



UNIWERSYTET ŚLĄSKI  
W KATOWICACH

**Uniwersytet Śląski w Katowicach**  
**Wydział Nauk Przyrodniczych**  
**Instytut Biologii, Biotechnologii i Ochrony Środowiska**

**Alicja Tomasiak**

**PRACA DOKTORSKA**

**Kompleksowa analiza epigenetyczna procesów reprogramowania  
komórkowego w tkankach hodowanych *in vitro* oraz *in vivo*-  
badania porównawcze gatunków *Fagopyrum***

**Promotor:**

dr hab. Alexander Betekhtin, prof. UŚ  
Uniwersytet Śląski w Katowicach

**Promotor pomocniczy:**

dr Agnieszka Brąszewska  
Uniwersytet Śląski w Katowicach

Katowice, 2024

### *Podziękowania*

*Składam serdeczne podziękowania Promotorowi prof. dr hab. Alexandrowi Betekhtinowi prof. UŚ za wsparcie merytoryczne i cierpliwość podczas całego procesu kształcenia oraz podczas postawiania tej rozprawy doktorskiej.*

*Pragnę podziękować Promotorowi Pomocniczemu, dr Agnieszce Brąszewskiej za cenne uwagi, wskazówki i informacje zwrotne.*

*Wielkie podziękowania dla Katarzyny Sali-Cholewy i Artura Pińskiego za pomoc w pracy naukowej oraz pomoc w powstawaniu rozprawy doktorskiej.*

*Składam również podziękowania współautorom publikacji naukowych, Członkom Zespołu Cytogenetyki i Biologii Molekularnej Roślin za pomoc naukową.*

*Dziękuję również mojej Mamie i Siostrze za wsparcie i motywację.*

## Spis treści

|  |    |
|--|----|
| 1. Wykaz publikacji wchodzących w skład rozprawy doktorskiej.....  | 4  |
| 2. Wykaz używanych skrótów.....  | 7  |
| 3. Streszczenie.....   | 8  |
| 4. Summary.....  | 10 |
| 5. Wstęp.....  | 12 |
| 6. Cel, hipotezy i zadania badawcze .....  | 19 |
| 7. Materiały i metody.....   | 21 |
| 8. Omówienie wyników przeprowadzonych badań.....   | 23 |
| 8.1 Omówienie badań przeprowadzonych <i>in vitro</i> .....   | 23 |
| 8.1.1 Przegląd dostępnej literatury podsumowujących dotychczasowe badania na gatunkach <i>Fagopyrum</i> w kulturach <i>in vitro</i> .....  | 24 |
| Publikacja P1.....   | 26 |
| 8.1.2 Ocena globalnych zmian w modyfikacjach białek histonowych i metylacji DNA w kalusach o zróżnicowanym potencjale embriogennym .....   | 27 |
| Publikacja P2.....   | 30 |
| 8.1.3 Zbadanie korelacji między poziomem modyfikacji epigenetycznych w genach kodujących białka i polisacharydy ściany komórkowej, a procesami odróżnicowania i różnicowania w kalusach <i>F. tataricum</i> o różnej zdolności do regeneracji..... | 31 |
| Publikacja P3.....   | 35 |
| 8.2 Omówienie wyników badań przeprowadzonych <i>in vivo</i> .....  | 37 |
| 8.2.1 Ocena poziomu zmian metylacji DNA oraz genów kodujących metylazy i demetylazy DNA wkwiatkach zamkniętych oraz otwartych samopylnej gryki tatarskiej i obcopylnej gryki zwyczajnej.....   | 38 |
| Publikacja P4.....   | 41 |
| 9. Podsumowanie i wnioski.....   | 43 |
| 10. Literatura.....  | 48 |
| 11. Oświadczenia autorów publikacji wchodzących w skład rozprawy doktorskiej ..  | 52 |

## 1. Wykaz publikacji wchodzących w skład rozprawy doktorskiej

### Publikacja 1 (P1):

**Tomasiak A.**, Zhou M., Betekhtin A. Buckwheat in tissue culture research: current status and future perspectives.

International Journal of Molecular Sciences, **2022**, 23(4)

<https://doi.org/10.3390/ijms23042298>

IF<sub>2022</sub>: 5,6

Punkty MNiSW: 140

### Publikacja 2 (P2):

**Tomasiak A.**, Sala-Cholewa K., Berg L.S., Brąszewska A., Betekhtin A. Global epigenetic analysis revealed dynamic fluctuations in levels of DNA methylation and histone modifications in the calli of *Fagopyrum* with different capacity for morphogenesis.

Plant Cell, Tissue and Organ Culture **2023**, 155, 743–757

<https://doi.org/10.1007/s11240-023-02595-3>

IF<sub>2023</sub>: 2,3

Punkty MNiSW: 100

### Publikacja 3 (P3):

**Tomasiak A.**, Pinski A., Milewska-Hendel A., Borowska-Żuchowska N., Morończyk J., Moreno-Romero J., Betekhtin A. H3K4me3 changes occur in cell wall genes during the development of *Fagopyrum tataricum* morphogenic and non-morphogenic calli.

Frontiers in Plant Science, **2024**, 15, 1465514

<https://doi.org/10.3389/fpls.2024.1465514>

IF<sub>2024</sub>: 4,1

Punkty MNiSW: 100

**Publikacja 4 (P4):**

Sala-Cholewa K.\*, **Tomasiak A.\***, Nowak K., Piński A., Betekhtin A. DNA methylation analysis of floral parts revealed dynamic changes during the development of homostylous *Fagopyrum tataricum* and heterostylous *F. esculentum* flowers.

BMC Plant Biology, **2024**, 24, 448

<https://doi.org/10.1186/s12870-024-05162-w>

\* równorzędny pierwszy autor

**IF<sub>2024</sub>**: 4,3

**Punkty MNiSW**: 100

**Sumaryczny IF**: 16,3

**Sumaryczne punkty MNiSW**: 440

Praca doktorska została wykonana w ramach badań realizowanych w projekcie finansowanym przez Narodowe Centrum Nauki pt.:

**Procesy reprogramowania komórek: analiza epigenetyczna i proteomiczna losów komórek gryki zwyczajnej i tataraki**

Nr grantu: 2020/37/B/NZ9/01499

Projekt w ramach konkursu OPUS 19 realizowanego w latach 2020-2024

Kierownik projektu: dr hab. Alexander Betekhtin, prof. UŚ

W trakcie realizacji pracy doktorskiej odbyłam dwumiesięczny staż zagraniczny w ramach programu Erasmus+ na Uniwersytecie Autonomicznym w Barcelonie, Wydział Biochemii i Biologii Molekularnej, pod kierownictwem dr Jordi Moreno-Romero.

## 2. Wykaz używanych skrótów

**2,4-D:** Kwas 2,4-dichlorofenoksyoctowy

**5mC:** 5-metylocytozyna

**BSA:** Albumina surowicy bydłęcej

**CMT3:** *CHROMOMETYLAZA3*

**DAPI:** 4',6-diamidyno-2-fenylindol

**DME:** *DEMETER*, glikozydaza 5-metylocytozyny

**DML2:** *DME-like 2*, *DME-like 2* glikozydaza 5-metylocytozyny

**DML3:** *DME-like 3*, *DME-like 3* glikozydaza 5-metylocytozyny

**DRMs:** *DOMAINS REARRANGED METHYLTRANSFERASEs*

**EDTA:** Kwas wersenowy

**EXTs:** *EKSTENSYNY*

**H3K18ac:** Acetylacja histonu H3 na lizynie 18

**H3K36me3:** Trimetylacja histonu H3 na lizynie 36

**H3K4me2:** Dimetylacja histonu H3 na lizynie 4

**H3K4me3:** Trimetylacja histonu H3 na lizynie 4

**H4K12ac:** Acetylacja histonu H4 na lizynie 12

**H4K16ac:** Acetylacja histonu H4 na lizynie 16

**H4K5ac:** Acetylacja histonu H4 na lizynie 5

**IAA:** Kwas indolilo-3-octowy

**KIN:** Kinetyna

**MET1:** *METYLOTRANSFERAZA DNA 1*

**NAA:** Kwas 1-naftylooctowy

**PBS:** Zbuforowany roztwór soli fizjologicznej

**PGs:** *POLIGALAKTURONAZY*

**PME:** *METYLOESTERAZA PEKTYNOWA*

**PMEI:** *INHIBITOR METYLOESTERAZY PEKTYNOWEJ*

**PXs:** *PEROKSYDAZY*

**ROS1:** *REPRESOR OF SILENCING 1*, glikozydaza 5-metylocytozyny

**SDS:** Laurylosiarczan sodu

**S-ELF3:** *S-LOCUS EARLY FLOWERING 3*

**TBO:** Błękit Toluidyny O

### 3. Streszczenie

Pierwszy etap pracy doktorskiej dotyczył badań nad procesami różnicowania komórek kalusa embriogenego (EK) *F. esculentum* oraz kalusa morfogenego (MK) i niemorfogenego (NK) *F. tataricum* w wybranych dniach kultury. EK i MK indukowano z niedojrzałych zarodków zygocycznych. EK *F. esculentum* charakteryzuje się budową typową dla embriogenicznej tkanki kalusowej. Składa się z mas embriogenicznych i komórek parenchymatycznych, zachowuje stabilność przez okres do dwóch lat hodowli, a jego morfologia charakteryzuje się gęstą, kulistą strukturą. MK *F. tataricum* charakteryzuje się zdolnością do morfogenezy lub embriogenezy somatycznej przez około 10 lat hodowli, wykazując wysoki poziom stabilności genomu. NK pojawia się na powierzchni MK po około dwóch latach hodowli w wyniku endoreplikacji. Charakteryzuje się aneuploidią, szybkim tempem wzrostu, wysokim poziomem stresu oksydacyjnego oraz całkowitą utratą zdolności do morfogenezy.

Celem pracy w pierwszym etapie było określenie zmian w poziomie występowania wybranych markerów epigenetycznych dotyczących poziomu metylacji DNA oraz metylacji i acetylacji histonów podczas odróżnicowania i ponownego różnicowania komórek wyżej wymienionych typów kalusów w wybranych dniach pasażu. Wykazano między innymi, że: obniżony poziom H3K4me2 jest skorelowany z odróżnicowaniem komórek u EK *F. esculentum* i MK *F. tataricum*; natomiast obniżony poziom metylacji DNA jest najprawdopodobniej powiązany z nabyciem potencjału embriogenicznego i ponowną inicjacją proembriogenicznych kompleksów komórkowych w MK *F. tataricum*. Spośród wszystkich badanych modyfikacji acetylacja histonów, czyli modyfikacje H4K16ac i H4K5ac, wykazały największą zmienność w NK, co można odnieść do procesów endoreplikacji, charakterystycznych dla rozwoju tego typu kalusa.

Dodatkowo, otrzymane wyniki pozwoliły na wybór jednej modyfikacji epigenetycznej (H3K4me3), którą użyto do badań immunoprecypitacji chromatyny. Celem badań była analiza i porównanie poziomu ekspresji i poziomu H3K4me3 w genach ściany komórkowej pomiędzy MK i NK *F. tataricum*. Analizy bioinformatyczne sekwencjonowania DNA tkanek poddanych immunoprecypitacji chromatyny wykazały, że genomowa zawartość H3K4me3 jest większa w NK. Natomiast w genach kodujących konkretne enzymy odpowiadające za reorganizację składników ściany komórkowej, tj. metyloesterazy pektynowe oraz peroksydazy, NK charakteryzował się obniżonym poziomem H3K4me3, co powiązano z brakiem zdolności do morfogenezy komórek tego typu kalusa. W MK w badanych genach ściany komórkowej



poziom H3K4me3 wzrastał wraz z progresją pasażu, co może oznaczać wzmożoną aktywność enzymów zaangażowanych w przemiany składników ściany komórkowej podczas procesów odróżnicowania komórkowego i dezintegracji proembriogennych kompleksów komórkowych. Wysłunięto wniosek, że modyfikacja H3K4me3 odgrywa kluczową rolę w aktywacji genów zaangażowanych w biosyntezę i reorganizację ściany komórkowej.

W drugiej części projektu przeprowadzono analizy poziomu metylacji DNA podczas rozwoju kwiatów *in vivo*. Poziom metylacji badano w elementach (płatki, nektarniki, zalążnie, znamiona słupka) kwiatów zamkniętych i otwartych obcopolnego gatunku *F. esculentum* cechującego się heterostylią (kwiaty typu Pin i Thrum) i samopolnego gatunku *F. tataricum*. W porównaniu do kwiatów zamkniętych, w otwartych kwiatach zaobserwowano spadek metylacji DNA w znamionach słupka, płatkach i zalążniach (z wyjątkiem zalążni w typie Thrum). Stwierdzono również znaczące różnice w poziomach metylacji DNA między morfotypami Pin i Thrum, jak i w kwiatach *F. tataricum*. Wykazano również, że spadek metylacji DNA korelował z obniżoną ekspresją genów kodujących metylotransferazy DNA. W otwartych kwiatach Thrum ekspresja *MET1* była ponad 45 razy niższa niż w zamkniętych, natomiast w zamkniętych i otwartych kwiatach Pin zmiana w poziomie ekspresji *MET1* była nieistotna statystycznie. Obserwowano również obniżoną transkrypcję innych analizowanych genów (*CMET3*, *DME1*, *DME3*, *ROS1*) w otwartych kwiatach Pin. Ponadto, gen *ROS1*, kodujący demetylazę DNA, wykazywał obniżoną ekspresję w otwartych kwiatach *F. esculentum* i *F. tataricum*. Ponieważ niedostępne są dane literaturowe na temat zmian epigenetycznych podczas rozwoju kwiatów gatunków *Fagopyrum* można zakładać, że wyższy poziom metylacji DNA oraz poziom ekspresji genów kodujących metylotransferazy i demetylazy DNA w zamkniętych kwiatach obu gatunków *Fagopyrum* wskazuje, że metylacja jest zaangażowana w procesy towarzyszące ich rozwojowi.

Słowa kluczowe: *Fagopyrum*, epigenetyka, heterostylia, H3K4me3, immunoprecypitacja chromatyny, kalus, kwiaty, metylacja DNA, odróżnicowanie, różnicowanie

## 4. Summary

The first stage of the research focused on the study of differentiation processes in embryogenic callus cells (EC) of *F. esculentum* and morphogenic (MC) and non-morphogenic (NC) callus of *F. tataricum* at selected days of culture. EC and MC were induced from immature zygotic embryos. *F. esculentum* EC is characterized by a structure typical of embryogenic callus tissue. It consists of embryogenic masses and parenchymatous cells, maintaining regeneration stability for up to two years of cultivation, with a morphology characterized by a dense, spherical structure. *F. tataricum* MC is capable of organogenesis or somatic embryogenesis for approximately ten years of cultivation, showing a high level of genome stability. NC appears on the surface of MC after approximately two years of cultivation as a result of endoreplication. It is characterized by aneuploidy, rapid growth rate, a high level of oxidative stress, and a complete loss of morphogenetic capacity.

The aim of the research in the first stages was to determine changes in the levels of selected epigenetic markers, including DNA methylation, histone methylation and acetylation, during dedifferentiation and re-differentiation of cells of the above-described calli on the selected days of culture. It was demonstrated, among others that a reduced level of H3K4me2 correlates with cell dedifferentiation in *F. esculentum* EC and *F. tataricum* MC. In contrast, the reduced level of DNA methylation is most likely associated with the acquisition of embryogenic potential and the re-initiation of proembryogenic cell complexes in *F. tataricum* MC. Among all the studied modifications, histone acetylation, particularly H4K16ac and H4K5ac, showed the greatest variability in NC, which can be linked to the endoreduplication processes characteristic of the development of this type of callus.

The obtained results allowed the selection of one epigenetic modification (H3K4me3) for chromatin immunoprecipitation studies. The aim of this research was to analyze and compare gene expression levels and H3K4me3 levels in cell wall-related genes between *F. tataricum* MC and NC. Bioinformatic analyses of DNA sequencing of tissues subjected to chromatin immunoprecipitation revealed that the genomic content of H3K4me3 is higher in NC. However, in genes encoding specific enzymes responsible for the reorganization of cell wall components, such as pectin methylesterases and peroxidases, NC exhibited a reduced level of H3K4me3, which was associated with the lack of morphogenetic ability of this type of callus. In MC, the level of H3K4me3 in the studied cell wall genes increased with the progression of culture, which may indicate increased activity of enzymes involved in the transformation of cell wall components during cellular dedifferentiation processes and disintegration of

proembryogenic cell complexes. It was concluded that the H3K4me3 modification plays a key role in activating genes involved in cell wall biosynthesis and reorganization.

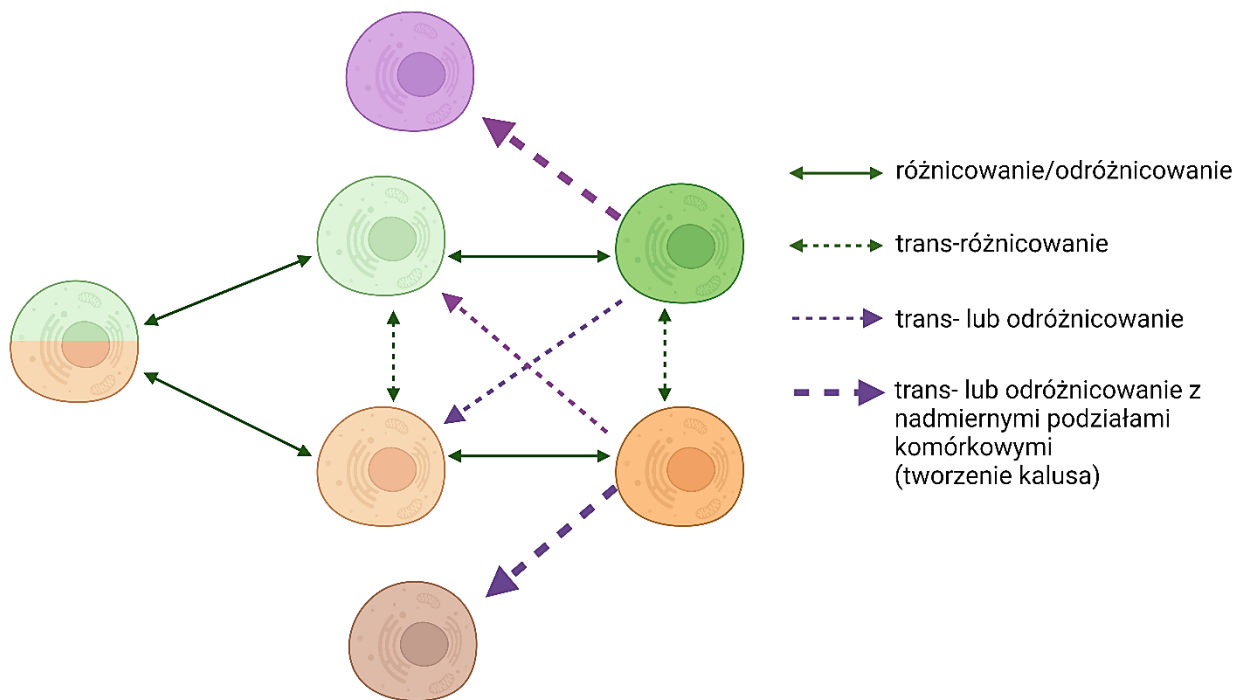
In the second part of the research, analyses of DNA methylation levels during flower development *in vivo* were conducted. Methylation levels were examined in the elements (petals, nectaries, ovaries, stigma) of closed and open flowers of the cross-pollinated species *F. esculentum*, which is characterised by heterostyly (Pin and Thrum morph flowers) and the self-pollinated species *F. tataricum*. Compared to closed flowers, open flowers showed a decrease in DNA methylation in the stigma, petals, and ovaries (except for the ovary in Thrum type). Significant differences in DNA methylation levels were also found between Pin and Thrum morphotypes, as well as in *F. tataricum* flowers. It was also demonstrated that the decrease in DNA methylation correlated with reduced expression of genes encoding DNA methyltransferases. In open Thrum flowers, *MET1* expression was over 45 times lower than in closed flowers, while in closed and open Pin flowers, the change in *MET1* expression level was not statistically significant. Reduced transcription of other analyzed genes (*CMET3*, *DME1*, *DME3*, *ROS1*) was observed in open Pin flowers. Additionally, the *ROS1* gene encoding DNA demethylase showed reduced expression in open *F. esculentum* and *F. tataricum* flowers. Since there is no available literature data on epigenetic changes during flower development in *Fagopyrum* species, it can be assumed that a higher level of DNA methylation and the expression levels of genes encoding DNA methyltransferases and demethylases in closed flowers of both *Fagopyrum* species indicate that methylation is involved in the processes accompanying their development.

Keywords: callus, chromatin immunoprecipitation, dedifferentiation, DNA methylation, epigenetics, flowers, gene expression, heterostyly, H3K4me3, redifferentiation.

## 5. Wstęp

Rośliny charakteryzują się wysoką zdolnością do regeneracji, w szczególności podczas hodowli w warunkach *in vitro*. Zróżnicowane komórki, pełniące określone funkcje w obrębie organizmu, mogą zatrzymać realizowany program rozwojowy pod wpływem konkretnego bodźca, następnie ‘zresetować się’ i rozpocząć realizację innego programu. Może to skutkować odtwarzaniem całego organizmu (lub jego części) w warunkach naturalnych pod wpływem czynników środowiskowych, albo podczas hodowli *in vitro* pod wpływem działania fitohormonów tj. auksyn i cytokinin. Szeroko pojęty termin ‘regeneracja’ dotyczy tych przemian. Dodatkowo, podczas rozwoju organów roślinnych, w tym kwiatów dochodzi do zmian na poziomie epigenetycznym, co wpływa na zmiany poziomów ekspresji genów, a przez to na uruchamianie konkretnych programów rozwojowych. W przedstawionej pracy wymienione wyżej zmiany losu komórek są określone jako reprogramowanie. Proces ten w kulturach *in vitro* może zachodzić na drodze odróżnicowania lub trans-różnicowania (Grafi, 2004). Oba procesy są powiązane z utratą cech charakterystycznych dla komórek poddanych indukcji, przy czym trans-różnicowanie wiąże się z nabyciem wyższego potencjału rozwojowego, czyli szerszego wachlarza potencjalnych dalszych dróg różnicowania w porównaniu do procesu odróżnicowania (Schemat 1) (Feher, 2019). Tworzenie kalusa można uznać za rodzaj trans-różnicowania, ponieważ w wielu kulturach *in vitro* obserwuje się występowanie grup komórek merystematycznych bądź embriogennych, z których powstają pędy (kaulogeneza), korzenie (ryzogeneza) lub zarodki somatyczne (embriogeneza somatyczna) co w odpowiednich warunkach hodowlanych prowadzi do otrzymania nowych roślin (Grafi, 2004, Sugimoto *i inni*, 2011, Sugimoto *i inni*, 2019).

Dotychczasowa literatura wskazuje, że oprócz czynników transkrypcyjnych i fitohormonów, epigenetyka odgrywa kluczową rolę w inicjacji, utrzymaniu i różnicowaniu komórek roślinnych. Indukcja i rozwój kalusa wiążą się ze zmianami epigenetycznymi (Miguel *i Marum*, 2011, Us-Camas *i inni*, 2014, Bednarek *i Orłowska*, 2019). Choć wiele modyfikacji epigenetycznych zostało zidentyfikowanych jako markery zmian losu komórek roślinnych, tylko nieliczne badania pokazują jak docelowo wpływają one na strukturę chromatyny i regulację transkrypcji (Szymanowska *i inni*, 2019).



**Schemat 1:** Schemat przedstawia drogi różnicowania, które może przejść komórka roślinna, oraz terminologię stosowaną do ich opisu. Różnicowanie wiąże się z obniżeniem potencjału rozwojowego komórki, natomiast odróżnicowanie z jej wzrostem. Odróżnicowanie może zajść w obrębie komórek tej samej linii rozwojowej, czyli komórek realizujących ten sam program rozwojowy i jest to równoznaczne z odwróceniem określonego wcześniej stanu zróżnicowania. Termin trans-różnicowanie natomiast jest używany do opisu zmian realizowanych przez komórki programu rozwojowego i są to zmiany niezależne od posiadanego potencjału rozwojowego, prowadzące do jego zwiększenia. W związku z różnorodnymi procesami zachodzącymi w obrębie kalusa, takimi jak trans-różnicowanie i intensywne podziały komórkowe, niektóre komórki mogą mieć zwiększony potencjał rozwojowy. Schemat i tekst zgodny z Feher (2019), zmodyfikowano. Schemat stworzony z użyciem platformy BioRender (<https://app.biorender.com>). Prawo do publikacji poświadczone licencją.

Metylacja DNA jest jedną z najlepiej zbadanych modyfikacji epigenetycznych i związana jest z różnorodnymi mechanizmami molekularnymi, takimi jak inaktywacja chromatyny czy regulacja aktywności genów (Park *i inni*, 2008, Springer i Schmitz, 2017, Ghosh *i inni*, 2021). Metylacja DNA zaangażowana jest w regulację wielu procesów komórkowych, natomiast jej rola w procesach różnicowania oraz odróżnicowania komórek podczas embriogenezy somatycznej i pokrewnych procesach zależy od gatunku oraz stadium rozwoju (Teyssier *i inni*, 2008). Obecność tej modyfikacji zazwyczaj związana jest z heterochromatyną i brakiem transkrypcji genów (Ghosh *i inni*, 2021). Natomiast inne badania wykazały, że metylacja DNA w regionach niepromotorowych, międzygenowych oraz w regionach aktywnych transkrypcyjnie (*ang. gene body*), ułatwia ekspresję genów i jest kluczowa dla zachowania słabo skondensowanej, aktywnej genetycznie chromatyny (Feng *i inni*, 2010, He *i inni*, 2011). W warunkach hodowli *in vitro* spadek poziomu metylacji DNA jest niezbędny do aktywacji podziałów komórkowych prowadzących do indukcji kalusa kukurydzy (*Zea mays*) (Stelpflug *i inni*, 2014, Han *i inni*, 2018). U brzoskwini (*Prunus persica*) spadek metylacji DNA miał pozytywny wpływ na procesy reprogramowania komórkowego i indukcji kalusa z komórek liścia (Zheng *i inni*, 2022). Z kolei, w kalusach soi (*Glycine max*) i kukurydzy zaobserwowano obniżenie poziomu metylacji DNA w wieloletnich kulturach, co sugeruje, że warunki hodowli *in vitro* skutkują utratą zdolności do utrzymania metylacji DNA na stałym poziomie (Han *i inni*, 2018, Ji *i inni*, 2019). Wykazano, że poziom metylacji DNA ma wpływ na embriogenezę somatyczną wielu gatunków roślin, w tym Akka Sellowa (*Acca sellowiana*), kawa (*Coffea canephora*), orchidea (*Doritaenopsis*) i żeń-szeń syberyjski (*Eleuterococcus senticosus*) (Chakrabarty *i inni*, 2003, Park *i inni*, 2008, Fraga *i inni*, 2012, Nic-Can *i inni*, 2013). Przykładowo, badania nad kalusami *Eleuterococcus senticosus* wykazały znacznie niższe poziomy metylacji DNA w kalusach embriogennych w porównaniu do kalusów nieembriogennych (Chakrabarty *i inni*, 2003). Podobne wyniki uzyskano dla *Agave furcroydes*, gdzie metylacja na wysokim, ale stabilnym poziomie była obecna przez cały okres hodowli w kalusie nieembriogennym (Monja-Mio *i inni*, 2018). Z drugiej strony, niższy poziom metylacji DNA w kalusie marchwi (*Daucus carota*), indukowanego z hipokotyli, hamował tworzenie komórek embriogennych (Yamamoto *i inni*, 2005).

Metylacja histonów jest niezbędnym czynnikiem w epigenetycznej regulacji ekspresji genów u roślin, gdyż mają na nią wpływ zarówno środowisko jak i sygnały rozwojowe, wywołane np. fitohormonami (tj. auksynami i cytokininami) (Yu *i inni*, 2009, Cheng *i inni*, 2020, Hu i Du, 2022). Występowanie markerów związanych z aktywną genetycznie chromatyną takich jak trimetylacja histonu H3 na lizynie 4 (H3K4me3) i trimetylacja histonu

H3 na lizynie 36 (H3K36me3) jest charakterystyczne dla komórek kalusa (Nic-Can *i inni*, 2013, Zhang *i inni*, 2015, Lee *i inni*, 2017, Ma *i inni*, 2022). Natomiast markery odpowiedzialne za stan heterochromatyny, takie jak di- i trimetylacja histonu H3 na lizynie 9 (H3K9me2/3) i di- lub trimetylacja histonu H3 na lizynie 27 (H3K27me2/3), są wykrywane na niższym poziomie w komórkach tkanki kalusowej (Lee i Seo, 2018, Hemenway i Gehring, 2023). Najnowsze badania wykazały, że obniżony poziom dimetylacji histonu H3 na lizynie 4 (H3K4me2) umożliwia aktywację genów niezbędnych do nabycia potencjału embriogenego podczas hodowli kalusa *Arabidopsis* (*Arabidopsis thaliana*) (Ishihara *i inni*, 2019). Stwierdzono również, że podwyższony poziom H3K36me3 towarzyszy procesom przejścia od zróżnicowanych komórek somatycznych do odróżnicowanych komórek kalusa *Arabidopsis* (Zhang *i inni*, 2015, Lee *i inni*, 2017, Ma *i inni*, 2022).

Acetylacja jest kolejnym istotnym czynnikiem regulującym transkrypcję genów związanych z nabywaniem potencjału embriogenego (np. *LEAFY COTYLEDON 1; 2*, *FUSCA 3* and *MYB DOMAIN PROTEIN 118*) (Moronczyk *i inni*, 2022). Transkrypcja genów z kolei, ma kluczowe znaczenie dla różnych zjawisk regeneracyjnych, w tym dla tworzenia kalusa, organogenezy i embriogenezy somatycznej (Birnbaum i Sanchez Alvarado, 2008, Us-Camas *i inni*, 2014). Acetylacja histonów jest powiązana z euchromatyną i aktywacją transkrypcji genów (Kouzarides, 2007). Wykazano, że podczas indukcji embriogenezy somatycznej wysokie poziomy acetylacji korelowały z ekspresją genów *SOMATIC EMBRYOGENESIS RECEPTOR-LIKE KINASE*, *BABY BOOM*, *LEAFY COTYLEDON*, *FUSCA3*, *CUP SHAPED COTYLEDONS*, i *WUSCHEL* u *Peaonia ostii* i *Arabidopsis* (Wickramasuriya i Dunwell, 2015, Ci *i inni*, 2022). Wykazano, że obniżony poziom acetylacji histonów, wynikający z nieprawidłowego działania acetylotransferaz histonowych (HATs), miał negatywny wpływ na procesy powstawania kalusa *Arabidopsis* (Kim *i inni*, 2018, Rymen *i inni*, 2019, Zhang *i inni*, 2020). U *Hevea brasiliensis* zaobserwowano obniżoną ekspresję genów dla deacetylaz histonów (HDACs) we wczesnych stadiach różnicowania kalusa (Li *i inni*, 2017a). Badanie dotyczące kalusa *Arabidopsis* wykazało, że acetylacja histonów jest niezbędna do nabycia potencjału morfogenego i regeneracji korzeni *de novo* poprzez aktywację transkrypcji genów w komórkach merystemu korzenia: *WUSCHEL-RELATED HOMEODOMAIN 5 (WOX5)*, *WOX15*, *SCARECROW*, *PLETHORA 1* i *PLETHORA 2* (Kim *i inni*, 2018).

Materiałem badawczym w przedstawionej pracy jest gryka - gatunek uprawny bogaty w związki fenolowe (głównie rutynę, kwercetynę i C-glikozyloflawony) oraz witaminy, które mają właściwości prozdrowotne dla człowieka (Ahmed *i inni*, 2013, Ge i Wang, 2020). Dodatkowo, gryka zawiera wysokiej jakości bezglutenowe białko i dostarcza konsumentom

szeroką gamę aminokwasów, błonnika pokarmowego oraz węglowodanów (Bonafacciaa *i inni*, 2003, Gonçalves *i inni*, 2016, Huda *i inni*, 2021). Do tej pory zidentyfikowano 22 gatunki gryki, przy czym dwoma najczęściej uprawianymi są: obcopolna gryka zwyczajna (*Fagopyrum esculentum*) i samopolna gryka tatarska (*Fagopyrum tataricum*) (Jha *i inni*, 2024). *F. esculentum* i *F. tataricum* cechują się dużymi różnicami pod względem morfologii, hodowli, plonowania, jak i rozwoju tkanki kalusowej w warunkach kultur *in vitro*.

W celu uniknięcia autoplagiatu w niniejszej rozprawie doktorskiej ryciny zawarte w publikacjach oznaczone zostały jako Figures, natomiast ryciny zawarte w tej pracy nazwano Rycinami 1 oraz 2, które zamieszczone są na końcu rozdziału Wstęp (strona 16).

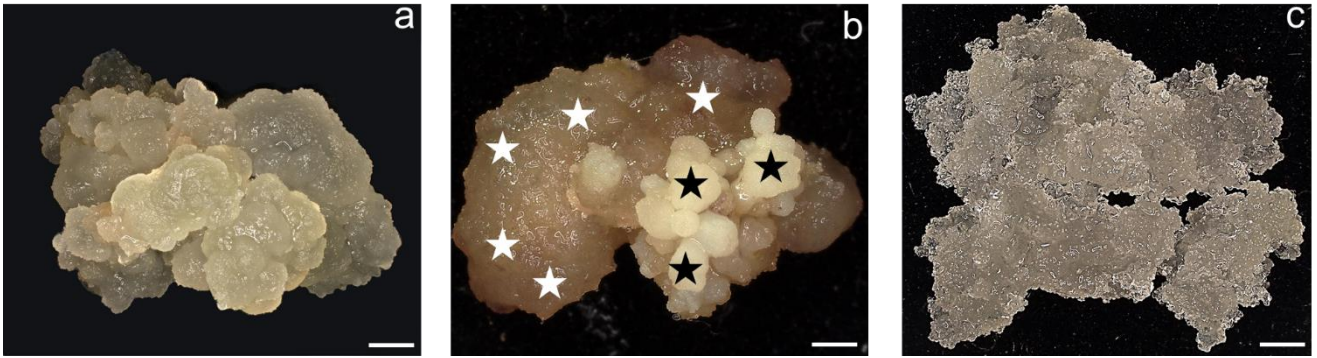
Kalusy: embriogeny (EK) *F. esculentum* (Ryc. 1a) i morfogeny (MK) *F. tataricum* (Ryc. 1b) indukowane były z niedojrzałych zarodków zygocytycznych. EK *F. esculentum* charakteryzuje się budową typową dla embriogenicznej tkanki kalusowej. Składa się z mas embriogenicznych, pozostaje stabilny przez okres do dwóch lat hodowli, a jego morfologia charakteryzuje się gęstą, kulistą strukturą. EK jest zdolny do tworzenia embrioidów z masy komórek embriogenicznych, regeneruje się poprzez embriogenezę somatyczną, ale nie wytwarza NK (Rumyantseva *i inni*, 2005). NK w przypadku *F. esculentum* natomiast może pojawić się w trakcie indukcji kalusa z zarodków zygocytycznych (Rumyantseva *i inni*, 2005). MK *F. tataricum* charakteryzuje się zdolnością do morfogenezy lub embriogenezy somatycznej przez około 10 lat prowadzenia kultury *in vitro*, wykazując niezwykle poziom stabilności genomu (Betekhtin *i inni*, 2017, Betekhtin *i inni*, 2019). MK składa się z proembriogenicznych kompleksów komórkowych (PEKK) (Ryc. 1b, czarne gwiazdki), struktur przypominających zarodki somatyczne zatrzymane w fazie preglobularnej, oraz z komórek ‘miękkiego’ kalusa (KMK) (Ryc. 1b, białe gwiazdki). Podczas pasażu MK przechodzi dwa cykle, które obejmują dezintegrację PEKK, proliferację i różnicowanie komórek, powstawanie KMK, co prowadzi do ponownego odtworzenia nowych PEKK. NK (Ryc. 1c) pojawia się na powierzchni MK po około dwóch latach hodowli w wyniku endoreplikacji. NK charakteryzuje się aneuploidią, szybkim tempem wzrostu, wysokim poziomem stresu oksydacyjnego oraz całkowitą utratą zdolności do morfogenezy (Sibgatullina *i inni*, 2012, Betekhtin *i inni*, 2017). Tkanki kalusowe obu gatunków, ze względu na zróżnicowanie potencjału rozwojowego, stanowią znakomity materiał do badań procesów reprogramowania komórek w kontekście zmian epigenetycznych.

Procesy reprogramowania komórek zachodzą nie tylko *in vitro*, ale również *in vivo*, na przykład podczas przejścia z fazy wegetatywnej do fazy generatywnej (Gehring, 2019). Dwa opisane powyżej gatunki *Fagopyrum* różnią się od siebie nie tylko typami kalusów, ale również typami kwiatów oraz sposobem ich zapylania. *F. esculentum* jest gatunkiem samo-niezdolnym,

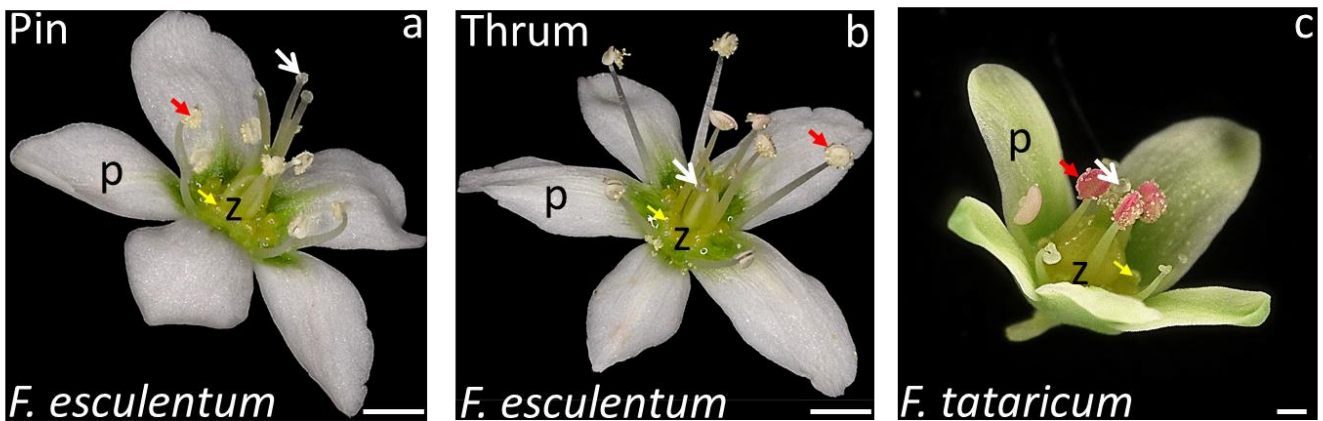


zapylanym krzyżowo, co oznacza, że roślina nie wytworzy nasion, jeśli zostanie zapyłona własnym pyłkiem. Jest to związane z heterostylią, czyli występowaniem dwóch morfologicznie odmiennych typów kwiatów (distylia) w obrębie tego samego gatunku, określanych jako Pin i Thrum (Ryc. 2. a-b) (Nagatomo T. i Adachi, 1985). Heterostylia u *F. esculentum* przejawia się w różnicach związanych z położeniem znamienia względem pylników w obu typach kwiatów, czyli długi słupek i krótsze pręciki w typie Pin (Ryc.2a), oraz krótszy słupek i dłuższe pręciki w typie Thrum (Ryc. 2b). Różnice w budowie kwiatów przekładają się na ich ograniczone zapylenie, niestabilny plon i w konsekwencji trudności w uprawie (Yasui i inni, 2012). Heterostylia *F. esculentum* jest kontrolowana przez klaster genów, tzw. supergen S (Cawoy i inni, 2006, Fawcett i inni, 2023). Niedawno wykazano, że gen *S-LOCUS EARLY FLOWERING 3 (S-ELF3)*, obecny w obrębie *locus* supergenu S, kontroluje długość słupka i niezgodność w szyjce słupka. Pojedyncza mutacja skutkująca inaktywacją *S-ELF3* doprowadziła do przełamania heterostylia poprzez regulację długości szyjki słupka i samozapylenia. U samozgodnych roślin występowały kwiaty o długich słupkach i pręcikach (tzn. długa homostylia) (Fawcett i inni, 2023). *F. tataricum* jest gatunkiem samopylnym, cechującym się homostylią, czyli występowaniem u wszystkich osobników kwiatów o zbliżonej długości słupków i nitek pręcików (Ryc. 2c), co eliminuje zależność od zapylaczy i skutkuje lepszym i stabilniejszym plonowaniem (Yasui i inni, 2016, Matsui i Yasui, 2020).

Metylacja DNA wpływa na różne aspekty rozwoju i morfologii kwiatów (Fulnecek i inni, 2011). Badania wykazały, że metylacja DNA odgrywa zasadniczą rolę w rozwoju kwiatów, przy czym niższy poziom metylacji DNA dominuje w kwiatach na wczesnym etapie rozwoju u *Arabidopsis* (Yang i inni, 2015). Dodatkowo, obniżony poziom metylacji DNA indukuje wczesne kwitnienie, co jest skorelowane ze zmianami w poziomach ekspresji genu *MET1* (Finnegan i inni, 1998, Yang i inni, 2015, Kumari i inni, 2022). Z kolei badania na pąkach i otwartych kwiatach *Azalea japonica* i *Arabidopsis* wykazały wzrost metylacji DNA podczas przejścia z fazy wegetatywnej do fazy kwitnienia (Ruiz-Garcia i inni, 2005, Meijón i inni, 2010). Metylacja reguluje kluczowe geny związane z kwitnieniem, takie jak *SOC1*, *API* i *SPL* oraz specyficzne geny czynników transkrypcyjnych, w tym geny *WUS* homeobox-containing (*WOX*) u jabłoni (Xing i inni, 2019). Podczas gdy liczne procesy związane z metylacją DNA w tkankach wegetatywnych roślin zostały szeroko zbadane, danych na temat metylacji DNA podczas rozwoju kwiatów, szczególnie kwiatów wykazujących różne cechy morfologiczne, jest niewiele.



**Rycina 1:** (a) kalus embriogeny *F. esculentum*; (b) kalus morfogeny *F. tataricum*, czarne gwiazdki - proembriogenne kompleksy komórkowe (PEKK), białe gwiazdki - komórki 'miękkiego' kalusa (KMK); (c) kalus niemorfogeny *F. tataricum*; skala - 1 cm. Fotografie: Alicja Tomasiak.



**Rycina 2:** Kwiaty *Fagopyrum esculentum*; (a) typ Pin; (b) typ Thrum; (c) kwiat *F. tataricum*; białe otwarte strzałki - znamiona, żółte strzałki - nektarniki, czerwone strzałki - pylniki, z - zalążnia, p - płatki, Skala - 0,3 cm. Fotografie - Alicja Tomasiak.

## 6. Cele i hipotezy badawcze

Epigenetyka odgrywa znaczącą rolę w procesach rozwojowych komórek roślinnych. Mechanizmy epigenetyczne regulują procesy reprogramowania komórkowego *in vitro* i *in vivo*. Gryka jest bardzo dobrym modelem do badania tego typu procesów, ponieważ posiada kalusy o zróżnicowanej zdolności do embriogenezy, jak i kwiaty o różnych cechach morfologicznych.

Zostały wyznaczone następujące cele badawcze:

1. Przegląd dostępnej literatury podsumowujący dotychczasowe badania na gatunkach *Fagopyrum* w kulturach *in vitro* (P1);
2. Ocena globalnych zmian w modyfikacjach białek histonowych i metylacji DNA w kalusach *F. esculentum* i *F. tataricum* o zróżnicowanej zdolności do embriogenezy (P2);
3. Zbadanie korelacji między poziomem modyfikacji epigenetycznych w genach kodujących białka i polisacharydy ściany komórkowej a procesami odróżnicowania i różnicowania w kalusach *F. tataricum* o różnym potencjale do regeneracji (P3);
4. Ocena poziomu zmian metylacji DNA oraz ekspresji genów kodujących metylazy i demetylazy DNA w kwiatkach na różnym etapie rozwoju (zamkniętych oraz otwartych) samopylnej gryki tatarskiej i obcopylnej gryki zwyczajnej (P4).

W pracy doktorskiej postawiono następujące hipotezy badawcze:

1. Procesom cyklicznego rozwoju kalusa gryki zwyczajnej i gryki tatarskiej w warunkach kultur *in vitro* towarzyszą zmiany w poziomach modyfikacji epigenetycznych i są one związane z procesami odróżnicowania i ponownego różnicowania komórek;
2. Występuje korelacja między zmianami epigenetycznymi a ekspresją genów kodujących białka i polisacharydy zaangażowane w przebudowę ściany komórkowej podczas procesów odróżnicowania i ponownego różnicowania komórek w kulturach *in vitro* kalusa gryki tatarskiej;
3. Kwiaty (*F. tataricum*, Pin i Thrum *F. esculentum*) na różnym etapie rozwoju (zamknięte i otwarte) różnią się poziomem metylacji DNA oraz ekspresją genów kodujących metylazy i demetylazy DNA.

## 7. Materiały i metody

W prowadzonych badaniach wykorzystano dwa gatunki gryki. Grykę zwyczajną (*F. esculentum*) genotyp Panda, który jest komercyjnie dostępną odmianą pozyskaną od Małopolskiej Hodowli Roślin (Polska), oraz grykę tatarkę (*F. tataricum*), genotyp k-17, której nasiona otrzymano od N.I. Instytutu Roślinnych Zasobów Genetycznych im. Wawilowa, Sankt Petersburg, (Rosja). Nasiona wysiewane były do doniczek wypełnionych ziemią wymieszaną z wermikulitem w stosunku 3:1, a następnie hodowane w szklarni w stałych warunkach temperatury  $25\pm 1$  °C, w warunkach fotoperiodu: 16 godz. światła i 8 godz. ciemności. Rośliny oświetlane były lampami emitującymi światło białe o strumieniu fotonów  $90 \mu\text{mol m}^{-2} \text{s}^{-1}$ . Kalus obu gatunków, tj. EK *F. esculentum* oraz MK *F. tataricum* indukowany był z niedojrzałych zarodków zygotycznych, natomiast NK *F. tataricum* pojawił się na powierzchni MK po około dwóch latach hodowli (Betekhtin *i inni*, 2017, Betekhtin *i inni*, 2019). Indukcja oraz hodowla kalusów w warunkach *in vitro* przeprowadzone były na pożywce RX o składzie mikro- i makroelementów oraz witamin według Gamborga zawierającej B5 z witaminami (Duchefa, Holandia, Gamborg *i inni* (1968)),  $2 \text{ g L}^{-1}$  N-Z aminy A (Sigma-Aldrich, USA),  $2 \text{ mg L}^{-1}$  kwasu 2,4-dichlorofenoksyoctowego (2, 4-D, Sigma-Aldrich),  $0,2 \text{ mg L}^{-1}$  kinetyny (KIN, Sigma-Aldrich, USA),  $0,5 \text{ mg L}^{-1}$  kwasu indolilo-3-octowego (IAA, Sigma-Aldrich, USA),  $0,5 \text{ mg L}^{-1}$  kwasu 1-naftylooctowego (NAA, Sigma-Aldrich, USA),  $25 \text{ g L}^{-1}$  sacharozy (Chempur, Polska) i  $7 \text{ g L}^{-1}$  fitoagaru (Duchefa, Holandia). Kalusy hodowano na szalkach Petriego w ciemności, umieszczonych w inkubatorze o temperaturze  $25^{\circ}\text{C} \pm 1$ . EK *F. esculentum* oraz MK *F. tataricum* pasażowano na świeżą pożywkę co cztery tygodnie. NK *F. tataricum* pasażowano co dwa tygodnie.

W zrealizowanych badaniach wykorzystano następujące techniki badawcze:

- Utrwalanie tkanek z wykorzystaniem paraformaldehydu, przesycanie utrwalonych tkanek woskiem Steedmana (Steedman, 1957), krojenie preparatów z użyciem mikrotomu rotacyjnego (**P2, P4**)
- Barwienia immunocytochemiczne z wykorzystaniem przeciwciał do modyfikacji epigenetycznych (5mC, H3K4me2, H3K4me3, H3K36me3, H3K18ac, H3K16ac, H4K12ac, H4K5ac) (**P2, P3**) oraz do epitopów białek i polisacharydów ściany komórkowej (LM5, LM6, LM19, LM20, JIM20) (**P4**)
- Barwienie tkanki kalusowej oraz kwiatów do analiz histologicznych z zastosowaniem błękitu toluidyny O (**P2, P4**)

- Obserwacje mikroskopowe z wykorzystaniem:
  - Mikroskopu cyfrowego Keyence VHX-970F (Japonia) (**P2, P3, P4**)
  - Mikroskopu jasnego pola Olympus BX43F (Polska) (**P2, P4**)
  - Mikroskopu konfokalnego Olympus FV1000 (Polska) (**P2, P4**)
  - Mikroskopu epifluorescencyjnego Axio Imager Z2 Zeiss (Niemcy) (**P4**)
- Reakcja immunoprecypitacji chromatyny (ChIP-qPCR), zawierająca następujące techniki molekularne: elektroforeza w żelu agarozowym, łańcuchowa reakcja polimerazy (*ang. polymerase chain reaction, PCR*), analiza ekspresji genów związanych ze ścianą komórkową metodą ilościowej reakcji łańcuchowej polimerazy w czasie rzeczywistym (*ang. real time quantitative polymerase chain reaction, RT-qPCR*) (**P3**).

Szczegółowe opisy wykorzystanych metod badań i eksperymentów, uzyskanych wyników wraz z ich dyskusją znajdują się w każdej publikacji wchodzącej w skład rozprawy doktorskiej, które oznaczone są numerami **P2**, **P3** oraz **P4**. Publikacje zamieszczono kolejno pod każdym omówieniem wyników badań. Przygotowanie skryptu do programu R Studio pozwalającego na przeprowadzenie analiz statystycznych zastosowanych w pracach **P2** oraz **P4** wykonane zostało przez mgr Leę Sophie Berg w ramach współpracy z Uniwersytetem w Bernie (Szwajcaria). Metoda ChIP-qPCR zastosowana w pracy **P3** została zoptymalizowana we współpracy z dr Jordi Moreno-Romero, Uniwersytet Autonomiczny w Barcelonie (Hiszpania).

## **8. Omówienie wyników przeprowadzonych badań**

### **8.1 Omówienie badań przeprowadzonych *in vitro***

### 8.1.1 Przegląd dostępnej literatury podsumowujących dotychczasowe badania na gatunkach *Fagopyrum* w kulturach *in vitro*

#### Publikacja P1:

**Tomasiak A.**, Zhou M., Betekhtin A. Buckwheat in tissue culture research: current status and future perspectives.

International Journal of Molecular Sciences, **2022**, 23(4):2298.

<https://doi.org/10.3390/ijms23042298>

IF<sub>2022</sub>: 5,6

Punkty MNiSW: 140

Publikacja opisuje badania i postępy w kulturach *in vitro* rodzaju *Fagopyrum*. Praca zawiera podrozdziały dotyczące indukcji kalusa, regeneracji roślin, kultur korzeni włósnikowatych, syntezy metabolitów wtórnych i otrzymywania roślin transgenicznych. Zamieszczono również oddzielny rozdział opisujący perspektywy w komercyjnym wykorzystaniu roślin z rodzaju *Fagopyrum*.

Podrozdział na temat indukcji kalusa opisuje typ eksplantatów używanych do indukcji, wykorzystywane pożywki i regulatory wzrostu. Najczęściej używanym eksplantatem do indukcji kalusa *F. esculentum* i *F. tataricum* były hipokotyle, hodowane na pożywce MS o składzie mikro- i makroelementów oraz witamin według Murashige i Skoog (1962), z dodatkiem kwasu 2,4-dichlorofenoksyoctowego (2,4-D) w stężeniu nieprzekraczającym 4.0 mg/L<sup>-1</sup> (Rajbhandari *i inni*, 1995, Han *i inni*, 2011, Kwon *i inni*, 2013). Do regeneracji roślin *F. esculentum* używane były głównie hipokotyle oraz liście na pożywce MS (Murashige i Skoog, 1962), z dodatkiem regulatorów wzrostu takich jak 2,4-D, 6-benzylaminopuryna (6-BA) oraz kinetyna (KIN) (Kumar, 2018, Fei *i inni*, 2019, Kumar i Saraswat, 2019). W przypadku *F. tataricum* do regeneracji roślin używano głównie hipokotyli, hodowanych na pożywce MS (Murashige i Skoog, 1962), a najczęściej wykorzystywanym regulatorem wzrostu był kwas 1-naftylooctowy (NAA) oraz 6-BA (Lachmann i Adachi, 1990, Han *i inni*, 2011, Wang *i inni*, 2016). W pracy opisano również regenerację *F. cymosum*, w przypadku którego użyto niedojrzałe kwiatostany (*ang. immature inflorescence*), pąki przybyszowe (*ang. adventitious buds*) oraz segmenty łodyg (*ang. nodal segments*) do regeneracji roślin na pożywce MS stosując głównie 6-BA (Takahata, 1988).



Kolejna część pracy opisuje kultury korzeni włośnikowatych, które zostały użyte do syntezy związków fenolowych. Podrozdział zawiera podsumowanie szlaków syntezy związków bioaktywnych takich jak m.in.: rutyna, kwercetyna, katechina, epikatechina, kwas kawowy oraz kwas chlorogenowy (Park *i inni*, 2012, Zhao *i inni*, 2014, Huang *i inni*, 2016, Li *i inni*, 2017b). Najczęściej używanym eksplantatem do indukcji korzeni włośnikowatych w przypadku *F. esculentum* były liście, hipokotyle i łodygi, natomiast w przypadku *F. tataricum* były to łodygi. Jako podłoże wykorzystywana była pożywka MS (Murashige i Skoog, 1962), a do transformacji użyto szczepów *Agrobacterium rhizogenes* ATCC 1584 oraz ATCC1000 (Lee *i inni*, 2007, Park *i inni*, 2012, Thwe *i inni*, 2013, Hou *i inni*, 2014, Huang *i inni*, 2016). Przy użyciu *A. tumefaciens*, uzyskano niewielki postęp odnośnie transformacji roślin z rodzaju *Fagopyrum* (Miljus-Djukić *i inni*, 1992, Kim *i inni*, 2001): nasiona otrzymane od zregenerowanych roślin w 75% wykazywały oporność na kanamycynę, co dowodzi integracji transgenu w genomie gryki.

Ostatni rozdział skupia się na perspektywach wykorzystania gryki, opisując, jak można wykorzystać hodowlę *in vitro* do przezwyciężenia ograniczeń związanych z uprawą *F. esculentum* (np. heterostylia, aborcja kwiatów). Fuzja protoplastów i hybrydyzacja somatyczna gatunków *Fagopyrum* została dotychczas opisana tylko w jednej pracy badawczej. Nie wspomniano natomiast, czy w wyniku regeneracji uzyskano funkcjonalne rośliny (Lachmann *i inni*, 1994). Edycja genomu przy użyciu systemu CRISPR/Cas9 (zgrupowane, regularnie rozproszone, krótkie, powtarzające się sekwencje palindromiczne, *ang. Clustered Regularly-Interspaced Short Palindromic Repeats*) umożliwia precyzyjną modyfikację genomu roślinnego. Nasza grupa, jako pierwsza na świecie, odniosła sukces w transformacji i modyfikacji genomu *F. tataricum* z wykorzystaniem systemu CRISPR/Cas9 na przykładzie inaktywacji genu kodującego desaturazę fitoenu. Uzyskane białe (albinotyczne) rośliny cechowały się obecnością indeli w obrębie sekwencji docelowej, wykazując skuteczną i precyzyjną modyfikację genomu gryki (Pinski i Betekhtin, 2023).

Podsumowując, prezentowana praca zawiera szczegółowy przegląd aktualnych badań, optymalnych warunków do hodowli i regeneracji roślin gryki w warunkach kultur *in vitro*.

**Publikacja P1:** Buckwheat in tissue culture research: current status and future perspectives.

**Tomasiak A., Zhou M., Betekhtin A.** Buckwheat in tissue culture research: current status and future perspectives.

International Journal of Molecular Sciences, **2022**, 23(4): 2298.

<https://doi.org/10.3390/ijms23042298>

**IF<sub>2022</sub>:** 5,6

**Punkty MNiSW:** 140



Review

# Buckwheat in Tissue Culture Research: Current Status and Future Perspectives

Alicja Tomasiak <sup>1</sup>, Meiliang Zhou <sup>2</sup> and Alexander Betekhtin <sup>1,\*</sup>

<sup>1</sup> Institute of Biology, Biotechnology and Environmental Protection, Faculty of Natural Sciences, University of Silesia in Katowice, 28 Jagiellonska St., 40-032 Katowice, Poland; alicja.tomasiak@us.edu.pl

<sup>2</sup> Institute of Crop Sciences, Chinese Academy of Agricultural Sciences, Room 405, National Crop Genebank Building, Zhongguancun South Street No. 12, Haidian District, Beijing 100081, China; zhoumeiliang@caas.cn

\* Correspondence: alexander.betekhtin@us.edu.pl

**Abstract:** Buckwheat is a member of a genus of 23 species, where the two most common species are *Fagopyrum esculentum* (common buckwheat) and *Fagopyrum tataricum* (Tartary buckwheat). This pseudocereal is a source of micro and macro nutrients, such as gluten-free proteins and amino acids, fatty acids, bioactive compounds, dietary fibre, fagopyrins, vitamins and minerals. It is gaining increasing attention due to its health-promoting properties. Buckwheat is widely susceptible to in vitro conditions which are used to study plantlet regeneration, callus induction, organogenesis, somatic embryogenesis, and the synthesis of phenolic compounds. This review summarises the development of buckwheat in in vitro culture and describes protocols for the regeneration of plantlets from various explants and differing concentrations of plant growth regulators. It also describes callus induction protocols as well as the role of calli in plantlet regeneration. Protocols for establishing hairy root cultures with the use of *Agrobacterium rhizogens* are useful in the synthesis of secondary metabolites, as well as protocols used for transgenic plants. The review also focuses on the future prospects of buckwheat in tissue culture and the challenges researchers are addressing.



**Citation:** Tomasiak, A.; Zhou, M.; Betekhtin, A. Buckwheat in Tissue Culture Research: Current Status and Future Perspectives. *Int. J. Mol. Sci.* **2022**, *23*, 2298. <https://doi.org/10.3390/ijms23042298>

Academic Editor: Anna M. Mastrangelo

Received: 4 February 2022

Accepted: 17 February 2022

Published: 18 February 2022

**Publisher's Note:** MDPI stays neutral with regard to jurisdictional claims in published maps and institutional affiliations.



**Copyright:** © 2022 by the authors. Licensee MDPI, Basel, Switzerland. This article is an open access article distributed under the terms and conditions of the Creative Commons Attribution (CC BY) license (<https://creativecommons.org/licenses/by/4.0/>).

**Keywords:** common buckwheat; in vitro callus induction; in vitro plantlet regeneration; Tartary buckwheat; tissue culture

## 1. Introduction

Plant tissue culture is considered to be an indispensable tool for plant regeneration, rapid multiplication, and propagation of material that is free of pathogens and disease, which characterises a plant with a better response to abiotic and biotic stresses and increased content of desired traits and characteristics [1]. It is, among others, used for research on organogenesis, direct and indirect somatic embryogenesis, callogenesis, hairy root formation, pathways of secondary metabolite production, genetic transformation, protoplast fusion, somatic hybridisation, and haploid plant production [2]. Tissue culture allows for the production of high throughput homogenous material in a short period [1,3]. Tissue culture aseptic conditions can be adjusted to obtain the desired results. These include medium pH, nutrient supply, hormone supply or lack thereof, optimal temperature and photoperiod. Plant tissue culture is widely used in studies on nutritionally and medicinally valuable plants [4,5]. In vitro culture revolves around the characteristics of cells called totipotency. Totipotent cells are considered to have the ability to regenerate into a new plant and express the full genome. However, it must be emphasised that the cell becomes totipotent under two conditions: its initiation has to be as a single cell and it must proceed autonomously as a single process [6,7]. Fehér [8] argued that, since plant regeneration needs to be induced through the process of organogenesis or somatic embryogenesis (SE) and callogenesis, cells regain totipotency, but have not always been totipotent. Fehér [8] describes the SE process as one where a single embryogenic cell is able to regenerate into a viable plantlet; therefore, this cell is totipotent. However, Fehér [8] also points out that if all

plant cells were totipotent, each plant cell would be capable of producing somatic embryos. Moreover, the same author highlights that somatic embryo formation does not always require dedifferentiated or totipotent cells during, for example, callo- and organogenesis where an embryo is initiated from procambial cells [8,9]. Regardless of the ambiguity surrounding the term “totipotency”, the principle of regeneration stays the same. It involves the adjustment of plant growth regulators (PGRs) and culture conditions to obtain the plant material with certain characteristics. PGRs are essential in order to determine the developmental pathway of cells in tissue culture. In vivo, plant calli form in response to wounding or pathogen infection, which further prompts changes in the regulation of PGRs, mainly auxin and cytokinin [10]. Fast-proliferating callus tissue is formed from the cambium cells; however, if the wound is not adjoined to cambium, live cells surrounding it undergo dedifferentiation, become meristematic and proliferate, resulting in callus formation [11]. A callus is a tissue with specific characteristics. It can form from one differentiated cell, and it is classified on the basis of the regeneration capacity. Under certain conditions, callus cells become pluripotent, which can lead to plantlet regeneration [6]. In vitro culture is a stressful environment for the plant. Artificial callus induction is caused in response to biotic and abiotic stresses and is affected by explants, media and PGRs [12]. Exogenous application of these hormones results in the induction of various processes. Increased concentration of PGRs result in the induction of various processes, i.e., increased concentration of auxin results in root formation, whereas a high concentration of cytokinin promotes the regeneration of shoots [1]. The balance between auxin and cytokinin govern callus states of dedifferentiation and differentiation. Adjusted concentrations of these hormones result in the induction of calli from explants under in vitro conditions [3]. In vitro callus induction provides an opportunity to extend the research of plant regeneration, cell totipotency, micropropagation and transgenics. Calli can be induced from various plant parts; reports describe induction from hypocotyls [13,14], young seedlings, cotyledon segments [15], shoots [16], immature inflorescence [17], anthers [18], and protoplasts [19,20].

It has been reported that callus induction involves transcriptional or post-transcriptional regulatory elements, which in turn result in global changes in the expression of genes and translation of proteins [21]. Some varieties of callus give rise to clones with inheritable traits different to those of parent plants. This is due to somaclonal variation, which is affected by explant source, age of parent plant, genotype and protocol for tissue culture [22].

Buckwheat belongs to a genus of 23 species, with the two most commonly cultivated species being *Fagopyrum esculentum* Moench (common buckwheat) and *Fagopyrum tataricum* Gaertn. (Tartary buckwheat) [23,24]. Common buckwheat is endemic to northern China and was subsequently introduced to Russia and Europe. The largest buckwheat producers are Russia, China, France, Poland and Ukraine, but it is also cultivated in North and South America [10,25,26]. It is a minor crop; however, the popularity of it is increasing among consumers because of the presence of gluten-free proteins and amino acids such as lysine, tryptophan, methionine, fatty acids, iminosugars, bioactive compounds such as rutin, orientin, quercetin, vixetin, isoorientin, and dietary fibre, fagopyrins, resistant starch, vitamin A, B-complex vitamins, zinc, sodium, copper, iron and other elements [11]. It has been proven that buckwheat has anti-oxidative, anti-tumour, anti-inflammatory, and anti-fungal, cardio-protective, hepato-protective, neuroprotective, anti-hypertension and anti-diabetic properties. Moreover, it can have cholesterol-lowering effects and improve cognition activities [11,27]. Tartary buckwheat is indigenous to west China and is grown in Bhutan, Nepal and northern part of India [28,29]. In Europe, Tartary buckwheat is cultivated in Luxemburg, Belgium, Germany, Italy and Slovenia [29,30]. It characterises with resistance to frost or drought, plant diseases, UV-B radiation damage and pests when compared with common buckwheat [28]. Moreover, Tartary buckwheat is characterised by over 100-fold higher content of rutin than common buckwheat [31]. It also contains resistance starch, balanced amino acids, increased levels of phenolics and was shown to alleviate symptoms of chronic diseases such as cardiovascular diseases, obesity, hypertension and can reduce intolerance of insulin and glucose in humans [28,32].

Buckwheat is widely susceptible to in vitro conditions which have been researched since 1974 [13] and have since been used to study plantlet regeneration from various explants, calli of different morphogenic capacity induction, organogenesis, somatic embryogenesis and synthesis of secondary metabolites such as phenolic compounds [33–35]. This review describes the research and progress of in vitro buckwheat cultures. It summarises reports on plant regeneration, callus induction, and protocols, as well as optimal physical, nutritional and hormonal conditions for buckwheat plant tissue culture. Additionally, it summarises the most recent studies on genetic transformation, hairy root cultures (HRCs), the efficacy of the process and optimal conditions and future prospects for buckwheat tissue culture.

## 2. Buckwheat Tissue Culture

### 2.1. Callus Induction

Plant tissue culture, also termed in vitro culture, is a widely used tool in agriculture and horticulture with different applications. The main advantage of the in vitro propagated material is the high yield of regenerants obtained in a short time. Regenerated plant populations are genetically homogenous, essentially disease-free and can possess desired traits such as low temperature, salinity and drought resistance [1]. Plant tissue culture is also important in terms of the germplasm preservation and imposing strategies for genetic interference and transformation as well as studying processes such as totipotency, differentiation and dedifferentiation and organogenesis [1]. As described by Ikeuchi et al. [36], the formation of a callus is a stage in plant regeneration and exhibits high and efficient regeneration potential.

Buckwheat characterises with high regeneration potential from calli [21]. Several studies have been conducted regarding the callus induction from various explants [13–15,18,20,35,37,38]. Table 1 summarises the optimal concentrations of hormones to induce calli from hypocotyls, cotyledons and immature embryos. Yamane [13] was the first to report callus induction from cotyledons and hypocotyls of common buckwheat using 10.0 mg/L of 2,4-dichlorophenoxyacetic acid (2,4-D). Takahata and Jumonji [14] conducted experiments with different concentrations of 2,4-D and 6-Benzylaminopurine (6-BA) and noticed that callus was induced with 6-BA, without the addition of 2,4-D. This is in contrast to work carried out by Yamane [13]. Rajbhandari et al. [16] noted improved callus induction in stem explants compared to leaf explants. Their experiments also showed that the supplementation of leaf and stem explants with naphthalene acetic acid (NAA) and indole acetic acid (IAA) at the concentrations of 0.5, 1.0 and 1.5 mg/L did not result in callus formation [16].

**Table 1.** Optimal conditions for the callus induction from different explants in *F. esculentum* and *F. tataricum*.

| Species              | Explant                      | Basal Medium                | PGRs                                    | References |
|----------------------|------------------------------|-----------------------------|---|------------|
| <i>F. esculentum</i> | Hypocotyl and cotyledon      | White's medium              | 5.0–10.0 mg/L 2,4-D                     | [13]       |
|                      | Hypocotyl                    | MS                          | 2.0 mg/L 2,4-D + 0.1–2.0 mg/L 6-BA      | [14]       |
|                      | Hypocotyl                    | B5                          | 1.0–5.0 mg/L 2,4-D + 0.05–2.0 mg/L 6-BA | [14]       |
|                      | Immature inflorescence       | B5                          | 1.0 mg/L 2,4-D + 2.0 mg/L NAA           | [17]       |
|                      | Hypocotyl derived protoplast | MS                          | 2.0 mg/L NAA + 1.0 mg/L 6-BA            | [19]       |
|                      | Leaf and stem                | MS                          | 1.0 mg/L 2,4-D                          | [16]       |
|                      | Hypocotyl and cotyledon      | MS                          | 2.0 mg/L 2,4-D + 0.5 mg/L 6-BA          | [38]       |
|                      | Leaf                         | MS                          | 1.0 mg/L 2,4-D                          | [39]       |
|                      | Cotyledon                    | MS                          | 2.0 mg/L 2,4-D + 0.2 mg/L KT            | [40]       |
|                      | Leaf                         | MS                          | 2.0 mg/L 2,4-D + 0.2 mg/L KT            | [41]       |
|                      | Hypocotyl                    | MS                          | 2.0 mg/L 2,4-D + 1.0 mg/L 6-BA          | [42]       |
|                      | Hypocotyl                    | MS                          | 1.0–2.0 mg/L 2,4-D + 1.5 mg/L 6-BA      | [43]       |
|                      | Anther                       | B5                          | 1.0 mg/L NAA + 2.0 mg/L 6-BA            | [18]       |
| Anther               | MS                           | 2.0 mg/L KT + 2.0 mg/L 6-BA | [44]                                    |            |

Table 1. Cont.

| Species             | Explant                      | Basal Medium | PGRs  | References |
|---------------------|------------------------------|--------------|---|------------|
| <i>F. tataricum</i> | Immature embryos             | B5           | 2.0 mg/L thiamine + 1.0 mg/L pyrioxidine + 1.0 mg/L nicotinic acid + 2000 mg/L casein hydrolysate + 2.0 mg/L 2,4-D + 0.5 mg/L IAA + 0.5 mg/L NAA + 0.2mg/L KT | [34]       |
|                     | Hypocotyl derived protoplast | MS           | 1.0 mg/L NAA + 1.0 mg/L 6-BA  | [20]       |
|                     | Hypocotyl and cotyledon      | MS           | 2.0 mg/L 2,4-D + 1.0 mg/L KT  | [45]       |
|                     | Hypocotyl                    | MS           | 4.0 mg/L 2,4-D + 1.0 mg/L 6-BA  | [46]       |
|                     | Hypocotyl                    | MS           | 3.5 mg/L 2,4-D + 0.8 mg/L 6-BA  | [37]       |

Callus differentiation from hypocotyl-derived protoplasts was the most optimal with 1.0 mg/L 2,4-D and 0.1 mg/L 6-BA [19]. Adachi et al. [19] induced callus formation from hypocotyl-derived protoplasts on MS medium with 1.0 mg/L NAA and 1.0 mg/L 6-BA. Hao et al. [38] described the optimal conditions for callus induction from cotyledons and hypocotyls; it was noticed that a high level of sucrose had an enhancing effect on callus induction and further growth. On the other hand, Woo et al. [40] observed that the sucrose content in the induction of calli had no effect on subsequent somatic embryo development. Interestingly, Gumerova et al. [47], who used the same explants, have achieved optimal callus induction with different concentrations of PGRs. This may depend on buckwheat species specificity or the genotype.

In research on Tartary buckwheat, Rumyantseva et al. [34] used a different basal medium with a number of different vitamins and PGRs, namely 2.0 mg/L thiamine, 1.0 mg/L pyridoxine, 1.0 mg/L nicotinic acid, 2000 mg/L casein hydrolysate, 2.0 mg/L 2,4-D, 0.5 mg/L IAA, 0.5 mg/L NAA, and 0.2 mg/L KT and noted that the callus induction depends on explant species affiliation as well as the stage of immature embryo used during the induction. Wang et al. [45] used MS medium supplemented with 2.0 mg/L 2,4-D and 1.0 mg/L KT and obtained 98.96% induction rate. It is important to highlight that in the literature on buckwheat callus, the terminology is slightly ambiguous. Rumyantseva et al. [34] described four types of calli in common buckwheat: dense globular that proliferates slowly, dense slowly proliferating, loose and rapidly multiplying, and heterogenous slowly proliferating comprising loose globules, and one in Tartary buckwheat: heterogenous slowly growing. The same authors did not observe the loose and dense types; however, it was concluded that the characteristics of the callus during cultivation change, and that the heterogenous callus has the ability to establish calli with loose morphology. The common buckwheat dense-type callus and the heterogenous callus of Tartary buckwheat exhibited the highest organogenic capacity and after the transfer to the regeneration medium it prompted the emergence of stem apices. However, when globular calli (morphogenic) were transferred to the embryonic medium, embryo-like structures were observed after several days [34]. Woo et al. [41] describes somatic organogenesis from leaf explants calli which gave rise to somatic embryos. Park et al. [39] used leaf and stem segments and observed the emergence of proembryogenic/proembryonal complexes (PECCs) on explants and subsequent somatic embryogenesis. This was also observed by Gumerova et al. [33], who noted that the regeneration from PECCs can be achieved in three ways: via the formation of vegetative buds, via the formation of somatic embryos on the PECCs' surface and via the whole PECC transformation in a sprouting embryo. The term embryogenic callus is also used by Saraswat and Kumar [48], where it was induced from hypocotyls and cotyledons. On the other hand, Valieva et al. [49] describes an embryogenic callus, which can form embryoids, roots and buds, and a morphogenic callus, which can form vegetative buds and roots. They also describe histogenic calli, capable of vascular differentiation, and non-morphogenic callus (NC), which emerges on the surface of the morphogenic callus (MC) after two to three years of culture [49]. It is important to stress that the embryogenic callus is described as the one comprising PECCs and so called 'soft' callus by the authors [50].

Research on Tartary buckwheat by Betekhtin et al. [21] describes MC as the one with the ability to undergo somatic embryogenesis, organogenesis and subsequent plant regeneration. It comprises PECCs or pro-embryogenic masses (PEMs) and phenolic containing cells (PCC) on their surface [21]. In the course of callus cyclical development, mature PEMs collapse and new PEMs along with 'soft' callus cells (SCC) arise which are elongated and have large vacuoles and starch grains in the cytoplasm [21,34,50,51]. PCCs cover the surface of PEMs and parenchymatous cells localised in the central part of PEMs [21]. Calli exhibiting no apparent regeneration are classified as compact, friable or non-morphogenic calli [52]. The emergence of NC is correlated with metabolic changes of the cells. Calli lose the capability of accumulating and synthesizing pigments such as anthocyanins during a prolonged period of culture [13,21,49,51]. It emerges seldomly from separate foci (once per 30–40 passages) [53]. Tartary buckwheat calli with different morphogenic capacities allow us to conduct comparative analyses of physiological, biochemical and cytological features in long-term cultivated callus lines.

## 2.2. Buckwheat Plant Regeneration

Protocols for buckwheat regeneration from several explants such as hypocotyls [14,20,42,46,47,54–56], immature inflorescence [17], nodal segments [57], immature embryos [34,58], anthers [44,59], leaf petioles [60] and cotyledons [40,54,61,62] were developed. In Table 2, the optimal conditions for the plantlet regeneration from different explants, *F. esculentum*, *F. tataricum* and *F. cymosum*, are summarised.

The first description of common buckwheat plantlet regeneration from explants was reported by Yamane [13]. It was reported that plant calli could regenerate plants even after 48 months of culture. Moreover, shoot and root formation was observed in calli transferred to modified LS (Linsmaier and Skoog) medium (supplemented with 15% coconut milk and 3.0 mg/L yeast extract) after 30 to 60 days [13]. Srejovic and Neskovic [15] classified the stages of explants' growth via organogenesis. Takahata and Jumonji [14] were able to produce regenerants of common buckwheat on MS (Murashige and Skoog) medium with up to 5.0 mg/L 2,4-D and up to 2.0 mg/L, and it was concluded that calli can be induced only with 6-BA, without the addition of 2,4-D. Takahata [17] observed that direct formation of shoots from inflorescence was promoted by supplementation of the media with 0.2 mg/L NAA and 1.0 mg/L of 6-BA. Rajbhandari et al. [16] reported improved plantlet regeneration when MS medium was supplemented with 0.2 mg/L IAA and 2.0 mg/L 6-BA, and found dependency of regeneration on the genotype; however, somatic embryos were not observed. Hao et al. [38] noticed that carbohydrates have a shoot-promoting effect on the cutting site and act as osmotic stabilisers. A similar finding by Lachmann and Adachi [20] reported that the addition of sucrose was important for SE induction in buckwheat. On the contrary, Woo et al. [40] found that increased sucrose content did not have any effect on the callus induction or SE. In terms of callus induction and proliferation, Saraswat and Kumar [48] noticed that the hypocotyl explants responded better in media supplemented with glucose, while cotyledon explants responded better to the medium with sucrose as the carbohydrate source. Park et al. [39] were able to regenerate plants from leaf-derived calli on MS medium devoid of hormones, but the regeneration rate was low and failed to regenerate plantlets from stem-derived calli. Park and Park [62] reported direct organogenesis of multiple shoots from cotyledon explants. Berbec and Doroszewska [63] discovered that LS medium supplemented with TDZ (N-Phenyl-N'-1,2,3-thiadiazol-5-ylurea) is suitable for regeneration only when combined with IAA. When organogenesis was induced from leaf petioles, the optimal conditions were MS medium supplemented with 1.0 mg/L 6-BA, 1.0 mg/L 2iP (6-( $\gamma,\gamma$ -Dimethylallylamino) purine) and 1.0 mg/L 2,3,5-TIBA (2,3,5-triiodobenzoic acid). It is speculated that TIBA controls the shoot initiation process by contracting endogenous auxins. This research has also revealed a finding that the rate of seed abortion in regenerated plants is much lower compared to the ones grown directly from seeds [60]. Another investigation was conducted with the use of 7.0 mg/L of silver nitrate ( $\text{AgNO}_3$ ) and noted improvement in the frequency

of shoot regeneration of over 30% [64]. Similar results were obtained by Saraswat and Kumar [48] where the use of AgNO<sub>3</sub> showed improvements in shoot and root growth. The same authors tested the addition of KNO<sub>3</sub> to the medium. It was concluded that KNO<sub>3</sub> does not influence the maturation of somatic embryos, as is reported in SE in other species such as cotton [65]. Saraswat and Kumar [48] speculated that low maturity of somatic embryos supplemented with KNO<sub>3</sub> is due to the buckwheat being a salt-sensitive crop.

**Table 2.** Optimal conditions for the plantlet regeneration from different explants *F. esculentum*, *F. tataricum* and *F. cymosum*.

| Species                 | Explant                      | Basal Medium                               | PGRs  | References |
|-------------------------|------------------------------|--|---|------------|
| <i>F. esculentum</i>    | Hypocotyl                    | LS   | 1.0–10.0 mg/L 2,4-D + 2.0 mg/L NAA                      | [13]       |
|                         | Cotyledon                    | B5   | 0.1 mg/L 6-BA + 0.1 mg/L IAA                            | [15]       |
|                         | Hypocotyl                    | MS   | 0.1–0.2 mg/L NAA + 1.0–2.0 mg/L 6-BA                    | [14]       |
|                         | Immature embryo              | B5   | 2.2 mg/L 6-BA + 0.17 mg/L IAA + 0.5 mg/L IBA            | [58]       |
|                         | Shoot apex                   | MS   | 0.5 mg/L IAA + 2.0 mg/L 6-BA                            | [66]       |
|                         | Immature inflorescence       | B5   | 0.2 mg/L NAA + 1.0 mg/L 6-BA                            | [17]       |
|                         | Anther                       | MS   | 1.0 mg/L 6-BA + 0.2 mg/L IAA                            | [59]       |
|                         | Hypocotyl derived protoplast | MS   | 0.1 mg/L NAA + 0.5 mg/L 6-BA + 0.1 mg/L GA <sub>3</sub> | [19]       |
|                         | Leaf and stem                | MS   | 0.2 mg/L IAA + 2.0 mg/L 6-BA                            | [16]       |
|                         | Anther                       | MS   | 2.5 mg/L 6-BA + 0.5 mg/L IAA                            | [44]       |
|                         | Cotyledon                    | MS + B5 vits                               | 0.5 mg/L IAA + 0.25 mg/L IBA                            | [61]       |
|                         | Hypocotyl and cotyledon      | LS   | 0.05–0.1 mg/L TDZ + 0.5 mg/L IAA                        | [63]       |
|                         | Leaf and stem                | MS   | Hormone free  | [39]       |
|                         | Cotyledon                    | MS   | 2.0 mg/L 6-BA + 0.2 mg/L KT                             | [40]       |
|                         | Nodal segment                | MS   | 1.0 mg/L KT   | [67]       |
|                         | Anther                       | B5   | 1.0 mg/L NAA + 1.0–2.0 mg/L 6-BA                        | [18]       |
|                         | Hypocotyl                    | MS   | 2.0 mg/L 6-BA + 1.0 mg/L KT                             | [43]       |
|                         | Hypocotyl                    | B5   | 2.23 mg/L 6-BA + 0.17 mg/L IAA                          | [33,47]    |
|                         | Leaf                         | MS   | 0.2 mg/L KT + 2.0–3.0 mg/L 6-BA                         | [41]       |
|                         | Cotyledon and hypocotyl      | MS + B5 vits                               | 1.0 mg/L 6-BA   | [57]       |
|                         | Nodal segment and shoot apex | MS + B5 vits                               | 2.0 mg/L 6-BA + 0.2 mg/L IAA                            | [57]       |
|                         | Cotyledon                    | MS   | 4.0 mg/L 6-BA + 7.0 mg/L AgNO <sub>3</sub>              | [68]       |
|                         | Leaf petiole                 | MS   | 1.0 mg/L 6-BA + 1.0 mg/L 2iP + 1.0 mg/L TIBA            | [60]       |
| Hypocotyl               | MS                           | 1.0 mg/L KT + 1.0 mg/L 6-BA + 2.0 mg/L IAA | [42]  |            |
| Hypocotyl               | MS                           | 1.0 mg/L NAA + 1.0 mg/L 6-BA               | [55]  |            |
| Hypocotyl and cotyledon | MS                           | 0.2 mg/L 6-BA + 0.5 mg/L AgNO <sub>3</sub> | [48]  |            |
| <i>F. tataricum</i>     | Immature embryos             | MS   | 0.1 mg/L 6-BA + 0.1 mg/L IAA                            | [34]       |
|                         | Hypocotyl derived protoplast | MS   | 2.0 mg/L NAA + 1.0 mg/L 6-BA                            | [20]       |
|                         | Hypocotyl                    | MS   | 1.0 mg/L NAA + 0.5 mg/L 6-BA                            | [55]       |
|                         | Hypocotyl and cotyledon      | MS   | 3.0 mg/L 6-BA + 1.0 mg/L TDZ                            | [45]       |
| <i>F. cymosum</i>       | Immature inflorescence       | B5   | 1.0 mg/L NAA + 1.0 mg/L 6-BA                            | [17]       |
|                         | Adventitious buds            | MS   | 2.0 mg/L 6-BA + 0.5 mg/L TDZ + 0.2 mg/L NAA             | [69]       |
|                         | Nodal segments               | MS   | 2.5 mg/L IBA  | [5]        |



Reports on Tartary buckwheat regenerations were first described by Rumyantseva et al. [34] who were able to demonstrate plant regeneration from calli cultured for a period of 18 months. It was noticed that the embryoids developed faster and spontaneous embryogenesis occurred more frequently, compared to common buckwheat. Han et al. [46] reported moderate frequency of Tartary buckwheat plantlet regeneration by supplementing MS medium with 1.0 mg/L IAA, 1.0 mg/L KT, 2.0 mg/L 6-BA and 0.5 mg/L TDZ. However, the authors did not mention the percentage of regenerated plants. Wang et al. [45] reported 56% plantlet regeneration level from callus on the MS medium supplemented with 2.0 mg/L 6-BA and 1.0 mg/L KT. These authors observed the level of shoot induction of 69% on MS basal medium with the addition of 3.0 mg/L 6-BA and 1.0 mg/L TDZ. Induction of roots was obtained on half-strength ( $\frac{1}{2}$ ) MS medium with 1.0 mg/L IBA, which resulted in 75% of plantlets surviving after being transferred to soil with field conditions [45]. Advances in buckwheat regeneration protocols can be used as protocol for transformation which in turn will create opportunities to examine metabolic and molecular regulation of significant components such as gluten-free proteins, fatty acids, flavonoids and vitamins. The literature in terms of callus induction in buckwheat focuses only on common and Tartary buckwheat, while it is important to highlight that there are 23 buckwheat species.

### 2.3. Hairy Root Culture

A type of tissue culture which has received increasing attention in recent years is the hairy root cultures (HRCs) [64,70–83]. These are derived from infecting the explants with *Agrobacterium rhizogenes* and occurs via the transfer of the root-inducing (Ri) bacterial plasmid, which in consequence prompts the induction of hairy root (HR) syndrome [84] and results in the abundant growth of neoplastic roots that can be cultured under in vitro conditions [77]. Neoplastic roots are singular due to their biosynthetic and genetic stability, which improves the activity of growth regulators [78]. There are multiple advantages of HRCs, which makes them a valuable system for research on secondary plant metabolites such as flavonoids. Other advantages include high growth rates without the addition of PGRs, and in certain cases, without incubation under light. HRCs are genetically stable and respond well when the conditions of culture such as carbon source and concentration, medium pH, white fluorescent light and temperature are adjusted for optimal secondary metabolite secretion [85]. However, the most prominent feature of HRCs is the fact that *A. rhizogenes* is able to manipulate the host in order to increase the chance of a successful transformation. Thus, the *Agrobacterium*-mediated transformation of HRCs provides an easy and fast way to introduce and express foreign genes in cells that are able to carry out the synthesis of certain secondary metabolites [86]. It has been reported that *A. rhizogenes* strain number 15,834 is one of the most widely used strains for hairy root induction as well as their production of secondary metabolites [76,87–89]. As for the production of secondary metabolites in callus cultures of *Fagopyrum* species, it was reported by Moumou and Trotin [90] that the flavonoid content was relatively low in calli grown in darkness compared to ones grown under the light. Nonetheless, secondary metabolite content was significant, especially the content of two dimeric proanthocyanidins: B2 and B2-3'-O-gallate and two catechins: epicatechin and epicatechin 3-O-gallate [90–92]. Therefore, as a source of bioactive secondary metabolites such as flavonoids, transgenic technology involving *Fagopyrum* species, especially through HRCs is important in the investigation of their molecular and metabolic regulation and genetic engineering. In Table 3, the optimal conditions for the production of bioactive compounds with *A. rhizogenes* from different explants, *F. esculentum* and *F. tataricum*, are summarised.

The first reports on HRCs in common buckwheat date to 1990 when Neskovic et al. [93] researched the inoculation of *A. rhizogenes*, which led to the development of hairy roots on stems. Two strains were used, i.e., ATCC 15834 and ATCC 13332, to induce HRCs and obtain the efficiency of HRCs formation at 75.8% and 24.1%, respectively, and overall formation of HRCs from inoculated explants was 39.7%. It was concluded that this species is very responsive to *Agrobacterium* which in the future could be used as a vector in genetic

transformation [93]. Moumou and co-workers [91] discovered that selected cultures of calli induced from common buckwheat hypocotyls produced significantly high quantities of flavonoids, procyanidins and catechins in particular, which were not present in original plants. Trotin et al. [94] established HRCs by infecting hypocotyl explants of common buckwheat with *A. rhizogenes* strain ATCC 15834 and observed the synthesis of flavonoids: catechin, epicatechin, epicatechin-3-O-gallate, procyanidin B2 and procyanidin BZ3'-O-gallate. It was concluded that the HRCs exhibited the highest concentration of procyanidin B2-3'-O-gallate, suggesting that HRCs characterise in the preferential synthesis of galloylated derivatives of monomeric and dimeric classes as well as inverted content of catechin and epicatechin when compared to calli, confirming that HRCs contain more flavonoids than regular roots, in vitro normal roots and calli. Polyphenolics were also investigated in HRCs induced by *A. rhizogenes* strain MAFF 03-01724, which induces similar secondary metabolite production in roots compared to those in intact plants [95]. The effect of different media on HRCs was investigated and led to the conclusion that the most suited is MS medium; however, the most promising result was that the HRCs produced ten times more rutin than the field-cultivated plants [95]. About a decade later, Lee et al. [96] used a different strain of *A. rhizogenes* (R1000) and tested the production of rutin in common buckwheat HRCs. It was found that the quantity of rutin produced by HRCs was notably higher when compared with the control. It was also noticed that the addition of auxins (IAA) positively affected rutin production and the most suitable medium for the highest yield of HRCs was  $\frac{1}{2}$  MS. Research led by Kim et al. [86] provided a protocol for common buckwheat HRCs transformation via affecting stems with *A. rhizogenes* strain ATCC 15834 containing pB1121 binary vector. Rapidly growing clones were obtained, which produced 2.6 times more rutin than the wild type roots [97]. This work provided the efficient and multifaceted system for investigating the molecular regulation of phenolic compound biosynthesis as well as evaluating the system's potential for metabolically engineering and rutin production [97]. Park et al. [74] demonstrated that the expression of the transcription factor AtMYB12 resulted in increased levels of rutin in common buckwheat transgenic HRCs. The family of MYB transcription factor is commonly present within higher plants [74]. It is known to participate in diverse biochemical and physiological processes, which include, among others, response to abiotic stress, influencing secondary metabolism pathways and controlling cell morphogenesis [98]. The accumulation of flavonols was observed as a result of the over expression of AtMYB12, which was primarily identified in *Arabidopsis thaliana* [99,100]. As a conclusion of Park et al. [75], it was noted that although AtMYB12 notably affected the production of rutin in transgenic buckwheat HRCs, a more effectively engineered metabolic pathway is required in order to allow the identification of transcription factors from the *Fagopyrum* species [75]. Gabr et al. [70] measured the content of phenolic acids in HRCs of common buckwheat obtained by infecting roots, stems and leaves with *A. rhizogenes* strain A4 and observed three-fold higher content of chlorogenic acid than in the control in all treated explants, with HRCs from roots containing most of the acid. HRCs from roots also exhibited an increased content of p-anisic and caffeic acids. The same authors in 2019 investigated the content of rutin in HRCs of common buckwheat in explants from leaves, stems and roots. It was reported that the rutin content was higher in control root compared to HRCs from stem and leaves, which led to the conclusion that the suppression of rutin accumulation in HRCs is a form of plant defence against stress. It was also concluded that the production of rutin depends on the type of explant, and moreover that HRCs displayed increased levels of histidine, valine, lysine and isoleucine and total content of flavonoids and the antioxidant activity [71].

**Table 3.** Optimal conditions for the production of bioactive compounds with *A. rhizogenes* from different explants *F. esculentum*, *F. tataricum*.

| Species              | Explant             | <i>A. rhizogenes</i> Strain | Basal Medium                     | Bioactive Compounds   | References |
|----------------------|---------------------|-----------------------------|----------------------------------|---|------------|
| <i>F. esculentum</i> | Stem                | ATCC 15834<br>ATCC 13332    | $\frac{1}{2}$ B5 (half strength) | -   | [93]       |
|                      | Hypocotyl           | ATCC 15834                  | B5                               | Catechin, epicatechin, epicatechin-3-O-gallate, procyanidin B2 and procyanidin B2-3'-O-gallate  | [94]       |
|                      | Leaf                | MAFF 03-01724               | MS                               | catechin, epicatechin, epicatechin 3-O-gallate procyanidin B-1 and procyanidin B-2 3'-O-gallate   | [95]       |
|                      | Leaf                | R1000                       | MS                               | Rutin   | [96]       |
|                      | Stem                | ATCC 15834                  | MS                               | Rutin   | [97]       |
|                      | Stem                | R1000                       | MS                               | Rutin   | [75]       |
|                      | Leaf, stem and root | A4                          | MS                               | Rutin, chlorogenic acid, hyperoside, caffeic acid, p-anisic acid  | [70]       |
|                      | Steam, leaf         | A4                          | MS                               | Rutin, hesperidine, kaempferol-3-O-rutinoside   | [71]       |
| <i>F. tataricum</i>  | Stem                | R1000                       | MS                               | Rutin, quercetin, epicatechin, catechin hydrate, gallic acid, ferulic acid, chlorogenic acid, and caffeic acid                          | [86]       |
|                      | Stem                | R1000                       | MS                               | Rutin, epicatechin, gallic acid, epigallocatechin, caffeic acid, catechin hydrate, chlorogenic acid                                     | [74]       |
|                      | Stem                | R1000                       | $\frac{1}{2}$ SH                 | Rutin, epicatechin, gallic acid, epigallocatechin, caffeic acid, catechin hydrate, chlorogenic acid                                     | [81]       |
|                      | Hypocotyl           | R1000                       | MS                               | Rutin, quercetin, gallic acid, caffeic acid, ferulic acid, 4-hydroxybenzoic acid  | [79,80]    |
|                      | Leaf                | Ri1601                      | MS                               | Rutin and quercetin   | [99,100]   |
|                      | Hypocotyl           | R1000                       | $\frac{1}{2}$ MS                 | Cyanidin 3-O-glucoside, cyanidin 3-O-rutinoside   | [64]       |
|                      | Stem                | R1000                       | $\frac{1}{2}$ MS                 | Rutin, quercetin, chlorogenic acid, 4-hydroxybenzoic acid, caffeic acid, ferulic acid, cyanidin 3-O-glucoside, cyanidin 3-O-rutinoside, | [72]       |

Tartary buckwheat has over 26-fold higher content of rutin than common buckwheat making it more suitable for researching HRCs and their production of bioactive compounds [101]. Kim et al. [86] quantified rutin, quercetin, epicatechin, catechin hydrate, gallic acid, ferulic acid, chlorogenic acid, and caffeic acid in HRCs of Tartary buckwheat obtained from stems infected with an *A. rhizogenes* R1000 strain. The results showed that rutin and epicatechin in HRCs were 10 times and 5 times higher, respectively, compared with wild-type roots [86]. Park et al. [74] used the same *Agrobacterium* strain as Kim et al. [86] to produce HRCs from Tartary buckwheat stems and observed two morphological phenotypes emerging in their cultures. Approximately 80% of the established HRCs had well-developed primary roots and a few secondary roots, and are therefore termed as a “thick phenotype”, and the remaining 20% displayed traits characteristic of those of primary roots with a profusion of root hairs, which they named the “thin phenotype”. The “thin phenotype” had a higher number of hairy roots as well as higher growth rate than the “thick phenotype”. Park et al. [74] concluded that selecting the optimal morphological phenotype of HRCs is crucial for improved production of secondary metabolites under in vitro conditions. Attempts to optimise the growth and enhance the synthesis of phenolic compounds in HRCs with the basal medium and the addition of PGRs were made with the use of R1000 strain in Tartary buckwheat stems [81]. It was established that the optimal medium for HRC growth and phenolic compounds biosynthesis was half-strength SH (Schenk and Hildebrandt) medium. As for the PGRs, the best results were obtained with 0.5 mg/L indole-3-butyric acid (IBA), which resulted in 24% more growth than in the control [81]. In contrast to these findings, Park et al. [64] showed that

high concentration auxins, namely IBA, NAA and 2,4-D had no effect on HRC growth. However, enhanced growth of HRCs with the application of low concentration of 2,4-D followed by IAA was noted. Zhao et al. [82] reported that with the addition of yeast polysaccharide elicitor (YPS) to HRCs, rutin and quercetin content increased two times when compared with the control. Further experiments resulted in a three-fold increase on flavonols, when YPS treatment phenylpropanoid pathway stimulation was combined with the process of medium renewal. As YPSs are commercially available, this research demonstrated an enhanced way for phenolic compound synthesis in HRCs [82]. Ethephon is a PGR that releases ethylene which is subsequently absorbed by plants. It results in enhanced flowering, fruit ripening and secondary metabolite production [102]. Li et al. [72] tested the effect of ethephon on HRCs of Tartary buckwheat and noted enhancement in anthocyanin biosynthesis when supplemented with a concentration of 0.5 mg/L. This led them to conclude that the biosynthesis of anthocyanin plays a crucial part in the response of buckwheat to ethephon-induced stress [72].

Research into gene transformation in Tartary buckwheat focused on transcription factors (TFs) of the MYB family, which are common in plants [103]. Jasmonates (JAs) are plant hormones known to induce the biosynthesis of different secondary metabolites. Transcriptional repressors, jasmonate ZIM domain (JAZ) proteins interact with different TFs that have various roles in regulating JA-responsive expression of genes [104]. For example, genes which encode JAZ are the integral factor in the anthocyanin synthesis as a response to a certain type of stress [103]. Another one of the types that takes part in JA-induced biosynthesis of secondary metabolites is MYB type. R2R3-MYB TFs are known to play a substantial part in regulating the biosynthesis of secondary metabolites [105]. To examine the characteristics of MYB TFs and their derivatives in planta, Zhou et al. [83] investigated rutin accumulation in HRCs of Tartary buckwheat. A previously unknown R2R3-MYB TF FtMYB11 was isolated and classified as a subgroup 4 of R2R3-MYB TFs. It was also found that the level of FtMYB11 expression was substantially induced by Jas, which led to the conclusion that FtMYB11 is a JA-responsive TF and its activity might be regulated by JAZ repressors. Analysis of rutin biosynthesis genes in HRCs qRT-PCR revealed that FtMYB11 repressed the expression of most of the key enzyme genes, which led to the conclusion that FtMYB11 is a master regulator repressing rutin biosynthesis [106]. A subsequent study of HRCs described a clade of JA-responsive MYB repressors (FtMYB13, FtMYB14, FtMYB15, and FtMYB16) and their key involvement in repressing phenylpropanoid biosynthesis. A study that focused on FtMYB16 interactions with Ftimportin- $\alpha$ 1 (FtPinG0006805200) and subsequent regulation of rutin biosynthesis concluded that FtMYB16 act as a repressor in both root growth and rutin accumulation [107]. Moreover, Ftimportin- $\alpha$ 1 directly regulates the import of FtMYB16 to the nucleus and acts as a promoter of FtMYB16 transcriptional activity on its target genes [108].

#### 2.4. Transgenic Buckwheat Plants

Genetic plant transformation has become one of the highly promising tools in plant breeding and research [73]. It has been previously engaged in defining plants' genes functions [109]. Although an efficient protocol for *A. tumefaciens* for common buckwheat was developed by Neskovic et al. [93] who established HRCs with *A. rhizogenes*, limited research regarding the subject followed in subsequent years. Miljus-Djukic et al. [110] studied the efficiency of various strains of *A. tumefaciens* and their experiments showed that the A281 strain exhibited stronger virulence than the other strains (Ach5 and A6). The same authors genetically transformed buckwheat plants using *A. tumefaciens* A281 strain as vectors. Incubated cotyledon fragments with A281 strain harbouring pGA472 were carrying the *neomycin phosphotransferase II (nptII)* gene responsible for kanamycin resistance. Regenerated seedlings exhibited the ratio of resistant to sensitive approximately three to one [110]. To test the efficiency of different strains in planta of *A. tumefaciens* (LBA4404 and pBI121) apical meristems of young buckwheat seedlings were inoculated. The results showed the transformation efficiency of 36% and 70% with strain LBA4404 and pBI121

strain, respectively [109]. Transgenic plants of common buckwheat were also obtained from infecting hypocotyl fragments with *A. tumefaciens* LBA4404 strain harbouring vector pBI121 which contains genes of *neomycin phosphotransferase II* (*npt II*) and  $\beta$ -glucuronidase (*gus*) [56]. Moreover, these authors tested cotyledon and hypocotyl explants and, contrarily to Miljus-Djukic et al. [110], observed better efficiency of the latter for the production and recovery of regenerants [56]. These reports allowed for the improvement of protocols in buckwheat *Agrobacterium*-mediated genetic transformation.

HRCs have also been used in the attempts to improve gene transformation efficiency with the use of *A. tumefaciens* [111]. It has been shown to influence the production of certain phytohormones and subsequently enhanced proliferation and tumour formation [112]. Transformation of common buckwheat via the establishment of in vitro callus was achieved by using the *A. tumefaciens* LBA4404 strain, which contained pHZX1 binary vector. Transgenic plants that exhibited overexpression of *AtNHX1* were regenerated. *AtNHX1* is a vacuolar Na<sup>+</sup>/H<sup>+</sup> antiporter gene from *Arabidopsis thaliana*. Overexpression of *AtNHX1* showed improved salt tolerance in other species: tomato [113], *Brassica napus* [114], rice [115], perennial ryegrass [116] and wheat [117]. In regenerated transgenic common buckwheat, line growth was less inhibited by salt stress when compared to wild type, which demonstrated that overexpressing Na<sup>+</sup>/H<sup>+</sup> antiporter cDNA can have a positive effect on improved salt tolerance [118]. Deciphering metabolic pathways will in future provide molecular bases for metabolic engineering studies.

### 3. Future Perspectives

Buckwheat, due to its high content of micro- and macronutrients, as well as its health benefits and potential, was established as functional food and pharmaceutical plant. However, as the population and the environment are exposed to constant and rapid changes, combined with scientific progress, there are therefore several aspects of buckwheat research that have to be addressed. As described in this review, in vitro callus induction and plantlet regeneration of common and Tartary buckwheat is rather well researched. There are some challenges plant breeders are faced with. The main problem with common buckwheat is the short life of its single flower and a growing period which lasts from 70 to 90 days [119]. Indeterminate type of growth and flowering makes it difficult to determine harvesting time. Susceptibility of buckwheat to biotic stresses such as ground frost, low water supply, drought and photoperiod causes flowering and embryo abortions. *F. homotropicum* has been cross-pollinated with common buckwheat and Tartary buckwheat in order to transfer genes that have a greater resistance to frost and a higher seed yield. These attempts, however, have been unsuccessful due to the barriers preventing cross-pollination between different species [120]. Common buckwheat plants are dimorphic with two types of flowers—Pin with pistils longer than stamens, and Thrum with pistils shorter than stamens—resulting in self-incompatibility [19,119]. Fertilisation occurs between both flower types after cross-pollination [121]. Tartary buckwheat is a homostylous species with flowers that contain anthers and stigmas of the same height. Among the most important reasons for the low yield are: self-incompatibility; insufficient fertilisation; embryo abortion; sensitivity to heat and drought stress; and assimilation deficiency that occurs in aging plants [122].

Protoplast fusion and subsequent in vitro plant regeneration, which leads to somatic hybridisation, offers opportunities for transferring entire genomes from one plant into another regardless of the interspecific crossing barriers [123]. Somatic hybridisation has been successfully used for a number of intra- and inter-specific, intergenetic, inter-tribal and even inter-familial combinations [124,125]. The literature data about the protoplast fusion of the buckwheat species are limited. There was only one success with obtaining hybrid calli of common buckwheat (+) Tartary buckwheat achieved by Lachmann et al. [126] using polyethylene glycol (PEG)-mediated protoplast fusion. Although the authors highlighted the hybrid nature of obtained calli, the possibility of plant regeneration was not shown. Currently, the most promising and efficient technique is protoplast electrofusion by staining

the protoplasts with different fluorescent colours, enabling the hybrid cells to be selected at the beginning of the experiments.

Draft genome sequences for common and Tartary buckwheat will help in gaining understanding of genetic mechanisms and regulation of specific traits, proteomic, transcriptomic, metabolomics and epigenomic approaches. For example, Penin et al. [127] characterised 1.5 Gb genome along with the reference assembly of common buckwheat. This will lead to opportunities to determine functions that will help in the population improvement programmes as well as to examine their mechanisms. These authors used the draft genome in order to reference it with genotyping-by-sequencing (GBS) analysis and discover the location of the 5.4 Mbp S-allelic region along with candidate genes responsible for controlling buckwheat heteromorphic self-incompatibility [127].

Genome editing with the RNA-guided clustered regularly interspaced short palindromic repeats-associated protein 9 (CRISPR/Cas9) technology is emerging as a valuable tool in research on plant functional genomics [128]. It has the potential to revolutionise the modification of traits and characteristics in plants by functional gain or loss via insertion of single-guide RNA (sgRNA) into the plant genome [129]. CRISPR/Cas9 is far more efficient, simpler and gives the possibility to edit multiple target genes concurrently, compared with zinc finger nucleases (ZFNs) and transcription activator-like effector nucleases (TALENs) [130]. Developing efficient protocol for buckwheat will help to generate plant varieties with improved traits such as better resistance to biotic and abiotic stresses and improved breeding timelines. CRISPR/Cas9 gene editing technology was successfully used in *Brachypodium* [131], *Arabidopsis thaliana*, sorghum [132], rice [133], barley [134], wheat [135] and corn [136], but not in *Fagopyrum* species. The CRISPR/Cas9 system can also be used in targeting microRNAs (miRNA) in order to gain insight into miRNA regulatory pathways. This has been performed in soybean [137] and in rice [138]. *Agrobacterium*-mediated genetic transformation, particle bombardment and PEG-transformation and protoplast fusion allowed us to obtain genome-modified lettuce [73], *Arabidopsis*, tobacco [139] and rice [140], apple [141], petunia [142]; however, no regenerants were obtained. The approach to standardize factors affecting genetic transformation in buckwheat by particle bombardment or via any of the direct-DNA delivery methods will help to excel the scarce research which mainly focused on optimising the method protocols.

To summarise, understanding the morphological, physiological and molecular parameters that affect the development of buckwheat plants will be relevant for revealing the complex mechanisms. This in turn will have an impact on successfully modulating yield productivity and stability for future buckwheat breeding programmes.

**Author Contributions:** Conceptualisation—A.T., A.B.; preparing the original draft—A.T.; reviewing and editing—A.B., M.Z.; supervising—A.B.; acquiring funding—A.B. All authors have read and agreed to the published version of the manuscript.

**Funding:** This research was funded by the National Science Centre Poland (grant number 2020/37/B/NZ9/01499) and grants from the National Natural Science Foundation of China (31871536).

**Institutional Review Board Statement:** Not Applicable.

**Informed Consent Statement:** Not Applicable.

**Data Availability Statement:** Not Applicable.

**Acknowledgments:** We thank Agnieszka Braszewska (University of Silesia, Katowice) for valuable comments on the manuscript, and Aaron Mills for editing.

**Conflicts of Interest:** The authors declare no conflict of interest.

## References

1. Hussain, A.; Qarshi, I.A.; Nazir, H.; Ullah, I. Plant Tissue Culture: Current Status and Opportunities, Recent Advances in Plant in vitro Culture. In *Recent Advances in Plant In Vitro Culture*; Leva, A., Rinaldi, L.M.R., Eds.; IntechOpen: Rijeka, Croatia, 2012.
2. Luthar, Z.; Fabjan, P.; Mlinarić, K. Biotechnological methods for buckwheat breeding. *Plants* **2021**, *10*, 1547. [CrossRef] [PubMed]
3. Kumar, P.P.; Loh, C.S. Plant tissue culture for biotechnology. In *Plant Biotechnology and Agriculture*; Academic Press: Cambridge, MA, USA, 2012; pp. 131–138.
4. Abobkar, I.M.; Ahmed, M. Plant tissue culture media. In *Recent Advances in Plant In Vitro Culture*; IntechOpen: Rijeka, Croatia, 2012.
5. Majid, A.; Kaloo, Z.A.; Padder, B.M.; Munshi, A.H. An efficient in vitro regeneration protocol for an endangered medicinally important herb *Fagopyrum dibotrys* growing in Kashmir Himalaya. *CIBTech. J. Biotechnol.* **2015**, *4*, 12–15.
6. Verdeil, J.L.; Alemanno, L.; Niemenak, N.; Tranbarger, T.J. Pluripotent versus totipotent plant stem cells: Dependence versus autonomy? *Trends Plant Sci.* **2007**, *12*, 245–252. [CrossRef] [PubMed]
7. Condic, M.L. Totipotency: What it is and what it is not. *Stem Cells Dev.* **2014**, *23*, 796–812. [CrossRef]
8. Fehér, A. Callus, dedifferentiation, totipotency, somatic embryogenesis: What these terms mean in the era of molecular plant biology? *Front. Plant Sci.* **2019**, *10*, 536. [CrossRef]
9. Guzzo, F.; Baldan, B.; Mariani, P.; Lo Schiavo, F.; Terzi, M. Studies on the origin of totipotent cells in explants of *Daucus carota* L. *J. Exp. Bot.* **1994**, *45*, 1427–1432. [CrossRef]
10. Sinkovič, L.; Kokalj, D.; Vidrih, R.; Meglič, V. Milling fractions fatty acid composition of common (*Fagopyrum esculentum* Moench) and tartary (*Fagopyrum tataricum* (L.) Gaertn) buckwheat. *J. Stored Prod. Res.* **2020**, *85*, 101551. [CrossRef]
11. Gonçalves, F.M.F.; Debiage, R.R.; Gonçalves da Silva, R.M.; Porto, P.P.; Yoshihara, E.; de Mello Peixoto, E.C.T. *Fagopyrum esculentum* Moench: A crop with many purposes in agriculture and human nutrition. *Afr. J. Agric. Res.* **2016**, *11*, 983–989.
12. Rose, R.J.; Mantiri, F.R.; Kurdyukov, S.; Chen, S.; Wang, X.; Nolan, K.E. Developmental biology of somatic embryogenesis. In *Plant Developmental Biology—Biotechnological Perspectives*; Pua, E., Davey, M., Eds.; Springer: Berlin/Heidelberg, Germany, 2010; Volume 2.
13. Yamane, Y. Induced differentiation of buckwheat plants from subcultured calluses in vitro. *Jpn. J. Genet.* **1974**, *49*, 139–146. [CrossRef]
14. Takahata, Y.; Jumonji, E. Plant regeneration from hypocotyl section and callus in buckwheat (*Fagopyrum esculentum* Moench.). *Ann. Rep. Fac. Educ.* **1985**, *45*, 137–142.
15. Srejovic, V.; Neskovic, M. Regeneration of plants from cotyledon fragments of buckwheat (*Fagopyrum esculentum* Moench.). *Z. Pflanzenphysiol.* **1981**, *104*, 37–42. [CrossRef]
16. Rajbhandari, B.P.; Dhaubhadel, S.; Gautam, D.M.; Gautam, B.R. Plant regeneration via calli of leaf and stem explants in common buckwheat ecotypes. In *Current Advances in Buckwheat Research*; Shinshu University Press: Nagano, Japan, 1995; pp. 191–196.
17. Takahata, Y. Plant regeneration from cultured immature inflorescence of common buckwheat (*Fagopyrum esculentum* MOENCH) and perennial buckwheat (*F. cymosum* meisn.). *Jpn. J. Breed.* **1988**, *38*, 409–413. [CrossRef]
18. Yui, M.; Yoshida, T. Callus induction and plant regeneration in anther culture of Japanese buckwheat cultivars (*Fagopyrum esculentum* Moench). *Fagopyrum* **2001**, *18*, 27–35.
19. Adachi, T.; Yamaguchi, A.; Miike, Y.; Hoffmann, F. Plant regeneration from protoplasts of common buckwheat (*Fagopyrum esculentum*). *Plant Cell Rep.* **1989**, *8*, 247–250. [CrossRef] [PubMed]
20. Lachmann, S.; Adachi, T. Callus regeneration from hypocotyl protoplasts of tartary buckwheat (*Fagopyrum tataricum* Gaertn.). *Fagopyrum* **1990**, *10*, 62–64.
21. Betekhtin, A.; Rojek, M.; Jaskowiak, J.; Milewska-Hendel, A.; Kwasniewska, J.; Kostyukova, Y.; Kurczynska, E.; Rummyantseva, N.; Hasterok, R. Nuclear genome stability in long-term cultivated callus lines of *Fagopyrum tataricum* (L.) Gaertn. *PLoS ONE* **2017**, *12*, e0173537. [CrossRef] [PubMed]
22. Perez-Garcia, P.; Moreno-Risueno, M.A. Stem cells and plant regeneration. *Dev. Biol.* **2018**, *442*, 3–12. [CrossRef]
23. Ahmed, A.; Khalid, N.; Ahmad, A.; Abbasi, N.A.; Latif, M.S.Z.; Randhawa, M.A. Phytochemicals and biofunctional properties of buckwheat: A review. *J. Agric. Sci.* **2013**, *152*, 349–369. [CrossRef]
24. Kwon, S.J.; Roy, S.K.; Choi, J.; Park, J.; Cho, S.; Sarker, K. Recent research updates on functional components in buckwheat. *J. Agric. Sci.* **2018**, *34*, 1–8.
25. Ji, X.; Han, L.; Liu, F.; Yin, S.; Peng, Q.; Wang, M. A mini-review of isolation, chemical properties and bioactivities of polysaccharides from buckwheat (*Fagopyrum* Mill). *Int. J. Biol. Macromol.* **2019**, *127*, 204–209. [CrossRef]
26. FAO. Crops and Livestock Products FAOSTAT Statistical Database. Available online: <https://www.fao.org/faostat/en/#data/QCL> (accessed on 5 January 2022).
27. Huda, M.N.; Lu, S.; Jahan, T.; Ding, M.; Jha, R.; Zhang, K.; Zhang, W.; Georgiev, M.I.; Park, S.U.; Zhou, M. Treasure from garden: Bioactive compounds of buckwheat. *Food Chem.* **2021**, *335*, 127653. [CrossRef] [PubMed]
28. Zhang, K.; He, M.; Fan, Y.; Zhao, H.; Gao, B.; Yang, K.; Li, F.; Tang, Y.; Gao, Q.; Lin, T.; et al. Resequencing of global Tartary buckwheat accessions reveals multiple domestication events and key loci associated with agronomic traits. *Genome Biol.* **2021**, *22*, 23. [CrossRef] [PubMed]
29. Bonafaccia, G.; Marocchini, M.; Kreft, I. Composition and technological properties of the flour and bran from common and tartary buckwheat. *Food Chem.* **2003**, *80*, 9–15. [CrossRef]
30. Giupponi, L.; Borgonovo, G.; Panseri, S.; Giorgi, A. Multidisciplinary study of a little known landrace of *Fagopyrum tataricum* Gaertn. of Valtellina (Italian Alps). *Genet. Resour. Crop Evol.* **2019**, *66*, 783–796. [CrossRef]

31. Fabjan, N.; Rode, J.; Kosir, I.J.; Wang, Z.; Zhang, Z.; Kreft, I. Tartary buckwheat (*Fagopyrum tataricum* Gaertn.) as a source of dietary rutin and quercitrin. *J. Agric. Food Chem.* **2003**, *51*, 6452–6455. [[CrossRef](#)]
32. Skrabanja, V.; Liljeberg Elmstahl, H.G.; Kreft, I.; Björck, I.M. Nutritional properties of starch in buckwheat products: Studies in vitro and in vivo. *J. Agric. Food Chem.* **2001**, *49*, 490–496. [[CrossRef](#)]
33. Gumerova, E.; Gatina, E.; Chuenkova, S.; Rummyantseva, N. Somatic embryogenesis in common buckwheat *Fagopyrum esculentum* Moench. In Proceedings of the 8th International Symposium on Buckwheat, Chunchon, Korea, 30 August–2 September 2001; pp. 377–381.
34. Rummyantseva, N.; Sergejewa, N.; Khakimova, L.E.; Salnikov, V.V.; Gumerova, E.A. Organogenesis and somatic embryogenesis in tissue culture of two buckwheat species. *Russ. J. Plant Physiol.* **1989**, *36*, 189–194.
35. Rummyantseva, N.I.; Sal'nikov, V.V.; Lebedeva, V.V. Structural changes of cell surface in callus of *Fagopyrum esculentum* Moench. during induction of morphogenesis. *Russ. J. Plant Physiol.* **2005**, *52*, 381–387. [[CrossRef](#)]
36. Ikeuchi, M.; Ogawa, Y.; Iwase, A.; Sugimoto, K. Plant regeneration: Cellular origins and molecular mechanisms. *Development* **2016**, *143*, 1442–1451. [[CrossRef](#)]
37. Dong, Q.; Zhao, H.; Zhao, X.; Lv, B.; Li, Q.; Wang, X.; Li, C.; Chen, H.; Wu, Q. Callus induction of tartary buckwheat and enhancement of its flavonoids via *FtCHS1* overexpression. *PeerJ Prepr.* **2019**, *7*, e27862v1.
38. Hao, J.; Pei, Y.; Qu, Y.; Zheng, C. Study on callus differentiation conditions of common buckwheat. In Proceedings of the 7th International Symposium on Buckwheat, Winnipeg, MB, Canada, 12–14 August 1998; pp. 33–37.
39. Park, C.; Lee, S.; Chung, C.; Shin, Y.; Kim, N.; Kim, Y.; Yoon, K.; Choi, Y. Somatic embryogenesis and plant regeneration from leaf and stem explants of buckwheat. *Fagopyrum* **1999**, *16*, 53–56.
40. Woo, S.H.; Nair, A.; Adachi, T. Plant regeneration from cotyledon tissues of common buckwheat (*Fagopyrum esculentum* Moench). *Vitr. Cell. Dev. Biol.—Plant* **2000**, *36*, 358–361. [[CrossRef](#)]
41. Woo, S.H.; Takaoka, M.; Kim, H.S.; Park, C.H.; Adachi, T.; Jong, S.K. Plant regeneration via shoot organogenesis from leaf callus culture of common buckwheat (*Fagopyrum esculentum* Moench.). In Proceedings of the 9th International Symposium on Buckwheat, Prague, Czech Republic, 18–22 August 2004; pp. 61–65.
42. Kwon, S.-J.; Han, M.-H.; Huh, Y.-S.; Roy, S.K.; Lee, C.-W.; Woo, S.H. Plantlet regeneration via somatic embryogenesis from hypocotyls of common buckwheat (*Fagopyrum esculentum* Moench.). *Korean J. Crop Sci.* **2013**, *58*, 331–335. [[CrossRef](#)]
43. Jin, H.; Jia, J.F.; Hao, J.G. Efficient plant regeneration in vitro in buckwheat. *Plant Cell Tissue Organ Cult.* **2002**, *69*, 293–295. [[CrossRef](#)]
44. Bohanec, B.; Nešković, M.; Vujčić, R. Anther culture and androgenetic plant regeneration in buckwheat (*Fagopyrum esculentum* Moench). *Plant Cell Tissue Organ Cult.* **1993**, *35*, 259–266. [[CrossRef](#)]
45. Wang, C.; Dong, X.; Ding, M.; Tang, Y.; Zhu, X.; Wu, Y.; Zhou, M.; Shao, J. Plantlet regeneration of Tartary buckwheat (*Fagopyrum tataricum* Gaertn.) in vitro tissue cultures. *Protein Peptide Lett.* **2016**, *23*, 468–477. [[CrossRef](#)]
46. Han, M.; Kamal, A.; Huh, Y.; Jeon, A.Y.; Bae, J.; Chung, K.Y.; Lee, M.S.; Park, S.U.; Jeong, H.; Woo, S.H. Regeneration of plantlet via somatic embryogenesis from hypocotyls of Tartary Buckwheat (*Fagopyrum tataricum*). *Aust. J. Crop Sci.* **2011**, *5*, 865–869.
47. Gumerova, E.A.; Galeeva, E.I.; Chuyenkova, S.A.; Rummyantseva, N.I. Somatic embryogenesis and bud formation on cultured *Fagopyrum esculentum* hypocotyls. *Russ. J. Plant Physiol.* **2003**, *50*, 640–645. [[CrossRef](#)]
48. Saraswat, R.; Kumar, M. Plant regeneration in buckwheat (*Fagopyrum esculentum* Moench.) via somatic embryogenesis and induction of meristemoids in abnormal embryos. *Plant Tissue Cult. Biotechnol.* **2019**, *29*, 33–47. [[CrossRef](#)]
49. Valieva, A.; Mukhitov, A.; Rummyantseva, N.I. Patterns of proteins and its glycosylated forms in buckwheat calli with different morphogenic ability. In Proceedings of the 8th International Symposium of Buckwheat, Chunchon, Korea, 30 August–2 September 2001; pp. 50–56.
50. Rummyantseva, N.I.; Samaj, J.; Ensikat, H.J.; Sal'nikov, V.V.; Kostyukova, Y.A.; Baluska, F. Changes in the extracellular matrix surface network during cyclic reproduction of proembryonic cell complexes in the *Fagopyrum tataricum* (L.) Gaertn callus. *Dokl. Biol. Sci.* **2003**, *391*, 375–378. [[CrossRef](#)]
51. Rummyantseva, N.I.; Akulov, A.N.; Mukhitov, A.R. Extracellular polymers in callus cultures of *Fagopyrum tataricum* (L.) Gaertn. with different morphogenic activities: Time courses during the culture cycle. *Prikl. Biokhim. Mikrobiol.* **2004**, *40*, 571–578. [[CrossRef](#)]
52. Ikeuchi, M.; Sugimoto, K.; Iwase, A. Plant callus: Mechanisms of induction and repression. *Plant Cell* **2013**, *25*, 3159–3173. [[CrossRef](#)] [[PubMed](#)]
53. Akulov, A.N.; Gumerova, E.A.; Rummyantseva, N.I. Cell cultures of *Fagopyrum tataricum* as a source of biologically active phenolic compounds. In *Buckwheat Germplasm in the World*; Academic Press: Cambridge, MA, USA, 2018; pp. 259–270.
54. Fei, Y.; Wang, L.-X.; Fang, Z.-W.; Liu, Z.-X. Somatic embryogenesis and plant regeneration from cotyledon and hypocotyl explants of *Fagopyrum esculentum* Moench lpls mutant. *Agronomy* **2019**, *9*, 768. [[CrossRef](#)]
55. Hou, S.; Sun, Z.; Linghu, B.; Wang, Y.; Huang, K.; Xu, D.; Han, Y. Regeneration of buckwheat plantlets from hypocotyl and the influence of exogenous hormones on rutin content and rutin biosynthetic gene expression in vitro. *Plant Cell Tissue Organ Cult.* **2014**, *120*, 1159–1167. [[CrossRef](#)]
56. Kim, S.H.; Kang, H.J.; Lee, Y.T.; Lee, S.Y.; Ko, J.A.; Rha, E.S. Direct regeneration of transgenic buckwheat from hypocotyl segments by *Agrobacterium*-mediated transformation. *Korean J. Crop Sci.* **2001**, *46*, 375–379.
57. Klčova, L.; Gubisova, M. Evaluation of different approaches to buckwheat (*Fagopyrum esculentum* Moench.) micropropagation. *Czech J. Genet. Plant Breed.* **2008**, *44*, 66–72. [[CrossRef](#)]



58. Nešković, M.; Vujičić, R.; Budimir, S. Somatic embryogenesis and bud formation from immature embryos of buckwheat (*Fagopyrum esculentum* Moench.). *Plant Cell Rep.* **1987**, *6*, 423–426.
59. Adachi, T.; Suputtitada, S.; Miike, Y. Plant regeneration from anther cultures in common buckwheat (*Fagopyrum esculentum*). *Fagopyrum* **1988**, *8*, 5–9.
60. Slawinska, J.; Kantartzi, S.K.; Obendorf, R.L. In vitro organogenesis of *Fagopyrum esculentum* Moench (Polygonaceae) as a method to study seed set in buckwheat. *J. Plant Sci. Biotechnol.* **2009**, *3*, 75–78.
61. Luthar, Z.; Marchetti, S. Plant regeneration from mature cotyledons in a buckwheat (*Fagopyrum esculentum* Moench) germplasm collection. *Fagopyrum* **1994**, *14*, 65–69.
62. Park, S.; Park, C. Multiple shoot organogenesis and plant regeneration from cotyledons of buckwheat (*Fagopyrum esculentum* Moench). In Proceedings of the 8th International Symposium on Buckwheat, Chunchon, Korea, 30 August–2 September 2001; pp. 427–430.
63. Berbec, A.; Doroszewska, T. Regeneration in vitro of three cultivars of buckwheat (*Fagopyrum esculentum* Moench.) as affected by medium composition. *Fagopyrum* **1999**, *16*, 49–52.
64. Park, C.H.; AyeThwe, A.; Kim, S.J.; Park, J.S.; Arasu, M.; Al-Dhabi, N.; Park, N.A.; Park, S.U. Effect of auxins on anthocyanin accumulation in hairy root cultures of Tartary buckwheat cultivar Hokkai T10. *Nat. Prod. Commun.* **2016**, *11*, 1283–1286. [[CrossRef](#)] [[PubMed](#)]
65. Trolinder, N.L.; Goodin, J.R. Somatic embryogenesis and plant regeneration in cotton (*Gossypium hirsutum* L.). *Plant Cell Rep.* **1987**, *6*, 231–234. [[CrossRef](#)] [[PubMed](#)]
66. Bohanec, B. Improvements in buckwheat (*Fagopyrum esculentum* Moench) micropropagation procedures. *Fagopyrum* **1987**, *7*, 13–15.
67. Kachonpadungkitti, Y.; Romchatngoen, S.; Hasegawa, K.; Hisajima, S. Efficient flower induction from cultured buckwheat (*Fagopyrum esculentum* L.) node segments in vitro. *Plant Growth Regul.* **2001**, *35*, 37–45. [[CrossRef](#)]
68. Lee, Y.K.; Kim, K.Y.; Uddin, M.R.; Park, N.I.; Park, S.U. An efficient protocol for shoot organogenesis and plant regeneration of buckwheat (*Fagopyrum esculentum* Moench.). *Roman. Biotechnol. Lett.* **2009**, *14*, 4524–4529.
69. Chen, C.; Lan, J.; Xie, S.; Cui, S.; Li, A. In vitro propagation and quality evaluation of long-term micro-propagated and conventionally grown *Fagopyrum dibotrys* Hara mutant, an important medicinal plant. *J. Med. Plants Res.* **2012**, *6*, 3003–3012.
70. Gabr, A.; Sytar, O.; Abdelrahman, A.; Smetanska, I. Production of phenolic acids and antioxidant activity in hairy root cultures of different explant sources of common buckwheat (*Fagopyrum esculentum* M). *Aust. J. Basic Appl. Sci.* **2012**, *6*, 577–586.
71. Gabr, A.M.M.; Sytar, O.; Ghareeb, H.; Brestic, M. Accumulation of amino acids and flavonoids in hairy root cultures of common buckwheat (*Fagopyrum esculentum*). *Physiol. Mol. Biol. Plants* **2019**, *25*, 787–797. [[CrossRef](#)]
72. Li, X.; Thwe, A.A.; Park, C.H.; Kim, S.J.; Arasu, M.V.; Al-Dhabi, N.A.; Lee, S.Y.; Park, S.U. Ethephon-induced phenylpropanoid accumulation and related gene expression in tartary buckwheat (*Fagopyrum tataricum* (L.) Gaertn.) hairy root. *Biotechnol. Biotechnol. Equip.* **2017**, *31*, 304–311. [[CrossRef](#)]
73. Matvieieva, N.A. Agrobacterium-mediated transformation of compositae plants. I. Construction of transgenic plants and «hairy» roots with new properties. *Biotechnol. Acta* **2015**, *8*, 19–31. [[CrossRef](#)]
74. Park, N.; Xiaohua, L.; Uddin, R.; Park, S. Phenolic compound production by different morphological phenotypes in hairy root cultures of *Fagopyrum tataricum* Gaertn. *Arch. Biol. Sci.* **2011**, *63*, 193–198. [[CrossRef](#)]
75. Park, N.I.; Li, X.; Thwe, A.A.; Lee, S.Y.; Kim, S.G.; Wu, Q.; Park, S.U. Enhancement of rutin in *Fagopyrum esculentum* hairy root cultures by the Arabidopsis transcription factor AtMYB12. *Biotechnol. Lett.* **2012**, *34*, 577–583. [[CrossRef](#)] [[PubMed](#)]
76. Putalun, W.; Yusakul, G.; Patanasethanont, D. Dicentrine production from a hairy roots culture of *Stephania suberosa*. *Z. Naturforsch. C J. Biosci.* **2009**, *64*, 692–696. [[CrossRef](#)] [[PubMed](#)]
77. Ron, M.; Kajala, K.; Pauluzzi, G.; Wang, D.; Reynoso, M.A.; Zumstein, K.; Garcha, J.; Winte, S.; Masson, H.; Inagaki, S.; et al. Hairy root transformation using *Agrobacterium rhizogenes* as a tool for exploring cell type-specific gene expression and function using tomato as a model. *Plant Physiol.* **2014**, *166*, 455–469. [[CrossRef](#)] [[PubMed](#)]
78. Arafa, N.M.; Gabr, A.M.M.; Ibrahim, N.M.; Shevchenko, Y.; Smetanska, I. Study the effect of hairy root transformation on rapid growth (growth morphology) of *Nepeta cataria* in vitro cultures. *J. Innov. Pharm. Biol. Sci.* **2015**, *2*, 439–450.
79. Thwe, A.; Kim, J.K.; Li, X.; Bok Kim, Y.; Romij, U.; Kim, S.J.; Suzuki, T.; Park, N.; Park, S.U. Metabolomic analysis and phenylpropanoid biosynthesis in hairy root culture of Tartary buckwheat cultivars. *PLoS ONE* **2013**, *8*, e65349. [[CrossRef](#)]
80. Thwe, A.; Valan Arasu, M.; Li, X.; Park, C.H.; Kim, S.J.; Al-Dhabi, N.A.; Park, S.U. Effect of different *Agrobacterium rhizogenes* strains on hairy root induction and phenylpropanoid biosynthesis in Tartary buckwheat (*Fagopyrum tataricum* Gaertn). *Front. Microbiol.* **2016**, *7*, 318. [[CrossRef](#)]
81. Uddin, M.R.; Li, X.; Won, O.J.; Park, S.U.; Pyon, J.Y. Herbicidal activity of phenolic compounds from hairy root cultures of *Fagopyrum tataricum*. *Weed Res.* **2012**, *52*, 25–33. [[CrossRef](#)]
82. Zhao, J.L.; Zou, L.; Zhang, C.Q.; Li, Y.Y.; Peng, L.X.; Xiang, D.B.; Zhao, G. Efficient production of flavonoids in *Fagopyrum tataricum* hairy root cultures with yeast polysaccharide elicitation and medium renewal process. *Pharmacogn. Mag.* **2014**, *10*, 234–240. [[CrossRef](#)]
83. Zhou, M.; Sun, Z.; Ding, M.; Logacheva, M.D.; Kreft, I.; Wang, D.; Yan, M.; Shao, J.; Tang, Y.; Wu, Y.; et al. FtSAD2 and FtJAZ1 regulate activity of the FtMYB11 transcription repressor of the phenylpropanoid pathway in *Fagopyrum tataricum*. *New Phytol.* **2017**, *216*, 814–828. [[CrossRef](#)] [[PubMed](#)]
84. Gelvin, S.B. Agrobacterium in the genomics age. *Plant Phys.* **2009**, *150*, 1665–1676. [[CrossRef](#)] [[PubMed](#)]

85. Bathia, S.; Bera, T. Classical and nonclassical techniques for secondary metabolite production in plant cell culture. In *Modern Applications of Plant Biotechnology in Pharmaceutical Sciences*; Elsevier: London, UK, 2015.
86. Kim, Y.K.; Li, X.; Xu, H.; Park, N.I.; Uddin, M.R.; Pyon, J.Y.; Park, S.U. Production of phenolic compounds in hairy root culture of tartary buckwheat (*Fagopyrum tataricum* Gaertn.). *J. Crop Sci. Biotechnol.* **2009**, *12*, 53–57. [[CrossRef](#)]
87. Luczkiewicz, M.; Kokotkiewicz, A. *Genista tinctoria* hairy root cultures for selective production of isoliquiritigenin. *Z. Nat. C* **2005**, *60*, 687–875. [[CrossRef](#)]
88. Giri, A.; Ravindra, S.T.; Dhingra, V.; Narasu, M.L. Influence of different strains of *Agrobacterium rhizogenes* on induction of hairy roots and artemisinin production in *Artemisia annua*. *Curr. Sci.* **2001**, *81*, 378–382.
89. Putalun, W.; Prasarnsiwamai, P.; Tanaka, H.; Shoyama, Y. Solasodine glycoside production by hairy root cultures of *Physalis minima*. *Biotechnol. Lett.* **2004**, *26*, 545–548. [[CrossRef](#)]
90. Moumou, Y.; Trotin, F. Influence of culture conditions on polyphenol production by *Fagopyrum esculentum* tissue culture. *J. Nat. Prod.* **1992**, *55*, 33–38. [[CrossRef](#)]
91. Moumou, Y.; Vasseur, J.; Trotin, F.; Dubois, J. Catechin production by callus cultures of *Fagopyrum esculentum*. *Phytochemistry* **1992**, *31*, 1239–1241. [[CrossRef](#)]
92. Moumou, Y.; Trotin, F.; Vasseur, J.; Vermeersch, G.; Guyon, R.; Dubois, J.; Pinkas, M. Procyanidin production by *Fagopyrum esculentum* callus cultures. *Planta Med.* **1992**, *58*, 516–519. [[CrossRef](#)]
93. Neskovic, M.; Vinterhalter, B.; Miljus-Djukic, J.; Ninkovic, S.; Vinterhalter, D.; Jovanovic, V.; Knezevic, J. Susceptibility of buckwheat (*Fagopyrum esculentum* Moench.) to *Agrobacterium tumefaciens* and *A. rhizogenes*. *Fagopyrum* **1990**, *10*, 57–61.
94. Trotin, F.; Moumou, Y.; Vasseur, J. Flavanol production by *Fagopyrum esculentum* hairy root and normal root cultures. *Phytochemistry* **1993**, *32*, 929–931. [[CrossRef](#)]
95. Tanaka, N.; Yoshimatsu, K.; Shimomura, K.; Ishimaru, K. Rutin and other polyphenols in *Fagopyrum esculentum* hairy root. *Nat. Med.* **1996**, *50*, 269–272.
96. Lee, S.Y.; Cho, S.I.; Park, M.H.; Kim, Y.K.; Choi, J.E.; Park, S.U. Growth and rutin production in hairy root cultures of buckwheat (*Fagopyrum esculentum* M.). *Prep. Biochem. Biotechnol.* **2007**, *37*, 239–246. [[CrossRef](#)] [[PubMed](#)]
97. Kim, Y.K.; Xu, H.; Park, W.T.; Park, N.I.; Lee, S.Y.; Park, S.U. Genetic transformation of buckwheat (*Fagopyrum esculentum* M.) with *Agrobacterium rhizogenes* and production of rutin in transformed root cultures. *Aust. J. Crop Sci.* **2010**, *4*, 485–490.
98. Du, H.; Zhang, L.; Liu, L.; Tang, X.-F.; Yang, W.-J.; Wu, Y.-M.; Huang, Y.-B.; Tang, Y.-X. Biochemical and molecular characterization of plant MYB transcription factor family. *Biochemistry* **2009**, *74*, 1–11. [[CrossRef](#)] [[PubMed](#)]
99. Mehrrens, F.; Kranz, H.; Bednarek, P.; Weisshaar, B. The arabidopsis transcription factor MYB12 is a flavanol-specific regulator of phenylpropanoid biosynthesis. *Plant Physiol.* **2005**, *138*, 1083–1096. [[CrossRef](#)] [[PubMed](#)]
100. Zhou, M.; Wang, C.; Qi, L.; Yang, X.; Sun, Z.; Tang, Y.; Tang, Y.; Shao, J.; Wu, Y. Ectopic Expression of *Fagopyrum tataricum* FtMYB12 Improves Cold Tolerance in *Arabidopsis thaliana*. *J. Plant Growth Regul.* **2015**, *34*, 362–371. [[CrossRef](#)]
101. Podolska, G.; Gujska, E.; Klepacka, J.; Aleksandrowicz, E. Bioactive compounds in different buckwheat species. *Plants* **2021**, *10*, 961. [[CrossRef](#)]
102. Sun, Z.Y.; Zhang, T.J.; Su, J.Q.; Chow, W.S.; Liu, J.Q.; Chen, L.L.; Li, W.H.; Peng, S.L.; Peng, C.L. A novel role of ethephon in controlling the noxious weed *Ipomoea cairica* (Linn.) Sweet. *Sci. Rep.* **2015**, *5*, 11372. [[CrossRef](#)]
103. Luo, X.P.; Li, S.-J.; Yao, P.-F.; Li, C.-L.; Chen, H.; Wu, Q.; Zhao, H.-X. The jasmonate-ZIM domain protein FtJAZ2 interacts with the R2R3-MYB transcription factor FtMYB3 to affect anthocyanin biosynthesis in Tartary buckwheat. *Turk. J. Biol.* **2017**, *41*, 526–534. [[CrossRef](#)]
104. Dubos, C.; Stracke, R.; Grotewold, E.; Weisshaar, B.; Martin, C.; Lepiniec, L. MYB transcription factors in Arabidopsis. *Trends Plant Sci.* **2010**, *15*, 573–581. [[CrossRef](#)] [[PubMed](#)]
105. Zhou, M.; Memelink, J. Jasmonate-responsive transcription factors regulating plant secondary metabolism. *Biotechnol. Adv.* **2016**, *34*, 441–449. [[CrossRef](#)] [[PubMed](#)]
106. Zhang, K.; Logacheva, M.D.; Meng, Y.; Hu, J.; Wan, D.; Li, L.; Janovska, D.; Wang, Z.; Georgiev, M.I.; Yu, Z.; et al. Jasmonate-responsive MYB factors spatially repress rutin biosynthesis in *Fagopyrum tataricum*. *J. Exp. Bot.* **2018**, *69*, 1955–1966. [[CrossRef](#)]
107. Li, J.; Zhang, K.; Meng, Y.; Li, Q.; Ding, M.; Zhou, M. FtMYB16 interacts with Ftimportin- $\alpha$ 1 to regulate rutin biosynthesis in tartary buckwheat. *Plant Biotechnol. J.* **2019**, *17*, 1479–1481. [[CrossRef](#)]
108. Tyagi, R.K.; Agrawal, A.; Mahalakshmi, C.; Hussain, Z.; Tyagi, H. Low-cost media for in vitro conservation of turmeric (*Curcuma longa* L.) and genetic stability assessment using RAPD markers. *Vitr. Cell. Dev. Biol. Plant* **2007**, *43*, 51–58. [[CrossRef](#)]
109. Kojima, M.; Arai, Y.; Iwase, N.; Shirotori, K. Development of a simple and efficient method for transformation of buckwheat plants (*Fagopyrum esculentum*) using *Agrobacterium tumefaciens*. *Biosci. Biotechnol. Biochem.* **2000**, *64*, 845–847. [[CrossRef](#)]
110. Miljus-Djukic, J.; Neskovic, M.; Ninkovic, S.; Cekvenjakov, R. *Agrobacterium*-mediated transformation and plant regeneration of buckwheat (*Fagopyrum esculentum* Moench.). *Plant Cell Tissue Organ Cult.* **1992**, *29*, 101–108. [[CrossRef](#)]
111. Gohlke, J.; Deeken, R. Plant responses to *Agrobacterium tumefaciens* and crown gall development. *Front. Plant Sci.* **2014**, *5*, 155. [[CrossRef](#)] [[PubMed](#)]
112. Staskiewicz, B.; Ausubel, F.M.; Baker, B.J.; Ellis, J.G.; Jones, J.D.G. Molecular genetics of plant disease resistance. *Science* **1995**, *268*, 661–667. [[CrossRef](#)] [[PubMed](#)]
113. Zhang, H.X.; Blumwald, E. Transgenic salt-tolerant tomato plants accumulate salt in foliage but not in fruit. *Nat. Biotechnol.* **2001**, *19*, 765–768. [[CrossRef](#)]

114. Zhang, H.X.; Hodson, J.N.; Williams, J.P.; Blumwald, E. Engineering salt-tolerant *Brassica* plants: Characterization of yield and seed oil quality in transgenic plants with increased vacuolar sodium accumulation. *Proc. Natl. Acad. Sci. USA* **2001**, *98*, 12832–12836. [[CrossRef](#)] [[PubMed](#)]
115. Ohta, M.; Hayashi, Y.; Nakashima, A.; Hamada, A.; Tanaka, A.; Nakamura, T.; Hayakawa, T. Introduction of a Na<sup>+</sup>/H<sup>+</sup> antiporter gene from *Atriplex gmelini* confers salt tolerance to rice. *FEBS Lett.* **2002**, *532*, 279–282. [[CrossRef](#)]
116. Wu, Y.-Y.; Chen, Q.; Chen, M.; Chen, J.; Wang, X.-C. Salt-tolerant transgenic perennial ryegrass (*Lolium perenne* L.) obtained by *Agrobacterium tumefaciens*-mediated transformation of the vacuolar Na<sup>+</sup>/H<sup>+</sup> antiporter gene. *Plant Sci.* **2005**, *169*, 65–73. [[CrossRef](#)]
117. Xue, Z.-Y.; Zhi, D.-Y.; Xue, G.-P.; Zhang, H.; Zhao, Y.-X.; Xia, G.-M. Enhanced salt tolerance of transgenic wheat (*Triticum aestivum* L.) expressing a vacuolar Na<sup>+</sup>/H<sup>+</sup> antiporter gene with improved grain yields in saline soils in the field and a reduced level of leaf Na<sup>+</sup>. *Plant Sci.* **2004**, *167*, 849–859. [[CrossRef](#)]
118. Chen, L.H.; Zhang, B.; Xu, Z.Q. Salt tolerance conferred by overexpression of Arabidopsis vacuolar Na<sup>(+)</sup>/H<sup>(+)</sup> antiporter gene *AtNHX1* in common buckwheat (*Fagopyrum esculentum*). *Transgenic Res.* **2008**, *17*, 121–132. [[CrossRef](#)]
119. Cawoy, V.; Ledent, J.F.; Kinet, J.-M.; Jacquemart, A.L. Floral biology of common buckwheat (*Fagopyrum esculentum* Moench). *Eur. J. Plant Sci. Biotechnol.* **2009**, *3*, 1–9.
120. Woo, S.H.; Ohmoto, T.; Campbell, C.; Adachi, T.; Jong, S.K. Pre- and post-fertilization to backcrossing in interspecific hybridization between *Fagopyrum esculentum* and *F. homotropicum* with *F. esculentum*. In Proceedings of the 8th International Symposium on Buckwheat, Chunchon, Korea, 30 August–2 September 2001; pp. 450–455.
121. Cawoy, V.; Deblauwe, V.; Halbrech, B.; Ledent, J.F.; Kinet, J.M.; Jacquemart, A.L. Morph differences and honeybee morph preference in the distylous species *Fagopyrum esculentum* Moench. *Int. J. Plant Sci.* **2006**, *167*, 853–861. [[CrossRef](#)]
122. Taylor, D.P.; Obendorf, R.L. Quantitative assessment of some factors limiting seed set in buckwheat. *Crop Sci.* **2001**, *41*, 1792–1799. [[CrossRef](#)]
123. Eeckhaut, T.; Lakshmanan, P.S.; Deryckere, D.; Van Bockstaele, E.; Van Huylenbroeck, J. Progress in plant protoplast research. *Planta* **2013**, *238*, 991–1003. [[CrossRef](#)]
124. Dudits, D.; Maroy, E.; Praznovszky, T.; Olah, Z.; Gyorgyey, J.; Cella, R. Transfer of resistance traits from carrot into tobacco by asymmetric somatic hybridization: Regeneration of fertile plants. *Proc. Natl. Acad. Sci. USA* **1987**, *84*, 8434–8438. [[CrossRef](#)]
125. Kisaka, H.; Lee, H.; Kisama, M.; Kanno, A.; Kang, K.; Kameya, T. Production and analysis of asymmetric hybrid plants between monocotyledon (*Oryza sativa* L.) and dicotyledon (*Daucus carota* L.). *Theor. Appl. Genet.* **1994**, *84*, 365–371. [[CrossRef](#)] [[PubMed](#)]
126. Lachmann, S.; Kishima, Y.; Adachi, T. Protoplast fusion in buckwheat: Preliminary results on somatic hybridisation. *Fagopyrum* **1994**, *14*, 7–12.
127. Penin, A.A.; Kasianov, A.S.; Klepikova, A.V.; Kirov, I.V.; Gerasimov, E.S.; Fesenko, A.N.; Logacheva, M.D. High-resolution transcriptome atlas and improved genome assembly of common buckwheat, *Fagopyrum esculentum*. *Front. Plant Sci.* **2021**, *12*, 612382. [[CrossRef](#)]
128. Bortesi, L.; Fischer, R. The CRISPR/Cas9 system for plant genome editing and beyond. *Biotechnol. Adv.* **2015**, *33*, 41–52. [[CrossRef](#)] [[PubMed](#)]
129. Joshi, D.C.; Zhang, K.; Wang, C.; Chandora, R.; Khurshid, M.; Li, J.; He, M.; Georgiev, M.I.; Zhou, M. Strategic enhancement of genetic gain for nutraceutical development in buckwheat: A genomics-driven perspective. *Biotechnol. Adv.* **2019**, *39*, 107479. [[CrossRef](#)] [[PubMed](#)]
130. Zhao, H.W.; Lv, X.; Yin, W. The CRISPR/Cas9 system: A novel strategy for targeted genome engineering. *J. Pathog. Biol.* **2015**, *10*, 281–284.
131. Hus, K.; Betekhtin, A.; Pinski, A.; Rojek-Jelonek, M.; Grzebelus, E.; Nibau, C.; Gao, M.; Jaeger, K.E.; Jenking, G.; Doonan, J.H.; et al. A CRISPR/Cas9-based mutagenesis protocol for *Brachypodium distachyon* and its allopolyploid relative, *Brachypodium hybridum*. *Front. Plant Sci.* **2020**, *11*, 614. [[CrossRef](#)]
132. Mao, Y.; Zhang, H.; Xu, N.; Zhang, B.; Gou, F.; Zhu, J.K. Application of the CRISPR-Cas system for efficient genome engineering in plants. *Mol. Plant* **2013**, *6*, 2008–2011. [[CrossRef](#)]
133. Jiang, W.; Zhou, H.; Bi, H.; Fromm, M.; Yang, B.; Weeks, D.P. Demonstration of CRISPR/Cas9/sgRNA-mediated targeted gene modification in Arabidopsis, tobacco, sorghum and rice. *Nucleic Acids Res.* **2013**, *41*, e188. [[CrossRef](#)]
134. Lawrenson, T.; Shorinola, O.; Stacey, N.; Li, C.; Ostergaard, L.; Patron, N.; Uauy, C.; Harwood, W. Induction of targeted, heritable mutations in barley and *Brassica oleracea* using RNA-guided Cas9 nuclease. *Genome Biol.* **2015**, *16*, 258. [[CrossRef](#)]
135. Wang, Y.; Cheng, X.; Shan, Q.; Zhang, Y.; Liu, J.; Gao, C.; Qiu, J.-L. Simultaneous editing of three homoeoalleles in hexaploid bread wheat confers heritable resistance to powdery mildew. *Nat. Biotechnol.* **2014**, *32*, 947–951. [[CrossRef](#)] [[PubMed](#)]
136. Liang, Z.; Zhang, K.; Chen, K.; Gao, C. Targeted mutagenesis in *Zea mays* using TALENs and the CRISPR/Cas system. *J. Genet. Genom.* **2014**, *41*, 63–68. [[CrossRef](#)]
137. Jacobs, T.B.; LaFayette, P.R.; Schmitz, R.J.; Parrott, W.A. Targeted genome modifications in soybean with CRISPR/Cas9. *BMC Biotechnol.* **2015**, *15*, 16. [[CrossRef](#)]
138. Li, M.; Li, M.; Lin, H.; Wang, J.; Jin, Y.; Han, F. Characterization of the novel T4-like *Salmonella enterica* bacteriophage STP4-a and its endolysin. *Arch. Virol.* **2015**, *161*, 377–384. [[CrossRef](#)] [[PubMed](#)]
139. Yin, K.; Han, T.; Liu, G.; Chen, T.; Wang, Y.; Yu, A.Y.; Liu, Y. A geminivirus-based guide RNA delivery system for CRISPR/Cas9 mediated plant genome editing. *Sci. Rep.* **2015**, *5*, 14926. [[CrossRef](#)] [[PubMed](#)]

140. Miao, J.; Guo, D.; Zhang, J.; Huang, Q.; Qin, G.; Zhang, X.; Wan, J.; Gu, H.; Qu, L.J. Targeted mutagenesis in rice using CRISPR-Cas system. *Cell Res.* **2013**, *23*, 1233–1236. [[CrossRef](#)]
141. Malnoy, M.; Viola, R.; Jung, M.H.; Koo, O.J.; Kim, S.; Kim, J.S.; Velasco, R.; Kanchiswamy, N.C. DNA-free genetically edited grapevine and apple protoplast using CRISPR/Cas9 ribonucleoproteins. *Front. Plant Sci.* **2016**, *7*, 1904. [[CrossRef](#)]
142. Subburaj, S.; Chung, S.J.; Lee, C.; Ryu, S.-M.; Kim, D.H.; Kim, J.S.; Bae, S.; Lee, G.J. Site-directed mutagenesis in *Petunia × hybrida* protoplast system using direct delivery of purified recombinant Cas9 ribonucleoproteins. *Plant Cell Rep.* **2016**, *35*, 1535–1544. [[CrossRef](#)]

## 8.1.2 Ocena globalnych zmian w modyfikacjach białek histonowych i metylacji DNA w kalusach o zróżnicowanym potencjale embriogennym

### Publikacja P2:

**Tomasiak A.**, Sala-Cholewa K., Berg L.S., Brąszewska A., Betekhtin A. Global epigenetic analysis revealed dynamic fluctuations in levels of DNA methylation and histone modifications in the calli of *Fagopyrum* with different capacity for morphogenesis.

Plant Cell, Tissue and Organ Culture **2023**, 155, 743–757

<https://doi.org/10.1007/s11240-023-02595-3>

IF<sub>2023</sub>: 2,3

Punkty MNiSW: 100

Badania zostały przeprowadzone w celu oceny wpływu modyfikacji epigenetycznych na zmianę losu komórek w długoterminowych hodowlach linii kalusa *Fagopyrum* o zróżnicowanej zdolności do embriogenezy. Określenie poziomów metylacji DNA i histonów oraz acetylacji histonów podczas przejścia komórek ze stanu zróżnicowanego do odróżnicowanego miało na celu przybliżyć role modyfikacji epigenetycznych w nabywaniu potencjału embriogennego. Użyto EK *F. esculentum* oraz MK i NK *F. tataricum* w wybranych dniach pasażu, tj. w dniach zerowym, drugim, szóstym i jedenastym. Po przeniesieniu na świeże podłoże w przypadku *F. tataricum* inicjowana jest dezintegracja proembriogennych kompleksów komórkowych (PEKK), co powoduje powstawanie komórek ‘miękkiego’ kalusa (KMK). Jest to zauważalne w drugim dniu pasażu; około dnia szóstego następują procesy różnicowania komórek prowadzące do odtworzenia PEKK, które stają się widoczne około dnia jedenastego. Wtedy również rozpoczyna się drugi cykl dezintegracji PEKK.

Morfologia (Figure 1) oraz histologia (Figure 2) poszczególnych typów kalusów w dynamice pasażu zawarta jest w publikacji **P2**. EK *F. esculentum* (Fig. 2a) zawiera komórki embriogenne (Fig. 2a, prostokąt, a1 groty strzałek, a2 strzałka, a3 strzałka), które mają gęstą cytoplazmę, centralnie położone jądro i bardzo niski stopień wakuolizacji (Fig. 2, a3, strzałka). Są one otoczone zwakuolizowanymi komórkami parenchymatycznymi posiadającymi przyściennie zlokalizowane jądro komórkowe (Fig. 2a, a1, a2 gwiazdki). W EK obecne są również komórki zawierające związki fenolowe, które akumulują je w swoich wakuolach (Fig.

2a, strzałka). EK zawiera także komórki, które wykazują podobieństwo fenotypowe do komórek epidermalnych (Fig. 2a, a2 otwarte strzałki).

Kalus MK *F. tataricum*, charakteryzuje się odmienną strukturą. Powierzchnia PEKK jest pokryta komórkami zawierającymi związki fenolowe (Fig. 2b, prostokąt, strzałki na Fig. 2b1). W warstwie poniżej znajdują się słabo zwakuolizowane komórki merystematyczne (Fig. 2b1, podwójne strzałki), które posiadają gęstą cytoplazmę, okrągłe jądro i centralnie położone jąderko. Komórki parenchymatyczne stanowią centralną część PEKK (Fig. 2b1, otwarte strzałki). Natomiast NK *F. tataricum* (Fig. 2c) składa się wyłącznie z cienkościennej, zwakuolizowanych komórek z dużym, nieregularnym jądrem położonym przyściennie (Fig. 2c, strzałki), które często zawiera wiele jąder (Fig. 2c, wstawka, otwarte strzałki).

W publikacji analizowano globalne zmiany w poziomach modyfikacji epigenetycznych (metylacji DNA, metylacji i acetylacji histonów) podczas odróżnicowania i ponownego różnicowania komórek kalusów gatunków *Fagopyrum* o zróżnicowanej zdolności do embriogenezy. Metylacja DNA warunkuje powstawanie, zwartej i nieaktywnej genetycznie chromatyny, oraz reguluje ekspresję genów. Immunobarwienie oraz następnie analiza statystyczna poziomu metylacji DNA (Fig. 3a) pokazała, że w EK *F. esculentum* poziom tej modyfikacji w badanych dniach pasażu jest zróżnicowany. Modyfikacja 5mC była obserwowana na dość wysokim poziomie i wzrastała ona od drugiego dnia pasażu. Poziom trimetylacji histonu H3 na lizynie 36 (H3K36me3) (Fig. 3b) wahał się od wysokich wartości w dniu zerowym i szóstym do niskich w dniu drugim i jedenastym. Di- i trimetylacja histonu H3 na lizynie 4 (H3K4me2 i H3K4me3) (Fig. 3c, d) wykazywały natomiast najniższe poziomy w dniu szóstym i jedenastym. Te modyfikacje związane są z nieskondensowanym stanem chromatyny i aktywną transkrypcją genów (Nic-Can *i inni*, 2013). Spadek H3K4me3 sugeruje, że dynamiczne różnicowanie komórek w EK *F. esculentum* zachodzi w późniejszych dniach pasażu. Zwiększenie acetylacji histonu H4 i acetylacji H3K18 jest związane z wejściem w fazę S cyklu komórkowego (Jasencakova *i inni*, 2003). Poziom acetylacji histonu H3 na lizynie 18 (H3K18ac) (Fig. 4a) utrzymywał się na wysokim poziomie i spadał wraz z postępem pasażu, podobny wzorzec wykazywały poziomy acetylacji histonu H3 na lizynie 12 (H4K12ac) (Fig. 4b), korelując z wynikami uzyskanymi dla metylacji H3K4me2. Poziomy acetylacji histonu H4 na lizynie 16 (H4K16ac) (Fig. 4c) były najniższe w dniu zerowym i wzrastały wraz z kolejnymi badanymi dniami pasażu. Acetylacja histonu H4 na lizynie 5 (H4K5ac) (Fig. 4d) wykazywała odwrotny wzorzec, malejąc w trakcie pasażu, z wyjątkiem wzrostu w dniu jedenastym.

Analizy immunocytochemiczne ujawniły także dynamiczne zmiany epigenetyczne w kalusach *F. tataricum* o zróżnicowanym potencjale do embriogenezy. Najbardziej wyraźnym

wzorcem modyfikacji epigenetycznych w trakcie pasażu MK *F. tataricum* charakteryzowała się metylacja DNA (Fig. 3e). W dniu zerowym i jedenastym poziom 5mC był znacząco obniżony w porównaniu do dnia drugiego i szóstego. Może to wynikać z faktu, że PEKK w dniu zerowym mają najwyższy potencjał morfogeny, co może powodować hipometylację; natomiast po dezintegracji i utracie potencjału - zawartość 5mC wzrastała. Kolejna reinicjacja PEKK w dniu jedenastym skutkowałą odzyskaniem potencjału morfogenego i spadkiem poziomu metylacji DNA. Poziom 5mC w NK (Fig. 3i) był na znacznie wyższym poziomie w porównaniu do MK i pozostawał na stabilnym poziomie w trakcie pasażu (z wyjątkiem dnia szóstego). Poziom H3K36me3 był stabilny przez wszystkie badane dni pasażu w MK i NK (Fig. 3f, j). H3K4me2 i H3K4me3 (Fig. 3g, h) były obecne na niższych poziomach w dniach zerowym i drugim w MK. Obniżony poziom H3K4me2 wskazuje, że odróżnicowanie może być inicjowane w pierwszych dniach pasażu MK. W NK poziom H3K4me2 (Fig. 3k) był na stabilnym wysokim poziomie przez cały czas trwania pasażu, natomiast poziom H3K4me3 (Fig. 3l) był zmniejszony w dniach zerowym i drugim, podobnie do MK. Poziomy H3K18ac w MK i NK były na wysokim poziomie (Fig. 4e, i). W NK najniższy poziom H3K18ac występował w dniu zerowym i jedenastym, wzrastając w dniach drugim i szóstym. H4K12ac jest markerem związanym z euchromatyną i aktywną transkrypcją; w MK i NK jej wzór jest przeciwny, mianowicie w MK poziom H4K12ac (Fig. 4f) był najwyższy w dniu zerowym i jedenastym, podczas gdy w NK (Fig. 4j) w wymienione dni poziom był najniższy. Może to wynikać z aktywnej ekspresji genów skorelowanych z reinicjacją PEKK. Podwyższone poziomy H4K12ac w NK w dniach drugim i szóstym, a także H4K5ac (Fig. 4k) w dniu zerowym i H4K16ac (Fig. 4l) w dniu szóstym mogą być skorelowane z endoreplikacją. Poziom H4K16ac w MK pozostawał na niższych poziomach w dniu zerowym i jedenastym oraz podwyższonych poziomach w dniach drugim i szóstym, co może być powiązane z intensywnymi podziałami komórkowymi i wzrostem aktywności mitotycznej. Wzór poziomu H4K5ac w MK (Fig. 4g) przedstawiał stopniowy wzrost od dnia zerowego do jedenastego, podczas gdy w NK zaobserwowano znaczną redukcję tej modyfikacji w dniu zerowym, drugim i jedenastym. Podwyższony poziom tej modyfikacji w dniu szóstym może oznaczać, że w tym dniu transkrypcja jest aktywowana i zachodzi w szybkim tempie. NK wykazywał stosunkowo stabilny, ale wysoki poziom metylacji DNA oraz acetylacji histonów H3K18 i H4K12 (Fig. 4i, j), prawdopodobnie ze względu na szybkie tempo wzrostu i stały stan stresu oksydacyjnego.

**Publikacja P2:** Global epigenetic analysis revealed dynamic fluctuations in levels of DNA methylation and histone modifications in the calli of *Fagopyrum* with different capacity for morphogenesis.

**Tomasiak A.,** Sala-Cholewa K., Berg L.S., Braszewska A., Betekhtin A. Global epigenetic analysis revealed dynamic fluctuations in levels of DNA methylation and histone modifications in the calli of *Fagopyrum* with different capacity for morphogenesis.

Plant Cell, Tissue and Organ Culture **2023**, 155, 743–757

<https://doi.org/10.1007/s11240-023-02595-3>

IF<sub>2023</sub>: 2,3

**Punkty MNiSW:** 100

Materiały uzupełniające dostępne online

**Supplementary file 1:** Dane liczbowe z pomiarów intensywności fluorescencji

[https://static-content.springer.com/esm/art%3A10.1007%2Fs11240-023-02595-3/MediaObjects/11240\\_2023\\_2595\\_MOESM1\\_ESM.xlsx](https://static-content.springer.com/esm/art%3A10.1007%2Fs11240-023-02595-3/MediaObjects/11240_2023_2595_MOESM1_ESM.xlsx)

**Supplementary file 2:** Analiza statystyczna pomiarów fluorescencji w kontroli; niezmodyfikowanym histonie H3 i H4

[https://static-content.springer.com/esm/art%3A10.1007%2Fs11240-023-02595-3/MediaObjects/11240\\_2023\\_2595\\_MOESM2\\_ESM.pptx](https://static-content.springer.com/esm/art%3A10.1007%2Fs11240-023-02595-3/MediaObjects/11240_2023_2595_MOESM2_ESM.pptx)

**Supplementary file 3:** Skrypt z programu R studio (2022.12.0 wersja 353) użyty do analizy statystycznej i graficznej wizualizacji wyników z pomiarów fluorescencji

[https://static-content.springer.com/esm/art%3A10.1007%2Fs11240-023-02595-3/MediaObjects/11240\\_2023\\_2595\\_MOESM3\\_ESM.docx](https://static-content.springer.com/esm/art%3A10.1007%2Fs11240-023-02595-3/MediaObjects/11240_2023_2595_MOESM3_ESM.docx)





# Global epigenetic analysis revealed dynamic fluctuations in levels of DNA methylation and histone modifications in the calli of *Fagopyrum* with different capacity for morphogenesis

Alicja Tomasiak<sup>1</sup> · Katarzyna Sala-Cholewa<sup>1</sup> · Lea Sophie Berg<sup>2</sup> · Agnieszka Braszewska<sup>1</sup> · Alexander Betekhtin<sup>1</sup>

Received: 20 March 2023 / Accepted: 25 August 2023 / Published online: 12 September 2023  
© The Author(s) 2023

## Abstract

Buckwheat characterises with high susceptibility to in vitro tissue culture conditions, which have been researched extensively to study a plethora of processes. *F. tataricum* morphogenic callus (MC) is characterised by its capacity for morphogenesis for up to ten years of culture, displaying an extraordinary level of genome stability, and comprises of proembryogenic cell complexes (PECC), which are the structures resembling somatic embryos arrested on the pre-globular stage. The non-morphogenic callus (NC) that appears on the surface of MC after approximately two years of culture due to endoreduplication cycles, is characterised by aneuploidy, rapid growth rate and high level of oxidative stress. *F. esculentum* embryogenic callus (EC) has different morphological and histological features, remains stable for up to three years of culture, has a dense, globular structure, and is capable of forming embryoids from the masses of embryogenic cells, but does not produce a non-embryogenic clone. In this work, immunocytochemical analyses revealed dynamic epigenetic changes in *Fagopyrum* calli. We demonstrated that; decreased level of H3K4me2 seems to be associated with pluripotency acquisition in *F. esculentum* EC and *F. tataricum* MC; DNA hypomethylation appears to be connected with the acquisition of the embryogenic potential and PECC reinitiation in *F. tataricum* MC. Moreover, we observed that H4K16ac and H4K5ac exhibited the highest variability during the course of passage in NC. Elevated levels of these modifications on day zero and day six for H4K16ac and H4K5ac, respectively, seem to be connected with endoreplication peaks, the processes which are characteristic of this callus.

## Key message

Epigenetic changes accompany the dedifferentiation and re-differentiation processes in long-term callus cultures of *Fagopyrum* with different capacity for morphogenesis.

**Keywords** In vitro callus culture · DNA methylation · Epigenetic modifications · *Fagopyrum* · Histone acetylation · Morphogenic callus · Non-morphogenic callus · Embryogenic callus

## Abbreviations

5mC      5-Methylcytosine  
H3K18ac      Acetylation of Histone H3 on lysine 18

H4K16ac      Acetylation of Histone H4 on lysine 16  
H4K12ac      Acetylation of Histone H4 on lysine 12  
H4K5ac      Acetylation of Histone H4 on lysine 5  
H3K4me2      Dimethylation of Histone H3 on lysine 4  
H3K4me3      Trimethylation of Histone H3 on lysine 4  
H3K36me3      Trimethylation of Histone H3 on lysine 36  
PTMs      Post-Translational Modifications  
SE      Somatic embryogenesis  
TBO      Toluidine Blue O

Communicated by Danny Geelen.

✉ Alexander Betekhtin  
alexander.betekhtin@us.edu.pl

<sup>1</sup> Faculty of Natural Sciences, Institute of Biology, Biotechnology and Environmental Protection, University of Silesia in Katowice, Katowice, Poland

<sup>2</sup> Institute of Plant Sciences, University of Bern, Bern, Switzerland

## Introduction

The buckwheat genus comprises 23 species, and the two most cultivated are *Fagopyrum esculentum* Moench (common buckwheat) and *Fagopyrum tataricum* Gaertn. (Tartary buckwheat) (Tomasiak et al. 2022). Buckwheat is highly susceptible to in vitro conditions which have been researched extensively to study the induction of callus, plantlet regeneration from a variety of explants, organogenesis, somatic embryogenesis (SE) and synthesis of secondary metabolites (Fei et al. 2019; Rummyantseva et al. 2005; Rummyantseva et al. 2003; Srejavic and Nesko- vic 1981; Takahata and Jumonji 1985; Yamane 1985). *F. tataricum* in vitro tissue culture of the morphogenic callus (MC) characterised by low chromosome variability and the capacity for morphogenesis for up to ten years of culture displaying an extraordinary level of stability (Betekhtin et al. 2017; Rummyantseva et al. 2003). On the contrary, the non-morphogenic callus (NC) of *F. tataricum* appears on the surface of MC after approximately two years of culture due to endoreduplication cycles (Betekhtin et al. 2019, 2017). NC is characterised by aneuploidy, rapid growth rate and high content of hydrogen peroxide, an indication that NC is in a constant state of oxidative stress (Betekhtin et al. 2017; Kamalova et al. 2009). *F. esculentum* embryogenic callus (EC) displays different morphological and histological features, remains stable for up to three years of culture, has a dense, globular structure, and is capable of forming embryoids (Rummyantseva et al. 2005) but does not produce a non-embryogenic clone.

Sessile organisms, such as plants, are subjected to the ever-changing environment and have developed a high level of phenotypic plasticity, which to a vast degree, is controlled by the post-translational modifications (PTMs) (Bennett et al. 2021; Ghosh et al. 2021; Miguel and Marum 2011). Under certain circumstances, differentiated plant cells have the ability to return to a previous developmental state (dedifferentiate) and regain pluri- or totipotency, resulting in organogenesis and SE, processes largely involving PTMs (Birnbaum and Sanchez Alvarado 2008; Simsek Geyik et al. 2022; Xu and Huang 2014). The process of dedifferentiation and re-entry into the cell cycle was found to be associated with the global reorganisation of chromatin and changes in gene expression (Avivi et al. 2004; Williams et al. 2003; Zhao et al. 2001). In vitro tissue culture is a good system for studying these processes since they can be easily induced, influenced and modified under controlled conditions. According to the available evidence, it is believed that in vitro conditions destabilise the genetic and epigenetic programs of the plant tissue and can result in alteration of chromosome and DNA sequence, transposon activation or repression, generation

of somaclonal variants and recalcitrance (Ckurshumova and Berleth 2015; Neelakandan and Wang 2012).

DNA methylation, one of the most researched modifications, is associated with a variety of molecular mechanisms, including inactivation of the chromatin, gene regulation and plant cell differentiation, among others (Ghosh et al. 2021; Kaeppeler et al. 2000; Park et al. 2008; Springer and Schmitz 2017). Highly dynamic mechanisms of global and local DNA methylation changes were found to occur during cell dedifferentiation and re-differentiation processes in callus formation (Horstman et al. 2017; Li et al. 2017b). Recent studies conducted in peach (*Prunus persica*) demonstrated the beneficial influence of DNA hypomethylation during the transition from leaf to callus (Zheng et al. 2022), and subsequently that genes involved in DNA and histone methylation are up regulated in five-year old callus when compared to newly formed callus (Gao et al. 2023) showing dynamic changes in these epigenetic marks during the callus culture. In *Glycine max* and *Zea mays* on the other hand, losses in DNA methylation were observed after many years of consecutive culture which led to the conclusion that tissue culture results in diminishing ability to maintain DNA methylation (Han et al. 2018; Ji et al. 2019). Studies on *Eleuterococcus senticosus* embryogenic and non-embryogenic calli demonstrated significantly lower global DNA methylation rates in embryogenic calli (Chakrabarty et al. 2003). Similar results were obtained for *Agave furcroydes*, where hypermethylation on a high but stable level was present throughout the culture in non-embryogenic callus (Monja-Mio et al. 2018). DNA methylation has also been found to be engaged in SE (Chakrabarty et al. 2003; Fraga et al. 2012; Nic-Can et al. 2013; Park et al. 2008). Results obtained for *Daucus carota* showed that DNA hypomethylation suppressed the formation of embryogenic cells (Yamamoto et al. 2005). DNA methylation contributes to a plethora of processes; however, its role in the cell differentiation/dedifferentiation switch and SE and related processes seem to be species-dependent.

Callus formation and its developmental processes were found to involve global changes in global epigenetic make-up (Bednarek and Orłowska 2019; Miguel and Marum 2011; Us-Camas et al. 2014). Marks involved in open chromatin state such as acetylation on histone H3 and H4, as well as methylation H3K4me3 and H3K36me3 have a tendency to be enriched in the callus cells when compared to somatic cells, while marks responsible for heterochromatin such as H3K9me2/3 and H3K27me2/3 are decreased in dedifferentiated cells (Hemenway and Gehring 2023; Lee and Seo 2018). Histone methylation is an indispensable player in the epigenetic regulation of the gene expression orchestrated by environmental and developmental cues in plants (Cheng et al. 2020; Hu and Du 2022; Yu et al. 2009). Recent research demonstrated that reduced levels of H3K4me2 allow the activation of genes essential for the acquisition of regenerative competency

during the callus culture of *Arabidopsis* (Ishihara et al. 2019). Another study on *Arabidopsis* reported the reduced accumulation of H3K4me3 during early stages of callus formation (Lee et al. 2019). Similarly, in *Coffea canephora* global levels of H3K4me were decreased at the beginning of SE induction (Nic-Can et al. 2013). Another modification associated with active transcription H3K36me3 was found to be accompanying the transition processes from differentiated somatic cells to dedifferentiated pluripotent stem cells during the formation of callus in *Arabidopsis*, leading to the conclusion that this PTM promotes early stages of cellular dedifferentiation by creating an open chromatin structure and maintaining transcriptionally competent state (Lee et al. 2017; Ma et al. 2022; Zhang et al. 2015). Histone acetylation is associated with relaxed euchromatin and transcriptional activation (Kouzarides 2007). It has been reported that reduced levels of histone acetylation due to the compromised function of histone acetyltransferases and deacetylases had a negative effect on morphogenic responses such as callus formation (Kim et al. 2018; Lee et al. 2016; Rymen et al. 2019; Zhang et al. 2020). Indirect evidence of the correlation between dynamic epigenetic changes during SE induction was also demonstrated in *Hevea brasiliensis*, *Peonia ostii* and *Arabidopsis*, where patterns of expression of the histone acetyltransferases (HAT) and histone deacetylases (HDAC) genes fluctuated during the SE induction (Ci et al. 2022; Li et al. 2017a; Wickramasuriya and Dunwell 2015). In *Hevea brasiliensis*, reduction in histone deacetylases was observed in the early stages of callus differentiation (Li et al. 2020). Study on *Arabidopsis* demonstrated that histone acetylation is essential for in vitro acquisition of pluripotency by promoting transcriptional activation of several root-meristem gene loci (Kim et al. 2018). There is limited evidence available in literature decoding the exact function of the histone acetylation, however, the research implicates that acetylation is an essential factor for the appropriate regulation of transcription (Birnbaum and Roudier 2017; Us-Camas et al. 2014).

This study was conducted in order to decipher how the epigenetic modifications influence cell fate transition in long-term cultivated *Fagopyrum* callus lines with different capacity for morphogenesis. Depicting levels of DNA and histone methylation as well as histone acetylation during the transition from non-embryogenic to embryogenic state will help to comprehend what role the PTMs play in the acquisition of embryogenic potential, thereby expanding the limited evidence available on this topic.

## Materials and methods

### Plant material

The seeds of *F. tataricum*, sample k-17 were acquired from the collection of the N.I. Vavilov Institute of Plant Genetic

Resources, Saint Petersburg, Russia (plants were grown in field conditions during the period from May to September). For *F. esculentum* commercially available seeds of the Panda cultivar (the Malopolska Plant Breeding, Poland) were used. EC of *F. esculentum* and *F. tataricum* MC were induced from immature zygotic embryos. NC of *F. tataricum* appears on the surface of MC after approximately two years of culture (Betekhtin et al. 2017). For the present study, EC's age was approximately one year old and MC's eight years old, and NC's five years old. Calli were cultivated in the dark in an incubator at  $25\text{ }^{\circ}\text{C} \pm 1$  on an RX medium, according to Betekhtin et al. (2019). It composed of Gamborg B5 including vitamins (Duchefa, Netherlands) (Gamborg et al. 1968),  $2\text{ g L}^{-1}$  N-Z amine A (Sigma-Aldrich, USA),  $2\text{ mg L}^{-1}$  2,4-dichlorophenoxyacetic acid (2,4-D, Sigma-Aldrich),  $0.2\text{ mg L}^{-1}$  kinetin (KIN, Sigma-Aldrich, USA),  $0.5\text{ mg L}^{-1}$  3-indoleacetic acid (IAA, Sigma-Aldrich, USA),  $0.5\text{ mg L}^{-1}$  1-naphthaleneacetic acid (NAA, Sigma-Aldrich, USA),  $25\text{ g L}^{-1}$  sucrose (Chempur, Poland) and  $7\text{ g L}^{-1}$  phyto agar (Duchefa, Netherlands). EC of *F. esculentum*, MC and NC of *F. tataricum* were subcultured every four and two weeks, respectively.

### Histological and immunostaining procedures

Proembryogenic cell complexes (PECC) from *F. tataricum* MC were carefully selected in sterile conditions under the stereoscopic Nikon microscope (Japan) and transferred onto a fresh medium for each time point, i.e. day zero, two, six and eleven of the passage. For immunocytochemical analysis NC of *F. tataricum* and EC of *F. esculentum* pieces of calli were put onto fresh medium for each time point. The same day, material from one petri dish of *F. tataricum* MC and NC and *F. esculentum* EC were fixed in 4% paraformaldehyde (Sigma-Aldrich, USA) in  $1\times$  phosphate buffered saline (PBS), pH 7.3 and placed in the vacuum desiccator for three hours with subsequent incubation in  $4\text{ }^{\circ}\text{C}$  overnight. The next day, the fixative was carefully replaced with  $1\times$  PBS and followed by dehydration in a graded ethanol series diluted in  $1\times$  PBS solution twice for 15 min in each concentration (10%, 30%, 50%, 70% and 90%) and 99,8% twice for 30 min each. The fixation process was repeated on day two, six and eleven.

The embedding procedure was performed according to Wolny et al. (2014). The de-embedding process involved placing the slides in 99,8% ethanol three times for 10 min, followed by rehydration in ethanol/  $1\times$  PBS solutions: 90%, 70%, 50%, 30% v/v and  $1\times$  PBS for 10 min each. The immunostaining and histological processes then commenced. For the histology, slides were stained with 0.05% aqueous solution of Toluidine blue (TBO, Sigma-Aldrich, USA) for 5 min and mounted with distilled water. Observations

and photographs were performed with an Olympus BX43F microscope equipped with a Olympus XC50 digital camera.

The immunostaining method used in this experiment was previously described by Braszewska-Zalewska et al. (2010); Braszewska-Zalewska et al. (2012); Braszewska-Zalewska et al. (2013). De-embedded slides were incubated with 5% bovine serum albumin (BSA, Sigma-Aldrich, USA) in 1xPBS for 1 h in the humid chamber at room temperature and subsequently, the primary antibody in 1% BSA in 1xPBS (1:100) was applied and incubated at 4 °C overnight. For 5mC primary antibody incubation was preceded with 2N HCl (Sigma-Aldrich, USA) digestion for 45 min. Next, the slides were rinsed by three washes in 1xPBS and secondary antibody in 1% BSA in 1xPBS (1:100) was applied. Samples were incubated at 37 °C in the humid chamber in the dark for one hour. After the incubation, three washes in 1xPBS were performed and nuclei were counterstained with 4',6-diamidyno-2-fenylindol (DAPI, 2.5 g/ml in Vectashield antifade buffer, Vector Laboratories, USA). The negative control was performed for each of the used modification by conducting the immunostaining procedure omitting the addition of the primary antibody. The antibodies used in the immunocytochemical analysis are listed in Table 1.

### Fluorescence intensity measurements and statistical analysis

Images were obtained using Olympus FV1000 confocal system (Olympus, Poland) equipped with an Olympus IX81 inverted microscope. Fluorescence of DAPI (excitation 405 nm, emission 425–475 nm) and Alexa488 (excitation 488 nm, emission 500–600 nm) was acquired from 60× Plan Apo oil-immersion objective lens (NA 1.35), a 50 mW 405 nm diode laser and a 100 mW multi-line argon

ion laser (Melles Griot BV, the Netherlands). Axial series of two-dimensional fluorescence images of the optical sections through the nuclei (z-stacks) was collected with the use of two separate photomultipliers (R6357, Hamamatsu, Japan) set to work in the integration mode at 4 μs pixel dwell time and 12-bit signal digitization (4096 intensity levels). Alexa488 and DAPI fluorescence intensity levels were measured in the ImageJ version 1.53 s software (Wayne Rasband, National Institutes of Health, USA). Images were converted to eight-bits and segmented with the threshold value parameter.

The fluorescence intensity of Alexa488 and DAPI was calculated as mean values from the Integrated Density (IntDen) parameter per one nucleus, which depicted the sum of all of the pixels within the region of interest. Results are presented in relative units. 500 nuclei were analysed for each callus type, four time points, for seven histone modifications, DNA methylation and two controls (unmodified histone H3 and H4). Numerical data is included in Supplementary Materials Fig. S1. Fluorescence data analysis and plotting was done using R, a software environment for statistical computing and graphics in R Studio 2022.12.0 Build 353 (Script included in Supplementary Materials Fig. S3), an integrated development environment for R (Team RC 2022; Team 2022b). An ANOVA's test with the R Stats package (Team 2022a) followed by Tukey's HSD test at the significance level  $p \leq 0.05$ . Standard errors were also calculated via the stats package. The package agricolae (Statistical Procedures for Agricultural Research) was used to find significant differences between means (Mendiburu 2021). Subsequently, data was plotted with packages dedicated to data visualization; ggplot2 (Wickham 2022) and ggpubr (Kassambara 2022). Letters on the graphs indicate statistically significant differences between samples.

**Table 1** List of antibodies used in the immunostaining

| Antibody                              | Catalogue number | Company            |
|---------------------------------------|------------------|--------------------|
| Anti-5-methylcytosine                 | ab73938          | Abcam, UK          |
| Anti-dimethyl-Histone H3 (Lysine 4)   | 04–790           | Sigma-Aldrich, USA |
| Anti-trimethyl-Histone H3 (Lysine 4)  | 04–745           | Sigma-Aldrich, USA |
| Anti-trimethyl-Histone H3 (Lysine 36) | abe305           | Sigma-Aldrich, USA |
| Anti-acetyl-Histone H3 (Lysine 18)    | ab1191           | Abcam, UK          |
| Anti-acetyl-Histone H4 (Lysine 16)    | ab109463         | Abcam, UK          |
| Anti-acetyl-Histone H4 (Lysine 12)    | 04–119           | Sigma-Aldrich, USA |
| Anti-acetyl-Histone H4 (Lysine 5)     | 04–118           | Sigma-Aldrich, USA |
| Unmodified H3                         | ab18521          | Abcam, UK          |
| Unmodified H4                         | ab10158          | Abcam, UK          |
| Goat Anti-Mouse IgG                   | ab150113         | Abcam, UK          |
| Goat Anti-Rabbit IgG                  | ab150077         | Abcam, UK          |

## Results and discussion

In general, callus tissue is of remarkable properties, it contains cells of increased developmental potency and can be formed through a variety of initial pathways which include the same gene regulatory network responsible for stress, hormonal and developmental cues (Feher 2019; Hemenway and Gehring 2023). These processes have also been linked with the chromatin accessibility indicating they are closely intertwined (Bednarek and Orłowska 2019; Birnbaum and Roudier 2017). *F. tataricum* MC characterises with a stable regeneration potential, the ability to undergo SE and organogenesis while maintaining low chromosome number ( $2n = 16$ ) throughout approximately ten years of culture (Betekhtin et al. 2017; Kamalova et al. 2009; Rumyantseva et al. 1989). MC's PECCs have a distinctive structure typical for embryogenic cultures, of the somatic embryos arrested at the pre-globular stage due to the presence of auxin in the culture media as demonstrated previously by Rumyantseva et al. (2003), Souter and Lindsey (2000). PECCs are known to be able to regenerate through organogenesis as well as SE, which makes it a perfect system for studying its response to hormonal cues, whereas an abnormal line, NC appears on the surface of MC due to endoreduplication cycles and is subdued to constant oxidative stress (Betekhtin et al. 2017), making it suitable for research on epigenetic mechanisms involved in stress response pathways. Since they originate from the same species, but are so extraordinary different in structure and responses to tissue culture conditions, comparative analyses can be performed to decipher the role of epigenetic mechanisms behind their development. Since, the closely related species *F. esculentum* produces an EC typical for that type of callus, able to regenerate through the means of SE, and is not as genetically stable as *F. tataricum* MC callus, it was significant to research the levels of the same epigenetic modifications to shed some light on similarities in mechanisms regulating responses to stress, hormonal and developmental signals.

### Morphology and histology of *Fagopyrum esculentum* EC, *Fagopyrum tataricum* MC, NC

Calli were examined on days zero, two, six and eleven of the passage (Fig. 1). Images of the morphology were acquired with the Keyence VHX-970F digital microscope (Japan) equipped with an ultra-small high-performance zoom lens VH-Z20R/Z20T and wide-area illumination adapter OP-87298. It provided real-time depth composition of images with the 3D scanning technique. The microscope produced images of extraordinary clarity

and texture, due to a high resolution dynamic range. In this experiment, day zero is the beginning of a new passage; a time point at which callus is transferred onto fresh RX medium. Most *F. esculentum* callus induction was obtained from hypocotyls, (Adachi et al. 1989; Hao et al. 1998; Jin et al. 2002; Kwon et al. 2013; Yamane 1985), however this could result in low embryogenic potential and elevated chromosome number. Callus induced from immature zygotic embryos characterised by the presence of meristemoids, was able to produce high amounts of somatic embryos suggesting that the genotype is an important factor for SE (Berbec and Doroszewska 1999; Nesković et al. 1987). EC of *F. esculentum* has a dense, globular structure, milky glittering surface and is comprised of embryogenic masses (Fig. 1 a–d). Upon transfer to the fresh medium, the secretion is triggered which is marked with red arrows (Fig. 1 a,b). EC of *F. esculentum* (Fig. 2a) contains embryogenic cells (Fig. 2a, rectangle, a1 arrowheads, a2 arrow, a3 arrow), which are poorly vacuolised, have dense cytoplasm and centrally located nucleus (Fig. 2, a3, arrow). They are surrounded by highly vacuolated parenchymatous cells (Fig. 2a, a1, a2 asterisks). Nucleus has a near-cell wall position. Phenolic containing (PC) cells that accumulate phenolics in their vacuoles are present (Fig. 2a, arrow). EC of *F. esculentum* also contains cells exhibiting epidermal phenotype (Fig. 2a, a2 open head arrows) which can form embryoids (Rumyantseva et al. 2005).

Upon transfer on fresh medium, in MC of *F. tataricum* PECC, which has a dense structure and light colour (Fig. 1e) is triggered to disintegrate, release secretion (Fig. 1 e, red arrows) giving rise to 'soft' callus cells (SCCs). This is evident on day two and day six (Fig. 1 f, g) where the number of SCCs rises and they become prominent brownish, with loose structure and more secretion (Fig. 1f, red arrows). SCCs may act as support tissue, providing nutrients such as proteins and sugars as well as other conditioning factors, which are secreted into the medium during the disintegration of the PECCs. SCCs do not divide but are metabolically active which postpones death through senescence (Betekhtin et al. 2017). New PECC blowout (white asterisks) supported by SCCs (black asterisks) is noticeable on day 11 (Fig. 1h). Previous study conducted on *F. tataricum* revealed two cycles of PECCs reinitiation during the course of the passage (Betekhtin et al. 2019, 2017; Rumyantseva et al. 2004). First one occurs approximately on the eleventh day, and the second one around day twenty-second, both supported by the spikes of the mitotic activity and release of the extracellular polymers into the culture medium (Rumyantseva et al. 2004). In this study one cycle was studied, since the events of the PECCs disintegration and reinitiation undergo the exact same processes after day eleven. PECC's surface (Fig. 2b) is covered by the PC cells (Fig. 2b, rectangle, b1

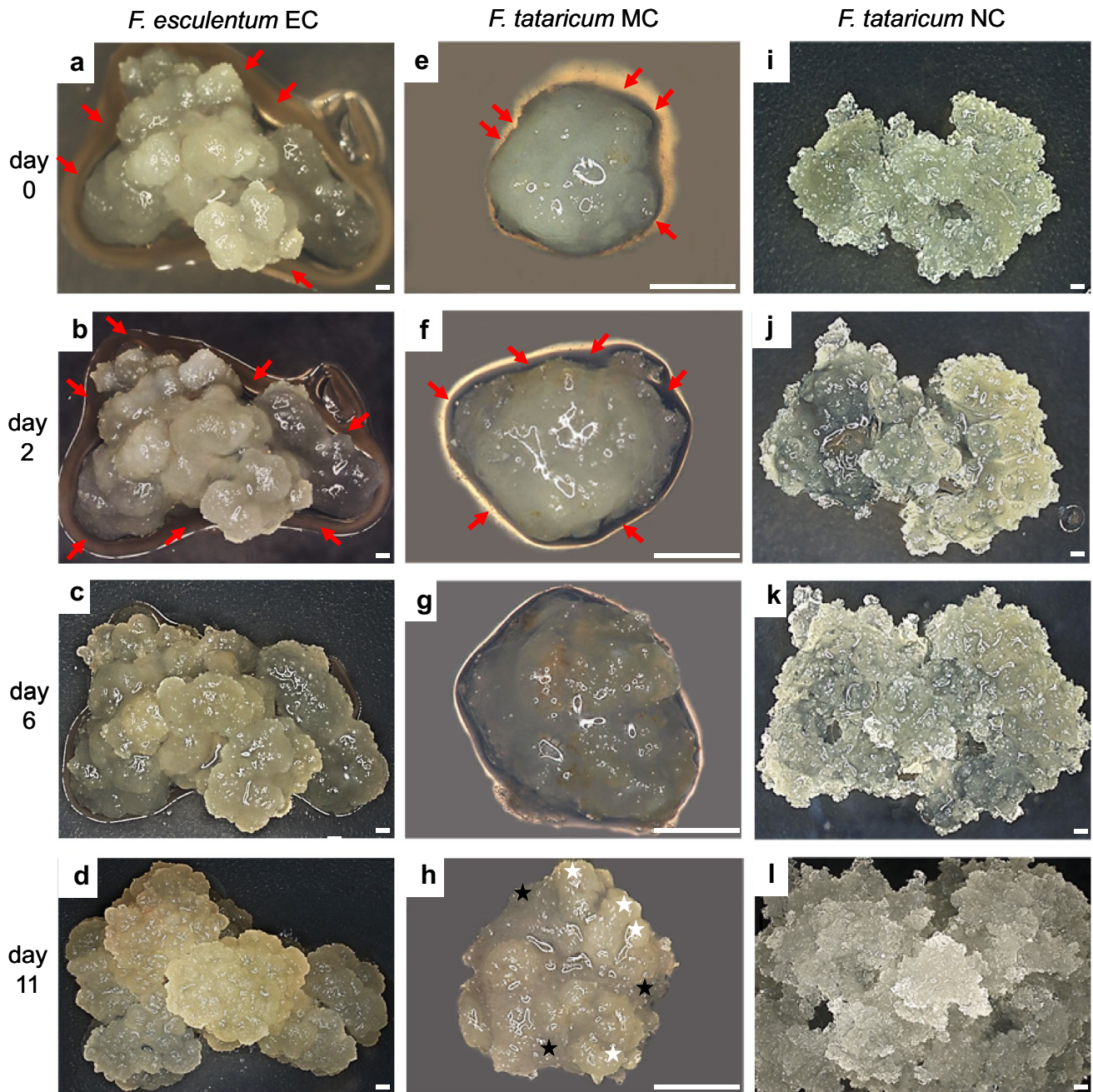


**Fig. 1** Morphology of *F. esculentum* EC **a–d**; embryonic complex of *F. tataricum* MC **e–h**; red arrows indicate the secretion, black asterisks indicate soft callus, white asterisks newly formed PECCs; NC of *F. tataricum* (**i–l**) on day zero, two, six and eleven; Scale bars: 0,5 mm

arrows). Below the PC cell layer, lay poorly vacuolised meristematic cells (Fig. 2b1, double arrows) with dense cytoplasm. Round nuclei and centrally located nucleolus—the source of embryogenically determined cells, from which embryoids and new PECCs can form. Parenchymatous, storage cells (Fig. 2b1, open arrows) containing large starch grains in their plastids and wall-adjacent large nucleolus are located below and constitute the largest part of the PECC. *F. tataricum* NC (Fig. 1i–l) has unorganised, frail structure,

is characterised by very fast growth rate and is devoid of the ability for morphogenesis (Betekhtin et al. 2017). *F. tataricum* NC (Fig. 2c) comprises exclusively of highly vacuolated parenchymatous cells with irregularly shaped wall-adjacent nucleus (Fig. 2c, arrows) that frequently contains multiple nucleoli (Betekhtin et al. 2017; Rumyantseva et al. 2003) (Fig. 2c, inset, open arrows) PCs are components of the antioxidant defence system in tissue cultures and take part in the regulation of morphogenesis processes (Debeaujon

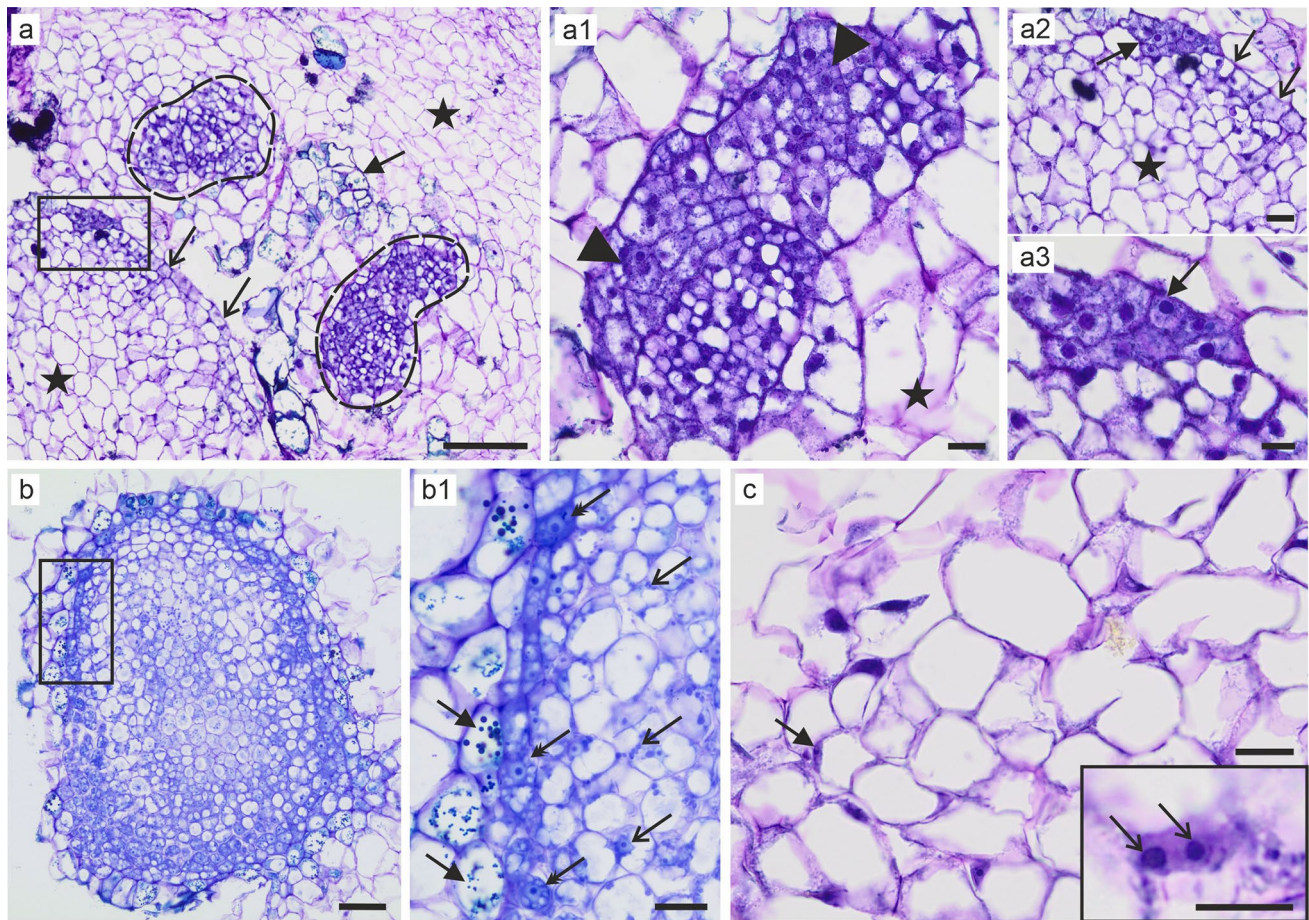


**Fig. 2 a** Histological section of the EC of *F. esculentum*; area in rectangle indicates embryogenic cells; open arrows—cells exhibiting epidermal phenotype; asterisks—parenchymatous cells; outlined areas—embryogenic masses; arrow—PCs; scale bar 100  $\mu\text{m}$  (a1) magnification, arrowheads—embryogenic masses; asterisk—parenchymatous cells; scale bar 20  $\mu\text{m}$  (a2) magnification, arrow—embryogenic cells, open arrows—cells exhibiting epidermal phenotype;

asterisk—parenchymatous cells; scale bar 20  $\mu\text{m}$  (a3) magnification, arrow—embryogenic cells; scale bar 10  $\mu\text{m}$  **b** Histological section of the proembryogenic complex of *F. tataricum* MC; scale bar 50  $\mu\text{m}$  (b1) magnification of area marked on b, arrows—PC, double arrows—meristematic cells; open arrows—parenchymatous cells with starch grains; scale bar 20  $\mu\text{m}$  **c** Histological section of *F. tataricum* NC; arrow—nucleus; inset: open arrows—nucleoli; scale bar 10  $\mu\text{m}$

et al. 2003; Sakar and Naik 2000). It has been previously demonstrated that MC accumulates much more phenolic compounds than the NC (Akulov et al. 2018). Moreover, NC cells poorly synthesize chlorophyll as a result of anomalies in the plastid development and lack the capacity to perform photosynthesis. Transformation of MC to the NC seems to be a result of the mutational or epigenetic changes in the DNA and subsequent silencing of genes involved in the PC biosynthesis (Akulov et al. 2018).

### Epigenetic modifications in *Fagopyrum esculentum* EC

The analysis of the level of epigenetic modifications in *F. esculentum* EC were preceded with the measurement of the unmodified histones H3 and H4 as controls where no significant differences were displayed across the examined days of

the passage (Fig. S2 a,b). Levels of DNA methylation across the examined days of the passage displayed significant differences (Fig. 3a). The content of 5mC decreased from day zero to day two which subsequently increased on day six and eleven. A similar result was obtained for *Beta vulgaris*, where hypomethylation was observed during callus formation (Zakrzewski et al. 2017). Similarly, in *Oryza sativa* callus, DNA hypermethylation was associated with dedifferentiated state (Stroud et al. 2013). In *Triticosecale* global DNA demethylation took place during tissue culture regeneration (Machczyńska et al. 2014). H3K36me3 levels (Fig. 3b) fluctuated from high on days zero and six to low on days two and eleven, whereas H3K4me (Fig. 3c, d) PTMs showed the lowest levels on day six and eleven. The deposition of H3K4me3 and H3K36me3 results in an open chromatin and transcriptional activation. H3K4me3 is typically enriched at the transcription start site and is associated with its initiation

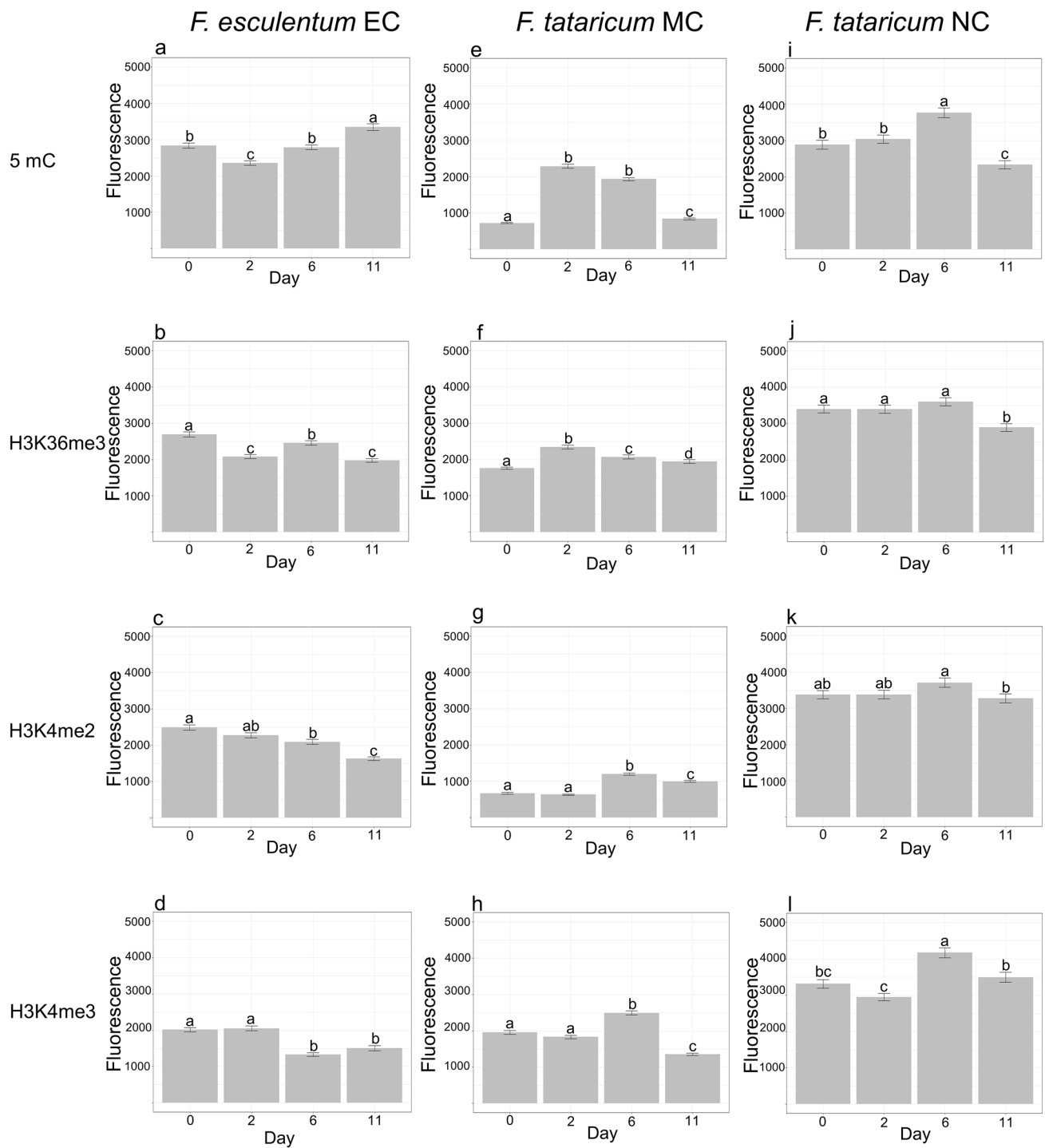


**Fig. 3** The levels of fluorescence intensity in DNA methylation and histone H3 methylation; in *F. esculentum* EC **a-d** and *F. tataricum* MC **e-h** and NC (**i-l**) across the passage. Letters indicate statistically significant differences between samples,  $P \leq 0.05$ ,  $n = 500$

whereas deposition of H3K36me3 is more widespread and associated with transcriptional elongation (Roudier et al. 2011). H3K4me and H3K36me3 are linked to a variety of developmental processes and responses to environmental cues (Roudier et al. 2011). In *Arabidopsis*, a mechanism

responsible for gene priming involving *LYSINE-SPECIFIC DEMETHYLASE 1-LIKE 3 (LDL3)* eliminates H3K4me2 during the callus formation and pluripotency acquisition (Ishihara et al. 2019). H3K4me3 increase was observed in *Oryza sativa* callus and was found to be mainly involved in



DNA replication (Zhao et al. 2020) hence suggesting that dynamic cell differentiation in *F. esculentum* EC takes place during the first days of the passage. H3K18ac was on an overall high level and decreased with the passage progression (Fig. 4a), a pattern displayed also by the levels of the

acetylation of H4K12 (Fig. 4b) correlating with the results obtained for histone H3K4me2 methylation. H3K18ac is also mainly found in regions adjacent to the transcription start site and correlated with transcription enhancers. Likewise is H4K12ac which is located on active coding genome

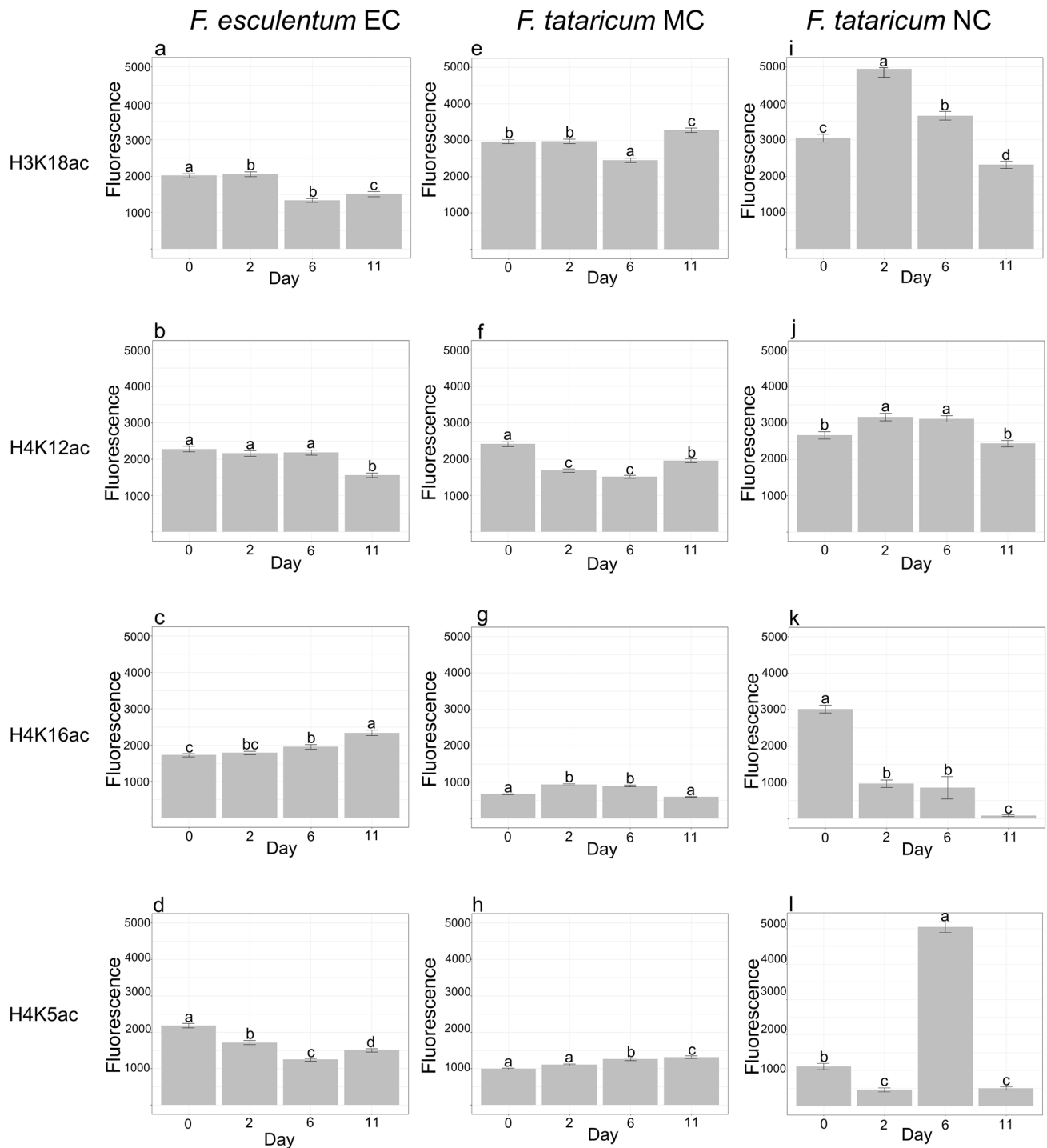


**Fig. 4** The levels of fluorescence intensity in histone H3 and H4 acetylation in *F. esculentum* EC **a-d** *F. tataricum* MC **e-h** and NC (i-l) callus; letters indicate statistically significant differences between samples,  $P \leq 0.05$ ,  $n = 500$

regions where it creates binding sites for regulatory factors and promotes transcription (Ayyappan et al. 2015; Inacio et al. 2018). In *Brassica napus* high levels of H3Ac and H4Ac were detected in the vacuolated microspore, which is a totipotent cell capable of reprogramming and re-entry into the cell cycle upon induction (Rodriguez-Sanz et al. 2014). H4K16ac (Fig. 4c) levels were the lowest on day zero and kept increasing with the passage progression. H4K5ac (Fig. 4d) presented a reverse pattern, decreasing across the passage, with the exception of an increase on day eleven. Both modifications are associated with active transcription suggesting that on day eleven gene transcription might occur in higher frequency and might be related with the acquisition of the embryogenic potential (Moronczyk et al. 2022). It has been previously reported that an increase in histone H4 acetylation was associated with the progression through the S-phase of the cell cycle (Desvoyes et al. 2014). In *Vicia faba*, *Hordeum vulgare* and *Arabidopsis* the intensity of histone H4 acetylation at lysine 5 and 12 was correlated with the cell cycle and evident ‘deposition-related’ acetylation at eu- and heterochromatin during DNA replication and subsequent deacetylation at heterochromatin towards mitosis. On the contrary, significant acetylation of H4K16ac within the chromocenters of endopolyploidy nuclei suggested delayed deacetylation after the endoreduplication (Jasencakova et al. 2001, 2000, 2003).

### Epigenetic modifications in *F. tataricum* NC and MC

Unmodified histone H3 and H4 levels in *F. tataricum* NC and MC were measured and showed no substantial differences across the examined days of the passage (Fig. S2 c-f). Immunocytochemical analyses revealed dynamic epigenetic changes in *F. tataricum* calli with different morphogenic potential. Differences in calli structure on the cellular level development might be a contributor to such immense changes in epigenetic modifications. NC is characterised by aneuploidy (Betekhtin et al. 2017; Kamalova et al. 2009). Increased cell ploidy has been related to an extended depth of the nuclear lobes as well as the nucleus area. The occurrence of high-level polyploid cells seemingly justifies the presence of lobed nuclei in the NC cells (Betekhtin et al. 2017). NC exhibited relatively stable but high level of DNA methylation (Fig. 3i), and histone H3K18, H4K12 acetylation (Fig. 4i, j) probably due to the rapid growth rate and high content of hydrogen peroxide, malonic dialdehyde, low catalase activity and high superoxide dismutase activity indicating that NC is in a constant state of oxidative stress (Kamalova et al. 2009). Additionally, NC has a high level of DNA damage across the passage, which is a normal physiological state for the NC and its cells appear to be adapted to it (Betekhtin et al. 2017). This can be correlated with the high levels of DNA methylation (Fig. 3i) and significantly

reduced and unstable levels of the acetylation of H4K16 and H4K5 (Fig. 4k, l) during the course of the passage.

The most noticeable and prominent pattern of the epigenetic modifications across the course of the passage in *F. tataricum* MC was DNA methylation (Fig. 3e). On day zero and eleven the levels of 5mC were significantly decreased when compared to day two and six. This might be due to the fact that PECCs on day zero have the highest morphogenic capacity, and upon disintegration and the loss of the capacity the 5mC content rises. Subsequent reinitiating of PECCs on day eleven results in regaining the morphogenic capacity and a decrease in the DNA methylation level. The levels of 5mC in NC (Fig. 3i), on the other hand were on a much higher level when compared to MC, however except for day six stayed on a stable level across the course of the passage. Betekhtin et al. (2019) examined the expression of DNA methyltransferases in *F. tataricum* calli and demonstrated significantly higher expression of *MET1* and *MET2* in the NC, while demethylases (*DME1*, *DME2*, *DME3*) expression was on the higher level in MC. Similar results were obtained for Siberian ginseng where significantly lower global DNA methylation rates in embryogenic calli were present in contrast to non-embryogenic calli (Chakrabarty et al. 2003). Additionally, in *Agave furcroydes*, hypermethylation on high but stable level was present throughout the culture in non-embryogenic callus and in the embryogenic clone the hypomethylation was observed in the beginning and towards the end of the passage (Monja-Mio et al. 2018), which correlates with the results obtained for MC of *F. tataricum*. H3K36me3 (Fig. 3f, j) was on the stable level with no vast fluctuations throughout the days of the passage in MC and in NC. H3K4me marks (Fig. 3g, h) were present in decreased levels on days zero and two in MC, similarly to *Coffea canephora* global levels of H3K4me which were decreased at the beginning of SE induction (Nic-Can et al. 2013). As mentioned earlier, elimination of H3K4me2 was observed in *Arabidopsis* during the pluripotency acquisition (Ishihara et al. 2019), therefore the differentiation/dedifferentiation switch might be initiated during the first days of the culture in MC. In NC, the level of H3K4me2 (Fig. 3k) was on the stable high level throughout the culture, whereas in H3K4me3 (Fig. 3l) it was decreased on days zero and two, comparable to MC. H3K18ac levels in MC and NC (Fig. 4e, i) were on an overall high level. However, an interesting pattern was prevalent in NC, where the lowest level presented on day zero and eleven, elevating on day two and six. H4K12ac is the mark associated with euchromatin and active transcription and in MC and NC (Fig. 4f, j) the pattern is opposing, namely in MC the H4K12ac level was the highest on day zero and eleven, whereas in NC those days levels were the lowest. This might be due to active gene expression correlated with PECCs reinitiating in the MC. An increase in the acetylation of histone H4 and acetylation of H3K18 has

been associated with the progression through the S-phase of the cell cycle (Jasencakova et al. 2001, 2003). Therefore, the elevated levels of H4K12ac (Fig. 4j) in NC on days two and six as well as H4K5ac (Fig. 4l) on day zero and H4K16ac (Fig. 4k) on day six might be a result of the endoreplication (Betekhtin et al. 2017). The levels of H4K16ac in MC (Fig. 4g) presented a pattern of lower levels on day zero and eleven and elevated levels on day two and six, which seem to correlate with intense cell division and an increase in the mitotic activity (Rumyantseva et al. 2003). H4K5ac in MC (Fig. 4h) presented a gradual increase from day zero to day eleven, while in NC the significant reduction of this modification was observed on day zero two and eleven. Elevated level of this modification on day six may suggest that upon this day the transcription is activated and rapid transcription takes place. Betekhtin et al. (2019) examined the expression of genes connected with ethylene biosynthesis, a factor with a significant role in the senescence processes, *1-AMINOCYCLOPROPANE-1-CARBOXYLIC SYNTHASE (ACS2* and *ACS6)*, *1-AMINOCYCLOPROPANE-1-CARBOXYLIC ACID OXIDASE (ACO1)* and *ETHYLENE RESPONSE FACTOR (ERF)*, in MC and NC. Their research showed that, *ACS2* and *ACS6* expression was higher in the NC, which led to the conclusion that such vast differences in the expression of these genes can result in the ethylene overproduction and the induction of fast senescence processes in the NC. Additionally, an increased expression of the *ERF1* in NC in comparison to MC seem to be related to the high levels of oxidative stress present throughout the culture. It was demonstrated, that *ERF1* is upregulated in the response to abiotic stress triggers such as salt and cold treatments or water deficit (Lestari et al. 2018; Makhloufi et al. 2014).

## Conclusions

This study investigated the influence of the epigenetic modifications on the cell fate transition in long-term cultivated in vitro *Fagopyrum* callus lines with different capacity for morphogenesis. It was exhibited that; decreased level of H3K4me2 seems to be connected with pluripotency acquisition in *F. esculentum* EC and *F. tataricum* MC; DNA hypomethylation appears to be correlated with the acquisition of the embryogenic potential and PECC reinitiation in *F. tataricum* MC; out of all examined PTMs, H4K16ac and H4K5ac revealed the highest variability during the course of passage in NC. Elevated levels of these modifications on day zero and day six for H4K16ac and H4K5ac respectively, seem to be correlated with endoreplication peaks, the processes which are distinctive for this callus. To sum up, while *F. esculentum* EC displays the characteristics typical to irregular, disorganised callus tissue, *F. tataricum* MC behaves in a completely different way. The cyclical development,

disintegration and reinitiation of PECCs allowed to examine epigenetic changes and associate them with these processes. Comprehending how the chromatin reprogramming underlies the changes in the cell fate can provide a way for future manipulation towards the crop improvement, since once established during the callus formation, those modifications can be inherited through the epigenetic allele's transmission and become strategies for the crop manipulation in the future (Hemenway and Gehring 2023; Lee and Seo 2018). In the future study, annotation of the genes involved in the process of dedifferentiation/re-differentiation switch, their expression and their epigenetic status in connection of the PTMs should be considered.

**Supplementary Information** The online version contains supplementary material available at <https://doi.org/10.1007/s11240-023-02595-3>.

**Acknowledgements** This research was funded by the National Science Centre Poland, Project OPUS19 grant number 2020/37/B/NZ9/01499.

**Author contributions** AB acquired funding, AB and ABr, conceived, designed the study and supervised its execution, AT carried out the experiments with supervision from KSC and ABr, LSB prepared the statistical analysis, AT, AB, ABr analysed the obtained results, AT drafted the manuscript with contributions from all of the authors, AB, ABr performed review and editing. All of the authors read and approved the final manuscript.

**Data availability** All data generated or analysed during this study are included in this published article.

## Declarations

**Conflict of interest** The authors declare that they have no conflict of interest.

**Ethical approval** The use of all plant materials in this study complies with relevant institutional, national, and international guidelines and legislation. Seeds of *F. tataricum* (sample k-17) are from the collections of the N. I. Vavilov Institute of Plant Genetic Resources, Saint Petersburg, Russia. Obtained seeds were multiplied in Plant Cytogenetic and Molecular Biology Group Institute of Biology, Biotechnology and Environmental Protection, Faculty of Natural Sciences, University of Silesia in Katowice, Poland. *F. tataricum* sample k-17 is a common cultivated landrace of *F. tataricum* and seeds are available on request from authors of the publication. Seeds of *F. esculentum* genotype Panda are commercially available and were purchased from the Malopolska Plant Breeding Company.

**Open Access** This article is licensed under a Creative Commons Attribution 4.0 International License, which permits use, sharing, adaptation, distribution and reproduction in any medium or format, as long as you give appropriate credit to the original author(s) and the source, provide a link to the Creative Commons licence, and indicate if changes were made. The images or other third party material in this article are included in the article's Creative Commons licence, unless indicated otherwise in a credit line to the material. If material is not included in the article's Creative Commons licence and your intended use is not permitted by statutory regulation or exceeds the permitted use, you will need to obtain permission directly from the copyright holder. To view a copy of this licence, visit <http://creativecommons.org/licenses/by/4.0/>.

## References

- Adachi T, Yamaguchi A, Miike Y, Hoffmann F (1989) Plant regeneration from protoplasts of common buckwheat (*Fagopyrum esculentum*). *Plant Cell Rep* 8:247–250
- Akulov AN, Gumerova EA & Romyantseva NI (2018) Cell cultures of *Fagopyrum tataricum* as a source of biologically active phenolic compounds. *Buckwheat Germplasm in the World*. 259–270
- Avivi Y, Morad V, Ben-Meir H, Zhao J, Kashkush K, Tzfira T, Citovsky V, Grafi G (2004) Reorganization of specific chromosomal domains and activation of silent genes in plant cells acquiring pluripotentiality. *Dev Dyn* 230(1):12–22. <https://doi.org/10.1002/dvdy.20006>
- Ayyappan V, Kalavacharla V, Thimmapuram J, Bhide KP, Sripathi VR, Smolinski TG, Manoharan M, Thurston Y, Todd A, Kingham B (2015) Genome-wide profiling of histone modifications (H3K9me2 and H4K12ac) and gene expression in rust (*Uromyces appendiculatus*) inoculated common bean (*Phaseolus vulgaris* L.). *PLoS One* 10(7):e0132176. <https://doi.org/10.1371/journal.pone.0132176>
- Bednarek PT, Orłowska R (2019) Plant tissue culture environment as a switch-key of (epi)genetic changes. *Plant Cell Tiss Org* 140(2):245–257. <https://doi.org/10.1007/s11240-019-01724-1>
- Bennett M, Cleaves K, Hewezi T (2021) Expression patterns of DNA methylation and demethylation genes during plant development and in response to phytohormones. *Int J Mo Sci* 22(18):9681. <https://doi.org/10.3390/ijms22189681>
- Berbec A, Doroszevska T (1999) Regeneration in vitro of three cultivars of buckwheat (*Fagopyrum esculentum* Moench.) as affected by medium composition. *Fagopyrum* 16:49–52
- Betekhtin A, Rojek M, Jaskowiak J, Milewska-Hendel A, Kwasniewska J, Kostyukova Y, Kurczynska E, Romyantseva N, Hasterok R (2017) Nuclear genome stability in long-term cultivated callus lines of *Fagopyrum tataricum* (L.) Gaertn. *PLoS One* 12(3):e0173537. <https://doi.org/10.1371/journal.pone.0173537>
- Betekhtin A, Pinski A, Milewska-Hendel A, Kurczynska E, Hasterok R (2019) Stability and instability processes in the calli of *Fagopyrum tataricum* that have different morphogenic potentials. *Plant Cell Tiss Org* 137(2):343–357. <https://doi.org/10.1007/s11240-019-01575-w>
- Birnbaum KD, Roudier F (2017) Epigenetic memory and cell fate reprogramming in plants. *Regeneration* 4(1):15–20. <https://doi.org/10.1002/reg2.73>
- Birnbaum KD, Sanchez Alvarado A (2008) Slicing across kingdoms: regeneration in plants and animals. *Cell* 132(4):697–710. <https://doi.org/10.1016/j.cell.2008.01.040>
- Braszewska-Zalewska A, Bernas T, Maluszynska J (2010) Epigenetic chromatin modifications in *Brassica* genomes. *Genome* 53(3):203–210. <https://doi.org/10.1139/g09-088>
- Braszewska-Zalewska A, Dziurlikowska A, Maluszynska J (2012) Histone H3 methylation patterns in *Brassica nigra*, *Brassica juncea*, and *Brassica carinata* species. *Genome* 55(1):68–74. <https://doi.org/10.1139/g11-076>
- Braszewska-Zalewska AJ, Wolny EA, Smialek L, Hasterok R (2013) Tissue-specific epigenetic modifications in root apical meristem cells of *Hordeum vulgare*. *PLoS One* 8(7):e69204. <https://doi.org/10.1371/journal.pone.0069204>
- Chakrabarty D, Yu KW, Paek KY (2003) Detection of DNA methylation changes during somatic embryogenesis of Siberian ginseng (*Eleutherococcus senticosus*). *Plant Sci* 165(1):61–68. [https://doi.org/10.1016/s0168-9452\(03\)00127-4](https://doi.org/10.1016/s0168-9452(03)00127-4)
- Cheng K, Xu Y, Yang C, Ouellette L, Niu L, Zhou X, Chu L, Zhuang F, Liu J, Wu H, Charron JB, Luo M (2020) Histone tales: lysine methylation, a protagonist in Arabidopsis development. *J Exp Bot* 71(3):793–807. <https://doi.org/10.1093/jxb/erz435>
- Ci H, Li C, Aung TT, Wang S, Yun C, Wang F, Ren X, Zhang X (2022) A Comparative transcriptome analysis reveals the molecular mechanisms that underlie somatic embryogenesis in *Peaonia ostii* “Fengdan.” *Int J Mol Sci* 23(18):10595. <https://doi.org/10.3390/ijms231810595>
- Ckurshumova W, Berleth T (2015) Overcoming recalcitrance - Auxin response factor functions in plant regeneration. *Plant Signal Behav* 10(7):e993293. <https://doi.org/10.4161/15592324.2014.993293>
- Debeaujon I, Nesi N, Perez P, Devic M, Grandjean O, Caboche M, Lepiniec L (2003) Proanthocyanidin-accumulating cells in Arabidopsis testa: regulation of differentiation and role in seed development. *Plant Cell* 15(11):2514–2531. <https://doi.org/10.1105/tpc.014043>
- Desvoyes B, Fernandez-Marcos M, Sequeira-Mendes J, Otero S, Vergara Z, Gutierrez C (2014) Looking at plant cell cycle from the chromatin window. *Front Plant Sci* 5:369. <https://doi.org/10.3389/fpls.2014.00369>
- Feher A (2019) Callus, dedifferentiation, totipotency, somatic embryogenesis: what these terms mean in the era of molecular plant biology? *Front Plant Sci* 10:536. <https://doi.org/10.3389/fpls.2019.00536>
- Fei Y, Wang LX, Fang ZW, Liu ZX (2019) Somatic embryogenesis and plant regeneration from cotyledon and hypocotyl explants of *Fagopyrum esculentum* Moench *lpls* mutant. *Agronomy* 9(11):768. <https://doi.org/10.3390/agronomy9110768>
- Fraga HP, Vieira LN, Caprestano CA, Steinmacher DA, Micke GA, Spudeit DA, Pescador R, Guerra MP (2012) 5-Azacytidine combined with 2,4-D improves somatic embryogenesis of *Acca sellowiana* (O. Berg) Burret by means of changes in global DNA methylation levels. *Plant Cell Rep* 31(12):2165–76. <https://doi.org/10.1007/s00299-012-1327-8>
- Gamborg OL, Miller RA, Ojima K (1968) Nutrient requirements of suspension cultures of soybean root cells. *Exp Cell Res* 50(1):151–158. [https://doi.org/10.1016/0014-4827\(68\)90403-5](https://doi.org/10.1016/0014-4827(68)90403-5)
- Gao L, Liu J, Liao L, Gao A, Njuguna BN, Zhao C, Zheng B, Han Y (2023) Callus induction and adventitious root regeneration of cotyledon explants in peach trees. *Horticulturae* 9(8):850. <https://doi.org/10.3390/horticulturae9080850>
- Ghosh A, Igamberdiev AU, Debnath SC (2021) Tissue culture-induced DNA methylation in crop plants: a review. *Mol Biol Rep* 48(1):823–841. <https://doi.org/10.1007/s11033-020-06062-6>
- Han Z, Crisp PA, Stelpflug S, Kaepler SM, Li Q, Springer NM (2018) Heritable epigenomic changes to the maize methylome resulting from tissue culture. *Genetics* 209(4):983–995. <https://doi.org/10.1534/genetics.118.300987>
- Hao J, Pei Y, Qu Y & Zheng C Study on callus differentiation conditions of common buckwheat. In: 7th International Symposium on Buckwheat, Winnipeg, MB, Canada., 12–14 August 1998. p 12–14
- Hemenway EA, Gehring M (2023) Epigenetic regulation during plant development and the capacity for epigenetic memory. *Annu Rev Plant Biol* 74:87–109. <https://doi.org/10.1146/annurev-arplant-070122-025047>
- Horstman A, Li M, Heidmann I, Weemen M, Chen B, Muino JM, Angenent GC, Boutilier K (2017) The *BABY BOOM* transcription factor activates the *LEC1-ABI3-FUS3-LEC2* network to induce somatic embryogenesis. *Plant Physiol* 175(2):848–857. <https://doi.org/10.1104/pp.17.00232>
- Hu H, Du J (2022) Structure and mechanism of histone methylation dynamics in Arabidopsis. *Curr Opin Plant Biol* 67:102211. <https://doi.org/10.1016/j.pbi.2022.102211>
- Inacio V, Martins MT, Graca J, Morais-Cecilio L (2018) Cork oak young and traumatic periderms show PCD typical chromatin patterns but different chromatin-modifying genes expression. *Front Plant Sci* 9:1194. <https://doi.org/10.3389/fpls.2018.01194>

- Ishihara H, Sugimoto K, Tarr PT, Temman H, Kadokura S, Inui Y, Sakamoto T, Sasaki T, Aida M, Suzuki T, Inagaki S, Morohashi K, Seki M, Kakutani T, Meyerowitz EM, Matsunaga S (2019) Primed histone demethylation regulates shoot regenerative competency. *Nat Commun* 10(1):1786. <https://doi.org/10.1038/s41467-019-09386-5>
- Jasencakova Z, Meister A, Walter J, Turner BM, Schubert I (2000) Histone H4 acetylation of euchromatin and heterochromatin is cell cycle dependent and correlated with replication rather than with transcription. *Plant Cell* 12:2087–2100
- Jasencakova Z, Meister A, Schubert I (2001) Chromatin organization and its relation to replication and histone acetylation during the cell cycle in barley. *Chromosoma* 110(2):83–92. <https://doi.org/10.1007/s004120100132>
- Jasencakova Z, Soppe WJ, Meister A, Gernand D, Turner BM, Schubert I (2003) Histone modifications in Arabidopsis- high methylation of H3 lysine 9 is dispensable for constitutive heterochromatin. *Plant J* 33(3):471–480. <https://doi.org/10.1046/j.1365-3113x.2003.01638.x>
- Ji L, Mathioni SM, Johnson S, Tucker D, Bewick AJ, Do Kim K, Daron J, Slotkin RK, Jackson SA, Parrott WA, Meyers BC, Schmitz RJ (2019) Genome-wide reinforcement of DNA methylation occurs during somatic embryogenesis in soybean. *Plant Cell* 31(10):2315–2331. <https://doi.org/10.1105/tpc.19.00255>
- Jiang D, Kong NC, Gu X, Li Z, He Y (2011) Arabidopsis COMPASS-like complexes mediate histone H3 lysine-4 trimethylation to control floral transition and plant development. *PLoS Genet* 7(3):e1001330. <https://doi.org/10.1371/journal.pgen.1001330>
- Jin H, Jia JF, Hao JG (2002) Efficient plant regeneration in vitro in buckwheat. *Plant Cell Tiss Org* 69:293–295
- Kaeppler SM, Keppeler HF, Rhee Y (2000) Epigenetic aspects of somaclonal variation in plants. *Plant Mol Biol* 43:179–188
- Kamalova GV, Akulov AN, Romyantseva NI (2009) Comparison of redox state of cells of tatar buckwheat morphogenic calluses and non-morphogenic calluses obtained from them. *Biochemistry (mosc)* 74(6):686–694. <https://doi.org/10.1134/s0006297909060145>
- Kassambara A (2022) 'ggplot2' Based Publication Ready Plots, R package version 0.4.0, <<https://CRAN.R-project.org/package=ggpubr>>. R package version 0.4.0 edn
- Kim JY, Yang W, Forner J, Lohmann JU, Noh B, Noh YS (2018) Epigenetic reprogramming by histone acetyltransferase HAG1/AtGCN5 is required for pluripotency acquisition in Arabidopsis. *EMBO J*. <https://doi.org/10.15252/embj.201798726>
- Kouzarides T (2007) Chromatin modifications and their function. *Cell* 128(4):693–705. <https://doi.org/10.1016/j.cell.2007.02.005>
- Kwon SJ, Han MH, Huh YS, Roy SK, Lee CW, Woo SH (2013) Plantlet regeneration via somatic embryogenesis from hypocotyls of common buckwheat (*Fagopyrum esculentum* Moench.). *Korean J Crop Sci* 58(4):331–335. <https://doi.org/10.7740/kjcs.2013.58.4.331>
- Lee K, Seo PJ (2018) Dynamic epigenetic changes during plant regeneration. *Trends Plant Sci* 23(3):235–247. <https://doi.org/10.1016/j.tplants.2017.11.009>
- Lee K, Park OS, Jung SJ, Seo PJ (2016) Histone deacetylation-mediated cellular dedifferentiation in Arabidopsis. *J Plant Physiol* 191:95–100. <https://doi.org/10.1016/j.jplph.2015.12.006>
- Lee KP, Park O-S, Seo PJ (2017) Arabidopsis ATXR2 deposits H3K36me3 at the promoters of LBD genes to facilitate cellular dedifferentiation. *Sic Signal* 10:eaan0316
- Lee K, Park OS, Choi CY, Seo PJ (2019) ARABIDOPSIS TRITHORAX 4 facilitates shoot identity establishment during the plant regeneration process. *Plant Cell Physiol* 60(4):826–834. <https://doi.org/10.1093/pcp/pcy248>
- Leljak-Levanic D, Bauer N, Mihaljevic S, Jelaska S (2004) Changes in DNA methylation during somatic embryogenesis in *Cucurbita pepo* L. *Plant Cell Rep* 23(3):120–127. <https://doi.org/10.1007/s00299-004-0819-6>
- Lestari R, Rio M, Martin F, Leclercq J, Woraathasin N, Roques S, Dessailly F, Clement-Vidal A, Sanier C, Fabre D, Melliti S, Suharsono S, Montoro P (2018) Overexpression of *Hevea brasiliensis* ethylene response factor HbERF-IXc5 enhances growth and tolerance to abiotic stress and affects laticifer differentiation. *Plant Biotechnol J* 16(1):322–336. <https://doi.org/10.1111/pbi.12774>
- Li HL, Guo D, Zhu JH, Wang Y, Peng SQ (2017) Identification and expression analysis of genes involved in histone acetylation in *Hevea brasiliensis*. *Tree Genet Genomes*. <https://doi.org/10.1007/s11295-017-1178-0>
- Li X, Han JD, Fang YH, Bai SN, Rao GY (2017) Expression analyses of embryogenesis-associated genes during somatic embryogenesis of *Adiantum capillus-veneris* L. in vitro: new insights into the evolution of reproductive organs in land plants. *Front Plant Sci* 8:658. <https://doi.org/10.3389/fpls.2017.00658>
- Li HL, Guo D, Zhu JH, Wang Y, Peng SQ (2020) Identification of histone methylation modifiers and their expression patterns during somatic embryogenesis in *Hevea brasiliensis*. *Genet Mol Biol* 43(1):e20180141. <https://doi.org/10.1590/1678-4685-GMB-2018-0141>
- Ma J, Li Q, Zhang L, Cai S, Liu Y, Lin J, Huang R, Yu Y, Wen M, Xu T (2022) High auxin stimulates callus through SDG8-mediated histone H3K36 methylation in *Arabidopsis*. *J Integr Plant Biol* 64(12):2425–2437. <https://doi.org/10.1111/jipb.13387>
- Machczyńska J, Orłowska R, Mańkowski DR, Zimny J, Bednarek PT (2014) DNA methylation changes in triticale due to in vitro culture plant regeneration and consecutive reproduction. *Plant Cell Tiss Org* 119(2):289–299. <https://doi.org/10.1007/s11240-014-0533-1>
- Makhloufi E, Yousfi FE, Marande W, Mila I, Hanana M, Berges H, Mzid R, Bouzayen M (2014) Isolation and molecular characterization of ERF1, an ethylene response factor gene from durum wheat (*Triticum turgidum* L. subsp. *durum*), potentially involved in salt-stress responses. *J Exp Bot* 65(22):6359–71. <https://doi.org/10.1093/jxb/eru352>
- Mendiburu F (2021) Statistical procedures for agricultural research, R package version 1.3–5, <<https://CRAN.R-project.org/package=agricolae>>. In: <https://CRAN.R-project.org/package=agricolae>
- Miguel C, Marum L (2011) An epigenetic view of plant cells cultured in vitro: somaclonal variation and beyond. *J Exp Bot* 62(11):3713–3725. <https://doi.org/10.1093/jxb/err155>
- Monja-Mio KM, Quiroz-Moreno A, Herrera-Herrera G, Montero-Muñoz JL, Sánchez-Teyer F, Robert ML (2018) Analysis of two clonal lines (embryogenic and non-embryogenic) of *Agave fourcroydes* using AFLP and MSAP. *A J Plant Sci* 9(4):745–762. <https://doi.org/10.4236/ajps.2018.94059>
- Moronczyk J, Braszewska A, Wojcikowska B, Chwialkowska K, Nowak K, Wojcik AM, Kwasniewski M, Gaj MD (2022) Insights into the histone acetylation-mediated regulation of the transcription factor genes that control the embryogenic transition in the somatic cells of Arabidopsis. *Cells* 11(5):863. <https://doi.org/10.3390/cells11050863>
- Neelakandan AK, Wang K (2012) Recent progress in the understanding of tissue culture-induced genome level changes in plants and potential applications. *Plant Cell Rep* 31(4):597–620. <https://doi.org/10.1007/s00299-011-1202-z>
- Nesković M, Vujčić R, Budimir S (1987) Somatic embryogenesis and bud formation from immature embryos of buckwheat (*Fagopyrum esculentum* Moench.). *Plant Cell Rep* 6:423–426
- Nic-Can GI, Lopez-Torres A, Barredo-Pool F, Wrobel K, Loyola-Vargas VM, Rojas-Herrera R, De-la-Pena C (2013) New insights into somatic embryogenesis: *LEAFY COTYLEDON1*, *BABY BOOM1* and *WUSCHEL-RELATED HOMEBOX4* are epigenetically regulated in *Coffea canephora*. *PLoS One* 8(8):e72160. <https://doi.org/10.1371/journal.pone.0072160>

- Park SY, Murthy HN, Chakrabarthi D, Paek KY (2008) Detection of epigenetic variation in tissue-culture-derived plants of *Doritaenopsis* by methylation-sensitive amplification polymorphism (MSAP) analysis. *In Vitro Cell Dev Biol Plant* 45(1):104–108. <https://doi.org/10.1007/s11627-008-9166-6>
- Rodriguez-Sanz H, Moreno-Romero J, Solis MT, Kohler C, Risueno MC, Testillano PS (2014) Changes in histone methylation and acetylation during microspore reprogramming to embryogenesis occur concomitantly with Bn HKMT and Bn HAT expression and are associated with cell totipotency, proliferation, and differentiation in *Brassica napus*. *Cytogenet Genome Res* 143(1–3):209–218. <https://doi.org/10.1159/000365261>
- Roudier F, Ahmed I, Berard C, Sarazin A, Mary-Huard T, Cortijo S, Bouyer D, Caillieux E, Duvernois-Berthet E, Al-Shikhley L, Giraut L, Despres B, Drevensek S, Barneche F, Derozier S, Brunaud V, Aubourg S, Schnittger A, Bowler C, Martin-Magniette ML, Robin S, Caboche M, Colot V (2011) Integrative epigenomic mapping defines four main chromatin states in Arabidopsis. *EMBO J* 30(10):1928–1938. <https://doi.org/10.1038/emboj.2011.103>
- Rumyantseva NI, Sergejewa NB, Khakimova LE, Salnikov BB, Gumerova EA, Lozowaja BB (1989) Organogenesis and somatic embryogenesis in tissue culture of two buckwheat species. *Russ J Plant Physiol* 36:187–194
- Rumyantseva NI, Samaj J, Ensikat H-J, Sal'nikov VV, Kostjukova YA, BaluSka F, Volkman D (2003) Changes in the extracellular matrix surface network during cyclic reproduction of proembryonic cell complexes in the *Fagopyrum tataricum* (L.) Gaertn callus. *Dokl Biol Sci* 391:375–378
- Rumyantseva NI, Akulov AN, Mukhitov AR (2004) Extracellular polymers in callus cultures of *Fagopyrum tataricum* (L.) Gaertn. with different morphogenic activities: time courses during the culture cycle. *Appl Biochem Microbiol* 40(5):494–500
- Rumyantseva NI, Sal'nikov VV, Lebedeva VV (2005) Structural changes of cell surface in callus of *Fagopyrum esculentum* Moench. during induction of morphogenesis. *Russ J Plant Physiol* 52(3):381–387
- Rymen B, Kawamura A, Lambomez A, Inagaki S, Takebayashi A, Iwase A, Sakamoto Y, Sako K, Favero DS, Ikeuchi M, Suzuki T, Seki M, Kakutani T, Roudier F, Sugimoto K (2019) Histone acetylation orchestrates wound-induced transcriptional activation and cellular reprogramming in Arabidopsis. *Commun Biol* 2:404. <https://doi.org/10.1038/s42003-019-0646-5>
- Sakar D, Naik PS (2000) Phloroglucinol enhances growth and rate of axillary shoot proliferation in potato shoot tip cultures in vitro. *Plant Cell Tiss Org* 60(2):139–149
- Simsek Geyik M, Yazicilar B, Bezirganoglu İ (2022) Microscopic and physiological analysis of somatic embryos under in vitro culture in Triticale. *Icontech Int J* 6(1):73–80. <https://doi.org/10.46291/ICONTECHvol6iss1pp73-80>
- Souter M, Lindsey K (2000) Polarity and signalling in plant embryogenesis. *J Exp Bot* 51(347):971–983. <https://doi.org/10.1093/jexbot/51.347.971>
- Springer NM, Schmitz RJ (2017) Exploiting induced and natural epigenetic variation for crop improvement. *Nat Rev Gen* 18(9):563–575. <https://doi.org/10.1038/nrg.2017.45>
- Srejovic V, Neskovic M (1981) Regeneration of plants from cotyledon fragments of buckwheat (*Fagopyrum esculentum* Moench.). *Z Pflanzenphysiol* 104:37–42
- Stroud H, Ding B, Simon SA, Feng S, Bellizzi M, Pellegrini M, Wang GL, Meyers BC, Jacobsen SE (2013) Plants regenerated from tissue culture contain stable epigenome changes in rice. *Elife* 2:e00354. <https://doi.org/10.7554/eLife.00354>
- Takahata YJ, Jumonji E (1985) Plant regeneration from hypocotyl section and callus in buckwheat (*Fagopyrum esculentum* Moench.). *Ann Rep Fac Educ* 45:137–142
- Team RC (2022a) R: A Language and environment for statistical computing. Vienna, Austria: R foundation for statistical computing. URL: <https://www.R-project.org/>. In: <https://www.R-project.org/> Accessed 1.02.2023
- Team RS (2022b) RStudio: Integrated development environment for R; RStudio, PBC, Boston, MA. URL: <http://www.rstudio.com/>. In: <http://www.rstudio.com/> Accessed 1.02.2023
- Tomasiak A, Zhou M, Betekhtin A (2022) Buckwheat in tissue culture research: current status and future perspectives. *Int J Mol Sci* 23(4):2298. <https://doi.org/10.3390/ijms23042298>
- Us-Camas R, Rivera-Solís G, Duarte-Aké F, De-la-Peña C (2014) In vitro culture: an epigenetic challenge for plants. *Plant Cell Tiss Org* 118(2):187–201. <https://doi.org/10.1007/s11240-014-0482-8>
- Viejo M, Rodriguez R, Valledor L, Perez M, Canal MJ, Hasbun R (2010) DNA methylation during sexual embryogenesis and implications on the induction of somatic embryogenesis in *Castanea sativa* Miller. *Sex Plant Reprod* 23(4):315–323. <https://doi.org/10.1007/s00497-010-0145-9>
- Wickham H (2022) Easily install and load the 'Tidyverse' R package version 1.2.0, <<https://CRAN.R-project.org/package=tidyverse>>. In: <https://cran.r-project.org/package=tidyverse>
- Wickramasuriya AM, Dunwell JM (2015) Global scale transcriptome analysis of Arabidopsis embryogenesis in vitro. *BMC Genomics* 16(1):301. <https://doi.org/10.1186/s12864-015-1504-6>
- Williams L, Zhao J, Morozova N, Li Y, Avivi Y, Grafi G (2003) Chromatin reorganization accompanying cellular dedifferentiation is associated with modifications of histone H3, redistribution of HP1, and activation of E2F-target genes. *Dev Dyn* 228(1):113–120. <https://doi.org/10.1002/dvdy.10348>
- Wolny E, Braszewska-Zalewska A, Hasterok R (2014) Spatial distribution of epigenetic modifications in *Brachypodium distachyon* embryos during seed maturation and germination. *PLoS One* 9(7):e101246. <https://doi.org/10.1371/journal.pone.0101246>
- Xu L, Huang H (2014) Genetic and epigenetic controls of plant regeneration. *Curr Top Dev Biol* 108:1–33. <https://doi.org/10.1016/B978-0-12-391498-9.00009-7>
- Yamamoto N, Kobayashi H, Togashi T, Mori Y, Kikuchi K, Kuriyama K, Tokui Y (2005) Formation of embryogenic cell clumps from carrot epidermal cells is suppressed by 5-azacytidine, a DNA methylation inhibitor. *J Plant Physiol* 162(1):47–54. <https://doi.org/10.1016/j.jplph.2004.05.013>
- Yamane Y (1985) Induced differentiation of buckwheat plants from subcultured calluses in vitro. *Jpn J Genet* 49:139–146
- Yao X, Feng H, Yu Y, Dong A, Shen WH (2013) SDG2-mediated H3K4 methylation is required for proper Arabidopsis root growth and development. *PLoS One* 8(2):e56537. <https://doi.org/10.1371/journal.pone.0056537>
- Yu Y, Bu Z, Shen W-H, Dong A (2009) An update on histone lysine methylation in plants. *Prog Nat Sci* 19(4):407–413. <https://doi.org/10.1016/j.pnsc.2008.07.015>
- Zakrzewski F, Schmidt M, Van Lijsebettens M, Schmidt T (2017) DNA methylation of retrotransposons, DNA transposons and genes in sugar beet (*Beta vulgaris* L.). *Plant J* 90(6):1156–1175. <https://doi.org/10.1111/tpj.13526>
- Zhang T, Cooper S, Brockdorff N (2015) The interplay of histone modifications-writers that read. *EMBO Rep* 16(11):1467–1481. <https://doi.org/10.15252/embr.201540945>
- Zhang H, Guo F, Qi P, Huang Y, Xie Y, Xu L, Han N, Xu L, Bian H (2020) OsHDA710-mediated histone deacetylation regulates callus formation of rice mature embryo. *Plant Cell Physiol* 61(9):1646–1660. <https://doi.org/10.1093/pcp/pcaa086>
- Zhao J, Morozova N, Williams L, Libs L, Avivi Y, Grafi G (2001) Two phases of chromatin decondensation during dedifferentiation of plant cells: distinction between competence for cell fate switch and a commitment for S phase. *J Biol Chem*

276(25):22772–22778. <https://doi.org/10.1074/jbc.M101756200>

Zhao N, Zhang K, Wang C, Yan H, Liu Y, Xu W, Su Z (2020) Systematic analysis of differential H3K27me3 and H3K4me3 deposition in callus and seedling reveals the epigenetic regulatory mechanisms involved in callus formation in rice. *Front Genet* 11:766. <https://doi.org/10.3389/fgene.2020.00766>

Zheng B, Liu J, Gao A, Chen X, Gao L, Liao L, Luo B, Ogutu CO, Han Y (2022) Epigenetic reprogramming of H3K27me3 and

DNA methylation during leaf-to-callus transition in peach. *Hortic Res* 9:uhac132. <https://doi.org/10.1093/hr/uhac132>

**Publisher's Note** Springer Nature remains neutral with regard to jurisdictional claims in published maps and institutional affiliations.

### 8.1.3 Zbadanie korelacji między poziomem modyfikacji epigenetycznych w genach kodujących białka i polisacharydy ściany komórkowej, a procesami odróżnicowania i różnicowania w kalusach *F. tataricum* o różnej zdolności do regeneracji

#### Publikacja P3:

**Tomasiak A.**, Pinski A., Milewska-Hendel A., Andreu Godall, I., Borowska-Żuchowska N., Morończyk J., Moreno-Romero J., Betekhtin A. H3K4me3 changes occur in cell wall genes during the development of *Fagopyrum tataricum* morphogenic and non-morphogenic calli.

Frontiers in Plant Science, **2024**, 15, 1465514

<https://doi.org/10.3389/fpls.2024.1465514>

IF<sub>2024</sub>: 4,1

Punkty MNiSW: 100

W przedstawionej pracy przeprowadzono analizę sekwencjonowania ChIP (ChIP-seq, z *ang. chromatin immunoprecipitation-sequencing*), która pozwoliła na stworzenie profilu trimetylacji histonu H3 na lizynie 4 (H3K4me3) w genomie *F. tataricum* i na porównanie genomowej zawartości tej modyfikacji pomiędzy MK i NK. Modyfikacja H3K4me3 jest związana z euchromatyną i ekspresją genów, wyselekcjonowana została na podstawie przeprowadzonych wcześniej analiz immunocytochemicznych (wyłoniły one różnice w globalnej zawartości tego markera pomiędzy dniem drugim i szóstym pasażu). Warto podkreślić, że na drugi dzień pasażu następuje dezintegracja PEKK, natomiast około dnia szóstego inicjowane są procesy związane z powstawaniem nowych PEKK. Wykorzystano również metodę immunoprecypitacji chromatyny tkanki nieutrwalonej (natywnej) (ChIP-qPCR, z *ang. ChIP- quantitative polymerase chain reaction*) do analizy zmian w poziomie H3K4me3 w genach kodujących białka i polisacharydy ściany komórkowej (*METYLOESTERAZA PEKTYNOWA (PME)*, *INHIBITOR METYLOESTERAZY PEKTYNOWEJ (PMEI)*, *PEROKSYDAZA (PX)*, *EKSTENSYNY (EXT1, EXT2)* i *POLIGALAKTURONAZY (PG1, PG2)* w MK oraz NK. Badania zostały uzupełnione analizą immunohistochemiczną pozwalającą na lokalizację epitopów białek oraz polisacharydów ściany komórkowej.

Analizy ChIP-seq zostały wykonane przez firmę Diagenode s. a. (Belgia). Tkanki MK i NK utrwalono w paraformaldehydzie zgodnie z instrukcjami firmy, w której następnie



przeprowadzono reakcję immunoprecypitacji tkanki usieciowanej (z *ang. crosslinked chromatin immunoprecipitation, X-ChIP*). Kolejno, tkanki po immunoprecypitacji poddano sekwencjonowaniu i użyto do przeprowadzenia analiz bioinformatycznych w celu porównania globalnego poziomu H3K4me3 w MK i NK. Odczyty sekwencjonowania zostały zmapowane na genom *F. tataricum*, co pozwoliło na uzyskanie tzw. ‘tagów’. Dystrybucja sygnału H3K4me3 w genomie *F. tataricum* wykazała, że 25,06% zmapowanych tagów występuje w regionie sekwencji kodujących, 46,54% jest zlokalizowanych w regionach międzygenowych, 12,10% występuje w regionie intronów, 10,03% w miejscach startu transkrypcji (z *ang. transcription start site; TSS*), a 6,27% w regionach końca transkrypcji (z *ang. transcription termination site; TTS*). Obecność H3K4me3 jest wyraźnie zaznaczona w TSS, natomiast brak jej w elementach powtarzalnych, takich jak transpozony. Analiza statystyczna porównująca interakcje białko histonowe - DNA (z *ang. differential binding analysis*) w intensywności zmapowanych tagów H3K4me3 między MK i NK wyłoniła 7372 lokalizacje, w których poziom H3K4me3 był statystycznie różny, czyli taki którego wysokość istotnie różni się od sygnału w rozkładzie tła. Spośród tych lokalizacji, 4289 wykazywało różnicę minimum 1,5 razy w intensywności sygnału H3K4me3 pomiędzy MK i NK. Rozkład genomowy tych 4289 regionów wykazał, że większość z nich związana jest z eksonami i regionami międzygenowymi. Regiony promotorowe i TSS stanowią tylko 10,03% tych regionów. Na podstawie rozkładu intensywności tagów H3K4me3 w TSS założono, że różnicowo wzbogacone regiony sklasyfikowane jako promotor (TSS) i pierwszy ekson odgrywają najważniejszą rolę w regulacji ekspresji genów. Z tego powodu przeanalizowano geny, których TSS był w bliskiej odległości (mniej niż 1 kb) od różnicowo wzbogaconych regionów. Uzyskano 1709 genów, spośród których w 1057 genach H3K4me3 była wyższa w MK, a w 652 genach wyższy poziom tej modyfikacji przeważał w NK. Wśród tych genów, skupiono się na tych związanych ze ścianą komórkową.

Do analiz ChIP-qPCR oraz RT-qPCR wyselekcjonowano następujące geny: *PMEI*, *PME*, *PX*, *EXT1* i *EXT2* oraz *PG1* i *PG2*. Celem badań była analiza poziomu ekspresji genów i poziomu H3K4me3 w dwóch punktach czasowych hodowli, tj. w dniu drugim i szóstym. Z genów, które były wzbogacone w H3K4me3 w NK w dniu jedenastym, zbadano *PMEI*, *PME* i *PX*. *PMEI* wykazał znaczny poziom tego markera w NK już w dniu drugim. Pomimo, że H3K4me3 była związana z wyższą aktywnością transkrypcyjną, wykazano statystycznie niższe poziomy ekspresji w NK zarówno w dniu drugim, jak i szóstym. Gen *PME* nie był wzbogacony w H3K4me3 w NK oraz MK w dniu drugim oraz szóstym, co sugeruje. Poziomy ekspresji *PME* były poniżej granic wykrywalności w RT-qPCR, co korelowało z niskim poziomem H3K4me3.

W przypadku *PX* poziomy H3K4me3 były istotnie wyższe tylko w NK w dniu szóstym. W tym przypadku, poziom ekspresji *PX* w NK w dniu szóstym wzrósł znacząco, osiągając poziom 39,4 razy wyższy niż w NK w dniu drugim, co korelowało z wyższym poziomem H3K4me3. Z genów, które wykazały wyższe poziomy H3K4me3 w MK niż w NK, analizowano *EXT1*, *EXT2*, *PG1* i *PG2*. Dla *EXT1* i *EXT2* nie zaobserwowano istotnych różnic w poziomach H3K4me3 w dniu drugim, natomiast znaczący wzrost zaobserwowano w dniu szóstym. Dla *EXT1*, ekspresja genu pozostała stabilna w obu punktach czasowych i w obu typach kalusa, podczas gdy *EXT2* wykazał wyższą ekspresję w NK w porównaniu do MK w dniu drugim, ale niższą ekspresję w NK w dniu szóstym (spadek o 41,7 razy w porównaniu do MK w dniu drugim). Podobnie jak w przypadku *PMEI*, ekspresja *EXT2* nie korelowała z poziomami H3K4me3. Poziom H3K4me3 w *PG1* i *PG2* w badanych dniach nie wykazał statystycznie istotnych różnic. Ekspresja *PG1* była istotnie wyższa w MK niż w NK w obu punktach czasowych hodowli. Podobnie jak w przypadku *PG1*, w *PG2* ekspresja w MK była wyższa niż w NK, ale miało to miejsce tylko w dniu drugim. Nagromadzenie H3K4me3 obserwowane w *PG1* i *PG2* w MK, mimo że nie było statystycznie istotne, wskazuje na potencjalną rolę tej modyfikacji w utrzymaniu wyższej ekspresji genów.

Badania immunohistochemiczne ściany komórkowej w MK i NK *F. tataricum* przeprowadzono z wykorzystaniem wybranych przeciwciał skierowanych przeciwko epitopom pektyn (LM5, LM6, LM19 i LM20) oraz ekstensyn (JIM20). Podobnie jak w przypadku analizy ChIP-qPCR oraz RT-qPCR, do badań wykorzystano kalus z drugiego i szóstego dnia pasażu. Wyniki pokazały zróżnicowanie występowania badanych epitopów zarówno między MK i NK, jak i między dniami pasażu. Epitop rozpoznawany przez przeciwciało LM5 był obecny w MK i NK jedynie w ścianie komórkowej, niezależnie od badanego dnia. Epitop rozpoznawany przez przeciwciało LM6 nie występował w NK, natomiast w MK był obserwowany od szóstego dnia pasażu i występował punktowo w kompartmentach cytoplazmatycznych. W przypadku epitopu rozpoznawanego przez przeciwciało LM19 nie zaobserwowano różnic w jego występowaniu między MK i NK. LM19 był obserwowany w obu badanych dniach pasażu i był zlokalizowany w ścianie komórkowej, kompartmentach cytoplazmatycznych, oraz na powierzchni komórek kalusa. Przeciwciało LM20 było wykryte zarówno w MK i NK bez względu na badany dzień. Epitop ten był zlokalizowany w ścianie komórkowej oraz na powierzchni komórek peryferycznych w obu kalusach, natomiast w NK dodatkowo był wykrywany w kompartmentach cytoplazmatycznych. Epitop JIM20 był obserwowany jedynie w MK w szóstym dniu pasażu w kompartmentach cytoplazmatycznych.

Podsumowując, przeprowadzone badania dostarczyły nowych informacji na temat epigenetycznej regulacji rozwoju kalusa *F. tataricum*. Podkreślono kluczową rolę modyfikacji H3K4me3 podczas aktywacji genów zaangażowanych w biosyntezę i modyfikację składników ściany komórkowej, niezbędnych dla morfogenezy i regeneracji tkanek roślinnych. Trzeba podkreślić, że jest to pierwsza praca wykorzystująca technikę ChIP-qPCR na tkankach gatunku *Fagopyrum*.

**Publikacja P3:** H3K4me3 changes occur in cell wall genes during the development of *Fagopyrum tataricum* morphogenic and non-morphogenic calli

**Tomasiak A.,** Pinski A., Milewska-Hendel A., Andreu Godall, I., Borowska-Żuchowska N., Morończyk J., Moreno-Romero J., Betekhtin A. H3K4me3 changes occur in cell wall genes during the development of *Fagopyrum tataricum* morphogenic and non-morphogenic calli

Frontiers in Plant Science, **2024**, 15, 1465514

<https://doi.org/10.3389/fpls.2024.1465514>

IF<sub>2024</sub>: 4,1

Punkty MNiSW: 100

Materiały uzupełniające dostępne online

<https://www.frontiersin.org/articles/10.3389/fpls.2024.1465514/full#supplementary-material>

**Supplementary Figure 1** Morfologia kalusa *F. tataricum*. (A) kalus morfogeny (MK); miękki kalus (czarne gwiazdki), nowo powstałe kompleksy proembriogenne (białe gwiazdki); (B) kalus niemorfogeny (NK). Skala: 0,5 cm

**Supplementary Figure 2** Graficzne przedstawienie schematu eksperymentu immunoprecypitacji chromatyny natywnej

**Supplementary Figure 3** Wzbogacenie markera H3K4me3 w regionach kontroli negatywnej. (A) graficzne przedstawienie poziomu H3K4me3 w regionach kontroli negatywnej: *PME* upstream (Figure 4) oraz *S-ELF3*. Wzbogacenie powtórzeń biologicznych przedstawione w tej samej skali dla każdego genu. Regiony starterów dla ChIP-qPCR zaznaczone poniżej na czerwono. (B) Wyniki ChIP-qPCR dla wzbogacenia regionów negatywnych w okolicy genu *S-ELF3* markerem H3K4me3. Wykresy pudełkowe przedstawiają rozkład znormalizowanych wyników z-score H3K4me3/Input dla MK i NK w różnych punktach czasowych (dzień drugi i dzień szósty).

**Supplementary Figure 4** Immunolokalizacja LM5 w MK i NK *F. tataricum* w dynamice pasażu, tj. dzień drugi i dzień szósty. FB – fluorescent brightener. Skala: 10 µm.

**Supplementary Figure 5** Immunolokalizacja LM6 w MK i NK *F. tataricum* w dynamice pasażu, tj. dzień drugi i dzień szósty. białe strzałki – sygnał w wewnętrznych przedziałach komórkowych. FB – fluorescent brightener. Skala: 10 µm.

**Supplementary Figure 6** Immunolokalizacja LM19 w MK i NK *F. tataricum* w dynamice pasażu, tj. dzień drugi i dzień szósty; sygnał na powierzchni kalusa: d2 i d2' – wstawka; d3 i d3' – wstawka. FB – fluorescent brightener. Skala: 10 µm.

**Supplementary Figure 7** Immunolokalizacja LM20 w MK i NK *F. tataricum* w dynamice pasażu, tj. dzień drugi i dzień szósty; sygnał na powierzchni kalusa: d2 i d2' – wstawka; d3 i d3' – wstawka. FB – fluorescent brightener. Skala: 10  $\mu\text{m}$ .

**Supplementary Figure 8** Immunolokalizacja JIM20 w MK i NK *F. tataricum* w dynamice pasażu, tj. dzień drugi i dzień szósty. FB – fluorescent brightener. Skala: 10  $\mu\text{m}$

**Supplementary Figure 9** Licencja publikacji BioRender.com dla Supplementary Figure 1; Graficznego przedstawienia schematu eksperymentu immunoprecypitacji chromatyny natywnej.



## OPEN ACCESS

## EDITED BY

Petra Prochazkova Schruppfova,  
Masaryk University, Czechia

## REVIEWED BY

Maria Luz Annacondia Lopez,  
University of Copenhagen, Denmark  
Juli Jing,  
Cornell University, United States

## \*CORRESPONDENCE

Jordi Moreno-Romero

✉ jordi.moreno.romero@uab.cat

Alexander Betekhtin

✉ alexander.betekhtin@us.edu.pl

RECEIVED 16 July 2024

ACCEPTED 05 September 2024

PUBLISHED 25 September 2024

## CITATION

Tomasiak A, Piński A, Milewska-Hendel A,  
Andreu Godall I, Borowska-Żuchowska N,  
Morończyk J, Moreno-Romero J and  
Betekhtin A (2024) H3K4me3 changes  
occur in cell wall genes during the  
development of *Fagopyrum tataricum*  
morphogenic and non-morphogenic calli.  
*Front. Plant Sci.* 15:1465514.  
doi: 10.3389/fpls.2024.1465514

## COPYRIGHT

© 2024 Tomasiak, Piński, Milewska-Hendel,  
Andreu Godall, Borowska-Żuchowska,  
Morończyk, Moreno-Romero and Betekhtin.  
This is an open-access article distributed under  
the terms of the [Creative Commons Attribution  
License \(CC BY\)](https://creativecommons.org/licenses/by/4.0/). The use, distribution or  
reproduction in other forums is permitted,  
provided the original author(s) and the  
copyright owner(s) are credited and that the  
original publication in this journal is cited, in  
accordance with accepted academic  
practice. No use, distribution or reproduction  
is permitted which does not comply with  
these terms.

# H3K4me3 changes occur in cell wall genes during the development of *Fagopyrum tataricum* morphogenic and non-morphogenic calli

Alicja Tomasiak<sup>1</sup>, Artur Piński<sup>1</sup>, Anna Milewska-Hendel<sup>1</sup>,  
Ignasi Andreu Godall<sup>2</sup>, Natalia Borowska-Żuchowska<sup>1</sup>,  
Joanna Morończyk<sup>1</sup>, Jordi Moreno-Romero<sup>3\*</sup>  
and Alexander Betekhtin<sup>1\*</sup>

<sup>1</sup>Institute of Biology, Biotechnology and Environmental Protection, Faculty of Natural Sciences, University of Silesia in Katowice, Katowice, Poland, <sup>2</sup>Centre for Research in Agricultural Genomics (CRAG), CSIC-IRTA-UAB-UB, Barcelona, Spain, <sup>3</sup>Departament de Bioquímica i Biologia Molecular, Universitat Autònoma de Barcelona, Cerdanyola del Vallès, Barcelona, Spain

Epigenetic changes accompany the dynamic changes in the cell wall composition during the development of callus cells. H3K4me3 is responsible for active gene expression and reaction to environmental cues. Chromatin immunoprecipitation (ChIP) is a powerful technique for studying the interplay between epigenetic modifications and the DNA regions of interest. In combination with sequencing, it can provide the genome-wide enrichment of the specific epigenetic mark, providing vital information on its involvement in the plethora of cellular processes. Here, we describe the genome-wide distribution of H3K4me3 in morphogenic and non-morphogenic callus of *Fagopyrum tataricum*. Levels of H3K4me3 were higher around the transcription start site, in agreement with the role of this mark in transcriptional activation. The global levels of methylation were higher in the non-morphogenic callus, which indicated increased gene activation compared to the morphogenic callus. We also employed ChIP to analyse the changes in the enrichment of this epigenetic mark on the cell wall-related genes in both calli types during the course of the passage. Enrichment of H3K4me3 on cell wall genes was specific for callus type, suggesting that the role of this mark in cell-wall remodelling is complex and involved in many processes related to dedifferentiation and redifferentiation. This intricacy of the cell wall composition was supported by the immunohistochemical analysis of the cell wall epitopes' distribution of pectins and extensins. Together, these data give a novel insight into the involvement of H3K4me3 in the regeneration processes in *F. tataricum* *in vitro* callus tissue culture.

## KEYWORDS

callus, cell wall, ChIP-sequencing, *Fagopyrum tataricum*, histone modification, morphogenic, native chromatin immunoprecipitation, non-morphogenic

## 1 Introduction

Plant tissue culture demonstrates remarkable capacity for cellular dedifferentiation and subsequent regeneration (Lee and Seo, 2018). Callus is a highly proliferative cell mass that is often considered dedifferentiated. Its growth and development under *in vitro* conditions depend on the activity of meristematic cells, which are capable of undergoing dedifferentiation and redifferentiation under specific conditions (Feher, 2019; Long et al., 2022). Callus tissue undergoes genomic reprogramming during its development, transitioning to a state allowing for the embryogenic cell formation and pluripotency (Ikeuchi et al., 2013). Consequently, the callus can exhibit the ability for direct organogenesis and embryogenesis. For those reasons, callus tissue grown *in vitro* offers a valuable model for exploring plant meristematic differentiation due to its sustained cell division, expansion and growth capacity (Feher, 2019). Cell fate transitions are governed by alterations of epigenetic patterns (Birnbaum and Roudier, 2017; Lee and Seo, 2018; Feher, 2019). Among other mechanisms, histone post-translational modifications are pivotal in governing gene transcription throughout the phases of cell growth and development, as well as in orchestrating the cell's reaction to both external and internal stimuli (Desvoyes et al., 2014; Birnbaum and Roudier, 2017; Bednarek and Orłowska, 2019). The trimethylation of histone H3 at lysine 4 (H3K4me3) mark in plants regulates gene expression and transcriptional memory, influences numerous developmental processes as well as stress responses (Foroozani et al., 2021). Multiple *Arabidopsis* mutants exhibit a locus-specific absence of H3K4me3, which manifests diverse developmental irregularities. These observations indicated that H3K4me3 likely plays crucial roles in upholding the typical expression of numerous genes (Guo et al., 2010). Accordingly, it has been shown an enrichment of H3K4me3 on multiple genes during the *Arabidopsis* leaf-to-callus transition (Hong et al., 2024). Previous research conducted by our group revealed that the levels of H3K4me3 mark in the morphogenic callus of *F. tataricum* increased with the acquisition of the regeneration potential (Tomasiak et al., 2023).

Among different changes, cellular reprogramming processes involve reorganising the cell wall components and specific gene expression (El-Tantawy et al., 2013; Su and Higashiyama, 2018). The primary cell wall is a highly dynamic structure and plays a crucial role in the life cycle of a plant (Sala et al., 2019; Leszczuk et al., 2023). It provides mechanical support to cells, participates in their growth and differentiation, and controls morphogenesis and the whole plant's architecture (Jamet et al., 2006; Corral-Martinez et al., 2016). The primary cell wall is structurally heterogeneous. The main components are pectins and glycoproteins such as hydroxyproline-rich glycoproteins (HRGPs) that include arabinogalactan proteins (AGPs) and extensins (Keller, 1993). By influencing the physical properties of the cell wall, they contribute to processes such as cell adhesion, expansion, intercellular communication and regulatory functions (Smertenko and Bozhkov, 2014). Extensins are one of the most crucial wall glycoproteins, which significantly impact growth processes and are essential for primary cell wall structure and plant development. They form networks that influence the extensibility of the cell wall, and their increased content

in the cell wall causes the termination of cell growth (Sala et al., 2019). Our previous research demonstrated the presence of extensins on the surface of morphogenic and non-morphogenic calli of *F. tataricum*, suggesting that they are crucial for cell proliferation, differentiation, cell extension (Betekhtin et al., 2019). Diverse groups of enzymes are also involved in the cell wall reorganisation and metabolism. Pectin methyl esterase inhibitors (PMEIs) are proteins that inhibit pectin methylesterase (PME) enzymes. By inhibiting their activity, PMEI maintains pectin in a more methylated state, affecting the rigidity and porosity of the cell wall (Wormit and Usadel, 2018). Moreover, PMEIs may affect the pH and consequently activate other cell wall degrading enzymes, thereby facilitating cell expansion, growth, and separation (Betekhtin et al., 2018). Overexpression of *PMEI* led to the development of callus-like structures without the addition of exogenous auxin, indicating that this cluster participates in cell reprogramming during callus formation (Xu et al., 2018). Polygalacturonases play a vital role in pectin degradation, essential for cell wall loosening and remodelling during growth and development (Shin et al., 2021). Studies on poplar established that overexpression of genes associated with cell wall degradation and loosening was upregulated during callus formation, which led to reduced pectin content. Researchers concluded that cell wall degradation and biosynthesis were required for cell fate transition (Cao et al., 2021; Zhang et al., 2024). Peroxidases take part in the formation and cross-linking of lignin and other components of the cell wall, providing structural support and rigidity. They regulate cell elongation, differentiation, and development (Nicolas et al., 2003). A study on *Linum usitatissimum* showed that fluctuations in peroxidase levels accompany shoot formation in callus. An increase in peroxidase activity was noticed during the induction of shoots callus, indicating a role for peroxidases in differentiation processes (McDougall et al., 1992). Altogether, substantial evidence was demonstrated that the dynamic changes in the cell wall composition occur during dedifferentiation and redifferentiation.

In this work, we aimed to link the changes of histone modifications in callus with cell wall related genes. To address that, we used chromatin immunoprecipitation (ChIP), a powerful technique to study the interactions of nuclear proteins with DNA (Gade and Kalvakolanu, 2012). The interplay of proteins and DNA is fundamental to numerous cellular processes, including DNA replication, repair, genomic stability maintenance, mitotic chromosome segregation, and gene expression regulation (Collas, 2010). ChIP-sequencing (ChIP-seq) is employed to identify the presence of chromatin-related proteins (e.g. histone modifications, transcription factors) along the genome (Nakato and Sakata, 2021). Here, we used the ChIP-seq for two types of *F. tataricum* calli, morphogenic (MC) and non-morphogenic (NC) to assess the enrichment of H3K4me3 genome-wide, as well as study specific loci of the genes coding for the cell wall proteins, to follow the dynamics of this histone mark in both calli during the transition from non-embryogenic to an embryogenic state. We also performed the immunohistochemical staining to compare the chemistry of cell wall components between calli developmental stages. Contrasting the epigenetic profiles of callus with different capacity for morphogenesis unveils shifts in chromatin state and the impact of diverse epigenetic changes on growth and development. This

comparison enables the identification of pivotal cell wall genes associated with plant growth and development, offering fresh perspectives on how these processes are regulated.

## 2 Materials and methods

### 2.1 Plant material

The seeds of *F. tataricum*, sample k-17 were acquired from the collection of the N.I. Vavilov Institute of Plant Genetic Resources, Saint Petersburg, Russia. *F. tataricum* MC was induced from immature zygotic embryos (Supplementary Figure S1A). NC of *F. tataricum* appears on the surface of MC after approximately two years of culture (Supplementary Figure S1B) (Betekhtin et al., 2017). Calli were cultivated in the dark in an incubator at 25°C ± 1 on an RX medium. It composed of Gamborg B5, including vitamins (Duchefa, Netherlands) (Gamborg et al., 1968), 2 g L<sup>-1</sup> N-Z amine A (Sigma-Aldrich, USA), 2 mg L<sup>-1</sup> 2,4-dichlorophenoxyacetic acid (2,4-D, Sigma-Aldrich, USA), 0.2 mg L<sup>-1</sup> kinetin (KIN, Sigma-Aldrich, USA), 0.5 mg L<sup>-1</sup> 3-indoleacetic acid (IAA, Sigma-Aldrich, USA), 0.5 mg L<sup>-1</sup> 1-naphthaleneacetic acid (NAA, Sigma-Aldrich, USA), 25 g L<sup>-1</sup> sucrose (Chempur, Poland) and 7 g L<sup>-1</sup> phyto agar (Duchefa, Netherlands). MC and NC were subcultured every four and two weeks, respectively.

### 2.2 Cross-linked chromatin immunoprecipitation and bioinformatic analysis

#### 2.2.1 Tissue preparation

MC and NC were harvested on eleventh day of cultivation and fixed according to the Diagenode s. a. (Belgium) company guidelines. Briefly, the tissues were rinsed in ddH<sub>2</sub>O, dried with paper towels, and placed in a crosslinking bag, which was then put in a 50 ml falcon tube with the crosslinking buffer (1 x phosphate buffered saline (PBS), 1% paraformaldehyde, ddH<sub>2</sub>O). Crosslinking took place in a vacuum desiccator (~ - 950 Millibars) for 15 minutes. 2.5 ml of the solution was replaced by 2.5ml of 1.25 M glycine in ddH<sub>2</sub>O, and placed in the vacuum for additional five minutes. Crosslinking solution was removed, and samples were washed three times in ddH<sub>2</sub>O. Tissues were removed from the bags, dried with paper towels and placed into new 50 ml falcon tubes. Tubes were snap-frozen and stored in -80°C till further processing. Chromatin immunoprecipitation was conducted by Diagenode ChIP-seq Profiling service (Diagenode Cat# G02010000) according to the company's guidelines using the antibody directed against H3K4me3 (Diagenode, Belgium, cat. No. C15410003).

#### 2.2.2 Alignment and peak calling

Data Analysis was performed by Diagenode Bioinformatics service (Diagenode Cat# G02010107). Sequencing was performed in paired-end 50 bp on an Illumina Novaseq, running Novaseq Control Software 1.7.0. Quality control of sequencing reads was

assessed using FastQC v0.11.9 (Andrews, 2010). Trimming of the adaptors was done with cutadapt v3.5 (Krueger, 2024). Trimmed reads were aligned to the reference genome (*Fagopyrum tataricum*) obtained from <https://www.mgbase.org/Pinkul/> (Zhang et al., 2017) using BWA software v.0.7.5a (Li and Durbin, 2009). PCR duplicates and multimapping reads were removed using samtools v1.15 (Li et al., 2009). Alignment statistics are collected in the Supplementary Table S1. Alignment coordinates were converted to BED format using BEDTools v.2.17 (Quinlan and Hall, 2010) and BED files were visualized by using the Integrated Genomic Viewer v2.17.4 (Robinson et al., 2011). Peak calling that corresponds to H3K4me3 enriched regions was performed using epic2 v0.0.52 (Stovner and Saetrom, 2019) with optimized peak calling parameters for histone modifications (undisclosed). General peak calling statistics are compiled in the Supplementary Table S2. The BED files were processed with deeptools2 v3.5.4 (Ramirez et al., 2016) to generate BigWig files of several bin size (10bp for Figures 1A, B, 50kb for Figure 1C). ThenkaryoploteR v.1.30.0 (Gel and Serra, 2017) was used to plot the density of H3K4me3 along genes and TE and across the chromosomes.

#### 2.2.3 Differential enrichment analysis

The differential enrichment quantitative analysis was performed with the R/Bioconductor package DiffBind (Stark and Brown, 2011; Ross-Innes et al., 2012). Difference in read concentration between MC and NC H3K4me3 peaks was estimated by comparing read densities computed over consensus peaks (peaks present in both replicates) (Figures 2A, B). The list of differentially enriched peaks between the two comparative groups is included in the Supplementary Table S3. Identified peaks were represented by Volcano plots in order to visualise which data points are differentially enriched (Figure 2C). Gene ontology analysis was performed by annotation of the genes with InterProScan 5.69-101.0 (Jones et al., 2014) and GO Enrichment implemented in Galaxy Australia version 21.09 (Figures 3A, B; Community, 2024).

### 2.3 Native chromatin immunoprecipitation

Chromatin immunoprecipitation experiments were carried out in four biological replicates, MC and NC samples were independently harvested on days two and six. A graphical depiction of the experiment was created with BioRender.com and is included in Supplementary Figure S2 (the confirmation of publication and licensing rights is included as the Supplementary Figure S9). The protocol employed in our experiment was according to Trejo-Arellano et al. (2017) with minor modifications. For this procedure one gram of callus tissue was ground with liquid nitrogen using a pestle and mortar. Trejo-Arellano et al. (2017) used 400 mg of the tissue; however, in our case, using over two times more of the starting material was necessary due to the high vacuolisation of callus cells. The ground powder was suspended in 10 ml Honda buffer (0.5% Triton X-100, 0.4 M Sucrose, 25mM 2-amino-2-(hydroxymethyl)-1,3-propanediol (Tris) pH 7.4, 10 mM MgCl<sub>2</sub>, 2.5% Ficoll 400, 5% Dextran T40, 10 Mm β-mercaptoethanol,



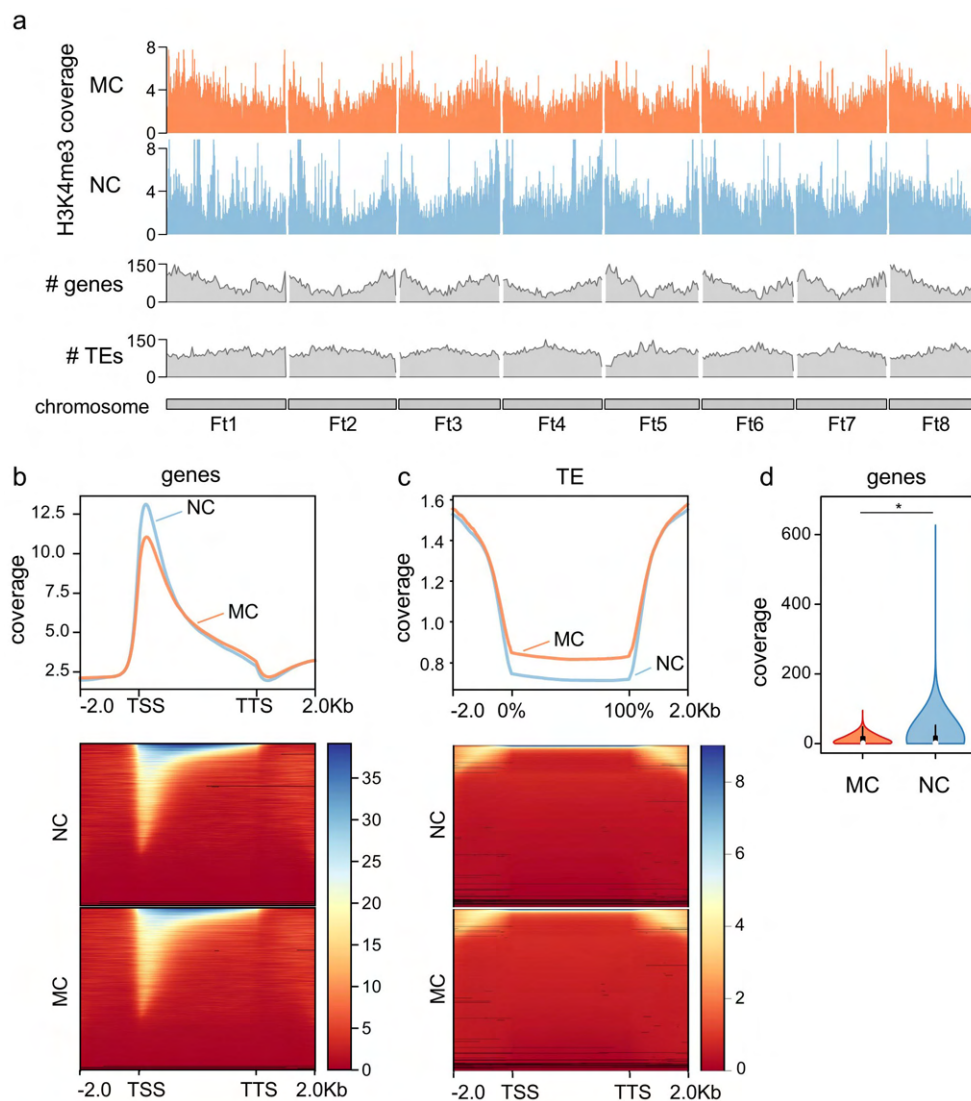


FIGURE 1

Genome-wide H3K4me3 distribution. (A) Chromosomal distribution of H3K4me3 in MC and NC, including genes and transposons (TEs) number along the chromosomes. (B) Metagene plot and heatmap of the distribution of H3K4me3 along genes, including -2.0 kb upstream the transcription start site (TSS) and +2.0 kb from the transcription termination site (TTS). (C) Metagene plot and heatmap of the distribution of H3K4me3 along TEs, including -2.0 kb upstream the TE body and +2.0 kb from the end of the TE. (D) Levels of H3K4me3 at the first 10% of the gene in MC and NC. Asterisk denote Mann–Whitney U test significant difference.

ddH<sub>2</sub>O) and placed on a rotator for 15-minute incubation in 4°C. Subsequently, the mixture was filtered twice through the miracloth, the first time with one layer and the second with two layers. Next, the tubes were centrifuged at 1500 g, 4°C for 5 minutes and the supernatant was discarded. The pellet was resuspended in 2 ml MNase buffer [50 mM Tris pH 8, 10 M NaCl, 5 mM CaCl<sub>2</sub> and protease inhibitors (Aprotinin, Antipain, Pepstatin A, Leupeptin, Sigma-Aldrich, USA)] and centrifuged again at 1500 g, 4°C for 5 minutes. Trejo-Arellano et al. (2017) protocol used the protease inhibitor cocktail (Roche - cOmplete™ Protease Inhibitor Tablets, Sigma-Aldrich, USA), however in our experiment employment of protease inhibitors prepared freshly before each experiment ensured their efficacy. The supernatant was discarded, and pellet was resuspended in 100 μl MNase buffer. Samples were placed on the thermoblock set at 14000 rpm, 25°C for 5 minutes, and MNase

(1 μl/50 μl) was added. Trejo-Arellano et al. (2017) protocol employs digestion at 37°C for 7 minutes, however for *F. tataricum* calli the best digestion effects were observed at lower temperature and shorter time. Digestion was quenched by adding 10 mM EDTA; samples were incubated on ice for 10 minutes, then centrifuged for 5 minutes at 2000g at 4°C. The supernatant was transferred to a fresh tube, and the pellet was resuspended in 100 μl S2 buffer (50 mM Tris pH 8, 100 mM EDTA and protease inhibitors), incubated for 30 minutes on ice and centrifuged 5 minutes at 2000 g at 4°C. Supernatants were combined, and the pellet discarded. To check the digestion efficiency, 40 μl of the aliquot was purified with a column DNA extraction kit and run on 1% agarose gel. DNA concentration of each sample was checked in the BioSpectrometer fluorescence (Eppendorf, Germany). The DNA concentration was adjusted to 15 μg/per sample, diluted in

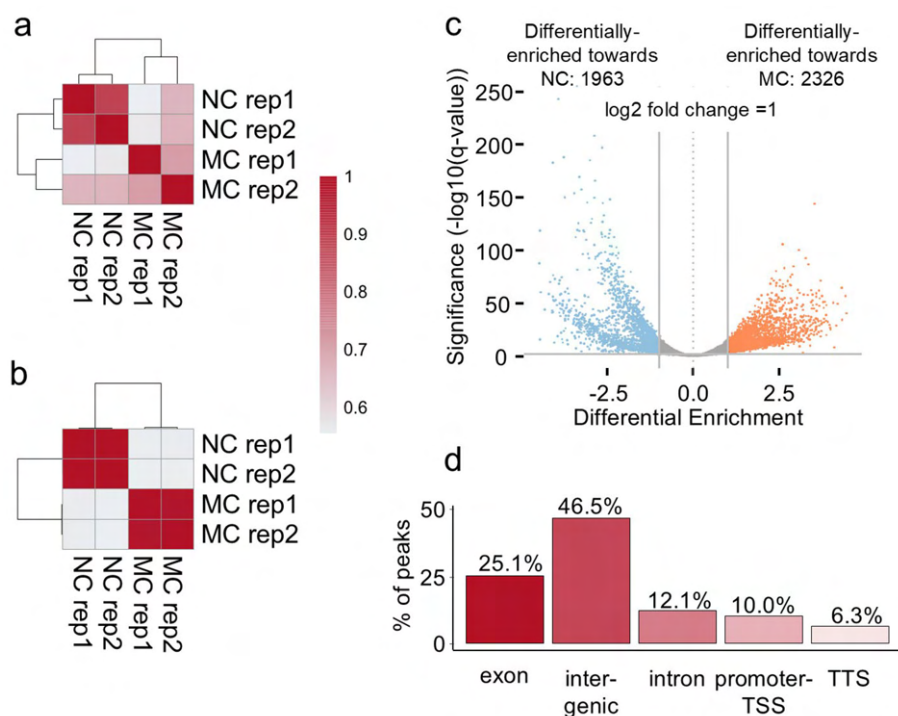


FIGURE 2

H3K4me3 differential enrichment of MC versus NC on day eleven of cultivation. (A) Pearson correlation on peaks detection of the MC and NC replicates. (B) Pearson correlation on peak enrichment of the MC and NC replicates. (C) Volcano plot of the differentially-enriched regions between MC and NC. The plot represents those 7372 differentially methylated regions, 4289 statistically significant regions with a two-fold change higher than one. 1963 regions displayed higher intensity in the NC (blue), whereas 2326 regions in the MC (orange). Regions in grey represent the peaks that are not passing the thresholds. The X-axis represents the log-fold differential enrichment. Vertical lines represent the threshold of the log<sub>2</sub> change. The Y-axis represents the significance at 0,01. In this plot, each point represents a genomic region identified as a binding site (peak). The plot also gives information on whether there is a global increase or reduction of binding affinity in the first or second group of the comparison by evaluating the significant data points in the positive or negative Log Fold Change. (D) genomic distribution of the differentially enriched 4289 regions (considering a log<sub>2</sub> fold change 1 and an adjusted p-value < 0.01 per annotation genomic features).

ChIP incubation buffer (1 M Tris pH 8, 0,5 M EDTA pH 8, 0,1% Triton X-100, 1 M NaCl and protease inhibitors) to obtain 350 µl of the solution sufficient for the immunoprecipitation (IP) by IgG and anti-H3K4me3 (150 µl per IP sample and 50 µl for the input sample). Input was removed and stored at 4°C till further processing. Samples were divided into separate Eppendorf tubes 150 µl each, and antibodies were added: 2 µl of rabbit IgG (Sigma-Aldrich, USA) and 1 µl of anti-trimethylation of histone H3 at lysine 4 (anti-H3K4me3, Sigma-Aldrich, USA). Tubes were incubated with gentle rotation overnight at 4°C. The next day, 8 µl/100 µl Protein-A Dynabeads (InvitroGen, USA) were washed with ChIP incubation buffer (with fresh proteinase inhibitors) on the Magnarack (InvitroGen, USA) five times. Subsequently, 12 µl of Dynabeads per sample were added, and the incubation continued for 90 minutes at 4°C. During incubation wash buffers were prepared: wash buffer 1 (25 mM Tris pH 8, 10 mM EDTA pH 8, 0,1% Triton X-100, 50 mM NaCl), wash buffer 2 (25 mM Tris pH 8, 10 mM EDTA pH 8, 0,1% Triton X-100, 100 mM NaCl) and wash buffer 3 (25 mM Tris pH 8, 10 mM EDTA pH 8, 0,1% Triton X-100, 150 mM NaCl). In the Trejo-Arellano et al. (2017) protocol protease inhibitor cocktail was used also in the above buffers, however we found adding protease inhibitors at this step was unnecessary. After the incubation, the beads were washed twice in each wash buffer.

Finally, one wash was performed with TE buffer (10 mM Tris pH 8, 1 mM EDTA pH 8). The beads were resuspended in 200 µl of freshly prepared ChIP elution buffer (1% SDS, 0,1M Na-HCO<sub>3</sub>) and incubated on a thermoblock at 65°C for 15 minutes with agitation. The supernatant was transferred to a fresh tube, and the beads were resuspended in 200 µl of ChIP elution buffer, and the incubation step was repeated. Supernatants were combined, beads were discarded. DNA purification of the input and ChIPed samples was performed by using phenol:chloroform. In the Trejo-Arellano et al. (2017) protocol, DNA elution and purification were done with IPure kit (Diagenode, Belgium), however for *F. tataricum* calli phenol:chloroform proved to be a more efficient method in terms of final quantity of recovered DNA.

## 2.4 Primer design, ChIP-quantitative PCR

Primers for ChIP were designed for selected regions on *F. tataricum* genome. The genomic sequence of *F. tataricum* cv. Pinkul1 was downloaded from <http://www.mgbkbase.org/Pinkul1/> (online access 4 February 2024) and loaded into Geneious 11.1.2 software (<http://www.geneious.com> (Kearse et al., 2012)). Gene-specific primers for positive and negative H3K4me3 regions were

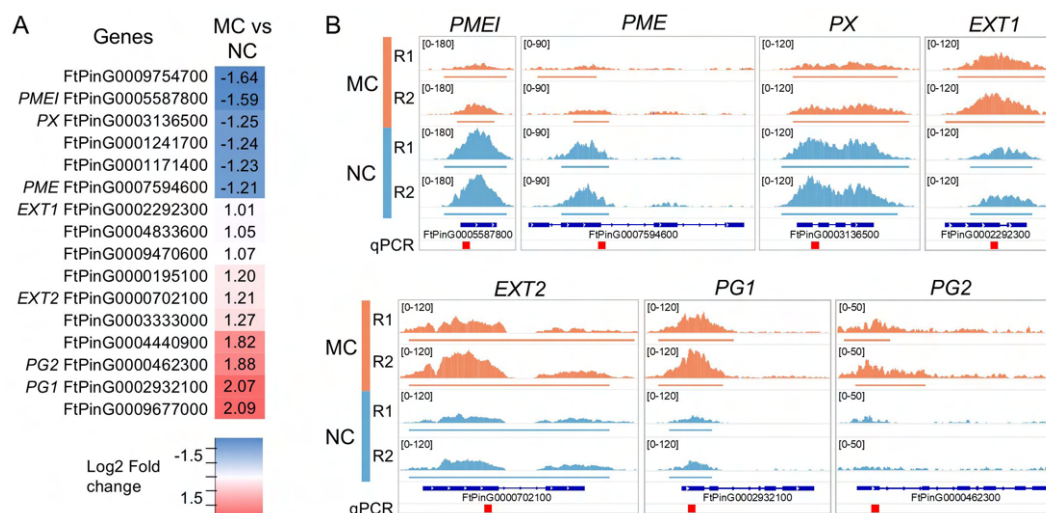


FIGURE 3

H3K4me3 in cell-wall related genes. (A) List of genes that presents a significantly enriched region (defined in Figure 1) in proximity of their TSS. Fold change (log<sub>2</sub>) is represented and names of the genes showed in (B) are indicated. The details of these genes can be found in the Supplementary Table S9. (B) Visual representation of the H3K4me3 enrichment on selected genes. Coverage of the replicas are represented in the same scale for each gene. Defined peaks are indicated below the coverage. Regions amplified by qPCR (Figure 2) are indicated as red square on the bottom. The Integrative Genomics Viewer was used for representation.

designed using the program's 'design primers' function. Primers used are listed in the Supplementary Table S4.

Input and ChIPed DNA samples quantification was performed by quantitative PCR (qPCR) using the 480 LightCycler<sup>®</sup> 480 SYBR Green I Master in a LightCycler<sup>®</sup> 480 Real-Time PCR System (Roche, Germany) in two technical replicates. Quantitative cycles were obtained and % input was calculated. To represent the ChIP data, results obtained from four independent biological replicates were calculated as z-scores of the % input (Figures 4A, B) z-scores were used to minimize intraexperimental technical variability that was not possible to be avoided because the ChIP workload did not allow the simultaneous execution of all the immunoprecipitation reactions. Ct values are available in Supplementary Table S5.

## 2.5 Reverse transcription quantitative PCR

Total RNA was isolated from MC and NC on days two and six of callus culture. Total RNA was extracted using the FastPure Plant Total RNA Isolation Kit (Polysaccharides and Polyphenolics-rich) from Vazyme Biotech (Red Maple Hi-tech Industry Park, PRC). The RNA concentrations were quantified with a Nano-Drop ND-1000 spectrophotometer (NanoDrop Technologies, USA). To remove any residual DNA, the RNA samples were treated with an RNase-free DNase Set (Qiagen, Germany). Reverse transcription (RT) was carried out using oligo-dT primers and the Maxima H Minus First Strand cDNA Synthesis Kit (Thermo Fisher Scientific, USA). The resulting cDNA was diluted four-fold with water, and 2 µl of this diluted cDNA was used in the qPCR reactions. The qPCR was performed in a 10 µl reaction volume using the LightCycler<sup>®</sup> 480 SYBR Green I Master mix (Roche, Switzerland). The same primers were used for ChIP-qPCR and RT-qPCR with exception of

*PX*, which is annotated in the Supplementary Table S4. Constitutive genes *SAND* and *ACTIN* were used as previously (Sala-Cholewa et al., 2024). qPCR was conducted on a LightCycler 480 system (Roche, Switzerland) under the following cycling conditions: an initial denaturation at 95°C for 5 minutes, followed by 40 cycles of 95°C for 10 seconds, a primer-specific annealing temperature for 20 seconds, and 72°C for 10 seconds. For melt curve analysis, denaturation was performed at 95°C for 5 seconds, followed by 65°C for 1 minute, and a gradual increase to 98°C (0.1°C/s) for fluorescence measurement. Ct values were determined using LinRegPCR software (version 11, Academic Medical Centre, The Netherlands). The plant tissues for the RT-qPCR analysis were prepared in three biological replicates, with each biological replicate having two technical replicates. Relative expression levels were calculated using the  $2^{-\Delta\Delta CT}$  method, where  $\Delta\Delta CT$  is defined as  $\Delta CT_{reference\ condition} - \Delta CT_{compared\ condition}$ . The one-way ANOVA ( $p < 0.05$ ) followed by Tukey's honestly-significant-difference test (Tukey HSD-test) ( $p < 0.05$ ) were used to calculate any significant differences between the experimental combinations (Figure 4C). Ct values are included in the Supplementary Table S6.

## 2.6 Immunohistochemical analysis

The MC and NC were fixed overnight at 4°C in a solution containing 4% paraformaldehyde and 1% glutaraldehyde in PBS (pH 7.3). Following fixation, the samples underwent three 15-minute washes in PBS and were then subjected to a dehydration process using increasing concentrations of ethanol (10%, 30%, 50%, 70%, 90%, 100%, each twice) before gradual embedding in London Resin (LR White resin, USA). Subsequently, the embedded samples were sliced into 1.5 µm thick cross-sections using an EM UC6

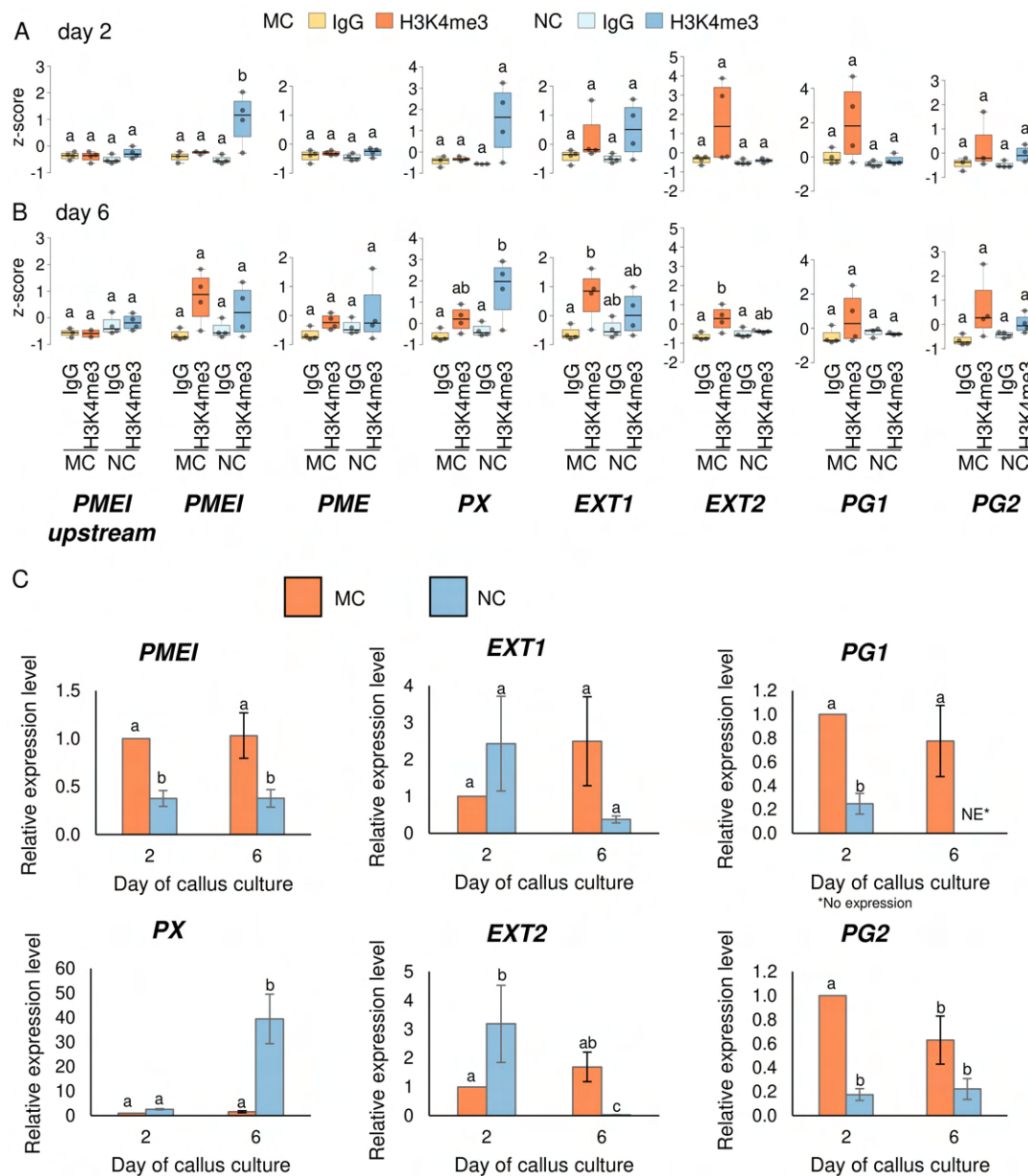


FIGURE 4

H3K4me3 enrichment in cell wall related genes at day two and six of the passage. ChIP-qPCR of H3K4me3 in MC and NC at day two (A) and day six (B) on selected genes. Box plots show the distribution of normalised z-scores of H3K4me3/Input of experiments performed simultaneously. One-way ANOVA followed by Tukey test was applied, and significance are marked by letters. (C) Relative expression level of *PME1*, *PX*, *EXT1*, *EXT2*, *PG1*, *PG2*. The expression level of genes in MC and NC was normalized with the constitutive genes *ACTIN* and *SAND* and calibrated to expression on day two in MC. Different letters indicate a significant difference between the tissues and days according to Tukey's HSD test ( $p < 0.05$ ;  $n = 3$ ; means  $\pm$  SE are given).

ultramicrotome (Leica Biosystems, Germany), and placed on glass slides coated with poly-L-lysine. For immunocytochemical analyses, the sections were treated with a blocking buffer (2% foetal calf serum and 2% bovine serum albumin in PBS) for 30 minutes at room temperature (RT). Next, the sections were incubated overnight at 4°C with primary monoclonal antibodies (Plant Probes, UK) diluted 1:20 in a blocking buffer. The antibodies used are listed in [Supplementary Table S7](#). After three washes in the blocking buffer, the sections were incubated with a secondary antibody, AlexaFluor 488 goat anti-rat IgG (Jackson ImmunoResearch Laboratories, UK), diluted 1:100 in the blocking buffer for two hours at RT. Following another wash in

the blocking buffer and rinsing three times in PBS, the sections were stained with calcofluor white (Sigma-Aldrich, USA) in PBS to visualise cell walls. After rinsing in PBS and distilled water, the dried sections were mounted on slides using Fluoromount (Sigma-Aldrich, USA).

As a negative control, the primary antibody was omitted, and the blocking buffer was applied along with all other procedure steps. Observations were performed, and the images were taken with an AxioImager Z2 epifluorescence microscope equipped with an AxioCam Mrm monochromatic camera (Zeiss, Germany) equipped with narrow-band filters for AlexaFluor 488 and DAPI.

## 3 Results

### 3.1 Morphology of *F. tataricum* morphogenic and non-morphogenic calli

A detailed description of the callus tissue morphology used in this research is available in our previous publications (Betekhtin et al., 2017, 2019; Tomasiak et al., 2023). The morphology of MC and NC is included in Supplementary Figure S1. Morphogenic callus (MC) comprises of proembryogenic cell complexes (PECCs) and soft callus cells (SCCs) (Supplementary Figure S1A, white and black asterisks, respectively). NC comprises solely of highly vacuolated, parenchymatous cells (Supplementary Figure S1B). Transfer to a fresh medium, which contains high auxin concentration, triggers PECCs disintegration, accompanied by the release of secretion, leading to the formation of new PECCs in the SCCs (between the 6<sup>th</sup> and 11<sup>th</sup> days of cultivation) (Rumyantseva et al., 2003; Betekhtin et al., 2017). Because the changes present during MC's development are major, day two was selected as a point where PECCs disintegrate, whereas day six was a point where subsequent new PECCs reinitiation processes begin. On day eleven of the culture, MC exhibits high content of embryogenic cells, whereas NC's parenchymatous cells characterise with high accumulation of the oxidative stress. Moreover, as demonstrated by our previous research, day two and day six exhibited the biggest changes in the global levels of H3K4me3 in MC and NC during the passage (Tomasiak et al., 2023).

### 3.2 H3K4me3 levels in MC and NC calli

Calli of *F. tataricum* with varying morphogenic capacities exhibited global epigenetic changes as demonstrated by fluctuations in DNA methylation and histone modifications (Tomasiak et al., 2023). To have a more precise picture of these changes, this work focused on the analysis of the genomic H3K4me3 mark distribution in MC and NC by performing a ChIP-seq in both callus types on day eleven of cultivation. The distribution of H3K4me3 along the *F. tataricum* chromosomes (Ft1-Ft8) (Figure 1) shows that the mark in both MC and NC is distributed along the chromosomes, with a pattern that follows gene distribution, and contrary to the transposable elements (TEs), indicating that H3K4me3 is distributed in the transcriptional active chromatin (where genes are located) and reduced in the silent chromatin (where enrichment of TEs occurs). In fact, when the H3K4me3 levels in both NC and MC are plotted on genes, the mark appears to be highly enriched, with clear higher levels of the mark at the transcriptional start site (TSS) (Figure 1B). On the contrary, H3K4me3 is absent in repetitive elements such as TEs (Figure 1C), as expected with a mark related to genes. As can be noted from the metagene plot (Figure 1B), the levels of H3K4me3 in the TSS are higher in NC than in MC. Accordingly, when we compared the coverage of H3K4me3 in the first 10% of the gene body, a significant increase of the mark was found in the NC, likewise the global content of the mark which is higher in NC than MC (Figure 1D) as previously reported by immunocytochemical analysis (Tomasiak et al., 2023).

Further analysis was conducted and H3K4me3 peaks were defined. Based on the detected peaks, the Pearson correlation between the samples analysed indicates that MC replicates and NC replicates form clusters together, both when peak location (Figure 2A) or the intensity of the peaks located at the same place (Figure 2B) were compared. The proper separation of the clustering demonstrates that MC and NC comparison presents a significant statistical difference in the peak intensity. By a differential analysis, 7372 regions were detected to be statistically different (adjusted p-value (q-value or FDR) < 0.01) (Figure 2C; Supplementary Table S3). Of those regions, 4289 not only statistically significant but also presented a log<sub>2</sub>-fold change higher than one. This cutoff signifies that the difference between the peak intensities is higher than the fold change of two. 1963 regions displayed higher intensity in the NC (blue), whereas 2326 regions in the MC (orange) (Figure 2C). The genomic distribution of these 4289 differential enriched regions (Figure 2D) shows that the majority of the regions were associated with exons and intergenic regions, with a lower amount of regions associated with introns and transcriptional termination site (TTS). Surprisingly, the promoter and TSS represent only 10.03% of those regions. However, from the regions classified as exon, 61% of them located in the first exon. Based on the distribution of the mark peaking at the TSS, we expect that the differentially enriched regions classified as promoter-TSS and first exon have the most important role in regulation of the gene expression. For that reason, we analysed the genes whose TSS was in close proximity (less than 1kb) to the differentially enriched regions. We obtained 1709 genes; in 1057 genes H3K4me3 was higher in MC and in 652 genes higher methylation prevailed in NC. A gene ontology analysis of these genes gave only significant enrichment on the list of genes with higher levels of the mark in MC (Supplementary Table S8). Many categories were photosynthesis-related activities (such as the photosynthesis itself, heme binding, oxidoreductase activity, iron ion binding), and some to metabolic pathways (glycogen (starch) synthase activity, UDP-glycosyltransferase activity) and the membrane (as cellular component category).

### 3.3 Comparison of H3K4me3 levels on cell wall related genes during the MC and NC growth

As cell wall phenolic composition in NC has been reported to be lower than in MC (Akulov et al., 2018), we explored among the genes that had in proximity of the TSS a differentially enriched region (log<sub>2</sub> FC < 1 and an adjusted p-value < 0.01), those related to cell wall (Figure 3A). We found that 16 genes presented differential methylation, 6 of them with enrichment towards NC and 10 towards MC, (Supplementary Table S9). Among the cell wall related genes enriched in NC, we found two genes related to xyloglucan catabolism, two related to pectin (*PECTIN METHYLESTERASE INHIBITOR*, *PMEI* and *PECTIN METHYLESTERASE*, *PME*), and a peroxidase (*PEROXIDASE*, *PX*). Polygalacturonase was also found, and two other *POLYGALACTURONASES* (named as *PG1* and *PG2*) were found as enriched in MC. Pectin-related genes were also found among the

H3K4me3-enriched in MC, but some other gene categories were specific, such the wall-associated receptor kinases and *EXTENSINS* (named as *EXT1* and *EXT2*).

Seven genes of these cell wall proteins were selected to explore their H3K4me3 levels by N-ChIP-qPCR (Figures 4A, B) and relative expression by RT-qPCR (Figure 4C) at two earlier time points of the culture: day two, when PECCs disintegrate, and day six, when new PECCs are formed. From the genes that were enriched in H3K4me3 in NC at day eleven (Figure 3A), *PMEI*, *PME* and *PX* were studied. *PMEI* showed significant enrichment of this mark in NC as early as day two. Despite the H3K4me3 levels on day six showed a certain enrichment compared to an H3K4me3-negative region upstream of the gene (Figures 4A, B; Supplementary Figure S3 for primer location and two other negative regions tested), this difference was not statistically significant compared to the basal levels (IgG signal). Although the H3K4me3 mark has been associated with higher transcriptional activity, expression results showed statistically lower levels of expression in NC on both, day two and day six, despite higher methylation. The *PME* gene was not enriched in H3K4me3 in either NC or MC on day two or day six, suggesting that NC methylation may occur after these time points, as this mark was present on day eleven. According to this low methylation, expression levels of *PME* were below the limits of detection by RT-qPCR (Supplementary Table S6). For *PX*, H3K4me3 were significantly higher only in NC on day six. In this case, the relative expression of *PX* positively correlated with methylation, as expression in NC on day six increased significantly, reaching a level 39.4 times higher than in MC on day two. From the genes that showed higher levels of H3K4me3 in MC than in NC on day eleven (Figure 3A), *EXT1*, *EXT2*, *PG1* and *PG2* were analysed. For *EXT1* and *EXT2*, no significant differences in H3K4me3 were observed on day two. A significant increase was only observed in these genes in MC on day six when compared to basal levels (IgG). Therefore, as with *PME*, levels of methylation on day eleven may have been established by day six. For *EXT1*, relative gene expression remained stable across the two time points and in the different callus type, while *EXT2* showed higher expression in NC compared to MC on day two, but lower expression in NC on day six (with a decrease being 41.7 times lower than in MC at day two). As with *PMEI*, expression on *EXT2* did not correlate with H3K4me3 levels. The enrichment of H3K4me3 in *PG1* and *PG2* across the examined days did not show statistically significant differences. The expression of *PG1* was significantly higher in MC than in NC on both culture time points (with expression levels below the technical limits on day six in NC). Similarly to *PG1*, in *PG2*, relative expression in MC was higher than in NC, but this occurred only on day two. The accumulation of H3K4me3 observed in *PG1* and *PG2* within MC, even though it was not statistically significant, points to a potential role for this modification in sustaining higher expression.

Altogether, the dynamic regulation of H3K4me3 methylation across different time points and callus types indicates a complex relationship between epigenetic modifications and gene expression in cell wall-related genes. While some genes, such as *PMEI* and *PX*, show a certain correlation between increased H3K4me3 levels and higher expression, others, like *PME* and *EXT2*, do not follow this pattern, suggesting that additional regulatory mechanisms may be involved.

### 3.4 Immunodetection of pectic and extensin epitopes

The specific cell wall epitope distribution was analysed on day two and six of the passage, corresponding to the days when H3K4me3 ChIP was conducted. Five different antibodies were applied using an immunocytochemical approach. Four were against different pectic epitopes (LM5, LM6, LM19 and LM20) and one against the extensin (JIM20). Results are summarised in Table 1, and the images from the immunolocalisation are included in Supplementary Figures S4–S8. Separating the fluorescence signals in the cell wall and the plasma membrane has proven difficult when using light microscopy. Therefore, those two compartments are described together.

Four antibodies were employed to analyse the pectin epitopes: LM5, LM6, LM19, and LM20. LM5 signal was present in MC and NC on each examined day in the cell wall but absent in the cell internal compartments and on the surface (Supplementary Figure S4). LM6, on the other hand, in MC was not present at the beginning of the passage, it appeared only on day six solely in a dotted manner in the inner cell compartments (Supplementary Figures S5A, B, b2 white arrows). In NC, this epitope was absent regardless of the day of the passage (Supplementary Figures S5C, D). LM19 was present both in MC and NC on all examined days, and all examined compartments and the callus surface (Supplementary Figure S6A, B, white arrows; d2 and d2' inset; d3 and d3' inset). LM20 was present in the MC across the passage in the cell wall and on the callus surface. In NC, LM20 was present not only in the cell wall and on the surface (Supplementary Figure S7; c2 and c2' inset; c3 and c3' inset) but also in the internal cell compartments (Supplementary Figure S7 d2, d3). The immunocytochemical analysis included one antibody against the extensins (JIM20); however, neither in MC nor NC was the reaction positive (Supplementary Figure S8).

## 4 Discussion

This research aimed to analyse and compare the enrichment of histone H3 at lysine K4 trimethylation (H3K4me3) in the genes coding for the cell wall proteins in *F. tataricum* MC and NC. To achieve this objective, the ChIP protocol was optimised to be applicable for *F. tataricum* callus tissue. To this date, a verified ChIP method has not been reported for *Fagopyrum* species, possibly due to its high content of phenolic compounds, which may affect immunoprecipitation efficiency. In plants, X-ChIP has been used, in some cases to address the role of histone marks in regulating the expression of genes related to cell wall biosynthesis. Experiments conducted on *Zea mays* demonstrated increased H3K9ac of two cell wall genes under the salt stress, suggesting that histone modifications may be important mitigating the harmful effects of excessive salinity on plants (Li et al., 2024). Native ChIP has not been commonly used in plant research (Ricardi et al., 2010; Huang et al., 2020). However, a few papers describe this method's use for studying plant pathogenic fungi (Cosseau et al., 2009; Soyer et al., 2014, 2015). The N-ChIP method beats traditional methods in profiling histones and histone modifications due to its superior antibody specificity, higher pull-down efficiency, reduced

TABLE 1 Summary of the immunocytochemical detection of selected epitopes in morphogenic and non-morphogenic callus (positive (+) or negative (-) reaction).

|          |       |       | Morphogenic callus (MC) |                            |                | Non-morphogenic callus (NC) |                            |                |
|----------|-------|-------|-------------------------|----------------------------|----------------|-----------------------------|----------------------------|----------------|
|          |       |       | Cell wall compartments  | Internal cell compartments | Callus surface | Cell wall compartments      | Internal cell compartments | Callus surface |
| Pectins  | LM5   | Day 2 | +                       | -                          | -              | +                           | -                          | -              |
|          |       | Day 6 | +                       | -                          | -              | +                           | -                          | -              |
|          | LM6   | Day 2 | -                       | -                          | -              | -                           | -                          | -              |
|          |       | Day 6 | -                       | +                          | -              | -                           | -                          | -              |
|          | LM19  | Day 2 | +                       | +                          | +              | +                           | +                          | +              |
|          |       | Day 6 | +                       | +                          | +              | +                           | +                          | +              |
|          | LM20  | Day 2 | +                       | -                          | +              | +                           | +                          | +              |
|          |       | Day 6 | +                       | -                          | +              | +                           | +                          | +              |
| Extensin | JIM20 | Day 2 | -                       | -                          | -              | -                           | -                          | -              |
|          |       | Day 6 | -                       | -                          | -              | -                           | -                          | -              |

background noise, and minimised bias towards open chromatin (O'Neill and Turner, 2003; Kasinathan et al., 2014), and it has been necessary in this work to be able to analyse *F. tataricum* callus material at early time points of the passage (day two and day six).

In this research, *F. tataricum* MC and NC samples underwent ChIP-seq to assess the global enrichment of H3K4me3. As a result, we were able to notice H3K4me3 distribution clearly differs between MC and NC (Figures 1, 2D), indicating that the enrichment of H3K4me3 could affect transcription potential of many different genes between those two tissue types. This link of H3K4me3 and transcriptionally active regions in *F. tataricum* is supported by the mark presence on genes and the strong enrichment around the TSS (Figure 1A). Available literature coincided with these results. A ChIP-seq analysis of rice callus demonstrated that H3K4me3 peaks are predominantly associated with gene regions, particularly near TSS, indicating its role in active transcription (Zhao et al., 2020). Research on *Eucalyptus grandis* showed that the vast majority of H3K4me3 peaks were gene-associated, particularly near exons and introns. It was also shown that H3K4me3 was present at several highly expressed genes involved in the secondary cell wall (Hussey et al., 2015).

Research demonstrated that the transcriptome analysis in the passage dynamics of soybean revealed active regulation of genes involved in cell wall modification. Those genes' expression proved to be essential for callus induction and proliferation. Researchers concluded that cell wall related genes, such as those responsible for cell wall degradation and synthesis, are differentially expressed during various stages of callus formation, indicating an intricate regulatory mechanism that includes H3K4me3 (Park et al., 2023). H3K4me3 has an indispensable role in maintaining the plasticity and dynamic nature of callus tissues, enabling the reprogramming of somatic cells into a pluripotent state capable of regeneration (Foroozani et al., 2021).

In this work, ChIP-seq H3K4me3 analysis on day eleven of cultivation acted as a reference point for further analysis. This led to selecting the genes coding for *PECTIN METHYLESTERASE INHIBITOR (PMEI)*, *PECTIN METHYLESTERASE (PME)*,

*PEROXIDASE (PX)*, two different regions coding for *EXTENSINS (EXT1, EXT2)*, and two regions coding for *POLYGALACTURONASES (PG1, PG2)*. *PMEI* and *PME* presented lower levels of H3K4me3 in MC on day eleven. *PME* did not show changes of methylation before day eleven, and its expression was undetectable. For *PMEI*, levels of H3K4me3 on day two were already elevated in NC. Despite this methylation pattern, expression in NC was lower than in MC. This suggests an increase in the activity of this enzyme during the MC's PECC disintegration. In *Arabidopsis*, the expression of *PMEI* genes has been linked to enhanced shoot regeneration from callus tissues. The maintenance of a higher degree of pectin methylesterification by *PMEI*s supports the structural changes required for the formation of new shoots from callus cells (Cao et al., 2021). Additionally, by regulating the activity of *PME*s, *PMEI*s regulate the level of pectin methylesterification, which is crucial for maintaining cell wall plasticity. It is essential for the callus' cells to undergo the modifications which are subsequently required for differentiation and development into specialised tissues with morphogenic potential (Zhang et al., 2024). Our immunohistochemical research revealed differences in the distribution pattern of low (LM19) and high methyl-esterified homogalacturonan (HG; LM20) that are strongly connected with *PME* activity. LM19 was present in all examined compartments and on the callus surface in MC and NC across the passage. LM20, on the other hand, was only absent in the internal cell compartments in MC. It has been shown that a reduction in wall stiffness was associated with increased pectin demethylesterification modulated by *PME* (Wormit and Usadel, 2018). The occurrence of both forms of HG in callus cells has been previously observed for other species in both monocots (Betekhtin et al., 2016, 2018) and dicots (Kuczak and Kurczynska, 2020; Popielarska-Konieczna et al., 2020). This may indicate that the presence of high and low methylesterified HG, and therefore the effects of *PME* and *PMEI*, play an important role in developmental processes in callus cells. Aside from differences in the occurrence of HG epitopes, our observations showed the presence of LM5 epitope in the cell wall compartments in MC and NC, whereas

LM6 was present on days six of the passage in MC but completely absent in NC. Antibodies LM5 and LM6 recognise carbohydrate residues within the galactan and arabinan side chains of rhamnogalacturonan I (RG-I), respectively (McCartney et al., 2000). These two forms of RG-I side chains show variable occurrence in cell walls and may be modified depending on both biotic and abiotic factors (Jaskowiak et al., 2019). Moreover, walls rich in galactan are strong and stiff, while those with arabinan predominance are flexible (Schols and Voragen, 1996). Previous immunocytochemical studies of *in vitro* cultures showed the presence of the LM5 epitope, especially in non-embryogenic cells, as well as a poor amount of LM6 epitope (Xu et al., 2011; Pilarska et al., 2013; Potocka et al., 2018), which is in accordance with the presented results.

Peroxidases facilitate the cross-linking cell wall polysaccharides and glycoproteins, increasing the cell wall's mechanical strength. This process is vital for stabilising callus cells and promoting their differentiation into specialised tissues. They are involved in the biosynthesis and polymerisation of lignin, especially during callus differentiation, which is crucial for the structural development of new tissues. *PX* enrichment in H3K4me3 is on an overall low level across the passage in MC with the course of the passage, in correlation with lower gene expression when the new PECCs arise. In peony callus, two peroxidase genes were found to be significantly down-regulated in callus with a high differentiation rate relative to callus with a low differentiation rate (Zhu et al., 2022). In NC, on the other hand, the high levels of H3K4me3 and increased relative expression of *PX* (~40 times) on the sixth day of the passagemay be involved in the rapid proliferation of this tissue.

Polygalacturonases (PGs), along with other cell wall-modifying enzymes, are part of a complex network that regulates the expression of genes involved in cell wall biosynthesis and modification. This network ensures that the cell wall remains dynamic and responsive to the needs of the differentiating cells. In *F. tataricum*, *PG1* and *PG2* are enriched in H3K4me3 in MC but not in NC on day eleven, suggesting active expression of those genes during cellular redifferentiation. Accordingly, gene expression of *PG1* and *PG2* on day two and six is higher in MC, also in agreement with a certain accumulation of H3K4me3 observed within MC, even though it is not statistically significant. Studies have shown that manipulating *PG* expression can influence the efficiency of callus formation and subsequent regeneration. For example, overexpression of *PG* genes can lead to enhanced callus proliferation and improved shoot regeneration from callus tissues (Zhang et al., 2024).

Obtained results suggest that the acquisition of embryogenic potential requires a complex and fine-tuned coordination between multiple processes and involves multiple components in the cell wall. Using two types of *F. tataricum* callus with different capacity for morphogenesis allowed us to conduct a comparative analysis of the H3K4me3 influence on gene expression coding for cell wall genes during the course of callus development.

## 5 Conclusions

The research aimed to analyse and compare the enrichment of H3K4me3 in genes coding for cell wall proteins in *F. tataricum* MC

and NC. The study also optimised the N-ChIP protocol for *F. tataricum* callus tissue, a challenging task due to the species' high phenolic content, which can hinder immunoprecipitation efficiency. ChIP-seq data revealed that H3K4me3 enrichment differs significantly between MC and NC. Further analysis revealed a higher enrichment of H3K4me3 near the TSS, indicating the importance of H3K4me3 on transcriptionally active regions. Additional ChIP-qPCR analysis showed that genes coding for *PME*, *PMEI*, *PX*, *EXTs* and *PGs* settled their enrichment to some extent in MC or NC already at day six or even day two of the passage, suggesting these genes became actively transcribed during callus differentiation and morphogenesis, and that these processes are highly dynamic. The increase in the relative expression of *PX* on day six in NC suggests that this gene is involved in the rapid proliferation of cells in NC.

In summary, this study provides novel insights into the epigenetic regulation of callus development in *F. tataricum*, highlighting the crucial role of H3K4me3 in activating genes involved in cell wall biosynthesis and modification, which are essential for the morphogenesis and regeneration of plant tissues. Our study offers new insights into the epigenetic mechanisms driving the cell wall composition during callus development in *F. tataricum*, offering valuable information in acquiring embryogenic potential.

## Data availability statement

The data presented in the study are deposited in the NCBI GenBank BioProject, accession number: PRJNA1142539.

## Author contributions

AT: Formal analysis, Investigation, Methodology, Visualization, Writing – original draft, Writing – review & editing. AP: Formal analysis, Investigation, Methodology, Visualization, Writing – original draft, Writing – review & editing. AM-H: Formal analysis, Investigation, Methodology, Visualization, Writing – original draft, Writing – review & editing. IAG: Formal analysis, Methodology, Visualization, Writing – review & editing. NB-Z: Methodology, Writing – review & editing. JM: Methodology, Writing – review & editing. JM-R: Formal analysis, Funding acquisition, Investigation, Methodology, Resources, Visualization, Writing – original draft, Writing – review & editing. AB: Conceptualization, Formal analysis, Funding acquisition, Investigation, Methodology, Resources, Supervision, Writing – original draft, Writing – review & editing.

## Funding

The author(s) declare financial support was received for the research, authorship, and/or publication of this article. This research was funded by the National Science Centre, Poland. Research project OPUS-19 (no. reg. 2020/37/B/NZ9/01499 awarded to AB) and the Generalitat de Catalunya AGAUR (2021-SGR0873 awarded to JM-R).



## Acknowledgments

We would like to extend our sincere gratitude to dr Katarzyna Nowak (University of Silesia in Katowice) for her immense help in the RT-qPCR part of this work.

## Conflict of interest

The authors declare that the research was conducted in the absence of any commercial or financial relationships that could be construed as a potential conflict of interest.

## Publisher's note

All claims expressed in this article are solely those of the authors and do not necessarily represent those of their affiliated organizations, or those of the publisher, the editors and the reviewers. Any product that may be evaluated in this article, or claim that may be made by its manufacturer, is not guaranteed or endorsed by the publisher.

## Supplementary material

The Supplementary Material for this article can be found online at: <https://www.frontiersin.org/articles/10.3389/fpls.2024.1465514/full#supplementary-material>

## References

- Akulov, A. N., Gumerova, E. A., and Rumyantseva, N. (2018). *Cell cultures of Fagopyrum tataricum as a source of biologically active phenolic compounds*. Eds. M. Zhang, I. Kreft, G. Suvorova, Y. Tang and S. H. Woo (Cambridge, UK: Academic Press), 259–270.
- Andrews, S. (2010). FastQC: a quality control tool for high throughput sequence data [Online]. Babraham Institute. Available online at: <http://www.bioinformatics.babraham.ac.uk/projects/fastqc>.
- Bednarek, P. T., and Orłowska, R. (2019). Plant tissue culture environment as a switch-key of (epi)genetic changes. *Plant Cell Tissue Organ Cult.* 140, 245–257. doi: 10.1007/s11240-019-01724-1
- Betekhtin, A., Pinski, A., Milewska-Hendel, A., Kurczynska, E., and Hasterok, R. (2019). Stability and instability processes in the calli of *Fagopyrum tataricum* that have different morphogenic potentials. *Plant Cell Tissue Organ Cult.* 137, 343–357. doi: 10.1007/s11240-019-01575-w
- Betekhtin, A., Rojek, M., Jaskowiak, J., Milewska-Hendel, A., Kwasniewska, J., Kostyukova, Y., et al. (2017). Nuclear genome stability in long-term cultivated callus lines of *Fagopyrum tataricum* (L.) Gaertn. *PLoS One* 12, e0173537. doi: 10.1371/journal.pone.0173537
- Betekhtin, A., Rojek, M., Milewska-Hendel, A., Gawecki, R., Karcz, J., Kurczynska, E., et al. (2016). Spatial distribution of selected chemical cell wall components in the embryogenic callus of *Brachypodium distachyon*. *PLoS One* 11, e0167426. doi: 10.1371/journal.pone.0167426
- Betekhtin, A., Rojek, M., Nowak, K., Pinski, A., Milewska-Hendel, A., Kurczynska, E., et al. (2018). Cell wall epitopes and endoploidy as reporters of embryogenic potential in *Brachypodium distachyon* callus culture. *Int. J. Mol. Sci.* 19 (12), 3811. doi: 10.3390/ijms19123811
- Birnbaum, K. D., and Roudier, F. (2017). Epigenetic memory and cell fate reprogramming in plants. *Regeneration* 4, 15–20. doi: 10.1002/reg.2.2017.4.issue-1
- Cao, Y., Zhang, Y., Chen, Y., Yu, N., Liaqat, S., Wu, W., et al. (2021). *OsPG1* encodes a polygalacturonase that determines cell wall architecture and affects resistance to bacterial blight pathogen in rice. *Rice* 14, 36. doi: 10.1186/s12284-021-00478-9
- Collas, P. (2010). The current state of chromatin immunoprecipitation. *Mol. Biotechnol.* 45, 87–100. doi: 10.1007/s12033-009-9239-8
- Community, T. G. (2024). The Galaxy platform for accessible, reproducible, and collaborative data analyses: 2024 update. *Nucleic Acids Res.* 52, 83–94. doi: 10.1093/nar/gkae410
- Corral-Martinez, P., Garcia-Fortea, E., Bernard, S., Driouch, A., and Segui-Simarro, J. M. (2016). Ultrastructural immunolocalization of arabinogalactan protein, pectin and hemicellulose epitopes through anther development in *Brassica napus*. *Plant Cell Physiol.* 57, 2161–2174. doi: 10.1093/pcp/pcw133
- Cosseau, C., Azzi, A., Smith, K., Freitag, M., Mitta, G., and Grunau, C. (2009). Native chromatin immunoprecipitation (N-ChIP) and ChIP-Seq of *Schistosoma mansoni*: critical experimental parameters. *Mol. Biochem. Parasitol.* 166, 70–76. doi: 10.1016/j.molbiopara.2009.02.015
- Desvoyes, B., Fernandez-Marcos, M., Sequeira-Mendes, J., Otero, S., Vergara, Z., and Gutierrez, C. (2014). Looking at plant cell cycle from the chromatin window. *Front. Plant Sci.* 5, 369. doi: 10.3389/fpls.2014.00369

### SUPPLEMENTARY FIGURE 1

Morphology of the *F. tataricum* calli. (A) morphogenic callus (MC); soft callus (black asterisks) and newly formed proembryogenic cell complexes (white asterisks); (B) non-morphogenic callus. Scale bar: 0.5 cm.

### SUPPLEMENTARY FIGURE 2

Graphical depiction of N-ChIP protocol.

### SUPPLEMENTARY FIGURE 3

H3K4me3 enrichment in negative control regions. (A) Visual representation of the H3K4me3 enrichment on negative control selected regions: *PME* upstream (Figure 4) and *S-ELF3*. Coverage of the replicas are represented in the same scale for each gene. Regions amplified by qPCR are indicated as red square on the bottom. (B) ChIP-qPCR of H3K4me3 levels of the negative regions around the *S-ELF3* gene. Box plots show the distribution of normalised z-scores of H3K4me3/Input for MC and NC across the time points (day two and day six).

### SUPPLEMENTARY FIGURE 4

Immunocalisation of LM5 in *F. tataricum* MC and NC in passage dynamics, i.e., day two and day six. *FB* fluorescent brightener. Scale bar: 10 µm.

### SUPPLEMENTARY FIGURE 5

Immunocalisation of LM6 in *F. tataricum* MC and NC in passage dynamics, i.e., day two and day six; white arrows- signal in the inner cell compartments. *FB* fluorescent brightener. Scale bar: 10 µm.

### SUPPLEMENTARY FIGURE 6

Immunocalisation of LM19 in *F. tataricum* MC and NC in passage dynamics, i.e., day two and day six; signal on the callus surface: d2 and d2' inset; d3 and d3' inset. *FB* fluorescent brightener. Scale bar: 10 µm.

### SUPPLEMENTARY FIGURE 7

Immunocalisation of LM20 in *F. tataricum* MC and NC in passage dynamics, i.e., day two and day six; signal on the callus surface: d2 and d2' inset; d3 and d3' inset. *FB* fluorescent brightener. Scale bar: 10 µm.

### SUPPLEMENTARY FIGURE 8

Immunocalisation of JIM20 in *F. tataricum* MC and NC in passage dynamics, i.e., day two and day six. *FB* fluorescent brightener. Scale bar: 10 µm.

### SUPPLEMENTARY FIGURE 9

BioRender.com publication licence for Supplementary Figure 1; graphical depiction of N-ChIP protocol.

- El-Tantawy, A. A., Solis, M. T., Da Costa, M. L., Coimbra, S., Risueno, M. C., and Testillano, P. S. (2013). Arabinogalactan protein profiles and distribution patterns during microspore embryogenesis and pollen development in *Brassica napus*. *Plant Reprod.* 26, 231–243. doi: 10.1007/s00497-013-0217-8
- Feher, A. (2019). Callus, dedifferentiation, totipotency, somatic embryogenesis: what these terms mean in the era of molecular plant biology? *Front. Plant Sci.* 10, 536. doi: 10.3389/fpls.2019.00536
- Foroozani, M., Vandal, M. P., and Smith, A. P. (2021). H3K4 trimethylation dynamics impact diverse developmental and environmental responses in plants. *Planta* 253, 4. doi: 10.1007/s00425-020-03520-0
- Gade, P., and Kalvakolanu, D. V. (2012). Chromatin immunoprecipitation assay as a tool for analyzing transcription factor activity. *Methods Mol. Biol.* 809, 85–104. doi: 10.1007/978-1-61779-376-9\_6
- Gamborg, O. L., Miller, R. A., and Ojima, K. (1968). Nutrient requirements of suspension cultures of soybean root cells. *Exp. Cell Res.* 50, 151–158. doi: 10.1016/0014-4827(68)90403-5
- Gel, B., and Serra, E. (2017). karyoploteR: an R/Bioconductor package to plot customizable genomes displaying arbitrary data. *Bioinformatics* 33, 3088–3090. doi: 10.1093/bioinformatics/btx346
- Guo, L., Yu, Y., Law, J. A., and Zhang, X. (2010). SET DOMAIN GROUP2 is the major histone H3 lysine 4 trimethyltransferase in *Arabidopsis*. *Proc. Natl. Acad. Sci. U.S.A.* 107, 18557–18562. doi: 10.1073/pnas.1010478107
- Hong, C., Lee, H. G., Shim, S., Park, O. S., Kim, J. H., Lee, K., et al. (2024). Histone modification-dependent production of peptide hormones facilitates acquisition of pluripotency during leaf-to-callus transition in *Arabidopsis*. *New Phytol.* 242, 1068–1083. doi: 10.1111/nph.v242.3
- Huang, X., Pan, Q., Lin, Y., Gu, T., and Li, Y. (2020). A native chromatin immunoprecipitation (ChIP) protocol for studying histone modifications in strawberry fruits. *Plant Methods* 16, 10. doi: 10.1186/s13007-020-0556-z
- Hussey, S. G., Mizrahi, E., Groover, A., Berger, D. K., and Myburg, A. A. (2015). Genome-wide mapping of histone H3 lysine 4 trimethylation in *Eucalyptus grandis* developing xylem. *BMC Plant Biol.* 15, 117. doi: 10.1186/s12870-015-0499-0
- Ikeuchi, M., Sugimoto, K., and Iwase, A. (2013). Plant callus: mechanisms of induction and repression. *Plant Cell* 25, 3159–3173. doi: 10.1105/tpc.113.116053
- Jamet, E., Canut, H., Boudart, G., and Pont-Lezica, R. F. (2006). Cell wall proteins: a new insight through proteomics. *Trends Plant Sci.* 11, 33–39. doi: 10.1016/j.tplants.2005.11.006
- Jaskowiak, J., Kwasniewska, J., Milewska-Hendel, A., Kurczynska, E. U., Szurman-Zubrzycka, M., and Szarejko, I. (2019). Aluminum alters the histology and pectin cell wall composition of barley roots. *Int. J. Mol. Sci.* 20 (12), 3039. doi: 10.3390/ijms20123039
- Jones, P., Binns, D., Chang, H. Y., Fraser, M., Li, W., Mcanulla, C., et al. (2014). InterProScan 5: genome-scale protein function classification. *Bioinformatics* 30, 1236–1240. doi: 10.1093/bioinformatics/btu031
- Kasinathan, S., Orsi, G. A., Zentner, G. E., Ahmad, K., and Henikoff, S. (2014). High-resolution mapping of transcription factor binding sites on native chromatin. *Nat. Methods* 11, 203–209. doi: 10.1038/nmeth.2766
- Kearse, M., Moir, R., Wilson, A., Stones-Havas, S., Cheung, M., Sturrock, S., et al. (2012). Geneious Basic: an integrated and extendable desktop software platform for the organization and analysis of sequence data. *Bioinformatics* 28, 1647–1649. doi: 10.1093/bioinformatics/bts199
- Keller, B. (1993). Structural cell wall proteins. *Plant Physiol.* 101, 1127–1130. doi: 10.1104/pp.101.4.1127
- Krueger, F. (2024). *Trim Galore* (Babraham Institute). Available online at: [https://www.bioinformatics.babraham.ac.uk/projects/trim\\_galore/](https://www.bioinformatics.babraham.ac.uk/projects/trim_galore/) (Accessed 5.08.2024).
- Kuczak, M., and Kurczynska, E. (2020). Cell wall composition as a marker of the reprogramming of the cell fate on the example of a *Daucus carota* (L.) hypocotyl in which somatic embryogenesis was induced. *Int. J. Mol. Sci.* 21 (21), 8126. doi: 10.3390/ijms21218126
- Lee, K., and Seo, P. J. (2018). Dynamic epigenetic changes during plant regeneration. *Trends Plant Sci.* 23, 235–247. doi: 10.1016/j.tplants.2017.11.009
- Leszczuk, A., Kalaitzis, P., Kulik, J., and Zdunek, A. (2023). Review: structure and modifications of arabinogalactan proteins (AGPs). *BMC Plant Biol.* 23, 45. doi: 10.1186/s12870-023-04066-5
- Li, H., and Durbin, R. (2009). Fast and accurate short read alignment with Burrows-Wheeler transform. *Bioinformatics* 25, 1754–1760. doi: 10.1093/bioinformatics/btp324
- Li, H., Handsaker, B., Wysoker, A., Fennell, T., Ruan, J., Homer, N., et al. (2009). The sequence alignment/map format and SAMtools. *Bioinformatics* 25, 2078–2079. doi: 10.1093/bioinformatics/btp352
- Li, H., Yan, S., Zhao, L., Tan, J., Zhang, Q., Gao, F., et al. (2024). Histone acetylation associated up-regulation of the cell wall related genes is involved in salt stress induced maize root swelling. *BMC Plant Biol.* 14. doi: 10.1186/1471-2229-14-105
- Long, Y., Yang, Y., Pan, G., and Shen, Y. (2022). New insights into tissue culture plant-regeneration mechanisms. *Front. Plant Sci.* 13, 926752. doi: 10.3389/fpls.2022.926752
- McCartney, L., Ormerod, A. P., Gidley, M. J., and Knox, J. P. (2000). Temporal and spatial regulation of pectic (1→4)-beta-D-galactan in cell walls of developing pea cotyledons: implications for mechanical properties. *Plant J.* 22, 105–113. doi: 10.1046/j.1365-313x.2000.00719.x
- McDougall, G. J., Davidson, D., and Millam, S. (1992). Alterations in surface-associated peroxidases during callus development and shoot formation in explants of *Linum usitatissimum*. *J. Plant Physiol.* 140, 195–200. doi: 10.1016/S0176-1617(11)80934-X
- Nakato, R., and Sakata, T. (2021). Methods for ChIP-seq analysis: A practical workflow and advanced applications. *Methods* 187, 44–53. doi: 10.1016/j.jmeth.2020.03.005
- Nicolas, J., Billaud, C., Philippon, J., and Rouet-Mayer, M. A. (2003). “Browning. Enzymatic – biochemical aspects,” in *Encyclopedia of Food Sciences and Nutrition (Second Edition)*. Ed. B. Caballero (Cambridge, MA, USA: Academic Press), 678–686.
- O'Neill, L. P., and Turner, B. M. (2003). Immunoprecipitation of native chromatin: NChIP. *Methods* 31, 76–82. doi: 10.1016/S1046-2023(03)00090-2
- Park, J. S., Choi, Y., Jeong, M. G., Jeong, Y. I., Han, J. H., and Choi, H. K. (2023). Uncovering transcriptional reprogramming during callus development in soybean: insights and implications. *Front. Plant Sci.* 14, 1239917. doi: 10.3389/fpls.2023.1239917
- Pilarska, M., Knox, J. P., and Konieczny, R. (2013). Arabinogalactan-protein and pectin epitopes in relation to an extracellular matrix surface network and somatic embryogenesis and callogenesis in *Trifolium nigrescens* Viv. *PCTOC* 115, 35–44. doi: 10.1007/s11240-013-0337-8
- Popielarska-Konieczna, M., Sala, K., Abdullah, M., Tuleja, M., and Kurczynska, E. (2020). Extracellular matrix and wall composition are diverse in the organogenic and non-organogenic calli of *Actinidia arguta*. *Plant Cell Rep.* 39, 779–798. doi: 10.1007/s00299-020-02530-2
- Potocka, I., Godel, K., Dobrowolska, I., and Kurczynska, E. (2018). Spatio-temporal localization of selected pectic and arabinogalactan protein epitopes and the ultrastructural characteristics of explant cells that accompany the changes in the cell fate during somatic embryogenesis in *Arabidopsis thaliana*. *Plant Physiol. Biochem.* 127, 573–589. doi: 10.1016/j.plaphy.2018.04.032
- Quinlan, A. R., and Hall, I. M. (2010). BEDTools: a flexible suite of utilities for comparing genomic features. *Bioinformatics* 26, 841–842. doi: 10.1093/bioinformatics/btq033
- Ramirez, F., Ryan, D. P., Gruning, B., Bhardwaj, V., Kilpert, F., Richter, A. S., et al. (2016). deepTools2: a next generation web server for deep-sequencing data analysis. *Nucleic Acids Res.* 44, W160–W165. doi: 10.1093/nar/gkw257
- Ricardi, M. M., González, R. M., and Iusem, N. D. (2010). Protocol: fine-tuning of a Chromatin Immunoprecipitation (ChIP) protocol in tomato. *Plant Methods* 6, 11. doi: 10.1186/1746-4811-6-11
- Robinson, J. T., Thorvaldsdóttir, H., Winckler, W., Guttman, M., Lander, E. S., Getz, G., et al. (2011). Integrative genomics viewer. *Nat. Biotechnol.* 29, 24–26. doi: 10.1038/nbt.1754
- Ross-Innes, C. S., Stark, R., Teschendorff, A. E., Holmes, K. A., Ali, H. R., Dunning, M. J., et al. (2012). Differential oestrogen receptor binding is associated with clinical outcome in breast cancer. *Nature* 481, 389–393. doi: 10.1038/nature10730
- Rumyantseva, N., Samaj, J., Ensikat, H., Salnikov, V., Kostyukova, Y., Baluska, F., et al. (2003). Changes in the extracellular matrix surface network during cyclic reproduction of preembryonic cell complexes in the *Fagopyrum tataricum* (L.) Gaertn callus. *Doklady Biol. Sci.* 391, 375–378. doi: 10.1023/A:1025127323165
- Sala, K., Karcz, J., Rypien, A., and Kurczynska, E. U. (2019). Unmethyl-esterified homogalacturonan and extensins seal *Arabidopsis* graft union. *BMC Plant Biol.* 19, 151. doi: 10.1186/s12870-019-1748-4
- Sala-Cholewa, K., Tomasiak, A., Nowak, K., Pinski, A., and Betekhtin, A. (2024). DNA methylation analysis of floral parts revealed dynamic changes during the development of homostylous *Fagopyrum tataricum* and heterostylous *F. esculentum* flowers. *BMC Plant Biol.* 24, 448. doi: 10.1186/s12870-024-05162-w
- Schols, H. A., and Voragen, A. G. J. (1996). Complex pectins: structure elucidation using enzymes. *Biotechnol. Prog.* 14, 3–19. doi: 10.1016/S0921-0423(96)80242-5
- Shin, Y., Chane, A., Jung, M., and Lee, Y. (2021). Recent advances in understanding the roles of pectin as an active participant in plant signaling networks. *Plants (Basel)* 10 (8), 1712. doi: 10.3390/plants10081712
- Smertenko, A., and Bozhkov, P. (2014). “The life and death signalling underlying cell fate determination during somatic embryogenesis,” in *Applied Plant Cell Biology. Plant Cell Monographs*. Eds. P. Nick and Z. Opatrny (Berlin, Germany: Springer), 131–178. doi: 10.1007/978-3-642-41787-0\_5
- Soyer, J. L., El Ghalid, M., Glaser, N., Ollivier, B., Linglin, J., Grandaubert, J., et al. (2014). Epigenetic control of effector gene expression in the plant pathogenic fungus *Leptosphaeria maculans*. *PLoS Genet.* 10, e1004227. doi: 10.1371/journal.pgen.1004227
- Soyer, J. L., Moller, M., Schotanus, K., Connolly, L. R., Galazka, J. M., Freitag, M., et al. (2015). Chromatin analyses of *Zymoseptoria tritici*: Methods for chromatin immunoprecipitation followed by high-throughput sequencing (ChIP-seq). *Fungal Genet. Biol.* 79, 63–70. doi: 10.1016/j.fgb.2015.03.006
- Stark, R., and Brown, G. D. (2011). DiffBind: Differential binding analysis of ChIP-Seq peak data. Bioconductor. [Online]. Cancer Research UK- Cambridge Institute: University of Cambridge. Available online at: <http://bioconductor.org/packages/release/bioc/html/DiffBind.html> (accessed 16.08.2024 2024).

- Stovner, E. B., and Saetrom, P. (2019). epic2 efficiently finds diffuse domains in ChIP-seq data. *Bioinformatics* 35, 4392–4393. doi: 10.1093/bioinformatics/btz232
- Su, S., and Higashiyama, T. (2018). Arabinogalactan proteins and their sugar chains: functions in plant reproduction, research methods, and biosynthesis. *Plant Reprod.* 31, 67–75. doi: 10.1007/s00497-018-0329-2
- Tomasiak, A., Sala-Cholewa, K., Berg, L. S., Braszewska, A., and Betekhtin, A. (2023). Global epigenetic analysis revealed dynamic fluctuations in levels of DNA methylation and histone modifications in the calli of *Fagopyrum* with different capacity for morphogenesis. *Plant Cell Tissue Organ Cult.* 155, 743–757. doi: 10.1007/s11240-023-02595-3
- Trejo-Arellano, M. S., Mahrez, W., Nakamura, M., Moreno-Romero, J., Nanni, P., Köhler, C., et al. (2017). H3K23me1 is an evolutionarily conserved histone modification associated with CG DNA methylation in *Arabidopsis*. *Plant J.* 90, 293–303. doi: 10.1111/tpj.13489
- Wormit, A., and Usadel, B. (2018). The multifaceted role of pectin methyltransferase inhibitors (PMEIs). *Int. J. Mol. Sci.* 19 (10), 2878. doi: 10.3390/ijms19102878
- Xu, C., Cao, H., Xu, E., Zhang, S., and Hu, Y. (2018). Genome-wide identification of *Arabidopsis* LBD29 target genes reveals the molecular events behind auxin-induced cell reprogramming during callus formation. *Plant Cell Physiol.* 59, 744–755. doi: 10.1093/pcp/pcx168
- Xu, C., Zhao, L., Pan, X., and Samaj, J. (2011). Developmental localization and methylesterification of pectin epitopes during somatic embryogenesis of banana (*Musa* spp. AAA). *PLoS One* 6 (8), e22992. doi: 10.1371/journal.pone.0022992
- Zhang, G., Liu, P., Zhang, G., Yao, X., Wang, X., Zhang, Y., et al. (2024). Cell wall remodeling promotes callus formation in poplar. *Mol. Hort.* 4, 16. doi: 10.1186/s43897-024-00093-4
- Zhang, L., Li, X., Ma, B., Gao, Q., Du, H., Han, Y., et al. (2017). The Tartary buckwheat genome provides insights into rutin biosynthesis and abiotic stress tolerance. *Mol. Plant* 10, 1224–1237. doi: 10.1016/j.molp.2017.08.013
- Zhao, N., Zhang, K., Wang, C., Yan, H., Liu, Y., Xu, W., et al. (2020). Systematic analysis of differential H3K27me3 and H3K4me3 deposition in callus and seedling reveals the epigenetic regulatory mechanisms involved in callus formation in rice. *Front. Genet.* 11, 766. doi: 10.3389/fgene.2020.00766
- Zhu, X., Zhu, H., Ji, W., Hong, E., Lu, Z., Li, B., et al. (2022). Callus induction and transcriptomic analysis of *in vitro* embryos at different developmental stages of peony. *Front. Plant Sci.* 13, 1046881. doi: 10.3389/fpls.2022.1046881

## **8.2 Omówienie wyników badań przeprowadzonych *in vivo***

## 8.2.1 Ocena poziomu zmian metylacji DNA oraz genów kodujących metylazy i demetylazy DNA w kwiatach zamkniętych oraz otwartych samopylnej gryki tatarskiej i obcopolnej gryki zwyczajnej

### Publikacja P4:

Sala-Cholewa K.\*, Tomasiak A.\*, Nowak K., Piński A., Betekhtin A. DNA methylation analysis of floral parts revealed dynamic changes during the development of homostylous *Fagopyrum tataricum* and heterostylous *F. esculentum* flowers.

BMC Plant Biology, 2024, 24, 448

<https://doi.org/10.1186/s12870-024-05162-w>

\* równorzędny pierwszy autor

IF<sub>2024</sub>: 4,3

Punkty MNiSW: 100

Celem badania było porównanie profili metylacji DNA pomiędzy elementami kwiatów (płatki, nektarniki, załącznik, znamiona słupka) *F. tataricum* oraz kwiatami typu Pin i Thrum *F. esculentum*. Porównano poziomy metylacji DNA w gatunku obcopolnym *F. esculentum*, charakteryzującym się heterostylią, z gatunkiem samopolnym *F. tataricum*. Kwiaty *F. esculentum* charakteryzują się dwoma morfotypami: kwiaty typu Pin posiadają długi słupek i krótsze pręciki (Ryc. 2a), natomiast kwiaty typu Thrum posiadają krótki słupek i dłuższe pręciki (Ryc. 2b). Otwarte kwiaty *F. tataricum* charakteryzowały się słupkiem i pręcikami o podobnej długości (Ryc. 2c).

Badania wykazały różnice w poziomie metylacji DNA. Płatki *F. esculentum* Thrum charakteryzowały się najwyższym początkowym poziomem metylacji DNA i najbardziej znaczącym spadkiem. U *F. tataricum*, natomiast najniższa wartość metylacji DNA obserwowana była w zamkniętych kwiatach. Kolejny analizowany element, znamię, to element słupka, kluczowy dla początkowych etapów zapylania. W tej części kwiatu zaobserwowano najwyższe wartości metylacji DNA w zamkniętych kwiatach oraz największą redukcję tego markera w otwartych kwiatach obu gatunków. Najwyższy poziom metylacji DNA w zamkniętych kwiatach oraz jej spadek (około pięciokrotny) zaobserwowano w typie Pin *F. esculentum*. Typ Thrum charakteryzował się natomiast niższym poziomem metylacji DNA i jednocześnie mniejszym spadkiem wartości metylacji DNA w porównaniu do Pin. Znamiona

*F. tataricum* wykazywały najniższy wyjściowy poziom metylacji DNA na etapie zamkniętych kwiatów i około dwukrotny spadek w otwartych kwiatach, podobnie jak w typie Thrum *F. esculentum*. Poziom metylacji DNA w zalążniach był najwyższy w zamkniętych kwiatach *F. tataricum*, następnie u *F. esculentum* w typie Pin, a najniższy w typie Thrum. Podczas rozwoju kwiatów zaobserwowano niewielki spadek poziomu metylacji DNA w zalążni zarówno w typie Pin *F. esculentum*, jak i u *F. tataricum*, w przeciwieństwie do zalążni morfotypu Thrum, w których wartości poziomu metylacji DNA wzrastały w otwartych kwiatach. W przeciwieństwie do innych elementów kwiatu (z wyjątkiem zalążni kwiatu typu Thrum), nektarniki otwartych kwiatów miały wyższe wartości metylacji DNA w porównaniu do wartości z zamkniętych kwiatów we wszystkich trzech typach (Pin, Thrum, *F. tataricum*). Jednakże, wzrost poziomu metylacji DNA był nieznaczny w przypadku typu Pin czy Thrum. Podsumowując, *F. esculentum* Pin i Thrum różnią się znacznie poziomem metylacji DNA w analizowanych elementach kwiatu. W zalążni, znamieniu i płatkach otwartych kwiatów typ Thrum wykazywał wyższe wartości poziomu metylacji DNA niż typ Pin. Wyniki uzyskane w przypadku gryki tatarskiej wykazują pewne podobieństwa do morfotypu Pin lub Thrum, w zależności od analizowanej części i stadium rozwojowego kwiatów.

Przeanalizowano również poziom ekspresji genów związanych z metylacją (*MET1*, *MET2*, *CMET3*) i demetylacją DNA (*DME1*, *DME3*, *ROS1*) w zamkniętych i otwartych kwiatach Pin i Thrum *F. esculentum* oraz kwiatach *F. tataricum*. Ekspresja wszystkich genów była wyższa (od 2,5 do ponad 9 razy wyższa) w zamkniętych kwiatach *F. esculentum* niż w kwiatach *F. tataricum*. Ponadto, wykryto różnice w ekspresji genów między kwiatami typu Pin i Thrum, zarówno zamkniętymi, jak i otwartymi. Ekspresja *MET2*, *DME1* i *ROS1* była niższa w kwiatach typu Pin w porównaniu do kwiatów typu Thrum. Pozostałe trzy analizowane geny (*MET1*, *CMET3*, *DME3*) charakteryzowały się wyższymi poziomami transkrypcji w kwiatach typu Thrum niż w typie Pin. Wyniki wykazały obniżenie ekspresji wszystkich genów w kwiatach typu Thrum. Najbardziej intensywny spadek ekspresji zaobserwowano dla *MET1*, który był ponad 45 razy niższy w otwartych niż w zamkniętych kwiatach typu Thrum. W przeciwieństwie do kwiatów typu Thrum, ekspresja *MET1* w otwartych kwiatach typu Pin nie różniła się statystycznie w porównaniu z kwiatami zamkniętymi. Obniżony poziom transkrypcji pozostałych analizowanych genów zaobserwowano w otwartych kwiatach typu Pin. Największy spadek był charakterystyczny dla genu *DME3* (14 razy niższy w otwartych niż w zamkniętych kwiatach typu Pin). Niższy poziom transkrypcji prawie wszystkich analizowanych genów zaobserwowano w otwartych kwiatach *F. tataricum*. Zasadniczo, podczas rozwoju kwiatów ekspresja genów kodujących metylazy i demetylazy DNA malała.

Przedstawiona praca ukazuje różne wzory metylacji DNA w wybranych elementach kwiatów typu Pin i Thrum u *F. esculentum*, oraz *F. tataricum*. Pozwoliło to na określenie potencjalnej roli tej modyfikacji epigenetycznej podczas rozwoju kwiatów gatunków *Fagopyrum*. Zrozumienie znaczenia metylacji DNA jest kluczowe dla rozwikłania molekularnych mechanizmów leżących u podstaw rozwoju i adaptacji kwiatów do zmian środowiskowych. Porównanie globalnej metylacji DNA i ekspresji genów w obu typach kwiatów *F. esculentum*, a także z blisko spokrewnionym samopylnym gatunkiem *F. tataricum*, wskazało na różnice między nimi, co może być zarówno przyczyną bądź skutkiem samo-niezhodności. Zwiększenie wiedzy o mechanizmach molekularnych heterostylii będzie pomocne w stworzeniu odmian samopylnych.

**Publikacja P4:** DNA methylation analysis of floral parts revealed dynamic changes during the development of homostylous *Fagopyrum tataricum* and heterostylous *F. esculentum* flowers.

Sala-Cholewa K.\*, **Tomasiak A.\***, Nowak K., Piński A., Betekhtin A. DNA methylation analysis of floral parts revealed dynamic changes during the development of homostylous *Fagopyrum tataricum* and heterostylous *F. esculentum* flowers.

BMC Plant Biology, **2024**, 24, 448

<https://doi.org/10.1186/s12870-024-05162-w>

\* równorzędny pierwszy autor

IF<sub>2024</sub>: 4,3

**Punkty MNiSW:** 100

Materiały uzupełniające dostępne online

**Additional file 1:** Graficzne przedstawienie schematu eksperymentu immunobarwienia i analizy obrazu

[https://static-content.springer.com/esm/art%3A10.1186%2Fs12870-024-05162-w/MediaObjects/12870\\_2024\\_5162\\_MOESM1\\_ESM.jpeg](https://static-content.springer.com/esm/art%3A10.1186%2Fs12870-024-05162-w/MediaObjects/12870_2024_5162_MOESM1_ESM.jpeg)

**Additional file 2:** Dane numeryczne z pomiarów intensywności fluorescencji

[https://static-content.springer.com/esm/art%3A10.1186%2Fs12870-024-05162-w/MediaObjects/12870\\_2024\\_5162\\_MOESM2\\_ESM.xlsx](https://static-content.springer.com/esm/art%3A10.1186%2Fs12870-024-05162-w/MediaObjects/12870_2024_5162_MOESM2_ESM.xlsx)

**Additional file 3:** Skrypt z programu R studio (2022.12.0 wersja 353) użyty do analizy statystycznej i graficznej wizualizacji wyników z pomiarów fluorescencji metylacji DNA

[https://static-content.springer.com/esm/art%3A10.1186%2Fs12870-024-05162-w/MediaObjects/12870\\_2024\\_5162\\_MOESM3\\_ESM.docx](https://static-content.springer.com/esm/art%3A10.1186%2Fs12870-024-05162-w/MediaObjects/12870_2024_5162_MOESM3_ESM.docx)

**Additional file 4:** Tabela zawierająca informacje na temat starterów genów metylaz i demetylaz DNA użytych to analiz RT-qPCR

[https://static-content.springer.com/esm/art%3A10.1186%2Fs12870-024-05162-w/MediaObjects/12870\\_2024\\_5162\\_MOESM4\\_ESM.xlsx](https://static-content.springer.com/esm/art%3A10.1186%2Fs12870-024-05162-w/MediaObjects/12870_2024_5162_MOESM4_ESM.xlsx)

**Additional file 5:** Certyfikat ze strony BioRender.com potwierdzający prawa do publikowania schematu eksperymentu immunobarwienia i analizy obrazu (Additional file 1)

[https://static-content.springer.com/esm/art%3A10.1186%2Fs12870-024-05162-w/MediaObjects/12870\\_2024\\_5162\\_MOESM5\\_ESM.pdf](https://static-content.springer.com/esm/art%3A10.1186%2Fs12870-024-05162-w/MediaObjects/12870_2024_5162_MOESM5_ESM.pdf)



**Additional file 6:** Histologia pylników z zamkniętych (a – c) i otwartych (d – f) kwiatów *F. esculentum* i *F. tataricum*

[https://static-content.springer.com/esm/art%3A10.1186%2Fs12870-024-05162-w/MediaObjects/12870\\_2024\\_5162\\_MOESM6\\_ESM.jpeg](https://static-content.springer.com/esm/art%3A10.1186%2Fs12870-024-05162-w/MediaObjects/12870_2024_5162_MOESM6_ESM.jpeg)

**Additional file 7:** Przykładowy obraz uzyskany z wykorzystaniem mikroskopu konfokalnego Olympus FV1000

[https://static-content.springer.com/esm/art%3A10.1186%2Fs12870-024-05162-w/MediaObjects/12870\\_2024\\_5162\\_MOESM7\\_ESM.jpeg](https://static-content.springer.com/esm/art%3A10.1186%2Fs12870-024-05162-w/MediaObjects/12870_2024_5162_MOESM7_ESM.jpeg)

RESEARCH

Open Access



# DNA methylation analysis of floral parts revealed dynamic changes during the development of homostylous *Fagopyrum tataricum* and heterostylous *F. esculentum* flowers

Katarzyna Sala-Cholewa<sup>1\*†</sup>, Alicja Tomasiak<sup>1†</sup>, Katarzyna Nowak<sup>1</sup>, Artur Piński<sup>1</sup> and Alexander Betekhtin<sup>1\*</sup>

## Abstract

**Background** Proper flower development is essential for plant reproduction, a crucial aspect of the plant life cycle. This process involves precisely coordinating transcription factors, enzymes, and epigenetic modifications. DNA methylation, a ubiquitous and heritable epigenetic mechanism, is pivotal in regulating gene expression and shaping chromatin structure. *Fagopyrum esculentum* demonstrates anti-hypertensive, anti-diabetic, anti-inflammatory, cardio-protective, hepato-protective, and neuroprotective properties. However, the heteromorphic heterostyly observed in *F. esculentum* poses a significant challenge in breeding efforts. *F. tataricum* has better resistance to high altitudes and harsh weather conditions such as drought, frost, UV-B radiation damage, and pests. Moreover, *F. tataricum* contains significantly higher levels of rutin and other phenolics, more flavonoids, and a balanced amino acid profile compared to common buckwheat, being recognised as functional food, rendering it an excellent candidate for functional food applications.

**Results** This study aimed to compare the DNA methylation profiles between the Pin and Thrum flower components of *F. esculentum*, with those of self-fertile species of *F. tataricum*, to understand the potential role of this epigenetic mechanism in *Fagopyrum* floral development. Notably, *F. tataricum* flowers are smaller than those of *F. esculentum* (Pin and Thrum morphs). The decline in DNA methylation levels in the developed open flower components, such as petals, stigmas and ovules, was consistent across both species, except for the ovule in the Thrum morph. Conversely, Pin and Tartary ovules exhibited a minor decrease in DNA methylation levels. The highest DNA methylation level was observed in Pin stigma from closed flowers, and the most significant decrease was in Pin stigma from open flowers.

<sup>†</sup>Katarzyna Sala-Cholewa and Alicja Tomasiak contributed equally to this work.

\*Correspondence:  
Katarzyna Sala-Cholewa  
katarzyna.sala@us.edu.pl  
Alexander Betekhtin  
alexander.betekhtin@us.edu.pl

Full list of author information is available at the end of the article



© The Author(s) 2024. **Open Access** This article is licensed under a Creative Commons Attribution 4.0 International License, which permits use, sharing, adaptation, distribution and reproduction in any medium or format, as long as you give appropriate credit to the original author(s) and the source, provide a link to the Creative Commons licence, and indicate if changes were made. The images or other third party material in this article are included in the article's Creative Commons licence, unless indicated otherwise in a credit line to the material. If material is not included in the article's Creative Commons licence and your intended use is not permitted by statutory regulation or exceeds the permitted use, you will need to obtain permission directly from the copyright holder. To view a copy of this licence, visit <http://creativecommons.org/licenses/by/4.0/>. The Creative Commons Public Domain Dedication waiver (<http://creativecommons.org/publicdomain/zero/1.0/>) applies to the data made available in this article, unless otherwise stated in a credit line to the data.

In opposition, the nectaries of open flowers exhibited higher levels of DNA methylation than those of closed flowers. The decrease in DNA methylation might correspond with the downregulation of genes encoding methyltransferases.

**Conclusions** Reduced overall DNA methylation and the expression of genes associated with these epigenetic markers in fully opened flowers of both species may indicate that demethylation is necessary to activate the expression of genes involved in floral development.

**Keywords** DNA methylation, Epigenetics, *Fagopyrum esculentum*, *Fagopyrum tataricum*, Flowers, Gene expression, Heterostyly

## Background

Buckwheat constitutes a small genus of 22 members [1]. Two of the most widely cultivated species of this genus are *Fagopyrum esculentum* Moench (common buckwheat) and *Fagopyrum tataricum* (Tartary buckwheat) [2, 3]. Common buckwheat is commonly cultivated in Russia, China, France, Poland, and the American regions [4, 5]. In terms of overall yield, buckwheat is a minor crop. However, its popularity among consumers steadily increases due to its remarkable properties. Common buckwheat is rich in beneficial phenolic compounds like rutin, quercetin and C-glycosyl flavones (orientin, isoorientin and vitexin). Additionally, it is gluten-free and provides amino acids, dietary fibre, resistant starch, and vitamins [6–8]. It was demonstrated that *F. esculentum* exhibits anti-hypertension, anti-diabetic, anti-inflammatory, cardio-protective, hepato-protective, and neuroprotective properties [7, 8]. Tartary buckwheat exhibits higher than common buckwheat resistance to high altitudes, harsh weather conditions such as drought, frost, UV-B radiation damage, and pests [9]. Additionally, compared to common buckwheat, *F. tataricum* contains more rutin and other phenolics and flavonoids, with well-balanced amino acids, making it a functional pseudocereal [10]. One significant advantage of Tartary buckwheat lies in the differences in flower structure and pollination methods, which directly impact yield. *F. esculentum* is an obligatory cross-pollinating, heterostylous species, while *F. tataricum* is self-pollinating, homostylous species eliminating reliance on external pollinators [11, 12]. *F. esculentum* has two floral morphs: Pin and Thrum, which differ in stamen and style length ratio, amount and size of the produced pollen grain, exine sculpturing, and nectar production [13, 14]. The distyly of *F. esculentum* is controlled by a cluster of genes, i.e. supergene S [13, 15]. Recently, the *S-LOCUS EARLY FLOWERING 3* gene (*S-ELF3*), present within the S supergene locus, was shown to control style length and style incompatibility. The inactivation of *S-ELF3* has led to the breakage of heterostyly and successful pollination [15]. While in the incompatible intra-morph pollination, the pollen tube growth within the style is inhibited [13, 16, 17].

Proper flower development ensures reproduction, one of the most vital parts of the plant's life cycle. This

process relies on fine-tuned machinery of transcription factors, enzymes and epigenetic modifications to function correctly. DNA methylation, a universal and heritable epigenetic mechanism, regulates gene expression and the chromatin structure [16, 18]. The extent of DNA methylation significantly shapes the plant genome's structure and function. Various molecular mechanisms are impacted by DNA methylation, highlighting its pivotal role in regulating cellular processes within plants [16, 19–22]. DNA methylation takes place at CG, CHG and CHH sites (H=A, T or C); methylation at these three sites is achieved by *DNA METHYLTRANSFERASE 1* (*MET1*), the plant-specific *CHROMOMETHYLASE 3* (*CMT3*), and *DOMAINS REARRANGED METHYLTRANSFERASEs* (*DRMs*), respectively [23, 24]. Each type is crucial for development and the ability to respond to environmental stresses [16, 25]. An opposite phenomenon, demethylation, is dependent on four bifunctional 5-methylcytosine glycosylases: *REPRESSOR OF SILENCING 1* (*ROS1*), *DEMETER* (*DME*), *DME-LIKE 2* (*DML2*), and *DML3*, which are involved in the removal of methylated bases and cleavage of the DNA backbone at abasic sites [26]. *ROS1* counteracts the DNA methylation pathway to prevent plant gene silencing [27]. Research demonstrated that DNA methylation plays an essential role in flower development, with demethylation dominating during early flower development [28]. It was also reported that decreased levels of DNA methylation induced early flowering and that demethylation activities are correlated with changes in the expression levels of DNA methylation genes [28–30]. On the other hand, experiments on *Azalea japonica* and *Arabidopsis* demonstrated an increase in global DNA methylation during the transition from the vegetative to the flowering stage [31, 32]. DNA methylation was determined to influence various aspects of flower development and morphology [33]. It affects floret closing in barley, and the development of bisexual flowers in *Populus cathayana* and *Fraxinus mandshurica* [34–36]. DNA methylation is also involved in forming double flowers and dichromatic petals [37, 38]. Moreover, it plays a crucial role in the expression of genes related to anthocyanin pigmentation in flower tissue [9, 39, 40]. Existing evidence suggests that methylation alterations accompany the flowering process

in plants. Methylation regulates key flowering-related genes such as *SOC1*, *API*, and *SPL* and specific transcription factor genes, including *WUS* homeobox-containing (*WOX*) genes in apple [41].

While numerous processes related to DNA methylation in plant vegetative tissues have been extensively studied, there remains a scarcity of information regarding DNA methylation during flower development, particularly in flowers exhibiting distinct morphologies. Thus, this study aimed to compare the DNA methylation status of Pin and Thrum flower components of *F. esculentum* that participate in pollination and embryo production with self-sufficient species of *F. tataricum*.

## Methods

### Plant material

*F. tataricum* seeds, sample k-17, were obtained from the N. I. Vavilov Institute of Plant Genetic Resources, Saint Petersburg, Russia. K-17 sample is a widely cultivated landrace of *F. tataricum*. Seeds are available upon request from the authors. *F. esculentum* seeds of the Panda cultivar are commercially available and were supplied from the Malopolska Plant Breeding, Poland. Both plant species were grown in pots with soil mixed with vermiculite (3:1, w/v) in a greenhouse at  $20 \pm 1$  °C, under a 16/8 h light/dark photoperiod, provided by lamps emitting white light at the intensity of  $90 \mu\text{mol m}^{-2} \text{s}^{-1}$ . After approximately three to four weeks, the flowers started to appear and were gradually collected, photographed with the use of Keyence VHX-970 F digital microscope (Japan) equipped with an ultra-small high-performance zoom lens VH-Z20R/Z20T and wide-area illumination adapter OP-87,298 and designated for further procedures.

For analysis, the closed flowers from both species were fixed in the intact state. Open flowers were dissected into parts that involved excised petals, stigmas and remains that contained ovaries and nectaries.

### Histological and immunostaining procedures

Closed and open flower components from *F. tataricum*, as well as closed and open Pin and Thrum flower components from *F. esculentum* were fixed in 4% paraformaldehyde (Sigma-Aldrich, USA) in 1x phosphate-buffered saline (PBS), pH 7.3 and placed in the vacuum desiccator for three hours (with 30 min intervals), after which the incubation at 4 °C overnight has followed. After approximately 24 h, the fixative was replaced with 1 × PBS (twice for 15 min) and followed by dehydration in a graded ethanol series diluted in 1xPBS solution in each

concentration (10%, 30%, 50%, 70% and 90%) and 99,8% twice for 30 min each. Subsequently, the embedding procedure was performed according to Wolny et al., 2014 [42]. 5 μm thick sections were prepared using a HYRAX M40 rotary microtome (Zeiss, Oberkochen, Germany) and placed on polysine-coated microscope slides (Epre-dia, Netherlands). Next, the de-embedding procedure comprised of placing the slides in 99,8% ethanol three times for 10 min, followed by the rehydration in ethanol/1xPBS solutions: 90%, 50%v/v and, finally in 1xPBS for 10 min each. Such prepared slides were used for both, the immunostaining and histological analysis. For the histological analysis, slides were stained with 0.05% aqueous solution of Toluidine blue O (TBO, Sigma-Aldrich, USA) for approximately 10 min, rinsed and mounted with 50% glycerol/ distilled water solution (v/v). Observations and photographs of histological sections were performed with an Olympus BX43F microscope equipped with an Olympus XC50 digital camera.

The immunostaining method was previously established by Braszewska-Zalewska et al., 2013 [43]. After the wax de-embedding described above, samples underwent the 2 N HCl (Sigma-Aldrich, USA) digestion for 45 min to denature DNA. Following, the slides were incubated with 5% bovine serum albumin (BSA, Sigma-Aldrich, USA) in 1xPBS for 1 h in the humid chamber at room temperature. Next, the primary antibody diluted in 1% BSA in 1xPBS (1:100) was applied, and slides were incubated at 4° C overnight (Table 1). After the incubation, the slides were washed three times in 1xPBS. Subsequently, a secondary antibody diluted in 1% BSA in 1xPBS (1:100) was applied, and samples were incubated at 37 ° C in the humid chamber in the dark for 1 h. After the incubation, the slides were again washed three times in 1xPBS and nuclei were counterstained with 4',6-diamidino-2-fenylindol (DAPI, 2.5 g/ml in Vectashield).

Graphical depiction of the experimental design is available in Additional Files, File 1.

### Fluorescence intensity measurements and statistical analysis

Images were captured with the Olympus FV1000 confocal system (Olympus, Poland) equipped with an Olympus IX81 inverted microscope. Fluorescence of Alexa488 (excitation 488 nm, emission 500–600 nm) was acquired from a 60x Plan Apo oil-immersion objective lens (NA 1.35), a 50 mW 405 nm diode laser and a 100 mW multiline argon ion laser (Melles Griot BV, the Netherlands). The confocal laser scanning microscope offers a significant advantage in obtaining high-resolution images of optical sections through fluorescently labelled nuclei (z-stacks) [44, 45]. The pixel-by-pixel image generation produces exceptional quality images [45], enabling visualization of fluorescence distribution corresponding to

**Table 1** List of antibodies used in the immunostaining

| Antibody              | Catalogue number | Company   |
|-----------------------|------------------|-----------|
| Anti-5-methylcytosine | ab73938          | Abcam, UK |
| Goat anti-mouse IgG   | ab150113         | Abcam, UK |

DNA methylation within the three-dimensional chromatin architecture of a nucleus. The nucleus area was used to standardise the fluorescence intensity, preventing any artificial positive correlation between intensity and nucleus size. Consequently, the fluorescence intensity-to-nucleus area ratio indicated the level of DNA methylation [46]. An axial series of two-dimensional fluorescence images of the optical sections through the nuclei (z-stacks) was collected with the use of two separate photomultipliers (R6357, Hamamatsu Photonics, Hamamatsu, Japan) set to work in the integration mode at 4  $\mu$ s pixel dwell time and 12-bit signal digitisation (4096 intensity levels). The fluorescence intensity levels of Alexa488 fluorochrome were subsequently measured in the ImageJ version 1.53s software (Wayne Rasband, National Institutes of Health, USA). ImageJ is a Java-based image processing program developed at the National Institutes of Health and the Laboratory for Optical and Computational Instrumentation (LOCI, University of Wisconsin) [47–50]. It performs various complex tasks such as editing, processing, and analysing 8-bit colour and grayscale images. ImageJ calculates area and pixel value statistics of selections and intensity-thresholded objects defined by the user and offers standard image processing [51–53]. Images were converted to eight bits and segmented with the threshold value parameter. Alexa488 fluorescence intensity was calculated as the mean values from the Integrated Density parameter per one nucleus, which depicted the sum of all pixels within the region of interest. Results are presented in relative units. Raw data obtained from the images were further analysed using statistical analysis software. This study utilised R Studio, an integrated development environment for R, a statistical programming language [54]. R is widely recognized as a statistical language, dominating other programming languages in developing statistical tools. It offers various packages suitable for scientific data analysis, including agricolae (Statistical Procedures for Agricultural Research), which can be used to determine significant differences between means [55], as well as other packages dedicated to data visualisation [56]. R facilitates the reproducible process of summarizing data after statistical analysis and visualizing it in graph form [57]. 500 nuclei were analysed from petals; 1000 nuclei from the nectary; 1500 nuclei from the ovary, and 1000 nuclei from the stigma in open and closed *F. tataricum* flowers and *F. esculentum* Pin open and closed and Thrum open and closed flower type. Numerical data is included in Additional File 2. Fluorescence data analysis and plotting was performed in R, a software environment for statistical computing and graphics in R Studio 2022.12.0 Build 353 (Script included in Additional File 3), an integrated development environment for R [58, 59]. One-way ANOVA test with the R Stats package [59]

was followed by Tukey's HSD test at the significance level  $p \leq 0.05$ . Standard errors were likewise calculated with the stats package. The package agricolae (Statistical Procedures for Agricultural Research) calculated significant differences between means [55]. Subsequently, data was plotted with packages dedicated to visualising data: ggplot2 [60] and ggpubr [56]. Letters on the graphs indicate statistically significant differences between samples. Full immunostaining procedure and the fluorescence intensity analysis is described for *Fagopyrum* species [61, 62].

#### RNA isolation and real-time qPCR

Total RNA was isolated from the closed and open flowers and Thrum and Pin types of *F. esculentum* and *F. tataricum*. Total RNA was isolated using a FastPure Plant Total RNA Isolation Kit (Polysaccharides and polyphenolics-rich) (Vazyme Biotech, Red Maple Hi-tech Industry Park, Nanjing, PRC). RNA concentrations were measured using a Nano-Drop ND-1000 (NanoDrop Technologies, Wilmington, DE, USA). The DNA was removed from the RNA samples by digesting them with an RNase-free DNase Set (Qiagen, Hilden, Germany). The oligo-dT primers and a Maxima H Minus First Strand cDNA Synthesis Kit (Thermo Fisher Scientific, Waltham, MA, USA) were used to produce the cDNA. The obtained cDNA was diluted four-fold with water and used at a volume of 2  $\mu$ l in a qPCR reaction. Analyses were performed in a 10  $\mu$ l volume using a LightCycler<sup>®</sup> 480 SYBR Green I Master (Roche, Basel, Switzerland). The primers were designed based on *Fagopyrum esculentum* "Pintian4" and *Fagopyrum tataricum* "Pinku1" references genomes with Primer3Plus (Additional File 4) [63]. The control genes (*SAND*, *ACTIN*) had a constant expression level in all tissue samples. Analyses were performed using a LightCycler 480 (Roche, Basel, Switzerland) under the following reaction conditions: initial denaturation of 5 min at 95 °C, followed by 10 s at 95 °C, 20 s at a temperature specific for the primers, 10 s at 72 °C, repeated in 40 cycles. Denaturation for the melt curve analysis was conducted for 5 s at 95 °C, followed by 1 min at 65 °C and heating to 98 °C (0.1 °C/s for the fluorescence measurement). The Ct values were calculated using LinRegPCR software (version 11, Academic Medical Centre, Amsterdam, The Netherlands). The plant tissues for the Real-Time qPCR analysis were produced in three biological repetitions, and two technical replicates of each repetition were analysed. The relative expression level was calculated using  $2^{-\Delta\Delta C_T}$ , where  $\Delta\Delta C_T$  represents  $\Delta C_{T \text{ reference condition}} - \Delta C_{T \text{ compared condition}}$ .

#### Statistical analysis

The Student t-test and one-way ANOVA ( $p < 0.05$ ) followed by Tukey's honestly-significant-difference test

(Tukey HSD-test) ( $p < 0.05$ ) were used to calculate any significant differences between the experimental combinations. The graphs show the average values with the standard error (SE) in Fig. 4 and the standard deviation (SD) in Fig. 5.

### Graphics

Photographs were cropped, adjusted (brightness, contrast) and arranged into figures in the Corel Draw 2020 program. A graphical depiction of the experimental design (Additional File 1) was prepared with BioRender (available online at: <https://app.biorender.com/>). Publication licences are included as Additional File 5.

## Results

### Anatomy and histology of the flowers

*F. tataricum* flowers, closed and open, were smaller than those of *F. esculentum* (Pin, Thrum) (Fig. 1). Closed flowers were coiled in petals of a greenish colour (Fig. 1a–c). In open flowers, the differences between two morphs were disclosed: Pin flowers featured a long style and shorter filaments (Fig. 1d), while Thrum had a short style and longer filaments (Fig. 1e). Open flowers of *F. tataricum* had green petals, with style and filaments of similar length (Fig. 1f).

In anthers of closed flowers, the developmental stage of pollen was advanced, with microspores enwrapped in egzine sheath, tapetum cells were already undergoing programmed cell death (Additional File 6a–c). The anthers of open flowers were fully developed and open, with mature pollen and no tapetum cell remains (Additional File 6d–f). Thus, the anthers were not considered in DNA methylation analysis due to the lack of reference (closed vs. open).

Petals of closed flowers were rich in polyphenols, which were detected in the epidermis and mesophyll cells (Fig. 2a–c). Although phenolic compounds were abundantly present in papillae and subpapillae cells of the stigma, the nuclei were visible (Fig. 2d–f). Within ovaries, the ovules comprised a double-layered integument with tightly adhered nucellus parenchyma cells and embryo sac (Fig. 2g–i). The nectaries were composed of the epidermis, nectary parenchyma, and secretory trichomes in which polyphenolic compounds, were mainly detected (Fig. 2m–o). Similarly to closed flowers, petals of open flowers contained large amounts of phenolic compounds, and the same for stigma papillae and subpapillae cells, where nuclei were “masked” with abundant polyphenol presence (Fig. 3a–f). Part of the nucellus parenchyma cells degenerated, leaving space within the

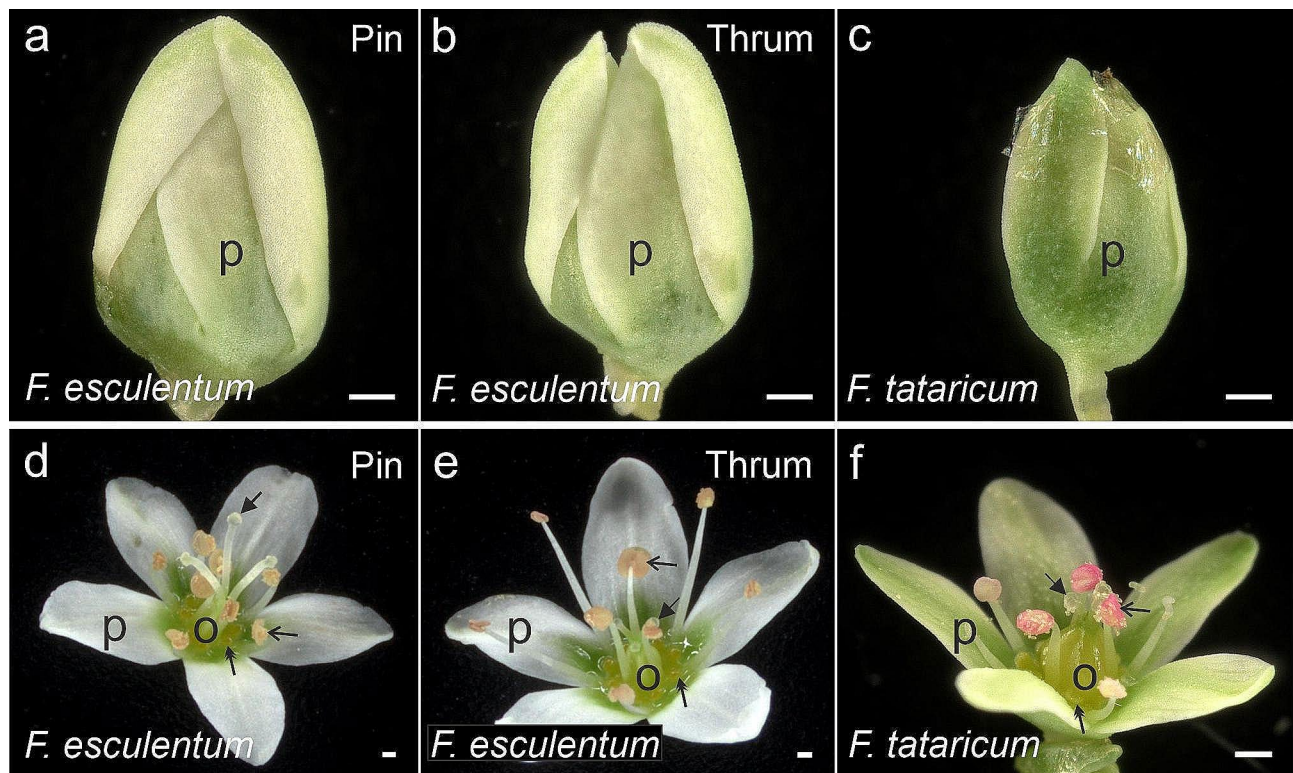


**Fig. 1** Morphology of analysed flowers. *F. esculentum* (a, d) Pin, (b, e) Thrum, and (c, f) *F. tataricum*. (a – c) closed flowers were tightly coiled in petals. (d – f) In open flowers, the anatomy is easily visible. Arrows – stigmas, double arrows – nectaries, open arrows – anthers, o – ovaries, p – petals. Scale bars: (a–f) = 300  $\mu$ m

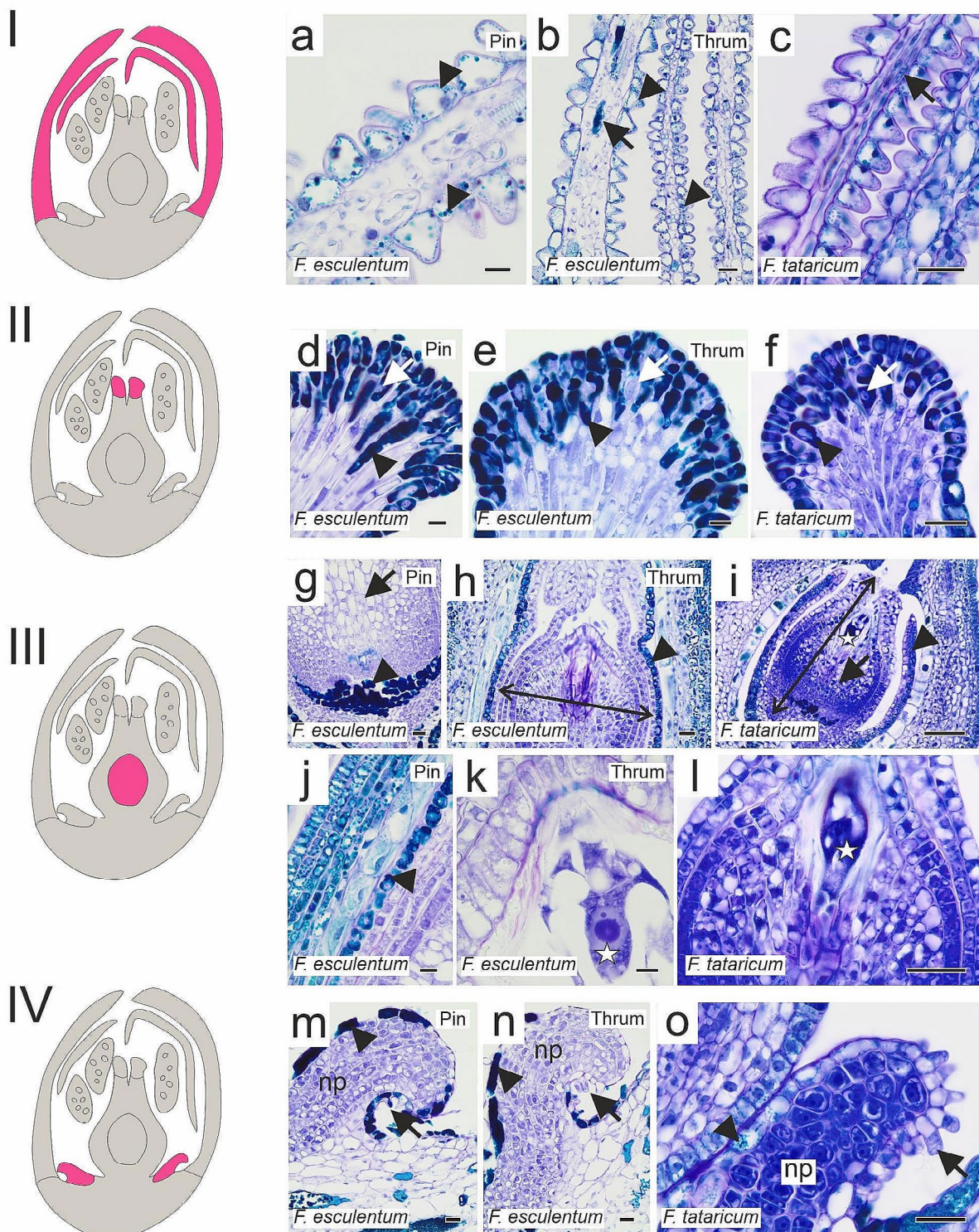


**Fig. 2** Histology of closed flower components (*F. esculentum* Pin, Thrum; *F. tataricum*). Schematic diagrams represent analysed flower components: I petals, II stigma, III ovary with ovule, IV nectary, marked in pink on the diagram. (a - c) petals, abundant polyphenols occurrence in epidermis (arrowheads) and mesophyll cells (arrows). (d - f) stigmas, papillae and subpapillae cells rich in polyphenols (arrowheads) but with visible nuclei (arrows). (g - l) ovaries and ovules, polyphenols present in basal part of ovule and in outer integument cells (arrowheads), arrows - nucellus parenchyma cells, embryo sacs (asterisks); double arrow stands for the extent of cells that were taken into account in the measurement of Alexa488 fluorescence intensity. (m - o) nectaries, epidermis rich in polyphenols (arrowheads), secretory trichomes (arrows), np nectary parenchyma. Scale bars: a, d, e, j, k = 10  $\mu$ m; b, f, g, h, l, m - o = 20  $\mu$ m; c, i = 50  $\mu$ m

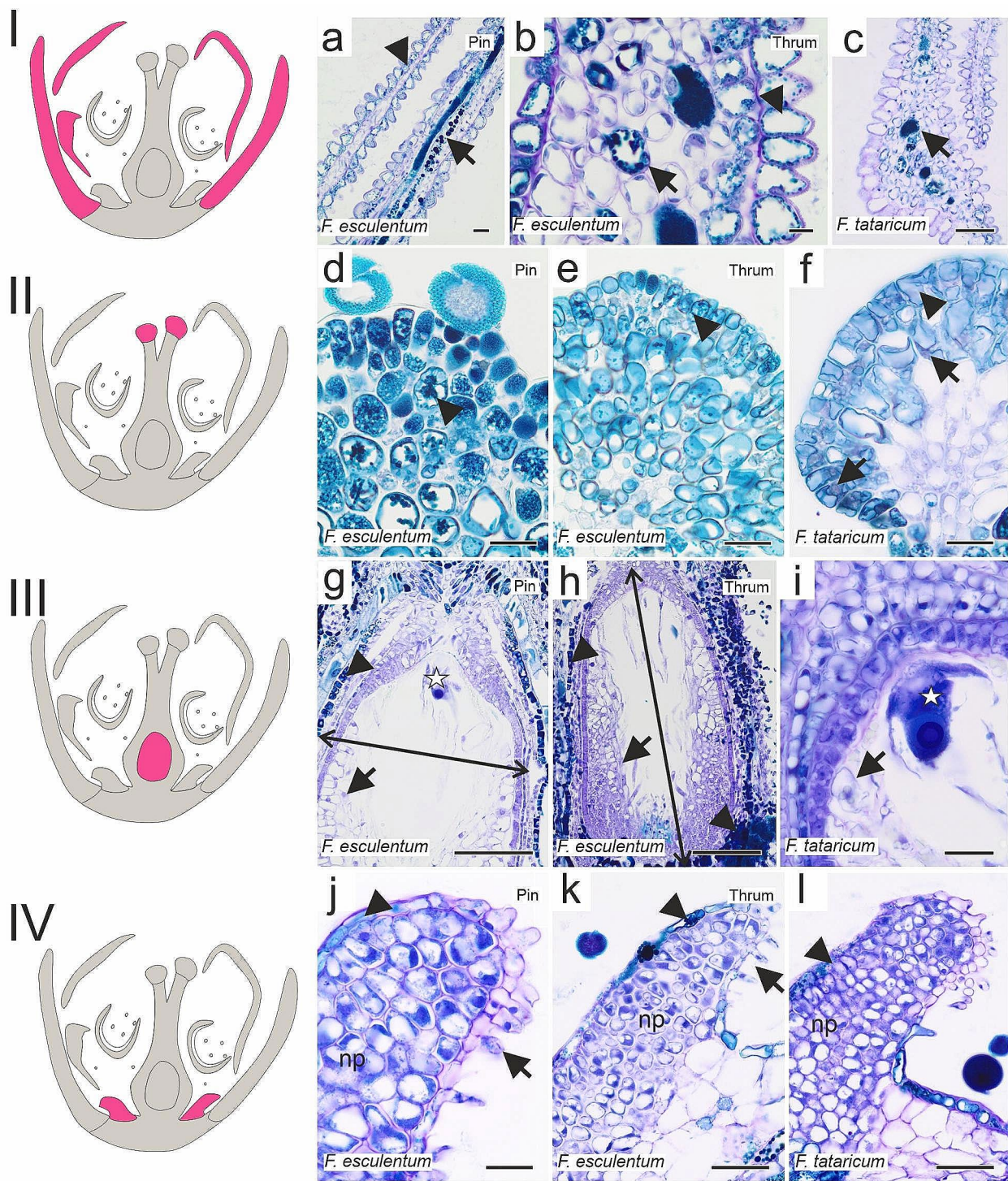


**Fig. 3** Histology of open flower components (*F. esculentum* Pin, Thrum; *F. tataricum*). Schematic diagrams represent analysed flower components: I petals, II stigma, III ovary with ovule, IV nectary, marked in pink on the diagram. (a – c) petals, abundant occurrence of polyphenols in the epidermis (arrowheads) and mesophyll cells (arrows). (d – f) stigmas, papillae and subpapillae cells containing polyphenols (arrowheads) and hardly visible nuclei (arrows). (g – i) ovaries and ovules, high polyphenolic content in the basal part of the ovule and in outer integument cells (arrowheads), arrows – nucellus parenchyma cells, embryo sacs (asterisks); double arrow stands for the extent of cells that were taken into account in the measurement of Alexa488 fluorescence intensity. (j – l) nectaries, epidermis rich in polyphenols (arrowheads), secretory trichomes (arrows), np nectary parenchyma. Scale bars: b = 10  $\mu$ m; a, d – f, i, j = 20  $\mu$ m; c, k, l = 50  $\mu$ m; g, h = 100  $\mu$ m



ovule (Fig. 3g–i). The histology of nectaries remained unchanged compared to closed flowers (Fig. 3j–l).

#### DNA methylation analysis

The highest DNA methylation level in petals from closed flowers was in the Thrum morph; the Pin morph exhibited slightly lower values, whereas the *F. tataricum* open flowers presented the lowest level of this modification. In open flowers, the methylation values decreased in each of the analysed floral parts, but the decrease was the most prominent in Thrum petals (Fig. 4a). Summarising, the *F. esculentum* Thrum morph petals were characterised by the highest starting DNA methylation level and the most eminent decrease; *F. tataricum*, exhibited the lowest DNA methylation value in closed flowers and the lowest decrease during petal development.

Stigma is a pistil component crucial for the first pollination stages. In this floral part, we observed the highest values of the DNA methylation levels in closed flowers among analysed specimens and each flower part and the most considerable reduction in the open flower stage. The highest output DNA methylation level in closed flowers, as well as the decrease (approximately five-fold drop), was noticed in Pin morph (Fig. 4b). Thrum morph was characterised by a lower DNA methylation level concurrently with the lower decrease of the methylation values in comparison to Pin morph (approximately two-fold drop; Fig. 4b). *F. tataricum* stigmas exhibited the lowest starting DNA methylation level among each variant at the closed flower stage, and around two-fold drop in an open flower, which is similar to value decrease observed in Thrum morph (Fig. 4b).

Among the analysed ovules, the DNA methylation level was highest in closed flowers of *F. tataricum*, then in the Pin morph and the lowest in the Thrum morph (Fig. 4c). During flower development, a slight reduction of DNA methylation level was observed for both Pin and Tartary (Fig. 4c) on the contrary to Thrum morph ovules, in which the values of methylation level increased in open flowers (Fig. 4c).

The highest DNA methylation level in nectaries from closed flowers was observed in Tartary buckwheat, lower in Pin, and the lowest in the Thrum morph (Fig. 4d). In contrast to other flower parts (except for the Thrum morph ovule), the nectaries from open flowers had higher values of DNA methylation (compared to values of closed flowers) in all three specimens (Fig. 4d). However, the increase in DNA methylation level was minor, not as prominent as in Pin or Thrum morph. In the opened flowers stage, the *F. esculentum* Pin morph exhibited the highest DNA methylation level, following Tartary, and the lowest values were noted in the Thrum morph.

In conclusion, *F. esculentum* Pin and Thrum morphs differ significantly in DNA methylation levels in the

analysed parts of the flower. In the ovule, stigma, and petals of open flowers, the Thrum morph exhibited higher values than the Pin. Results from Tartary buckwheat show some similarities to either Pin or Thrum, depending on the analysed part and stadium of the flower development.

The graphs show global DNA methylation analysis, but within parts such as ovules and nectaries, the DNA methylation level was not uniform in all nuclei. For example, in ovules, the nuclei from the embryo sac showed very low or no DNA methylation in contrast to other ovule nuclei (Additional File 7).

#### Gene expression analysis

We analysed the expression level of genes related to DNA methylation (*MET1*, *MET2*, *CMET3*) and demethylation (*DME1*, *DME3*, *ROS1*) in closed and open Pin and Thrum flowers of *F. esculentum* and flowers of *F. tataricum*. The results showed the down-regulation of all genes in Thrum flowers (Fig. 5a). The most intense decrease in expression was observed for *MET1*, which was over 45 times lower in the open than in closed Thrum flowers. In contrast to Thrum flowers, the expression of *MET1* in open Pin flowers was the same as in closed ones (Fig. 5b). The decreased transcript level of the rest of the analysed genes was observed in open Pin flowers. The highest reduction was characteristic for the *DME3* gene (14 times lower in open than in closed Pin flowers). The decreased transcript level of almost all analysed genes was observed in open flowers of *F. tataricum* (Fig. 5c). In general, during the development of flowers, the expression of genes encoding DNA methylases and demethylases was decreased.

In addition, we analysed the expression of the genes between flower types and species (Fig. 5d). The expression of all genes is higher (from 2.5 to over 9 times higher) in closed flowers of *F. esculentum* than in *F. tataricum*. Moreover, we observed the difference in expression of genes between Pin and Thrum flowers, both closed and open. *MET2*, *DME1*, and *ROS1* expression were lower in Pin than in Thrum flowers. The other three analysed genes (*MET1*, *CMET3*, *DME3*) are characterised by higher transcript levels in Thrum than in Pin flowers.

#### Discussion

The objective of this study was to compare the DNA methylation status between the Pin and Thrum flower components of *F. esculentum*, with that of self-pollinating species like *F. tataricum* in order to shed light on how this epigenetic mark may have a role in the floral development of the *Fagopyrum* species. *F. tataricum* flowers are smaller than those of *F. esculentum* (Pin, Thrum). In *F. esculentum* open flowers, Pin flowers feature a long style and shorter anther stamens, while Thrum has a

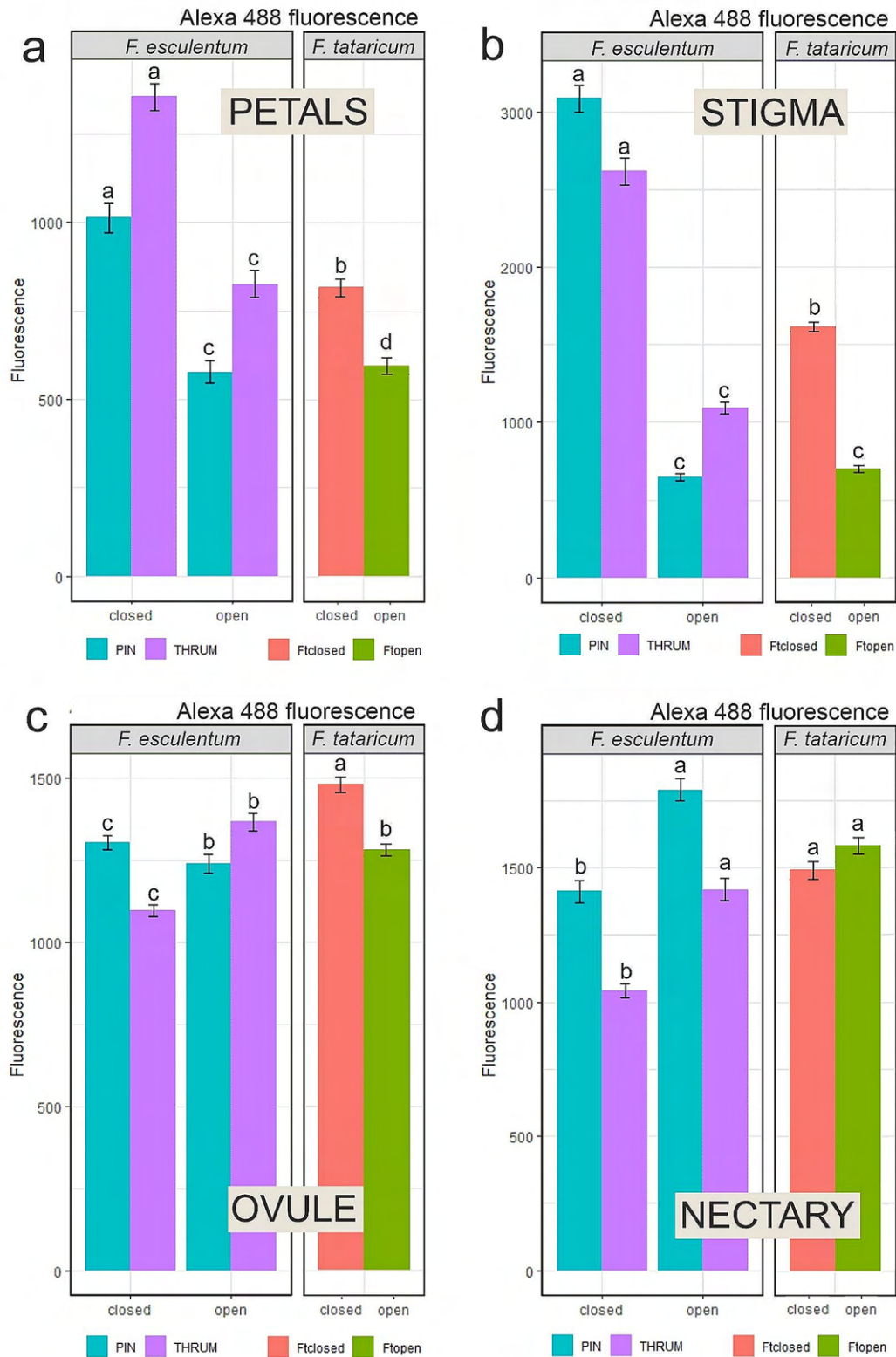


**Fig. 4** Fluorescence intensity measurements of DNA methylation levels. **(a)** petal;  $n=500$ , **(b)** stigma,  $n=1000$ , **(c)** ovule,  $n=1500$ , and **(d)** nectary,  $n=1000$  parts of the closed and the open flowers of *F. esculentum* and *F. tataricum*. Bars represent standard error; results presented in relative units, letters indicate statistically significant differences between the groups

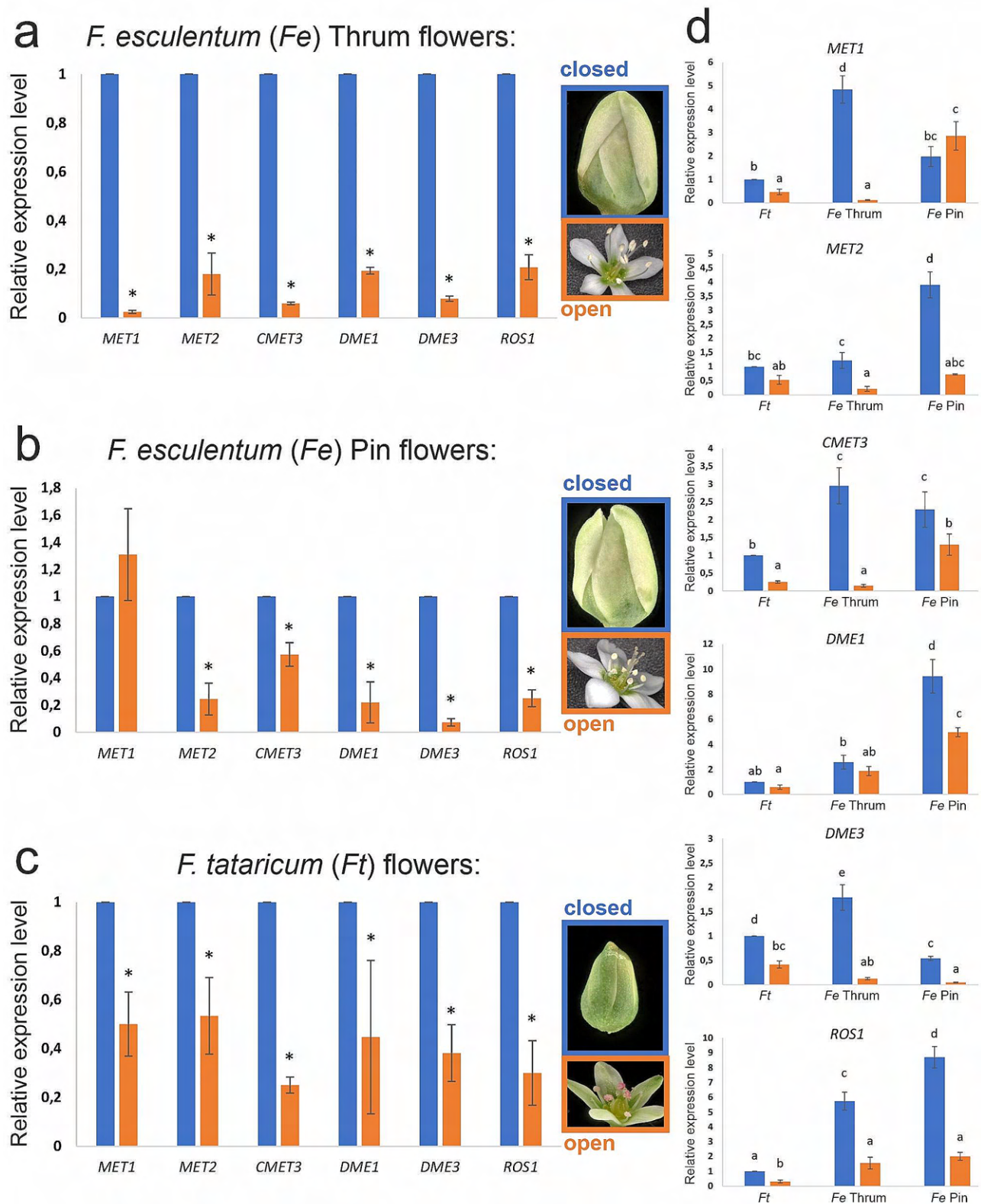


**Fig. 5** Expression level of *MET1*, *MET2*, *CMET3*, *DME1*, *DME3*, and *ROS1* in closed and open flowers, (a, d) Thrum and (b, d) Pin of *F. esculentum* and (c, d) *F. tataricum*. The expression level of genes in open flowers was calibrated to expression in closed flowers of the same type and species (a, b, c). \* - values significantly different from closed flowers of the same type and species (a, b, c) ( $p < 0.05$ ;  $n = 3$ ; means  $\pm$  SD are given). The expression level of genes in all types and species was calibrated to expression in closed flowers of the *F. tataricum* (d). Different letters indicate a significant difference between flower type and species according to Tukey's HSD test ( $p < 0.05$ ;  $n = 3$ ; means  $\pm$  SD are given)

short style and longer anther stamens. Open flowers of *F. tataricum* were characterised by green petals, style, and anthers of similar length. The heteromorphic heterostyly of *F. esculentum* is a significant limitation in breeding [15, 64]. Around a few thousand phenolic structures in the plant kingdom were reported – ranging from single, aromatic-ringed compounds to complex structures [65]. In *F. esculentum*, a total of 60 different phenolic substances were identified, with the highest number found in the flower part of the plant [66]. In tea, another species rich in this type of secondary metabolites, the accumulation of phenolics in leaves was developmentally regulated during bud or first leaf expansion [67]. Moreover, in tobacco, the subsequent stages of flower development were correlated with tissue contents of polyphenols and activities of L-phenylalanine ammonia-lyase, polyphenoloxidase and peroxidase [68]. Also, a large amount of polyphenols was accumulated in tobacco pistil [68] – both reports are consistent with our observations. Although the occurrence of phenolic compounds was not the main objective of our study, it cannot be excluded that DNA methylation changes also affect polyphenolic accumulation, as was reported for *Salvia* sp [69].

DNA methylation, one of the most researched epigenetic modifications, has been linked with regulating chromatin structure and gene expression [16, 25]. It is involved in various developmental processes in flowers, including developing the floral organs, regulating the flowering time, and floral patterning [19]. DNA methylation impacts floral development by modulating the expression of flowering genes via epigenetic alterations. Promoter methylation typically correlates with the suppression of gene expression, while the effects of gene body methylation remain ambiguous, with studies reporting both positive and negative associations [20, 70, 71]. A conducted study reported that DNA methylation in non-promoter, intergenic regions and gene bodies facilitates gene expression. Non-promoter DNA methylation appears crucial for preserving the active chromatin states of genes [26, 72, 73]. It has been previously demonstrated that this epigenetic mark is essential in flower development and that its enrichment fluctuates in various developmental stages [28, 35, 41]. Here, we demonstrated the differences in the level of DNA methylation in flowers at various developmental stages in two buckwheat species, *F. tataricum* with homostylous flower type and *F. esculentum* with heterostylous flowers. Only the nectaries from open flowers had higher values of DNA methylation in comparison to results from closed flowers. DNA methylation values decreased in petals, stigmas and ovules (except for Thrum morph) of each analysed variant in open, developed flowers. In studies conducted on lotus (*Nelumbo nucifera*), the stamen petaloid exhibited a global decrease in DNA methylation levels [74]. Studies

comparing DNA methylation patterns in ovules of the female-sterile rice and the wild-type, displayed a slightly lower whole-genome methylation level [75]. Research on hazel ovaries reported the reduction in DNA methylation levels of the ovule after pollination, indicating that the epigenetic mark is a crucial player in post-pollination stages [76]. It is known that stigma and pollen molecular cross-talk are crucial for successful pollination [77, 78]. During flower maturation, the papillae and sub-papillae cells of the stigma undergo histo- and biochemical changes to prepare for pollen reception, which involves cell loosening or exudate synthesis [79]. In our research, we observed a significant decrease in DNA methylation levels between stigmas of closed and open *F. esculentum* and *F. tataricum* flower; however, the divergence between DNA methylation levels in Pin and Thrum was the most prominent. This trait may point to differences between homo- and distylous species.

Studies conducted on *Lilium longiflorum* cv. Gelria focused on the analysis of the DNA methylation in pollen and reported that the vegetative nucleus in mature pollen grains was heavily methylated and that dramatic nonreplicative demethylation occurred during the pollen tube's development. In conclusion, it was established that DNA hypomethylation ensures the survival of pollen grains without external sources of nutrients until they reach the stigma [80]. Since open flowers in *Fagopyrum* already have produced pollen grains, this might have contributed to the global reduction in DNA methylation levels. The reduction in DNA methylation is correlated with the down-regulation of genes coding DNA methyltransferases. In the Thrum open flower, the expression of *MET1* was over 45 times lower in the open than in closed Thrum flowers.

In contrast to Thrum flowers, the expression of *MET1* in open Pin flowers was the same as in closed ones. It seems that in Pin open flowers, the decrease in DNA methylation level might be related to the down-regulation of genes other than *MET1* methyltransferase, such as *MET2* or *CMET3*. The differential expression of methyltransferases is observed between various tissues [81]; for example, in rice, the transcript of *MET1b* accumulates more abundantly than those of *MET1a* in many different tissues [82]. In our research, the decreased transcript level of the rest of the analysed genes was observed in open Pin flowers. *ROS1* encodes a nuclear protein containing an endonuclease III domain, exhibiting bifunctional DNA glycosylase/lyase activity specifically targeting methylated DNA while leaving unmethylated DNA unaffected [27]. It might explain why the levels of *ROS1* expression are reduced in open *Fagopyrum* flowers, which exhibit reduced DNA methylation levels. Lower transcript accumulation of genes engaged in DNA demethylation was observed in open flowers of

all analysed flower types and species. The DNA methylation level of analysed tissue is an interplay between DNA methylation and active demethylation. Methylation strongly affects flowering-related genes' expression and mobility of transposons [83]. Effective demethylation occurs on the maternal central cell before fertilisation, and in the endosperm, maternal alleles are less methylated than paternal ones [84]. Among others, imprinted genes such as *FLOWERING WAGENINGEN (FWA)*, *MEDEA (MEA)*, and *FERTILIZATION-INDEPENDENT SEED 2 (FIS2)* are methylated and silenced in the spermatid cell, so after fertilisation, only maternal alleles are expressed in the endosperm [85]. Thus, the methylation and demethylation of specific DNA sequences are essential in regulating genes for the proper development of flowers and embryos.

Acquisition of the flowering abilities and subsequent development is precisely governed by the synchronised and specific expression patterns of microRNAs associated with flowering in plants [86, 87]. MicroRNAs represent a new category of intrinsic molecules that modulate gene expression, particularly during the pathways of flower development in plants [83, 88, 89]. Research has shown that the relative expression levels of several potential miRNAs remain notably consistent while governing the flowering time phenotype in a spatial and temporal context [90].

## Conclusions

The current study illustrates the distinct DNA methylation patterns observed between the Pin and Thrum flower components of *F. esculentum*, as compared to self-pollinating species like *F. tataricum*, offering insights into the potential role of this epigenetic modification in the floral development of *Fagopyrum* species. Decreased overall DNA methylation and expression of genes connected with that epigenetic mark in open, developed flowers of both species might suggest that the demethylation is required to activate the expression of genes involved in floral development. Understanding the role of DNA methylation in flowers is crucial for unravelling the molecular mechanisms underlying floral development, adaptation to environmental changes, and the regulation of floral traits. It provides insights into how epigenetic modifications contribute to the diversity and complexity of flower morphology and function. Comparing the global methylation of DNA and expression of genes in both morphs of *F. esculentum*, as well as with a closely related, homostylous species, *F. tataricum* can lead to deciphering and understanding the differences between them and influence the self-incompatibility phenomenon to create self-compatible varieties. Our analyses offer insights into the potential roles of DNA methylation in gene expression and serve as valuable resources

for further exploration of the genetic pathways governing flower development.

## Abbreviations

|        |   |
|--------|---|
| BSA    | Bovine albumin serum  |
| CMT3   | <i>CHROMOMETHYLASE 3</i>                                      |
| DAPI   | 4',6-diamidino-2-phenylindol                                  |
| DME    | <i>Demeter, 5-methylcytosine glycosylase</i>                  |
| DML2   | <i>DME-like 2, 5-methylcytosine glycosylase</i>               |
| DML3   | <i>DME-like 3, 5-methylcytosine glycosylase</i>               |
| DRMs   | <i>DOMAINS REARRANGED METHYLTRANSFERASES</i>                  |
| MET1   | <i>DNA METHYLTRANSFERASE 1</i>                                |
| PBS    | 1x phosphate-buffered saline                                  |
| ROS1   | <i>Repressor of silencing 1, 5-methylcytosine glycosylase</i> |
| S-ELF3 | <i>S-LOCUS EARLY FLOWERING 3</i>                              |
| TBO    | Toluidine blue O  |

## Supplementary Information

The online version contains supplementary material available at <https://doi.org/10.1186/s12870-024-05162-w>.

**Additional File 1:** Graphical depiction of the experimental design

**Additional File 2:** Excel table containing raw numerical data for DNA methylation

**Additional File 3:** R-Studio script for statistical analysis and graphical depiction of the results

**Additional File 4:** Excel table containing forward and reverse primers for the RT-qPCR analysis

**Additional File 5:** BioRender certificate confirming the publication rights for Additional File

**Additional File 6:** Histology of anthers from closed (a – c) and open (d – f) flowers (not included in DNA methylation analysis)

**Additional File 7:** Selected images captured with the Olympus FV1000 confocal system

## Acknowledgements

The authors thank Lea Berg for preparing the R Studio script used in our analysis.

## Author contributions

Conceptualisation: AB; Methodology: KS-C, AT, KN, AP; Formal analysis: KS-C, AT, AB, KN, AP; Investigation: KS-C, AT, AB, KN, AP; Resources: AB; Writing—original draft: KS-C, AT, KN, AP; Writing—review & editing: KS-C, AT, KN, AP, AB; Visualisation: KS-C, AT, KN; Supervision: AB; Project administration: AB; Funding acquisition: AB. All authors have read and approved the final manuscript.

## Funding

This research was funded by the National Science Centre, Poland. Research project OPUS-19 (no. reg. 2020/37/B/NZ9/01499 awarded to AB) and the Research Excellence Initiative of the University of Silesia in Katowice.

## Data availability

All data generated or analysed during this study are included in this published article (and its additional information files).

## Declarations

### Ethics approval and consent to participate

The use of all plant materials in this study complies with relevant institutional, national, and international guidelines and legislation. Seeds of *F. tataricum* (sample k-17) are from the N. I. Vavilov Institute of Plant Genetic Resources collections, Saint Petersburg, Russia. The Plant Cytogenetic and Molecular Biology Group Institute of Biology, Biotechnology and Environmental

Protection, Faculty of Natural Sciences, University of Silesia in Katowice, Poland, multiplied the obtained seeds. *F. tataricum* sample k-17 is a common cultivated landrace of *F. tataricum*, and seeds are available upon request from the publication's authors. *F. esculentum* seeds of the Panda cultivar are commercially available and were supplied from the Malopolska Plant Breeding, Poland.

#### Consent for publication

Not applicable.

#### Competing interests

The authors declare no competing interests.

#### Author details

<sup>1</sup>Institute of Biology, Biotechnology and Environmental Protection, Faculty of Natural Sciences, University of Silesia in Katowice, 28 Jagiellonska St, Katowice 40-032, Poland

Received: 30 March 2024 / Accepted: 16 May 2024

Published online: 23 May 2024

#### References

- Jha R, Zhang K, He Y, Mandler-Drienovszki N, Magyar-Tábori K, Quinet M, Germ M, Kreft I, Meglič V, Ikeda K et al. Global nutritional challenges and opportunities: Buckwheat, a potential bridge between nutrient deficiency and food security. *Trends Food Sci Technol* 2024, 145.
- Tomasiak A, Zhou M, Betekhtin A. Buckwheat in tissue culture research: current status and future perspectives. *Int J Mol Sci* 2022, 23(4).
- Kwon SJ, Roy SK, Choi JY, Park JH, Cho SW, Sarker K, Woo SH. Recent research updates on functional components in buckwheat. *J Agr Sci*. 2018;34(1):1–8.
- Sinkovič L, Kokalj D, Vidrih R, Meglič V. Milling fractions fatty acid composition of common (*Fagopyrum esculentum* Moench) and tartary (*Fagopyrum tataricum* (L.) Gaertn) buckwheat. *J Stored Prod Res* 2020, 85.
- Ji X, Han L, Liu F, Yin S, Peng Q, Wang M. A mini-review of isolation, chemical properties and bioactivities of polysaccharides from buckwheat (*Fagopyrum Mill*). *Int J Biol Macromol*. 2019;127:204–9.
- Bonafaccia MM, Kreft I. Composition and technological properties of the flour and bran from common and tartary buckwheat. *Food Chem*. 2003;80:9–15.
- Gonçalves FMF, Debiage RR, Gonçalves da Silva RM, Porto PP, Yoshihara E, Cosendey E, Toledo De Mello Peixoto EC. *Fagopyrum esculentum* Moench: a crop with many purposes in agriculture and human nutrition. *Afr J Agric Res*. 2016;11(12):983–9.
- Huda MN, Lu S, Jahan T, Ding M, Jha R, Zhang K, Zhang W, Georgiev MI, Park SU, Zhou M. Treasure from garden: bioactive compounds of buckwheat. *Food Chem*. 2021;335:127653.
- Liu M, Sun W, Ma Z, Guo C, Chen J, Wu Q, Wang X, Chen H. Integrated network analyses identify MYB4R1 neofunctionalization in the UV-B adaptation of Tartary buckwheat. *Plant Commun*. 2022;3(6):100414.
- Sofi SA, Ahmed N, Farooq A, Rafiq S, Zargar SM, Kamran F, Dar TA, Mir SA, Dar BN, Mousavi Khaneghah A. Nutritional and bioactive characteristics of buckwheat, and its potential for developing gluten-free products: an updated overview. *Food Sci Nutr*. 2023;11(5):2256–76.
- Matsui K, Yasui Y. Genetic and genomic research for the development of an efficient breeding system in heterostylous self-incompatible common buckwheat (*Fagopyrum esculentum*). *Theor Appl Genet*. 2020;133(5):1641–53.
- Yasui Y, Hirakawa H, Ueno M, Matsui K, Katsube-Tanaka T, Yang SJ, Aii J, Sato S, Mori M. Assembly of the draft genome of buckwheat and its applications in identifying agronomically useful genes. *DNA Res*. 2016;23(3):215–24.
- Cawoy V, Deblauwe V, Halbrech B, Ledent JF, Kinet JM, Jacquemart AL. Morph differences and honeybee morph preference in the distylous species *Fagopyrum esculentum* Moench. *IJPS*. 2006;167(4):853–61.
- Quinet M, Cawoy V, Lefevre I, Van Miegroet F, Jacquemart AL, Kinet JM. Inflorescence structure and control of flowering time and duration by light in buckwheat (*Fagopyrum esculentum* Moench). *J Exp Bot*. 2004;55(402):1509–17.
- Fawcett JA, Takeshima R, Kikuchi S, Yazaki E, Katsube-Tanaka T, Dong Y, Li M, Hunt HV, Jones MK, Lister DL, et al. Genome sequencing reveals the genetic architecture of heterostyly and domestication history of common buckwheat. *Nat Plants*. 2023;9(8):1236–51.
- Zang Y, Xie L, Su J, Luo Z, Jia X, Ma X. Advances in DNA methylation and demethylation in medicinal plants: a review. *Mol Biol Rep*. 2023;50(9):7783–96.
- Zhang D, Li YY, Zhao X, Zhang C, Liu DK, Lan S, Yin W, Liu ZJ. Molecular insights into self-incompatibility systems: from evolution to breeding. *Plant Commun*. 2024;5(2):100719.
- Lin PY, Chang YT, Huang YC, Chen PY. Estimating genome-wide DNA methylation heterogeneity with methylation patterns. *Epigenet Chromatin*. 2023;16(1):44.
- Lucibelli F, Valoroso MC, Aceto S. Plant DNA methylation: an epigenetic mark in development, environmental interactions, and evolution. *Int J Mol Sci* 2022, 23(15).
- Zemach A, McDaniel I, Silva P, Zilberman D. Genome-wide evolutionary analysis of eukaryotic DNA methylation. *Science*. 2010;328(5980):916–9.
- Omony J, Nussbaumer T, Gutzat R. DNA methylation analysis in plants: review of computational tools and future perspectives. *Brief Bioinform*. 2020;21(3):906–18.
- Bednarek PT, Orłowska R. Plant tissue culture environment as a switch-key of (epi)genetic changes. *PCTOC*. 2019;140(2):245–57.
- Chan S, Henderson I, Jacobsen S. Gardening the genome: DNA methylation in *Arabidopsis thaliana*. *Nat Rev Genet*. 2005;6:351–60.
- Bennett M, Cleaves K, Hewezi T. Expression patterns of DNA methylation and demethylation genes during plant development and in response to phytohormones. *Int J Mol Sci* 2021, 22(18).
- Bird A. DNA methylation patterns and epigenetic memory. *Genes Dev*. 2002;16(1):6–21.
- He XJ, Chen T, Zhu JK. Regulation and function of DNA methylation in plants and animals. *Cell Res*. 2011;21(3):442–65.
- Gong Z, Morales-Ruiz T, Ariza RR, Roldan-Arjona T, David L, Zhu JK. *ROS1*, a repressor of transcriptional gene silencing in *Arabidopsis*, encodes a DNA glycosylase/lyase. *Cell*. 2002;111:803–14.
- Yang H, Chang F, You C, Cui J, Zhu G, Wang L, Zheng Y, Qi J, Ma H. Whole-genome DNA methylation patterns and complex associations with gene structure and expression during flower development in *Arabidopsis*. *Plant J*. 2015;81(2):268–81.
- Finnegan EJ, Genger RK, Kovac K, Peacock WJ, Dennis ES. DNA methylation and the promotion of flowering by vernalization. *Plant Biol*. 1998;95:5824–9.
- Kumari P, Khan S, Wani IA, Gupta R, Verma S, Alam P, Alaklabi A. Unravelling the role of epigenetic modifications in development and reproduction of angiosperms: a critical appraisal. *Front Genet*. 2022;13:819941.
- Meijón M, Feito I, Valledor L, Rodríguez R, Cañal MJ. Dynamics of DNA methylation and histone H4 acetylation during floral bud differentiation in azalea. *BMC Plant Biol* 2010, 10(10).
- Ruiz-García L, Cervera MT, Martínez-Zapater JM. DNA methylation increases throughout *Arabidopsis* development. *Planta*. 2005;222(2):301–6.
- Fulneček J, Matyasek R, Votruba I, Holy A, Krizova K, Kovarik A. Inhibition of 5AH-hydrolase activity during seed germination leads to deregulation of flowering genes and altered flower morphology in tobacco. *Mol Genet Genomics*. 2011;285(3):225–36.
- Wang N, Ning S, Wu J, Tagiri A, Komatsuda T. An epiallele at *clt1* affects the expression of floret closing (cleistogamy) in barley. *Genetics*. 2015;199(1):95–104.
- Zou JJ, Cai X, Yang J, Zeng X, Liu DX, Huang S, Chen X, Yang QY, Wang C, Chen H. DNA hypomethylation mediates flower opening and senescence in sweet osmanthus through auxin and ethylene responsive pathways. *Postharvest Biol Technol* 2023, 198.
- Zhang S, Jiang H, Zhao H, Korpelainen H, Li C. Sexually different physiological responses of *Populus cathayana* to nitrogen and phosphorus deficiencies. *Tree Physiol*. 2014;34(4):343–54.
- Sharifi A, Oizumi K, Kubota S, Bagheri A, Shafaroudi SM, Nakano M, Kanno A. Double flower formation in *Tricyrtis macranthopsis* is related to low expression of *AGAMOUS* ortholog gene. *Sci Hortic*. 2015;193:337–45.
- Wang Y, Zheng PC, Liu PP, Song XW, Guo F, Li YY, Ni DJ, Jiang CJ. Novel insight into the role of withering process in characteristic flavor formation of teas using transcriptome analysis and metabolite profiling. *Food Chem*. 2019;272:313–22.
- Liu XJ, Chuang YN, Chiou CY, Chin DC, Shen FQ, Yeh KW. Methylation effect on chalcone synthase gene expression determines anthocyanin pigmentation in floral tissues of two *Oncidium* orchid cultivars. *Planta*. 2012;236(2):401–9.

40. Wu X, Zhou Y, Yao D, Iqbal S, Gao Z, Zhang Z. DNA methylation of *LDOX* gene contributes to the floral colour variegation in peach. *J Plant Physiol* 2020, 246–7:153116.
41. Xing L, Li Y, Qi S, Zhang C, Ma W, Zuo X, Liang J, Gao C, Jia P, Shah K, et al. Comparative RNA-sequencing and DNA methylation analyses of apple (*Malus domestica* Borkh.) buds with diverse flowering capabilities reveal novel insights into the regulatory mechanisms of flower bud formation. *Plant Cell Physiol*. 2019;60(8):1702–21.
42. Wolny E, Braszewska-Zalewska A, Hasterok R. Spatial distribution of epigenetic modifications in *Brachypodium distachyon* embryos during seed maturation and germination. *PLoS ONE*. 2014;9(7):e101246.
43. Braszewska-Zalewska AJ, Wolny EA, Smialek L, Hasterok R. Tissue-specific epigenetic modifications in root apical meristem cells of *Hordeum vulgare*. *PLoS ONE*. 2013;8(7):e69204.
44. Pawley JB. Handbook of biological confocal microscopy: Third edition. 2006.
45. Wilson T. Resolution and optical sectioning in the confocal microscope. *J Microsc* 2011, 244.
46. Inacio V, Martins MT, Graca J, Morais-Cecilio L. Cork oak young and traumatic periderms show PCD typical chromatin patterns but different chromatin-modifying genes expression. *Front Plant Sci*. 2018;9:1194.
47. Bankhead P. Analyzing fluorescence microscopy images with ImageJ. *ImageJ*; 2014.
48. Abràmoff MD, Magalhães PJ, Ram SJ. Image processing with imageJ. *Biophotonics Int* 2004, 11.
49. Bourne R. *ImageJ. Fundamentals of Digital Imaging in Medicine* 2010.
50. Collins TJ. *ImageJ for microscopy*. Biotechniques 2007, 43.
51. Hartig SM. Basic image analysis and manipulation in imageJ. *Curr Protoc Mol Biol* 2013.
52. Schroeder AB, Dobson ETA, Rueden CT, Tomancak P, Jug F, Eliceiri KW. The ImageJ ecosystem: open-source software for image visualization, processing, and analysis. *Prot Sci* 2021, 30.
53. Ferreira T, Rasband W. *ImageJ user guide user guide ImageJ. Image J user Guide* 2012, 146r.
54. Martin G. R Studio. In: *An Introduction to Programming with R* 2021.
55. Mendiburu F. Statistical procedures for agricultural research. In: *Package 'agricolae'* 2022.
56. Kassambara A. 'ggplot2' Based Publication Ready Plots. In., 0.5.0 edn; 2022.
57. Toro ID, Dickson K, Hakes AS, Newman SL. Undergraduate Biostatistics & Data Science Introduction Using R, R Studio & the Tidyverse. *Am Biol Teach* 2022.
58. Team RC. R: A Language and environment for statistical computing. In. Vienna, Austria: R foundation for statistical computing; 2022.
59. Team RS. RStudio: Integrated development environment for R. In: *RStudio* Boston, Massachusetts: R Studio; 2022.
60. Wickham H. Easily Install and Load the 'Tidyverse'. In: *Package 'tidyverse'* 2022.
61. Tomasiak A, Sala K, Braszewska A. Immunostaining for epigenetic modifications in *Fagopyrum* calli. In: *Buckwheat Methods in Molecular Biology* Edited by Betekhtin A, Pinski, A., vol. 2791. Humana, New York: Springer; 2024: 15–22.
62. Tomasiak A, Berg LS, Sala K, Braszewska A. Quantitative analysis of epigenetic modifications in *Fagopyrum* nuclei with confocal microscope, ImageJ, and R Studio. In: *Buckwheat Methods in Molecular Biology* Edited by Betekhtin A, Pinski, A., vol. 2791. Humana, New York: Springer; 2024: 23–33.
63. He Q, Ma D, Li W, Xing L, Zhang H, Wang Y, Du C, Li X, Jia Z, Li X, et al. High-quality *Fagopyrum esculentum* genome provides insights into the flavonoid accumulation among different tissues and self-incompatibility. *J Integr Plant Biol*. 2023;65(6):1423–41.
64. Ueno M, Yasui Y, Aii J, Matsui K, Sato S, Ota T. Genetic analyses of the heteromorphic self-incompatibility (S) locus in buckwheat. In: *Mol Breed Nutritional Aspects Buckwheat* 2016: 411–21.
65. Crozier A, Jaganath I, Clifford MN. Phenols, polyphenol and tannins: an overview. In: *Plant secondary metabolites: occurrence, structure and role in human diet* 2007: 1–24.
66. Nesovic M, Gasic U, Tosti T, Horvacki N, Nedic N, Sredojevic M, Blagojevic S, Ignjatovic L, Tesic Z. Distribution of polyphenolic and sugar compounds in different buckwheat plant parts. *RSC Adv*. 2021;11(42):25816–29.
67. Jiang X, Liu Y, Li W, Zhao L, Meng F, Wang Y, Tan H, Yang H, Wei C, Wan X, et al. Tissue-specific, development-dependent phenolic compounds accumulation profile and gene expression pattern in tea plant [*Camellia sinensis*]. *PLoS ONE*. 2013;8(4):e62315.
68. Sheen SJ. Changes in amount of polyphenols and activity of related enzymes during growth of tobacco flower and capsule. *Plant Physiol*. 1973;51:839–44.
69. He X, Chen Y, Xia Y, Hong X, You H, Zhang R, Liang Z, Cui Q, Zhang S, Zhou M, et al. DNA methylation regulates biosynthesis of tanshinones and phenolic acids during growth of *Salvia miltiorrhiza*. *Plant Physiol*. 2024;194(4):2086–100.
70. Zhang X, Yazaki J, Sundaresan A, Cokus S, Chan SW, Chen H, Henderson IR, Shinn P, Pellegrini M, Jacobsen SE, et al. Genome-wide high-resolution mapping and functional analysis of DNA methylation in *Arabidopsis*. *Cell*. 2006;126(6):1189–201.
71. Zilberman D, Gehring M, Tran R, Ballinger T, Henikoff S. Genome-wide analysis of *Arabidopsis thaliana* DNA methylation uncovers an interdependence between methylation and transcription. *Nat Genet*. 2007;39:61–9.
72. Wu H, Coskun V, Tao J, Xie W, Ge W, Yoshikawa K, Li E, Zhang Y, Sun YE. *Dnmt3a*-dependent nonpromoter DNA methylation facilitates transcription of neurogenic genes. *Science*. 2010;329(5990):444–8.
73. Feng S, Cokus SJ, Zhang X, Chen PY, Bostick M, Goll MG, Hetzel J, Jain J, Strauss SH, Halpern ME, et al. Conservation and divergence of methylation patterning in plants and animals. *Proc Natl Acad Sci U S A*. 2010;107(19):8689–94.
74. Lin Z, Liu M, Damaris RN, Nyong'a TM, Cao D, Ou K, Yang P. Genome-wide DNA methylation profiling in the lotus (*Nelumbo nucifera*) flower showing its contribution to the stamen petaloid. *Plants* 2019, 8(5).
75. Liu H, Wu Y, Cao A, Mao B, Zhao B, Wang J. Genome-wide analysis of DNA methylation during ovule development of female-sterile rice *fsv1*. *G3* 2017, 7(11):3621–3635.
76. Cheng YQ, Wang J, Liu JF, Zhao YX, Geng WT, Z. H. D.: Analysis of ovary DNA methylation during delayed fertilization in hazel using the methylation-sensitive amplification technique. *Acta Physiol Plant* 2015, 37(231).
77. Cawoy V, Ledent JF, Kinet JM, Jacquemart AL. Floral biology of common buckwheat (*Fagopyrum esculentum* Moench). *EJPSB*. 2009;3(1):1–9.
78. Gao X-Q, Zhu D, Zhang X. Stigma factors regulating self-compatible pollination. *Front Biol*. 2010;5(2):156–63.
79. Çetinbaş-Genç A, Yanik F, Vardar F. Histochemical and biochemical alterations in the stigma of *Hibiscus syriacus* (Malvaceae) during flower development. *Caryologia*. 2019;72(4):3–13.
80. Janousek B, Zluvova J, Vyskot B. Histone H4 acetylation and DNA methylation dynamics during pollen development. *Protoplasma*. 2000;211:116–22.
81. Zhang H, Lang Z, Zhu JK. Dynamics and function of DNA methylation in plants. *Nat Rev Mol Cell Biol*. 2018;19(8):489–506.
82. Yamauchi T, Moritoh S, Johzuka-Hisatomi Y, Ono A, Terada R, Nakamura I, Iida S. Alternative splicing of the rice *OsMET1* genes encoding maintenance DNA methyltransferase. *J Plant Physiol*. 2008;165(17):1774–82.
83. Kim WJ, Ahn JH. MicroRNA-target interactions: important signaling modules regulating flowering time in diverse plant species. *Crit Rev Plant Sci*. 2014;33(6):470–85.
84. Klosinska M, Picard CL, Gehring M. Conserved imprinting associated with unique epigenetic signatures in the *Arabidopsis* genus. *Nat Plants*. 2016;2:16145.
85. Luo MB, Dennis P, Peacock ES, Chaudhury WJ. Expression and parent-of-origin effects for *FIS2*, *MEA*, and *FIE* in the endosperm and embryo of developing *Arabidopsis* seeds. *Proc Natl Acad Sci*. 2000;97:10637–42.
86. Arora S, Chaudhary B. Global expression dynamics and miRNA evolution profile govern floral/fiber architecture in the modern cotton (*Gossypium*). *Planta*. 2021;254(3):62.
87. Arora S, Pandey DK, Chaudhary B. Target-mimicry based diminution of miRNA167 reinforced flowering-time phenotypes in tobacco via spatial-transcriptional biases of flowering-associated miRNAs. *Gene*. 2019;682:67–80.
88. Hong Y, Jackson S. Floral induction and flower formation—the role and potential applications of miRNAs. *Plant Biotechnol J*. 2015;13(3):282–92.
89. Spanudakis E, Jackson S. The role of microRNAs in the control of flowering time. *J Exp Bot*. 2014;65(2):365–80.
90. Jin D, Wang Y, Zhao Y, Chen M. MicroRNAs and their cross-talks in plant development. *J Genet Genomics*. 2013;40(4):161–70.

## Publisher's Note

Springer Nature remains neutral with regard to jurisdictional claims in published maps and institutional affiliations.

## 9. Podsumowanie i wnioski

Do realizacji pierwszego etapu pracy doktorskiej użyto kalusów o zróżnicowanej zdolności do embriogenezy; kalus embriogeny *Fagopyrum esculentum*, kalus morfogeny oraz kalus niemorfogeny *Fagopyrum tataricum*. Natomiast w drugim etapie pracy doktorskiej skupiono się na badaniach kwiatów dwóch gatunków *Fagopyrum*. Kwiaty *F. esculentum*, cechują się heterostylią (dwa morfotypy: Pin i Thrum).

Te różnice stanowiły podstawy do przeprowadzenia analiz porównawczych w celu zrozumienia wpływu modyfikacji epigenetycznych na procesy odróżnicowania i ponownego różnicowania komórkowego w kulturach *in vitro*, jak i podczas rozwoju generatywnego roślin gryki. Zastosowane metody umożliwiły uzyskanie innowacyjnych i unikalnych wyników zarówno pod względem zdobytych informacji, jak i wykorzystanych technik. Hipotezy postawione w rozprawie doktorskiej zostały potwierdzone. Zaobserwowano zmiany w poziomach modyfikacji epigenetycznych podczas procesów odróżnicowania i różnicowania komórek w kalusach gryki zwyczajnej i gryki tatarskiej w warunkach kultur *in vitro*. Zidentyfikowano korelację między zmianami epigenetycznymi a ekspresją genów kodujących białka i polisacharydy zaangażowane w przebudowę ściany komórkowej podczas procesów odróżnicowania i różnicowania w kulturach *in vitro* kalusa gryki tatarskiej. Ponadto, opisano zmiany w poziomach metylacji DNA oraz poziomie ekspresji genów kodujących metylazy i demetylazy na różnych etapach rozwoju (zamknięte i otwarte) kwiatów (*F. tataricum*, Pin i Thrum *F. esculentum*).

Wnioski z przeprowadzonych w ramach pracy doktorskiej badań podzielono na podstawie warunków hodowli:

### Doświadczenia *in vitro*

1. Stwierdzono różnice w poziomie modyfikacji epigenetycznych w długoterminowych kulturach kalusów gatunków *Fagopyrum* o zróżnicowanej zdolności do embriogenezy (**P2**):

- Obniżony poziom modyfikacji związanych z aktywną transkrypcyjnie euchromatyną, di- i trimetylacji histonu H3 na lizynie 4 (H3K4me2, H3K4me3) jest związany z odróżnicowaniem komórek w kalusie embriogenym *F. esculentum* i w kalusie morfogenym *F. tataricum*;



- Obniżony poziom metylacji DNA w kalusie morfogenym *F. tataricum* jest skorelowany z dynamicznym różnicowaniem komórek i reinicjacją proembriogennych kompleksów komórkowych;
- Fluktuacje w poziomach acetylacji histonu H4 (H4K5ac, H4K16ac) mogą być spowodowane intensywnymi podziałami komórkowymi i endoreplikacją w kalusie niemorfogenym *F. tataricum*;

2. Wykazano szczegółowe różnice w poziomie trimetylacji histonu H3 na lizynie 4 (H3K4me3) pomiędzy kalusami morfogenym i niemorfogenym w *F. tataricum* (P3):

- W kalusie morfogenym *F. tataricum* w badanych genach białek oraz polisacharydów ściany komórkowej (*PMEI*, *PME*, *PX*, *EXT1* i *PG2*) poziom H3K4me3 wzrastał wraz z progresją pasażu, co oznacza ich wzmożoną aktywność podczas procesów odróżnicowania komórkowego i dezintegracji proembriogennych kompleksów komórkowych;
- Analiza sekwencjonowania CHIP wykazała wyższy poziom H3K4me3 w kalusie niemorfogenym *F. tataricum*. Natomiast kolejna analiza CHIP-qPCR przeprowadzona dla konkretnych genów (*PG1* oraz *EXT1*) wykazała niższy poziom tego markera, co najprawdopodobniej związane jest z brakiem zdolności komórek kalusa niemorfogenego do morfogenezy.

### **Doświadczenia *in vivo***

3. Zaobserwowano różnice w metylacji DNA oraz poziomie ekspresji genów kodujących metylazy i demetylazy DNA w kwiatach *F. esculentum* (Pin i Thrum) oraz *F. tataricum* podczas ich rozwoju (P4):

- Zwiększony w stosunku do kwiatów otwartych poziom metylacji DNA oraz poziom ekspresji genów kodujących metylotransferazy i demetylazy DNA w zamkniętych kwiatach obu gatunków *Fagopyrum* wskazuje, że metylacja jest zaangażowana w procesy towarzyszące ich rozwojowi.

## Uzupełnienie

Metodyka zastosowana w badaniach wykorzystanych w pracy doktorskiej została opublikowana jako dwa rozdziały monografii wydawnictwa Springer z serii „*Methods in Molecular Biology. Buckwheat: Methods in Molecular Biology*”.

**Tomasiak A**, Sala K, Braszewska A. Immunostaining for epigenetic modifications in *Fagopyrum calli*. w: *Buckwheat Methods in Molecular Biology* Edytorzy: Betekhtin A, Pinski, A., vol. 2791. Humana, Nowy Jork: Springer 2024: 15–22.

### Punkty MNiSW: 20

Rozdział zawiera szczegółowy protokół opisujący reakcje immunobarwienia, wykorzystywane powszechnie do identyfikacji poszczególnych epitopów w obrębie DNA, białek lub polisacharydów. Reakcja składa się z dwóch etapów: w pierwszym aplikowane jest nieoznakowane przeciwciało pierwszorzędowe, które wykrywa antygen, następnie nanoszone jest przeciwciało drugorzędowe, znakowane odpowiednim znacznikiem fluorescencyjnym umożliwiającym wizualizację poszukiwanego kompleksu. Do analizy użyto kalusy: EK *F. esculentum* oraz MK i NK *F. tataricum*. Opisano proces utrwalania tkanek oraz procedurę zatapiania w wosku Steedmana (Steedman, 1957). Rozdział zawiera również opis procesu przygotowania skrawków na mikrotomie rotacyjnym oraz opisuje etap odwoskowania i uwodnienia preparatów w celu przeprowadzenia reakcji immunohistochemicznej. Do analiz wykorzystano specyficzne przeciwciała pierwszorzędowe skierowane przeciwko zmodyfikowanym białkom histonowym - H3: dimetylacja histonu 3 na lizynie 4 (H3K4me2) trimetylacja histonu H3 na lizynie 4 (H3K4me3), trimetylacja histonu H3 na lizynie 36 (H3K4me36), acetylacja histonu 3 na lizynie 18 (H3K18ac); oraz H4: acetylacja histonu H4 na lizynie 12 (H4K12ac), acetylacja histonu H4 na lizynie 16 (H4K16ac), acetylacja histonu H4 na lizynie 5 (H4K5ac). Jako kontrole pozytywne użyto przeciwciał skierowanych przeciwko niezmodyfikowanym histonom H3 i H4. Oznaczenie metylacji DNA, poza aplikacją odpowiedniego przeciwciała, wymaga wcześniejszej denaturacji DNA kwasem solnym (HCl). Przeciwciało drugorzędowe zastosowane w przedstawionym protokole to poliklonalne IgG znakowane fluorochromem Alexa488.

Protokół pozwala na dokładne odtworzenie eksperymentu. Zawiera również użyteczne wskazówki (sekcja *Notes*) pozwalające na uniknięcie błędów podczas przeprowadzania reakcji oraz wszelkie niezbędne informacje dotyczące metody immunobarwienia cytochemicznego.

**Tomasiak A**, Berg LS, Sala K, Braszewska A. Quantitative analysis of epigenetic modifications in *Fagopyrum* nuclei with confocal microscope, ImageJ, and R Studio. w: Buckwheat Methods in Molecular Biology Edytorzy: Betekhtin A, Pinski, A., vol. 2791. Humana, Nowy Jork: Springer; 2024: 23–33.

### **Punkty MNiSW: 20**

Rozdział zawiera dokładny opis procedury, która pozwala na pozyskanie obrazu przy użyciu mikroskopii konfokalnej, jak i jego analizę przy użyciu profesjonalnych programów takich jak ImageJ oraz językiem programowania R. Protokół rozpoczyna się od dokładnego opisu ustawień mikroskopu konfokalnego Olympus FV1000 (Olympus, Polska). Kolejno protokół skupia się na analizie obrazu przy użyciu programu ImageJ wersja 1.53s (Wayne Rasband, National Institutes of Health, USA). Program ten jest cenionym narzędziem do analizy obrazów, wykorzystywanym w wielu dziedzinach nauki. Intensywność fluorescencji drugorzędowego przeciwciała Alexa488 została zmierzona jako średnia wartość z gęstości zintegrowanej (IntDen) z parametrem wartości progowej na jedno jądro, która przedstawia sumę wszystkich pikseli w obrębie wybranego obszaru. Protokół zawiera zrzuty ekranu wraz z opisem funkcji aby użytkownik mógł łatwo odtworzyć ścieżkę procedury. Dane liczbowe uzyskane z analizowanych obrazów poddano kolejno analizom statystycznym. W tym celu zastosowano R Studio 2022.12.0 Build 353. Jest to otwartoźródłowe, zintegrowane środowisko programistyczne dla języka R, który umożliwia łatwo odtwarzalny proces analizy statystycznej oraz wizualizacji danych. R jest głównie znany jako język statystyki, dlatego dominuje nad innymi językami programowania w tworzeniu narzędzi statystycznych. Zawiera różnorodne pakiety odpowiednie do naukowej analizy danych, takie jak agricolae (Procedury Statystyczne do Badań Rolniczych), który może być używany do znajdowania istotnych różnic między średnimi, oraz inne pakiety dedykowane wizualizacji danych. Umożliwia łatwe i powtarzalne uzyskiwanie podsumowania danych po analizie statystycznej i wizualizację ich w formie wykresów. Rozdział zawiera skrypt, który może być skopiowany i użyty do takiej analizy. W protokole zastosowano jednoczynnikową analizę wariancji (ANOVA), aby określić istotnie statystycznie różnice między porównywanymi grupami. Następnie zastosowano także test post-hoc Tukey’a, który miał na celu porównanie średnich w grupach.

Opisany protokół zawiera szczegółowy opis pomiaru fluorescencji z obrazów pozyskanych przy użyciu mikroskopii konfokalnej. Zawiera informacje na temat użytych programów, ich konfiguracji i ustawień odpowiednich do tego typu eksperymentów. Protokół można zastosować do różnorodnych badań pomiaru fluorescencji oraz, po zmodyfikowaniu dostępnego skryptu, analiz statystycznych.

**Wyniki otrzymane w rozprawie doktorskiej zaprezentowano na trzech konferencjach naukowych:**

1. 15 Międzynarodowe Sympozjum Gryki pt: „Buckwheat for health” zorganizowane przez Instytut Uprawy Nawożenia i Gleboznawstwa – Państwowy Instytut Badawczy w Puławach. Konferencja odbyła się w dniach 2-8 lipca 2023.

Tytuł wystąpienia: ‘Complex epigenetic analysis of the cell fate in long term cultivated *Fagopyrum* calli with different morphogenic capacity’. Prezentacja ustna.

2. 1st European Network for Protoplast regeneration and Microspore embryogenesis research zorganizowane przez Uniwersytet Gandawski w Gandawie. Konferencja odbyła się 9-10 września 2024.

Tytuł wystąpienia: ‘Cellular reprogramming processes in buckwheat from the epigenetic point of view’. Prezentacja ustna.

3. XVI Ogólnopolska Konferencja Kultur *In Vitro* i Biotechnologii Roślin, zorganizowana przez Uniwersytet Rolniczy w Krakowie. Konferencja odbyła się w dniach 23-25 września 2024.

Tytuł wystąpienia: ‘Gryka w kulturach *in vitro*: stan obecny i perspektywy’. Prezentacja ustna.

## 10. Literatura:

- Ahmed, A., Khalid, N., Ahmad, A., Abbasi, N.A., Latif, M.S.Z. i Randhawa, M.A. (2013) Phytochemicals and biofunctional properties of buckwheat: a review. *J Agric Sci*, **152**, 349-369.
- Bednarek, P.T. i Orłowska, R. (2019) Plant tissue culture environment as a switch-key of (epi)genetic changes. *Plant Cell Tiss Org*, **140**, 245-257.
- Betekhtin, A., Pinski, A., Milewska-Hendel, A., Kurczynska, E. i Hasterok, R. (2019) Stability and instability processes in the calli of *Fagopyrum tataricum* that have different morphogenic potentials. *Plant Cell Tiss Org*, **137**, 343-357.
- Betekhtin, A., Rojek, M., Jaskowiak, J., Milewska-Hendel, A., Kwasniewska, J., Kostyukova, Y., Kurczynska, E., Rumyantseva, N. i Hasterok, R. (2017) Nuclear genome stability in long-term cultivated callus lines of *Fagopyrum tataricum* (L.) Gaertn. *PLoS One*, **12**, e0173537.
- Birnbaum, K.D. i Sanchez Alvarado, A. (2008) Slicing across kingdoms: regeneration in plants and animals. *Cell*, **132**, 697-710.
- Bonafaccina, G., Marocchinia, M. i Kreft, I. (2003) Composition and technological properties of the flour and bran from common and tartary buckwheat. *Food chem*, **80**, 9-15.
- Cawoy, V., Deblauwe, V., Halbrech, B., Ledent, J.F., Kinet, J.M. i Jacquemart, A.L. (2006) Morph differences and honeybee morph preference in the distylous species *Fagopyrum esculentum* Moench. *Int J Plant Sci*, **167**, 853-861.
- Chakrabarty, D., Yu, K.W. i Paek, K.Y. (2003) Detection of DNA methylation changes during somatic embryogenesis of Siberian ginseng (*Eleuterococcus senticosus*) *Plant Sci*, **165**, 61-68.
- Cheng, K., Xu, Y., Yang, C., Ouellette, L., Niu, L., Zhou, X., Chu, L., Zhuang, F., Liu, J., Wu, H., Charron, J.B. i Luo, M. (2020) Histone tales: lysine methylation, a protagonist in *Arabidopsis* development. *J Exp Bot*, **71**, 793-807.
- Ci, H., Li, C., Aung, T.T., Wang, S., Yun, C., Wang, F., Ren, X. i Zhang, X. (2022) A comparative transcriptome analysis reveals the molecular mechanisms that underlie somatic embryogenesis in *Peaonia ostii* 'Fengdan'. *Int J Mol Sci*, **23**.
- Fawcett, J.A., Takeshima, R., Kikuchi, S., Yazaki, E., Katsube-Tanaka, T., Dong, Y., Li, M., Hunt, H.V., Jones, M.K., Lister, D.L., Ohsako, T., Ogiso-Tanaka, E., Fujii, K., Hara, T., Matsui, K., Mizuno, N., Nishimura, K., Nakazaki, T., Saito, H., Takeuchi, N., Ueno, M., Matsumoto, D., Norizuki, M., Shirasawa, K., Li, C., Hirakawa, H., Ota, T. i Yasui, Y. (2023) Genome sequencing reveals the genetic architecture of heterostyly and domestication history of common buckwheat. *Nat Plants*, **9**, 1236-1251.
- Feher, A. (2019) Callus, dedifferentiation, totipotency, somatic embryogenesis: what these terms mean in the era of molecular plant biology? *Front Plant Sci*, **10**, 536.
- Fei, Y., Wang, L.X., Fang, Z.W. i Liu, Z.X. (2019) Somatic embryogenesis and plant regeneration from cotyledon and hypocotyl explants of *Fagopyrum esculentum* Moench *lpls* mutant. *Agronomy*, **9**.
- Feng, S., Cokus, S.J., Zhang, X., Chen, P.Y., Bostick, M., Goll, M.G., Hetzel, J., Jain, J., Strauss, S.H., Halpern, M.E., Ukomadu, C., Sadler, K.C., Pradhan, S., Pellegrini, M. i Jacobsen, S.E. (2010) Conservation and divergence of methylation patterning in plants and animals. *Proc Natl Acad Sci U S A*, **107**, 8689-8694.
- Finnegan, E.J., Genger, R.K., Kovac, K., Peacock, W.J. i Dennis, E.S. (1998) DNA methylation and the promotion of flowering by vernalization. *Plant Biol*, **95**, 5824-5829.
- Fraga, H.P., Vieira, L.N., Caprestano, C.A., Steinmacher, D.A., Micke, G.A., Spudeit, D.A., Pescador, R. i Guerra, M.P. (2012) 5-Azacytidine combined with 2,4-D improves somatic embryogenesis of *Acca sellowiana* (O. Berg) Burret by means of changes in global DNA methylation levels. *Plant Cell Rep*, **31**, 2165-2176.
- Fulnecek, J., Matyasek, R., Votruba, I., Holy, A., Krizova, K. i Kovarik, A. (2011) Inhibition of SAH-hydrolase activity during seed germination leads to deregulation of flowering genes and altered flower morphology in tobacco. *Mol Genet Genomics*, **285**, 225-236.
- Gamborg, O.L., Miller, R.A. i Ojima, K. (1968) Nutrient requirements of suspension cultures of soybean root cells. *Exp Cell Res*, **50**, 151-158.
- Ge, R.H. i Wang, H. (2020) Nutrient components and bioactive compounds in tartary buckwheat bran and flour as affected by thermal processing. *Int J Food Prop*, **23**, 127-137.
- Gehring, M. (2019) Epigenetic dynamics during flowering plant reproduction: evidence for reprogramming? *New Phytol*, **224**, 91-96.
- Ghosh, A., Iqamberdiev, A.U. i Debnath, S.C. (2021) Tissue culture-induced DNA methylation in crop plants: a review. *Mol Biol Rep*, **48**, 823-841.

- Gonçalves, F.M.F., Debiage, R.R., Gonçalves da Silva, R.M., Porto, P.P., Yoshihara, E., Cosendey, E. i Toledo De Mello Peixoto, E.C.** (2016) *Fagopyrum esculentum* Moench: A crop with many purposes in agriculture and human nutrition. *Afr J Agric Res*, **11**, 983-989.
- Grafi, G.** (2004) How cells dedifferentiate: a lesson from plants. *Dev Biol*, **268**, 1-6.
- Han, M., Kamal, A., Huh, Y., Jeon, A.Y., Bae, J., Chung, K.Y., Lee, M.S., Park, S.U., Jeong, H. i Woo, S.H.** (2011) Regeneration of plantlet via somatic embryogenesis from hypocotyls of Tartary buckwheat (*Fagopyrum tataricum*). *Aust J Crop Sci*, **5**, 865-869.
- Han, Z., Crisp, P.A., Stelpflug, S., Kaeppler, S.M., Li, Q. i Springer, N.M.** (2018) Heritable epigenomic changes to the maize methylome resulting from tissue culture. *Genetics*, **209**, 983-995.
- He, X.J., Chen, T. i Zhu, J.K.** (2011) Regulation and function of DNA methylation in plants and animals. *Cell Res*, **21**, 442-465.
- Hemenway, E.A. i Gehring, M.** (2023) Epigenetic regulation during plant development and the capacity for epigenetic memory. *Annu Rev Plant Biol*, **74**, 87-109.
- Hou, S., Sun, Z., Linghu, B., Wang, Y., Huang, K., Xu, D. i Han, Y.** (2014) Regeneration of buckwheat plantlets from hypocotyl and the influence of exogenous hormones on rutin content and rutin biosynthetic gene expression *in vitro*. *Plant Cell Tiss Org*, **120**, 1159-1167.
- Hu, H. i Du, J.** (2022) Structure and mechanism of histone methylation dynamics in Arabidopsis. *Curr Opin Plant Biol*, **67**, 102211.
- Huang, X., Yao, J., Zhao, Y., Xie, D., Jiang, X. i Xu, Z.** (2016) Efficient rutin and quercetin biosynthesis through flavonoids-related gene expression in *Fagopyrum tataricum* Gaertn. hairy root cultures with UV-B irradiation. *Front Plant Sci*, **7**, 63.
- Huda, M.N., Lu, S., Jahan, T., Ding, M., Jha, R., Zhang, K., Zhang, W., Georgiev, M.I., Park, S.U. i Zhou, M.** (2021) Treasure from garden: Bioactive compounds of buckwheat. *Food Chem*, **335**, 127653.
- Ishihara, H., Sugimoto, K., Tarr, P.T., Temman, H., Kadokura, S., Inui, Y., Sakamoto, T., Sasaki, T., Aida, M., Suzuki, T., Inagaki, S., Morohashi, K., Seki, M., Kakutani, T., Meyerowitz, E.M. i Matsunaga, S.** (2019) Primed histone demethylation regulates shoot regenerative competency. *Nat Commun*, **10**, 1786.
- Jasencakova, Z., Soppe, W.J., Meister, A., Gernand, D., Turner, B.M. i Schubert, I.** (2003) Histone modifications in Arabidopsis- high methylation of H3 lysine 9 is dispensable for constitutive heterochromatin. *Plant J*, **33**, 471-480.
- Jha, R., Zhang, K., He, Y., Mandler-Drienyovszki, N., Magyar-Tábori, K., Quinet, M., Germ, M., Krefit, I., Meglič, V., Ikeda, K., Chapman, M.A., Janovská, D., Podolska, G., Woo, S.H., Bruno, S., Georgiev, M.I., Chrungoo, N., Betekhtin, A. i Zhou, M.** (2024) Global nutritional challenges and opportunities: Buckwheat, a potential bridge between nutrient deficiency and food security. *Trends Food Sci Technol*, **145**.
- Ji, L., Mathioni, S.M., Johnson, S., Tucker, D., Bewick, A.J., Do Kim, K., Daron, J., Slotkin, R.K., Jackson, S.A., Parrott, W.A., Meyers, B.C. i Schmitz, R.J.** (2019) Genome-wide reinforcement of DNA methylation occurs during somatic embryogenesis in soybean. *Plant Cell*, **31**.
- Kim, J.Y., Yang, W., Forner, J., Lohmann, J.U., Noh, B. i Noh, Y.S.** (2018) Epigenetic reprogramming by histone acetyltransferase HAG1/AtGCN5 is required for pluripotency acquisition in *Arabidopsis*. *EMBO J*, **37**.
- Kim, S.H., Kang, H.J., Lee, Y.T., Lee, S.Y., Ko, J.A. i Rha, E.S.** (2001) Direct regeneration of transgenic buckwheat from hypocotyl segments by *Agrobacterium*-mediated transformation. *Kor J Crop Sci*, **46**, 3775-3779.
- Kouzarides, T.** (2007) Chromatin modifications and their function. *Cell*, **128**, 693-705.
- Kumar, M.** (2018) Plant regeneration and genetic transformation in buckwheat (*Fagopyrum* spp.), a multipurpose gluten free crop of high nutraceutical importance: a critical review. *Ann Plant Sci*, **7**.
- Kumar, M. i Saraswat, R.** (2019) Plant regeneration in buckwheat (*Fagopyrum esculentum* Moench.) via somatic embryogenesis and induction of meristemoids in abnormal embryos. *Plant Tissue Cult Biotechnol*, **29**, 33-47.
- Kumari, P., Khan, S., Wani, I.A., Gupta, R., Verma, S., Alam, P. i Alaklabi, A.** (2022) Unravelling the role of epigenetic modifications in development and reproduction of Angiosperms: a critical appraisal. *Front Genet*, **13**, 819941.
- Kwon, S.J., Han, M.-H., Huh, Y.S., Roy, S.K., Lee, C.W. i Woo, S.H.** (2013) Plantlet regeneration via somatic embryogenesis from hypocotyls of common buckwheat (*Fagopyrum esculentum* Moench.). *Korean J Crop Sci*, **58**, 331-335.
- Lachmann, S. i Adachi, T.** (1990) Callus regeneration from hypocotyl protoplasts of tartary buckwheat (*Fagopyrum tataricum* Gartn.) *Fagopyrum*, **10**, 62-64.
- Lachmann, S., Kishima, Y. i Adachi, T.** (1994) Protoplast fusion in buckwheat: preliminary results on somatic hybridisation. *Fagopyrum*, **14**, 7-12.

- Lee, K. i Seo, P.J. (2018) Dynamic epigenetic changes during plant regeneration. *Trends Plant Sci*, **23**, 235-247.
- Lee, K.P., Park, O.S. i Seo, P.J. (2017) *Arabidopsis* ATXR2 deposits H3K36me3 at the promoters of *LBD* genes to facilitate cellular dedifferentiation. *Sci Signal*, **10**.
- Lee, S.Y., Cho, S.I., Park, M.H., Kim, Y.K., Choi, J.E. i Park, S.U. (2007) Growth and rutin production in hairy root cultures of buckwheat (*Fagopyrum esculentum* M.). *Prep Biochem Biotechnol*, **37**, 239-246.
- Li, H.L., Guo, D., Zhu, J.-H., Wang, Y. i Peng, S.Q. (2017a) Identification and expression analysis of genes involved in histone acetylation in *Hevea brasiliensis*. *Tree Genet Genomes*, **13**.
- Li, X., Thwe, A.A., Park, C.H., Kim, S.J., Arasu, M.V., Abdullah Al-Dhabi, N., Lee, S.Y. i Park, S.U. (2017b) Ethephon-induced phenylpropanoid accumulation and related gene expression in tartary buckwheat (*Fagopyrum tataricum* (L.) Gaertn.) hairy root. *Biotechnol Biotechnol Equip*, **31**, 304-311.
- Ma, J., Li, Q., Zhang, L., Cai, S., Liu, Y., Lin, J., Huang, R., Yu, Y., Wen, M. i Xu, T. (2022) High auxin stimulates callus through SDG8-mediated histone H3K36 methylation in *Arabidopsis*. *J Integr Plant Biol*, **64**, 2425-2437.
- Matsui, K. i Yasui, Y. (2020) Genetic and genomic research for the development of an efficient breeding system in heterostylous self-incompatible common buckwheat (*Fagopyrum esculentum*). *Theor Appl Genet*, **133**, 1641-1653.
- Meijón, M., Feito, I., Valledor, L., Rodríguez, R. i Cañal, M.J. (2010) Dynamics of DNA methylation and histone H4 acetylation during floral bud differentiation in azalea. *Plant Biol*, **10**.
- Miguel, C. i Marum, L. (2011) An epigenetic view of plant cells cultured *in vitro*: somaclonal variation and beyond. *J Exp Bot*, **62**, 3713-3725.
- Miljus-Djukić, J., Nesković, M., Ninković, S. i Cekvenjakov, R. (1992) *Agrobacterium*-mediated transformation and plant regeneration of buckwheat (*Fagopyrum esculentum* Moench.). *Plant Cell Tiss Org*, **29**, 101-108.
- Monja-Mio, K.M., Quiroz-Moreno, A., Herrera-Herrera, G., Montero-Muñoz, J.L., Sánchez-Teyer, F. i Robert, M.L. (2018) Analysis of two clonal lines (embryogenic and non-embryogenic) of *Agave fourcroydes* using AFLP and MSAP. *Am J Plant Sci*, **9**, 745-762.
- Moronczyk, J., Braszewska, A., Wojcikowska, B., Chwialkowska, K., Nowak, K., Wojcik, A.M., Kwasniewski, M. i Gaj, M.D. (2022) Insights into the histone acetylation-mediated regulation of the transcription factor genes that control the embryogenic transition in the somatic cells of *Arabidopsis*. *Cells*, **11**.
- Murashige, T. i Skoog, F. (1962) A revised medium for rapid growth and bio assays with tobacco tissue cultures. *Physiol Plantarum* **15**, 473-497.
- Nagatomo T. i Adachi, T. (1985) *Fagopyrum esculentum*. In *Handbook of flowering* (Halevy, A.H. ed. Boca Raton, Florida, USA: CRC Press, pp. 1-8.
- Nic-Can, G.I., Lopez-Torres, A., Barredo-Pool, F., Wrobel, K., Loyola-Vargas, V.M., Rojas-Herrera, R. i De-la-Pena, C. (2013) New insights into somatic embryogenesis: *LEAFY COTYLEDON1*, *BABY BOOM1* and *WUSCHEL*-related homeobox4 are epigenetically regulated in *Coffea canephora*. *PLoS One*, **8**.
- Park, N.I., Li, X., Thwe, A.A., Lee, S.Y., Kim, S.G., Wu, Q. i Park, S.U. (2012) Enhancement of rutin in *Fagopyrum esculentum* hairy root cultures by the *Arabidopsis* transcription factor AtMYB12. *Biotechnol Lett*, **34**, 577-583.
- Park, S.Y., Murthy, H.N., Chakrabarty, D. i Paek, K.Y. (2008) Detection of epigenetic variation in tissue-culture-derived plants of *Doritaenopsis* by methylation-sensitive amplification polymorphism (MSAP) analysis. *In Vitro Cell Dev Biol Plant* **45**, 104-108.
- Pinski, A. i Betekhtin, A. (2023) Efficient *Agrobacterium*-mediated transformation and genome editing of *Fagopyrum tataricum*. *Front Plant Sci*, **14**, 1270150.
- Rajbhandari, B.P., Dhaubhadel, S., Gautam, D.M. i B.R., G. (1995) Plant regeneration via calli of leaf and stem explants in common buckwheat ecotypes. In *Current Advances in Buckwheat Research* Nagano, Japan: Shinshu University Press, pp. 191-196.
- Ruiz-Garcia, L., Cervera, M.T. i Martinez-Zapater, J.M. (2005) DNA methylation increases throughout *Arabidopsis* development. *Planta*, **222**, 301-306.
- Rumyantseva, N.I., Sal'nikov, V.V. i Lebedeva, V.V. (2005) Structural changes of cell surface in callus of *Fagopyrum esculentum* Moench. during induction of morphogenesis. *Russ J Plant Physiol*, **52**, 381-387.
- Rymen, B., Kawamura, A., Lambolez, A., Inagaki, S., Takebayashi, A., Iwase, A., Sakamoto, Y., Sako, K., Favero, D.S., Ikeuchi, M., Suzuki, T., Seki, M., Kakutani, T., Roudier, F. i Sugimoto, K. (2019) Histone acetylation orchestrates wound-induced transcriptional activation and cellular reprogramming in *Arabidopsis*. *Commun Biol*, **2**, 404.

- Sibgatullina, G.V., Rumyantseva, N.I., Khaertdinova, L.R., Akulov, A.N., Tarasova, N.B. i Gumerova, E.A.** (2012) Establishment and characterization of the line of *Fagopyrum tataricum* morphogenic callus tolerant to aminotriazole. *Russ J Plant Physiol*, **59**, 662-669.
- Springer, N.M. i Schmitz, R.J.** (2017) Exploiting induced and natural epigenetic variation for crop improvement. *Nat Rev Genet*, **18**, 563-575.
- Steedman, H.** (1957) Polyester wax: a new ribboning embedding medium for histology. *Nature*, **179**, 1345.
- Stelpflug, S.C., Eichten, S.R., Hermanson, P.J., Springer, N.M. i Kaeppler, S.M.** (2014) Consistent and heritable alterations of DNA methylation are induced by tissue culture in maize. *Genetics*, **198**, 209-218.
- Sugimoto, K., Gordon, S.P. i Meyerowitz, E.M.** (2011) Regeneration in plants and animals: dedifferentiation, transdifferentiation, or just differentiation? *Trends Cell Biol*, **21**, 212-218.
- Sugimoto, K., Temman, H., Kadokura, S. i Matsunaga, S.** (2019) To regenerate or not to regenerate: factors that drive plant regeneration. *Curr Opin Plant Biol*, **47**, 138-150.
- Szymanowska, A., Gornowicz, A., Bielawska, A. i Bielawski, K.** (2019) Roślinne komórki macierzyste i ich zastosowanie w kosmetologii i medycynie regeneracyjnej. *Biul Wydz Farm WUM*, **7**, 36-42.
- Takahata, Y.** (1988) Plant regeneration from cultured immature inflorescence of common buckwheat (*Fagopyrum esculentum* Moench) and perennial buckwheat (*F. cymosum* Meisn.). *Jpn J Breed*, **38**, 409-413.
- Teysier, E., Bernacchia, G., Maury, S., How Kit, A., Stammitti-Bert, L., Rolin, D. i Gallusci, P.** (2008) Tissue dependent variations of DNA methylation and endoreduplication levels during tomato fruit development and ripening. *Planta*, **228**, 391-399.
- Thwe, A.A., Kim, J.K., Li, X., Kim, Y.B., Uddin, M.R., Kim, S.J., Suzuki, T., Park, N.I. i Park, S.U.** (2013) Metabolomic analysis and phenylpropanoid biosynthesis in hairy root culture of tartary buckwheat cultivars. *PLoS One*, **8**, e65349.
- Us-Camas, R., Rivera-Solís, G., Duarte-Aké, F. i De-la-Peña, C.** (2014) *In vitro* culture: an epigenetic challenge for plants. *Plant Cell Tiss Org*, **118**, 187-201.
- Wang, C., Dong, X., Ding, M., Tang, Y., Zhu, X., Wu, Y., Zhou, M. i Shao, J.** (2016) Plantlet regeneration of Tartary buckwheat (*Fagopyrum tataricum* Gaertn.) *in vitro* tissue cultures. *Protein Peptide Lett*, 468-477.
- Wickramasuriya, A.M. i Dunwell, J.M.** (2015) Global scale transcriptome analysis of *Arabidopsis* embryogenesis *in vitro*. *BMC Genomics*, **16**, 301.
- Xing, L., Li, Y., Qi, S., Zhang, C., Ma, W., Zuo, X., Liang, J., Gao, C., Jia, P., Shah, K., Zhang, D., An, N., Zhao, C., Han, M. i Zhao, J.** (2019) Comparative RNA-sequencing and DNA methylation analyses of apple (*Malus domestica* Borkh.) buds with diverse flowering capabilities reveal novel insights into the regulatory mechanisms of flower bud formation. *Plant Cell Physiol*, **60**, 1702-1721.
- Yamamoto, N., Kobayashi, H., Togashi, T., Mori, Y., Kikuchi, K., Kuriyama, K. i Tokuji, Y.** (2005) Formation of embryogenic cell clumps from carrot epidermal cells is suppressed by 5-azacytidine, a DNA methylation inhibitor. *J Plant Physiol*, **162**, 47-54.
- Yang, H., Chang, F., You, C., Cui, J., Zhu, G., Wang, L., Zheng, Y., Qi, J. i Ma, H.** (2015) Whole-genome DNA methylation patterns and complex associations with gene structure and expression during flower development in *Arabidopsis*. *Plant J*, **81**, 268-281.
- Yasui, Y., Hirakawa, H., Ueno, M., Matsui, K., Katsube-Tanaka, T., Yang, S.J., Aii, J., Sato, S. i Mori, M.** (2016) Assembly of the draft genome of buckwheat and its applications in identifying agronomically useful genes. *DNA Res*, **23**, 215-224.
- Yasui, Y., Mori, M., Aii, J., Abe, T., Matsumoto, D., Sato, S., Hayashi, Y., Ohnishi, O. i Ota, T.** (2012) *S-LOCUS EARLY FLOWERING 3* is exclusively present in the genomes of short-styled buckwheat plants that exhibit heteromorphic self-incompatibility. *PLoS One*, **7**.
- Yu, Y., Bu, Z., Shen, W.H. i Dong, A.** (2009) An update on histone lysine methylation in plants. *Prog Nat Sci*, **19**, 407-413.
- Zhang, H., Guo, F., Qi, P., Huang, Y., Xie, Y., Xu, L., Han, N., Xu, L. i Bian, H.** (2020) OsHDA710-mediated histone deacetylation regulates callus formation of rice mature embryo. *Plant Cell Physiol*, **61**, 1646-1660.
- Zhang, T., Cooper, S. i Brockdorff, N.** (2015) The interplay of histone modifications - writers that read. *EMBO Rep*, **16**, 1467-1481.
- Zhao, J.L., Zou, L., Zhang, C.Q., Li, Y.Y., Peng, L.X., Xiang, D.B. i Zhao, G.** (2014) Efficient production of flavonoids in *Fagopyrum tataricum* hairy root cultures with yeast polysaccharide elicitation and medium renewal process. *Pharmacogn Mag*, **10**, 234-240.
- Zheng, B., Liu, J., Gao, A., Chen, X., Gao, L., Liao, L., Luo, B., Ogutu, C.O. i Han, Y.** (2022) Epigenetic reprogramming of H3K27me3 and DNA methylation during leaf-to-callus transition in peach. *Hortic Res*, **9**.



## **11. Oświadczenia autorów publikacji wchodzących w skład rozprawy doktorskiej**

Katowice, 13.09.2024  
miejsowość, data

Alicja Tomasiak

imię i nazwisko kandydata

Instytut Biologii, Biotechnologii i Ochrony Środowiska,

Wydział Nauk Przyrodniczych,

Uniwersytet Śląski w Katowicach

Afiliacja

## OŚWIADCZENIE OSOBY UBIEGAJĄCEJ SIĘ O WŁASNYM WKŁADZIE W POWSTAWANIE PRACY

Oświadczam, że w pracy:

Tomasiak A., Zhou M., Betekhtin A. Buckwheat in tissue culture research: current status and future perspectives. International Journal of Molecular Sciences, 2022; 23(4):2298.

<https://doi.org/10.3390/ijms23042298>

Mój udział polegał na opracowaniu koncepcji publikacji, analizie dostępnej literatury i przygotowaniu pierwszej oraz finalnej wersji manuskryptu.



.....  
podpis

Prof. Meiliang Zhou

Beijing, 10.08.2024

Chinese Academy of Agricultural Sciences

Center for Crop Germplasm Resources

Institute of Crop Sciences

Beijing, China

## Authorship declaration

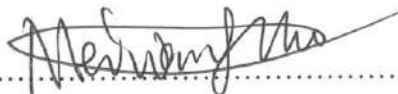
Buckwheat in tissue culture research: current status and future perspectives.

I declare that in the publication:

**Tomasiak A.**, Zhou M., Betekhtin A. Buckwheat in tissue culture research: current status and future perspectives.

International Journal of Molecular Sciences, 2022, 23(4).

my contribution was to review and edit the final version of the manuscript.



Prof. Meiliang Zhou

OŚWIADCZENIE WSPÓŁAUTORA OSOBY UBIEGAJĄcej SIĘ O WŁASNYM WKŁADZIE W  
POWSTAWANIE PRACY

Katowice, dnia 6.10.2024

dr hab. Alexander Betekhtin, prof. UŚ  
Imię i nazwisko współautora publikacji

Instytut Biologii, Biotechnologii i Ochrony Środowiska,

Wydział Nauk Przyrodniczych,

Uniwersytet Śląski w Katowicach  
Afilacja

**OŚWIADCZENIE**

Oświadczam, że w pracy:

Tomasiak A., Zhou M., Betekhtin A. Buckwheat in tissue culture research: current status and future perspectives. International Journal of Molecular Sciences, 2022, 23(4):2298.

<https://doi.org/10.3390/ijms23042298>

Mój udział polegał na opracowaniu koncepcji, pozyskaniu finansowania projektu, nadzorowaniu tworzenia oraz edycji manuskryptu. Jestem autorem korespondencyjnym.



.....  
Podpis współautora publikacji

Katowice, 13.09.2024  
miejsowość, data

Alicja Tomasiak

imię i nazwisko kandydata

Instytut Biologii, Biotechnologii i Ochrony Środowiska,

Wydział Nauk Przyrodniczych,

Uniwersytet Śląski w Katowicach

Afilacja

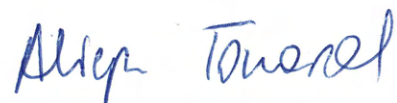
## OŚWIADCZENIE OSOBY UBIEGAJĄCEJ SIĘ O WŁASNYM WKŁADZIE W POWSTAWANIE PRACY

Oświadczam, że w pracy:

Tomasiak, A., Sala-Cholewa, K., Berg, L.S., Brąszewska, A., Betekhtin, A. Global epigenetic analysis revealed dynamic fluctuations in levels of DNA methylation and histone modifications in the calli of *Fagopyrum* with different capacity for morphogenesis. *Plant Cell Tissue and Organ Culture* 155, 743–757 (2023).

<https://doi.org/10.1007/s11240-023-02595-3>

Mój udział polegał na prowadzeniu materiału użytego do badań w kulturach *in vitro*, optymalizacji techniki immunobarwienia preparatów, wykonaniu preparatów do analiz histologicznych i immunocytochemicznych, obserwacji preparatów przy użyciu mikroskopii konfokalnej, analizie obrazów w programie ImageJ, analizie statystycznej i interpretacji wyników w programie R Studio, opracowaniu wyników i przygotowaniu ostatecznej wersji manuskryptu.



.....  
podpis

OŚWIADCZENIE WSPÓŁAUTORA OSOBY UBIEGAJĄCEJ SIĘ O WŁASNYM WKŁADZIE W  
POWSTAWIANIE PRACY

Katowice, dnia 30.09.2024

dr Katarzyna Sala-Cholewa  
Imię i nazwisko współautora publikacji

Instytut Biologii, Biotechnologii i Ochrony Środowiska,

Wydział Nauk Przyrodniczych,

Uniwersytet Śląski w Katowicach  
Afilacja

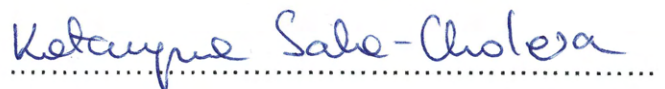
OŚWIADCZENIE

Oświadczam, że w pracy:

Tomasiak, A., Sala-Cholewa, K., Berg, L.S., Brąszewska, A., Betekhtin, A. Global epigenetic analysis revealed dynamic fluctuations in levels of DNA methylation and histone modifications in the calli of *Fagopyrum* with different capacity for morphogenesis. *Plant Cell Tissue and Organ Culture* 155, 743–757 (2023).

<https://doi.org/10.1007/s11240-023-02595-3>

Mój udział polegał na optymalizacji techniki przygotowania preparatów do analiz histologicznych i immunocytochemicznych, nadzorowaniu procedur immunobarwienia, obserwacji preparatów przy użyciu mikroskopii konfokalnej i edycji ostatecznej wersji manuskryptu.



Podpis współautora publikacji

A STATEMENT OF THE APPLICANT'S CO-AUTHOR OF THEIR CONTRIBUTION TO THE WORK

Bern, 1.10.2024

Lea Sophie Berg, MSc

First and last name of co-author of the publication

Institute of Plant Sciences

University of Bern

Bern, Switzerland

Affiliation

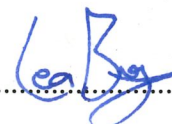
**STATEMENT**

I declare that for the following work:

Tomasiak, A., Sala-Cholewa, K., Berg, L.S., Brąszewska, A., Betekhtin, A. Global epigenetic analysis revealed dynamic fluctuations in levels of DNA methylation and histone modifications in the calli of *Fagopyrum* with different capacity for morphogenesis. *Plant Cell Tissue and Organ Culture* 155, 743–757 (2023).

<https://doi.org/10.1007/s11240-023-02595-3>

My participation consisted of providing an R Studio script used to perform the statistical analysis and the visualization of the results.



.....  
Signature of the co-author of the publication

OŚWIADCZENIE WSPÓŁAUTORA OSOBY UBIEGAJĄCEJ SIĘ O WŁASNYM WKŁADZIE W  
POWSTAWIANIE PRACY

Katowice, dnia 30.09.2024

dr Agnieszka Brąszewska  
Imię i nazwisko współautora publikacji

Instytut Biologii, Biotechnologii i Ochrony Środowiska,

Wydział Nauk Przyrodniczych,

Uniwersytet Śląski w Katowicach  
Afilacja

**OŚWIADCZENIE**

Oświadczam, że w pracy:

Tomasiak, A., Sala-Cholewa, K., Berg, L.S., Brąszewska, A., Betekhtin, A. Global epigenetic analysis revealed dynamic fluctuations in levels of DNA methylation and histone modifications in the calli of *Fagopyrum* with different capacity for morphogenesis. *Plant Cell Tissue and Organ Culture* 155, 743–757 (2023).

<https://doi.org/10.1007/s11240-023-02595-3>

Mój udział polegał na konceptualizacji badań, optymalizacji techniki barwienia preparatów do analiz immunocytochemicznych, interpretacji wyników oraz edycji ostatecznej wersji manuskryptu.



Podpis współautora publikacji



OŚWIADCZENIE WSPÓŁAUTORA OSOBY UBIEGAJĄCEJ SIĘ O WŁASNYM WKŁADZIE W  
POWSTAWIANIE PRACY

Katowice, dnia 6.10.2024

dr hab. Alexander Betekhtin, prof. UŚ  
Imię i nazwisko współautora publikacji

Instytut Biologii, Biotechnologii i Ochrony Środowiska,

Wydział Nauk Przyrodniczych,

Uniwersytet Śląski w Katowicach  
Afilacja

OŚWIADCZENIE

Oświadczam, że w pracy:

Tomasiak, A., Sala-Cholewa, K., Berg, L.S., Brąszewska, A., Betekhtin, A. Global epigenetic analysis revealed dynamic fluctuations in levels of DNA methylation and histone modifications in the calli of *Fagopyrum* with different capacity for morphogenesis. *Plant Cell Tissue and Organ Culture* 155, 743–757 (2023).

<https://doi.org/10.1007/s11240-023-02595-3>

Mój udział polegał na pozyskaniu finansowania projektu, planowaniu i nadzorze badań, interpretacji wyników oraz edycji manuskryptu. Jestem autorem korespondencyjnym.



Podpis współautora publikacji

Katowice, 13.09.2024  
miejsowość, data

Alicja Tomasiak

imię i nazwisko kandydata

Instytut Biologii, Biotechnologii i Ochrony Środowiska,

Wydział Nauk Przyrodniczych,

Uniwersytet Śląski w Katowicach

Afilacja

## OŚWIADCZENIE OSOBY UBIEGAJĄCEJ SIĘ O WŁASNYM WKŁADZIE W POWSTAWANIE PRACY

Oświadczam, że w pracy:

Tomasiak, A., Piński, A., Milewska-Hendel, A., Andreu Godall, I., Borowska-Żuchowska, N., Morończyk, J., Moreno-Romero, J., & Betekhtin, A. H3K4me3 changes occur in cell wall genes during the development of *Fagopyrum tataricum* morphogenic and non-morphogenic calli. *Frontiers in Plant Science*, 15, 1465514 (2024).

<https://doi.org/10.3389/fpls.2024.1465514>

Mój udział polegał na prowadzeniu materiału użytego do badań w kulturach *in vitro*, zaprojektowaniu starterów potrzebnych do analiz ekspresji genów metodą RT-qPCR i ChIP-qPCR, przygotowaniu, optymalizacji i wykonaniu eksperymentów immunoprecypitacji chromatyny, przygotowaniu materiału do badań immunohistochemicznych, obserwacji mikroskopowych preparatów po immunobarwieniu, analizie i interpretacji otrzymanych wyników, analizie statystycznej i opracowaniu otrzymanych wyników oraz przygotowaniu ostatecznej wersji manuskryptu.



.....  
podpis

OŚWIADCZENIE WSPÓŁAUTORA OSOBY UBIEGAJĄCEJ SIĘ O WŁASNYM WKŁADZIE W  
POWSTAWIANIE PRACY

Katowice, dnia 30.09.2024

dr Artur Piński  
Imię i nazwisko współautora publikacji

Instytut Biologii, Biotechnologii i Ochrony Środowiska,

Wydział Nauk Przyrodniczych,

Uniwersytet Śląski w Katowicach  
Afilacja

OŚWIADCZENIE

Oświadczam, że w pracy:

Tomasiak, A., Piński, A., Milewska-Hendel, A., Andreu Godall, I., Borowska-Żuchowska, N.,  
Morończyk, J., Moreno-Romero, J., & Betekhtin, A. H3K4me3 changes occur in cell wall genes  
during the development of *Fagopyrum tataricum* morphogenic and non-morphogenic calli.  
Frontiers in Plant Science, 15, 1465514 (2024).

<https://doi.org/10.3389/fpls.2024.1465514>

Mój udział polegał na wyborze genów do analiz RT-qPCR, analizie i opracowaniu otrzymanych  
wyników oraz przygotowaniu i edycji ostatecznej wersji manuskryptu.



Podpis współautora publikacji

OŚWIADCZENIE WSPÓŁAUTORA OSOBY UBIEGAJĄEJ SIĘ O WŁASNYM WKŁADZIE W  
POWSTAWANIE PRACY

Katowice, dnia 30.09.2024

dr Anna Milewska-Hendel  
Imię i nazwisko współautora publikacji

Instytut Biologii, Biotechnologii i Ochrony Środowiska,  
Wydział Nauk Przyrodniczych,  
Uniwersytet Śląski w Katowicach  
Afilacja

OŚWIADCZENIE

Oświadczam, że w pracy:

Tomasiak, A., Piński, A., Milewska-Hendel, A., Andreu Godall, I., Borowska-Żuchowska, N.,  
Morończyk, J., Moreno-Romero, J., & Betekhtin, A. H3K4me3 changes occur in cell wall genes  
during the development of *Fagopyrum tataricum* morphogenic and non-morphogenic calli.  
Frontiers in Plant Science, 15, 1465514 (2024).

<https://doi.org/10.3389/fpls.2024.1465514>

Mój udział polegał na przygotowaniu preparatów i przeprowadzeniu reakcji immunobarwienia,  
obserwacji mikroskopowych, analizie i interpretacji wyników, przygotowaniu i edycji ostatecznej  
wersji manuskryptu.

..... Milewska-Hendel .....

Podpis współautora publikacji

A STATEMENT OF THE APPLICANT'S CO-AUTHOR OF THEIR CONTRIBUTION TO THE WORK

Barcelona, 1.10.2024

Jordi Moreno-Romero, PhD

First and last name of co-author of the publication

Departament de Bioquímica i Biologia Molecular,

Universitat Autònoma de Barcelona,

Cerdanyola del Vallès, Barcelona, Spain

Affiliation

**STATEMENT**

I declare that for the following work:

Tomasiak, A., Piński, A., Milewska-Hendel, A., Andreu Godall, I., Borowska-Żuchowska, N., Morończyk, J., Moreno-Romero, J., & Betekhtin, A. H3K4me3 changes occur in cell wall genes during the development of *Fagopyrum tataricum* morphogenic and non-morphogenic calli. *Frontiers in Plant Science*, 15, 1465514 (2024).

<https://doi.org/10.3389/fpls.2024.1465514>

My participation consisted of acquiring the funding, supervision and guidance of the chromatin immunoprecipitation technique optimization, analysis and visualization of the obtained results, preparing and reviewing the final version of the manuscript. I am a corresponding author.

**JORDI MORENO  
ROMERO - DNI  
46827193K** Digitally signed by JORDI  
MORENO ROMERO - DNI  
46827193K  
Date: 2024.10.01  
17:23:42 +02'00'

.....  
Signature of the co-author of the publication

OŚWIADCZENIE WSPÓŁAUTORA OSOBY UBIEGAJĄEJ SIĘ O WŁASNYM WKŁADZIE W  
POWSTAWANIE PRACY

Katowice, dnia 6.10.2024

dr hab. Alexander Betekhtin, prof. UŚ  
Imię i nazwisko współautora publikacji

Instytut Biologii, Biotechnologii i Ochrony Środowiska,

Wydział Nauk Przyrodniczych,

Uniwersytet Śląski w Katowicach  
Afilacja

OŚWIADCZENIE

Oświadczam, że w pracy:

Tomasiak, A., Piński, A., Milewska-Hendel, A., Andreu Godall, I., Borowska-Żuchowska, N.,  
Morończyk, J., Moreno-Romero, J., & Betekhtin, A. H3K4me3 changes occur in cell wall genes  
during the development of *Fagopyrum tataricum* morphogenic and non-morphogenic calli.  
Frontiers in Plant Science, 15, 1465514 (2024).

<https://doi.org/10.3389/fpls.2024.1465514>

Mój udział polegał na pozyskaniu finansowania projektu, planowaniu oraz nadzorowaniu badań,  
interpretacji wyników oraz edycji manuskryptu. Jestem autorem korespondencyjnym.



Podpis współautora publikacji

OŚWIADCZENIE WSPÓŁAUTORA OSOBY UBIEGAJĄCEJ SIĘ O WŁASNYM WKŁADZIE W  
POWSTAWANIE PRACY

Katowice, dnia 30.09.2024

dr Katarzyna Sala-Cholewa  
Imię i nazwisko współautora publikacji

Instytut Biologii, Biotechnologii i Ochrony Środowiska,  
Wydział Nauk Przyrodniczych,  
Uniwersytet Śląski w Katowicach  
Afilacja

**OŚWIADCZENIE**

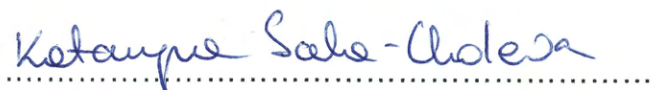
Oświadczam, że w pracy:

Sala-Cholewa, K.\*, Tomasiak, A.\*, Nowak, K., Piński, A., Betekhtin, A. DNA methylation analysis of floral parts revealed dynamic changes during the development of homostylous *Fagopyrum tataricum* and heterostylous *F. esculentum* flowers. *BMC Plant Biology* 24, 448 (2024).

<https://doi.org/10.1186/s12870-024-05162-w>

\* równorzędny pierwszy autor

Mój udział polegał na wykonaniu preparatów do analiz histologicznych i immunocytochemicznych obserwacji preparatów przy użyciu mikroskopii konfokalnej, ich analizy i interpretacji w programie ImageJ, analizie statystycznej otrzymanych wyników w programie R Studio, opracowaniu wyników i przygotowaniu ostatecznej wersji manuskryptu.



Podpis współautora publikacji

Katowice, 13.09.2024  
miejsowość, data

Alicja Tomasiak

imię i nazwisko kandydata

Instytut Biologii, Biotechnologii i Ochrony Środowiska,

Wydział Nauk Przyrodniczych,

Uniwersytet Śląski w Katowicach

Afiliacja

## OŚWIADCZENIE OSOBY UBIEGAJĄCEJ SIĘ O WŁASNYM WKŁADZIE W POWSTAWANIE PRACY

Oświadczam, że w pracy:

Sala-Cholewa, K.\*, Tomasiak, A.\*, Nowak, K., Piński, A., Betekhtin, A. DNA methylation analysis of floral parts revealed dynamic changes during the development of homostylous *Fagopyrum tataricum* and heterostylous *F. esculentum* flowers. BMC Plant Biology 24, 448 (2024).

<https://doi.org/10.1186/s12870-024-05162-w>

\* równorzędny pierwszy autor

Mój udział polegał na wykonaniu preparatów do analiz histologicznych i immunocytochemicznych, obserwacji preparatów przy użyciu mikroskopii konfokalnej, ich analizy i interpretacji w programie ImageJ, analizie statystycznej otrzymanych wyników w programie R Studio, opracowaniu wyników i przygotowaniu ostatecznej wersji manuskryptu.



.....  
podpis



OŚWIADCZENIE WSPÓŁAUTORA OSOBY UBIEGAJĄCEJ SIĘ O WŁASNYM WKŁADZIE W  
POWSTAWANIE PRACY

Katowice, dnia 30.09.2024

dr Katarzyna Nowak  
Imię i nazwisko współautora publikacji

Instytut Biologii, Biotechnologii i Ochrony Środowiska,

Wydział Nauk Przyrodniczych,

Uniwersytet Śląski w Katowicach  
Afilacja

OŚWIADCZENIE

Oświadczam, że w pracy:

Sala-Cholewa, K.\*, Tomasiak, A.\*, Nowak, K., Piński, A., Betekhtin, A. DNA methylation analysis of floral parts revealed dynamic changes during the development of homostylous *Fagopyrum tataricum* and heterostylous *F. esculentum* flowers. BMC Plant Biology 24, 448 (2024).

<https://doi.org/10.1186/s12870-024-05162-w>

\* równorzędny pierwszy autor

Mój udział polegał na przygotowaniu materiału do reakcji RT-qPCR, wykonaniu analiz ekspresji genów metodą RT-qPCR, analizie otrzymanych wyników oraz przygotowaniu ostatecznej wersji manuskryptu.

  
.....

Podpis współautora publikacji

OŚWIADCZENIE WSPÓŁAUTORA OSOBY UBIEGAJĄCEJ SIĘ O WŁASNYM WKŁADZIE W  
POWSTAWIANIE PRACY

Katowice, dnia 30.09.2024

dr Artur Piński

Imię i nazwisko współautora publikacji

Instytut Biologii, Biotechnologii i Ochrony Środowiska,

Wydział Nauk Przyrodniczych,

Uniwersytet Śląski w Katowicach

Afiliacja

OŚWIADCZENIE

Oświadczam, że w pracy:

Sala-Cholewa, K.\*, Tomasiak, A.\*, Nowak, K., Piński, A., Betekhtin, A. DNA methylation analysis of floral parts revealed dynamic changes during the development of homostylous *Fagopyrum tataricum* and heterostylous *F. esculentum* flowers. BMC Plant Biology 24, 448 (2024).

<https://doi.org/10.1186/s12870-024-05162-w>

\* równorzędny pierwszy autor

Mój udział polegał na przygotowaniu starterów potrzebnych do analiz ekspresji genów metodą RT-qPCR, analizie otrzymanych wyników oraz przygotowaniu ostatecznej wersji manuskryptu.



Podpis współautora publikacji

OŚWIADCZENIE WSPÓŁAUTORA OSOBY UBIEGAJĄCEJ SIĘ O WŁASNYM WKŁADZIE W  
POWSTAWANIE PRACY

Katowice, dnia 6.10.2024

dr hab. Alexander Betekhtin, prof. UŚ  
Imię i nazwisko współautora publikacji

Instytut Biologii, Biotechnologii i Ochrony Środowiska,

Wydział Nauk Przyrodniczych,

Uniwersytet Śląski w Katowicach  
Afilacja

**OŚWIADCZENIE**

Oświadczam, że w pracy:

Sala-Cholewa, K.\*, Tomasiak, A.\*, Nowak, K., Piński, A., Betekhtin, A. DNA methylation analysis of floral parts revealed dynamic changes during the development of homostylous *Fagopyrum tataricum* and heterostylous *F. esculentum* flowers. BMC Plant Biology 24, 448 (2024).

<https://doi.org/10.1186/s12870-024-05162-w>

\* równorzędny pierwszy autor

Mój udział polegał na pozyskaniu finansowania projektu, planowaniu oraz nadzorowaniu badań, interpretacji wyników oraz edycji manuskryptu. Jestem autorem korespondencyjnym.



Podpis współautora publikacji